

Copyright is owned by the Author of the thesis. Permission is given for a copy to be downloaded by an individual for the purpose of research and private study only. The thesis may not be reproduced elsewhere without the permission of the Author.

**AN INVESTIGATION OF THE APPLICATION  
OF REMOTE SENSING AND GEOGRAPHIC INFORMATION  
SYSTEMS FOR RESOURCE MANAGEMENT IN  
WESTLAND, NEW ZEALAND.**

A thesis presented in partial fulfilment  
of the requirements for the degree of  
Doctor of Philosophy in Soil Science  
at Massey University, New Zealand.

by

**Leonard John Brown**

**1995**

## ABSTRACT

Effective management of natural resources, and the side effects resulting from their use directly affects our environmental and economic wellbeing. This thesis was initiated to investigate the application of remote sensing, digital image processing and Geographic Information System (GIS) tools for natural resource management in Westland, New Zealand. From the multitude of potential applications, research was directed toward two issues: alluvial gold mining and indigenous forest management. This thesis focused on the use of personal computer (PC) applications.

A study of alluvial gold mining operations utilised black-and-white aerial photography taken at five dates in the period 1943 to 1988. The photographs were digitised, registered to a common base-image, and classified for bare ground, scrub and trees. A cadastral plan was also digitised, registered to the digital imagery and used to extract specific land-tenure parcels. The classified imagery was processed in an independent-classification change detection to identify change in land-cover between the dates of aerial photography.

The results demonstrated that digital image processing of black-and-white aerial photography could provide the quantitative and spatial land-cover information required for resource management in areas of alluvial gold mining. However, although the individual image classification accuracies exceeded 85%, error in the classifications generated areas of spurious change in the change detection imagery. Examination of subsequent change images revealed areas of land alternating between opposing change classes and indicated how a second, subsequent change image may be a useful tool to rapidly identify possible areas of spurious change.

An investigation of satellite imagery and digital image processing for management of indigenous forests compared a supervised classification of SPOT multispectral (XS) and Landsat Thematic Mapper (TM) imagery with an existing vegetation map. The images were classified with a maximum likelihood algorithm, applying vegetation classes derived from the map. The Landsat TM image achieved a higher overall classification accuracy (75%) compared to the SPOT XS (53%), indicating a superior information content for vegetation discrimination in the Landsat TM imagery. However neither image could achieve sufficient accuracy to be used for updating the existing map.

A second study of indigenous forestry applications investigated the use of integrated remote sensing and GIS analysis. A forest inventory comprising field-plots which recorded tree species and size-class information was interrogated within a GIS. The study illustrated

how GIS tools could be used to rapidly identify and map field-plots that contained trees suitable for harvesting in sustained-yield logging operations. This information is a prerequisite for any sustained-yield logging and would have been unfeasible to obtain without a GIS.

Two strategies were investigated for integrating the forest inventory with SPOT XS and Landsat TM imagery. The first approach applied a clustering procedure to generate the natural vegetative clusters within the forest inventory. A spectral signature for each plot was obtained by overlaying the plots on the digital imagery. A discriminant analysis was applied to determine whether the spectral information in the imagery could discriminate between the inventory clusters. The results revealed that this was not possible with overall classification accuracies of 39% and 48% for the SPOT XS and Landsat TM images respectively.

The second approach reversed the procedure and applied an unsupervised image classification to identify the spectral classes present in each image. The vegetative composition of each image class was investigated by examining the forest inventory plots within each class. The results demonstrated that the number of trees in the sub-canopy showed the most variation between classes, with minimal differences attributed to the species composition.

Analysis of the two approaches illustrated the difficulty of relating classifications derived from field survey and those from satellite imagery. While use of satellite imagery to map classes derived from field survey may result in disappointing results, an unsupervised approach provides a method to acquire an up-to-date, objective classification of the entire forest. The limitation is that the vegetation communities extracted from an unsupervised classification might well be different from those identified from analysis of forest inventory data and may not be of relevance to current resource management issues.

## ACKNOWLEDGEMENTS

I would like to express my gratitude to the following people who have assisted and encouraged me throughout this study:

My supervisors, Dr. Vince Neall and Mr Mike Tuohy of the Department of Soil Science, Massey University and Mr Peter Stephens of Manaaki Whenua - Landcare Research for their guidance throughout the course of this work. In particular I wish to thank Dr. Vince Neall for his encouragement during the latter stages of the thesis.

Mr Gernot Uhlig of Harihari, Westland for trusting me with the only copy of the Saltwater Forest inventory and for his helpful discussions and assistance during field visits to Saltwater Forest.

Mr Chris Pugsley, Mr Iain Gilbertson and staff of the Department of Conservation, Westland Conservancy for their financial support and for providing of much of the data used for the thesis.

The Earth Observation Satellite Company (EOSAT), for providing a Landsat TM image under their student data grant scheme.

Mr John Dymond of Manaaki Whenua - Landcare Research for his searching questions, thoughtful discussions and guidance.

My mother, extended family and friends, and in particular my wife Woody, for their continued moral support, patience, and tolerance of lost time together throughout the duration of this thesis.

## TABLE OF CONTENTS

ABSTRACT .....	ii
ACKNOWLEDGEMENTS .....	iv
TABLE OF CONTENTS .....	v
LIST OF FIGURES .....	vii
LIST OF TABLES .....	xii
<b>1: INTRODUCTION .....</b>	<b>1</b>
1.1 The Need for Resource Management .....	1
1.2 Information for Resource Management .....	2
1.3 Research Setting .....	3
1.4 Thesis Structure .....	4
<b>2: REMOTE SENSING AND GIS FOR RESOURCE MANAGEMENT .....</b>	<b>5</b>
2.1 Remote Sensing .....	5
2.11 Digital Image Processing .....	6
2.12 Image Calibration .....	12
2.13 Change Detection .....	13
2.14 Vegetation Indices .....	16
2.2 Remote Sensing for Resource Management .....	17
2.3 Geographic Information Systems .....	26
2.31 GIS Data Models .....	27
2.32 GIS Analysis .....	28
2.33 Error in GIS .....	29
2.4 GIS for Resource Management .....	32
2.5 Integrated Remote Sensing and GIS .....	34
2.6 Integrated Remote Sensing and GIS for Resource Management .....	36
<b>3: NATURAL RESOURCE MANAGEMENT IN WESTLAND .....</b>	<b>38</b>
3.1 Westland .....	38
3.2 Resource Management in Westland .....	40
3.3 Remote Sensing and GIS for Resource Management in Westland .....	46

<b>4: METHODOLOGY AND EXPERIMENTAL SITES</b> .....	49
4.1 Remote Sensing and GIS Methods to be Analysed .....	49
4.2 A PC Approach .....	50
4.3 Approaches to Methodology based on Computing Environment and Needs .....	51
4.4 Choice of Experimental Sites .....	52
<b>5: ALLUVIAL GOLD MINING</b> .....	53
5.1 Study Objective .....	53
5.2 Site Description .....	53
5.3 Methodology .....	55
5.4 Results and Discussion .....	63
5.5 Summary .....	81
<b>6: INDIGENOUS FORESTRY: SALTWATER ECOLOGICAL AREA</b> .....	83
6.1 Study Objective .....	83
6.2 Site Description .....	83
6.3 Methodology .....	86
6.4 Results and Discussion .....	91
6.5 Summary .....	101
<b>7: INDIGENOUS FORESTRY: SALTWATER FOREST</b> .....	103
7.1 Study Objective .....	103
7.2 Site Description .....	103
7.3 Methodology .....	105
7.4 Results and Discussion .....	112
7.5 Summary .....	128
<b>8: CONCLUSIONS &amp; RECOMMENDATIONS</b> .....	130
<b>REFERENCES</b> .....	136
<b>APPENDIX 1: The rms error for the image-to-image registration in the     Tuckers Flat alluvial gold mining study.</b> .....	162

## LIST OF FIGURES

### CHAPTER 2

- Figure 2.1:** The accumulation of error in a typical remote sensing through GIS data flow (From Lunetta *et al.*, 1991). . . . . 35

### CHAPTER 3

- Figure 3.1:** Westland - the West Coast of New Zealand's South Island . . . . . 39

### CHAPTER 5

- Figure 5.1:** A hydraulic excavator and rotary screening plant working at a mining claim within Tuckers Flat . . . . . 53
- Figure 5.2:** The location of Tuckers Flat - an area of alluvial gold mining. . . . . 54
- Figure 5.3:** The 1943 aerial photograph. The location of the Tuckers Flat area is indicated by the yellow box. . . . . 56
- Figure 5.4:** The 1976 aerial photograph. The location of the Tuckers Flat area is indicated by the yellow box . . . . . 56
- Figure 5.5:** The 1979 aerial photograph. The location of the Tuckers Flat area is indicated by the yellow box . . . . . 57
- Figure 5.6:** The 1986 aerial photograph. The location of the Tuckers Flat area is indicated by the yellow box. . . . . 57
- Figure 5.7:** The 1988 aerial photograph. The location of the Tuckers Flat area is indicated by the yellow box. . . . . 58
- Figure 5.8:** The 14 GCPs used in the registration superimposed on the 1976 image. Only a selection of GCPs were used to register a particular image. . . . . 58
- Figure 5.9:** The DoC cadastral plan used to obtain the land parcel boundaries for the Tuckers Flat area. The parcels used in this study were State Forest R.2106, State Forest R.2149, Rural Section 4668 and Gravel Reserve DP 1305. . . . . 59
- Figure 5.10:** The cadastral information derived from the DoC plan superimposed on the 1976 image. This image shows the misplacement of Tuckers Flat Road as drawn on the cadastral plan . . . . . 60
- Figure 5.11:** The cadastral information derived from the DoC plan superimposed on the 1976 image with the new Tuckers Flat Road that was digitised off the computer screen directly. . . . . 60
- Figure 5.12:** The 1976 image showing the roads (yellow) that were used to highlight errors in the image-to-image registration. . . . . 66

<b>Figure 5.13:</b> A test of the image-to-image registration accuracy - the 1943 image with roads from the 1976 base-image superimposed . . . . .	66
<b>Figure 5.14:</b> A test of the image-to-image registration accuracy - the 1979 image with roads from the 1976 base-image superimposed . . . . .	67
<b>Figure 5.15:</b> A test of the image-to-image registration accuracy - the 1986 image with roads from the 1976 base-image superimposed . . . . .	67
<b>Figure 5.16:</b> A test of the image-to-image registration accuracy - the 1988 image with roads from the 1976 base-image superimposed . . . . .	68
<b>Figure 5.17:</b> The classified image derived from the 1943 photograph showing the location of the bare land, tree and scrub classes. . . . .	72
<b>Figure 5.18:</b> The classified image derived from the 1976 photograph showing the location of the bare land, tree and scrub classes . . . . .	72
<b>Figure 5.19:</b> The classified image derived from the 1979 photograph showing the location of the bare land, tree and scrub classes . . . . .	73
<b>Figure 5.20:</b> The classified image derived from the 1986 photograph showing the location of the bare land, tree and scrub classes . . . . .	73
<b>Figure 5.21:</b> The classified image derived from the 1988 photograph showing the location of the bare land, tree and scrub classes . . . . .	74
<b>Figure 5.22:</b> An image showing the change in location of the bare ground, tree and scrub classes between the 1943 and 1976 classified images . . . . .	76
<b>Figure 5.23:</b> An image showing the change in location of the bare ground, tree and scrub classes between the 1976 and 1979 classified images . . . . .	77
<b>Figure 5.24:</b> An image showing the change in location of the bare ground, tree and scrub classes between the 1979 and 1986 classified images . . . . .	78
<b>Figure 5.25:</b> An image showing the change in location of the bare ground, tree and scrub classes between the 1986 and 1988 classified images . . . . .	79

## CHAPTER 6

<b>Figure 6.1:</b> A location map of Saltwater Ecological Area and Saltwater Forest . . . .	84
<b>Figure 6.2:</b> A road leading into Saltwater Ecological Area through Saltwater Forest. The road is runs right through the dense, predominantly rimu, forest on either side (photo L. J. Brown) . . . . .	85
<b>Figure 6.3:</b> One of the pakihi areas in Saltwater Ecological Area. Wire rush ( <i>Empodisma minus</i> ) is dominant in the foreground. The pakihi is bordered by forest where manuka ( <i>Leptospermum scoparium</i> ) is the dominant canopy species. This changes to rimu-dominated forest further from the pakihi (photo L. J. Brown) . . . . .	85

<b>Figure 6.4:</b> A band 3,2,1 (RGB) composite of the SPOT XS image. The location of Saltwater Forest and Saltwater Ecological Area is shown by the yellow rectangle .....	88
<b>Figure 6.5:</b> A band 3,2,1 (RGB) composite of the Landsat TM image. The location of Saltwater Forest and Saltwater Ecological Area is shown by the yellow rectangle .....	88
<b>Figure 6.6:</b> Norton and Leathwick's (1990) vegetation map of Saltwater Ecological Area. ....	89
<b>Figure 6.7:</b> The sample sites used to collect training data for classification of the SPOT XS image .....	90
<b>Figure 6.8:</b> The sample sites used to collect training data for classification of the Landsat TM (4,5,3 composite) image .....	90
<b>Figure 6.9:</b> Training data for classification of the SPOT XS image .....	92
<b>Figure 6.10:</b> The classified image showing the vegetation of Saltwater Ecological Area as derived from the SPOT XS image using the hybrid vegetation classes .....	95
<b>Figure 6.11:</b> Training data for classification of the Landsat TM image .....	96
<b>Figure 6.12:</b> The classified image of the Saltwater Ecological Area vegetation derived from the Landsat TM image. The image shows the 6 vegetation types based on the vegetation communities identified from an existing vegetation map (Figure 6.6) (Norton and Leathwick, 1990) .....	98

## CHAPTER 7

<b>Figure 7.1:</b> The centre of a hauler site used for selective logging of Saltwater Forest. The breaks in forest canopy indicate tracks where the logs were dragged across the forest floor before being loaded onto trucks (photo L. J. Brown). ....	104
<b>Figure 7.2:</b> Saltwater Forest in the SPOT XS (bands 3,3,1 (RGB) composite) image. This combination of bands provided the most visual discrimination within Saltwater Forest. The black line, digitised from a 1:25 000 forest map, indicates the extent of Saltwater Forest. Saltwater Ecological Area is to the west. ....	104
<b>Figure 7.3:</b> Saltwater Forest in the Landsat TM (bands 4,5,3 (RGB) composite) image. The contrast and brightness of the image have been stretched to reveal the spectral variation within Saltwater Forest. The black line, digitised from a 1:25 000 forest map, indicates the extent of Saltwater Forest. ....	105

**Figure 7.4:** A sample screen from the ArcView desktop mapping software. The 'theme' window (top left) indicates the layers of the database shown in the 'display' window (right). Only those layers with a tick in their check box are displayed. The 'display' window shows the distribution of the forest inventory plots and the roads of Saltwater Forest. The 'database' window (lower left) shows the result of clicking the mouse pointer on one of the plots. . . . . 107

**Figure 7.5:** A flow-chart indicating the method used to extract a pixel value for each plot from each image band . . . . . 110

**Figure 7.6:** A sample screen from the ArcView desktop mapping software. The 'display' window (right) shows the result of querying the forestry database to select all inventory plots that have rimu with a d.b.h greater than 1m present. The 'database' window (bottom left) shows the inventory database with all plots matching the search criteria coloured in magenta . . . . . 113

**Figure 7.7:** The rectified SPOT XS3 image with the roads digitised from the 1:25 000 forest map superimposed in yellow. . . . . 115

**Figure 7.8:** The rectified Landsat TM image with the roads digitised from the 1:25 000 forest map superimposed in yellow . . . . . 115

**Figure 7.9:** A box plot of the range of pixel values occurring within a plot as a percentage of the range across all plots. The colour of the box indicates the wavelength of light associated with the image band (yellow, cyan and magenta were chosen to represent the infrared bands). The line within each box is the mean. The boxes divide the data into quartiles . . . . . 117

**Figure 7.10:** The area occupied by the pixel value taken as representative for a particular plot. Total plot area is 2,000m<sup>2</sup>. The colour of the box indicates the wavelength of light associated with the image band (yellow, cyan and magenta were chosen to represent the infrared bands). The line within each box is the mean. The boxes divide the data into quartiles . . . . . 117

**Figure 7.11:** The range of pixel values observed within plots on the SPOT XS image. XS3 shows the greatest variation between plots. The colour of the box indicates the wavelength of light associated with the image band (yellow was chosen to represent the near-infrared band) . . . . . 118

**Figure 7.12:** The range of pixel values observed within plots for the Landsat TM image. TM4 (near-infrared) shows the greatest variation between plots. The colour of the box indicates the wavelength of light associated with the image band (yellow, cyan and magenta were chosen to represent the infrared bands) . . . . . 118

- Figure 7.13:** The Landsat TM NDVI values for each forest cluster. There is considerable overlap present in the range of NDVI recorded by the clusters ..... 122
- Figure 7.14:** Image classes derived from an unsupervised classification of the SPOT XS band 3 image. Three classes were chosen from visual inspection of the unclassified imagery. The roads of Saltwater Forest are superimposed ..... 123
- Figure 7.15:** The image classes derived from an unsupervised classification of the Landsat TM4,5,3 image. Four classes were chosen from visual inspection of the unclassified imagery. The roads of Saltwater Forest are superimposed ..... 124
- Figure 7.16:** The forest composition of the SPOT XS image classes. The number of trees refers to the median number of trees found in each grouping. The forest inventory axis shows the species ('mi' (miro), 'ri' (rimu), 'sp' (silver pine), 'ot' (others)) within each layer ('ab' (layer 1), ('cf' (layer 2), 'gtg' (layer 3)) e.g. 'riab' is the rimu in layer 1. 'Tot' refers to the total number of trees within a layer. Rimu was the only species present in layer 3. .... 126
- Figure 7.17:** The forest composition of the Landsat TM image classes. The number of trees refers to the median number of trees found in each grouping. The forest inventory axis shows the species ('mi' (miro), 'ri' (rimu), 'sp' (silver pine), 'ot' (others)) within each layer ('ab' (layer 1), ('cf' (layer 2), 'gtg' (layer 3)) e.g. 'riab' is the rimu in layer 1. 'Tot' refers to the total number of trees within a layer. Rimu was the only species present in layer 3. .... 127

## LIST OF TABLES

### CHAPTER 2

<b>Table 2.1:</b> The spectral resolution of the HRV (XS mode) and Landsat TM sensors .....	6
<b>Table 2.2:</b> A description of image enhancement techniques applied frequently in environmental remote sensing. ....	7
<b>Table 2.3:</b> A description of pixel interpolation algorithms .....	9
<b>Table 2.4:</b> A description of image classification algorithms applied frequently .....	11
<b>Table 2.5:</b> A comparison of raster and vector data models (adapted from Burrough, 1987) .....	28
<b>Table 2.6:</b> The total error at different map scales .....	31

### CHAPTER 5

<b>Table 5.1:</b> The black and white aerial photography used in the Tuckers Flat study .....	55
<b>Table 5.2:</b> The range of pixel values used to define each land-cover class. ....	62
<b>Table 5.3:</b> The relief displacement present in the aerial photographs over Tuckers Flat. ....	64
<b>Table 5.4:</b> The rms error between the 1943, 1979, 1986 and 1988 images and the 1976 base-image. ....	65
<b>Table 5.5:</b> The area (ha) classified in each land-cover class for each year .....	69
<b>Table 5.6:</b> A confusion matrix showing the number of pixels classified as each class for the 1943 classified image. The diagonal represents correct classifications. ....	74
<b>Table 5.7:</b> A confusion matrix showing the number of pixels classified as each class for the 1976 classified image. The diagonal represents correct classifications. ....	74
<b>Table 5.8:</b> A confusion matrix showing the number of pixels classified as each class for 1979 classified image. The diagonal represents correct classifications. ....	75
<b>Table 5.9:</b> A confusion matrix showing the number of pixels classified as each class for the 1986 classified image. The diagonal represents correct classifications. ....	75
<b>Table 5.10:</b> A confusion matrix showing the number of pixels classified as each class for the 1988 classified image. The diagonal represents correct classifications. ....	75

<b>Table 5.11:</b> An estimate of the overall change detection accuracy. The fourth column is the result of multiplying the two classification accuracy columns. ....	80
---	----

## CHAPTER 6

<b>Table 6.1:</b> The confusion matrix for the test classification of the SPOT XS image. The table shows the number of pixels classified from the image into each class as defined by the training data. The diagonal represents correct classifications. ....	93
<b>Table 6.2:</b> A summary of the results of the SPOT XS classification. The omission error shows for each reference class, the pixels that were classified as another class. The commission error shows the pixels classified incorrectly into a given image class ....	93
<b>Table 6.3:</b> The hybrid vegetation classes used for the SPOT XS classification. ....	94
<b>Table 6.4:</b> A confusion matrix for the SPOT XS classification applying the hybrid vegetation classes. The table shows the number of pixels classified from the image into each class as defined from the training data. The diagonal represents correct classifications ....	94
<b>Table 6.5:</b> A summary for the SPOT XS classification using the hybrid vegetation classes. The omission error shows for each reference class the pixels that were classified as another class. The commission error shows the pixels that were classified incorrectly into a given image class. ....	95
<b>Table 6.6:</b> A confusion matrix for the Landsat TM classification using the 6 vegetation classes. The table shows the number of pixels classified from the image into each class as defined by the training data. The diagonal represents correct classifications. ....	97
<b>Table 6.7:</b> A summary for the Landsat TM image classification using 6 vegetation classes. The omission error shows for each reference class, the pixels that were classified as another class. The commission error shows the pixels that were classified incorrectly into a given image class. ....	97

## CHAPTER 7

<b>Table 7.1:</b> A typical plot record from the Saltwater Forest inventory. ....	106
<b>Table 7.2:</b> The variables used in transformation of intensity values to apparent reflectance. $\alpha$ and $\beta$ are calibration coefficients and $E$ is the total irradiance for each band (from Price, 1987) ....	108
<b>Table 7.3:</b> The forest inventory clusters generated using the number of trees in each layer as the clustering variable ....	119

<b>Table 7.4:</b> The confusion matrix derived from classification of the SPOT XS imagery. The table shows the number of pixels classified from the image as each inventory cluster. The diagonal indicates correct classifications . . .	120
<b>Table 7.5:</b> A summary of the SPOT XS classification results. The omission error shows for each cluster the pixels that were classified as another cluster. The commission error shows the pixels that were classified incorrectly into a given cluster . . . . .	120
<b>Table 7.6:</b> The confusion matrix derived from classification of the Landsat TM imagery. The table shows the number of pixels classified from the image as each inventory cluster. The diagonal indicates correct classifications. . .	121
<b>Table 7.7:</b> A summary of the Landsat TM classification results. The omission error shows for each cluster the pixels that were classified as another cluster. The commission error shows the pixels that were classified incorrectly into a given cluster . . . . .	121
<b>Table 7.8:</b> The median, minimum and maximum number of trees occurring in each spectral class generated from the SPOT XS image. . . . .	126
<b>Table 7.9:</b> The median, minimum and maximum number of trees occurring in each spectral class generated from the Landsat TM image . . . . .	127

## 1: INTRODUCTION

### 1.1 The Need for Resource Management

Soil erosion, flooding, loss of indigenous forest and wetland, pests, weeds, water and air pollution, waste generation and disposal are problems that threaten the stability of the environment, affect our quality of life and impose economic costs on society. Effective management of our natural resources, and the side-effects resulting from their use, directly affects the environmental and the economic wellbeing of New Zealand. For future growth in the fishing, farming, horticulture, forestry, and mineral exploration industries, techniques are required to rapidly extract and manage information on the current resource level and to identify change in resource use. Ultimately management policies will need to be structured to ensure sustainable use of all natural resources.

A significant step toward an integrated approach to resource management in New Zealand began on October 1st, 1991 with the passing of the Resource Management Act 1991. This large and very complex piece of legislation provides the new legal framework for management of New Zealand's resources. The Act replaced much of the previous legislation dealing with resource consents and involved repealing more than 70 Acts, including the Town and Country Planning Act 1977 and the Water and Soil Conservation Act 1967.

The purpose of the Resource Management Act is to "*promote the sustainable management of ... natural and physical resources*" (section 5 (1)). All decision making and planning under the Act must aim to achieve this purpose.

Natural and physical resources are defined as

*"land, water, air, soil, minerals and energy, all forms of plants and animal (whether native to New Zealand or introduced) and all structures".*

Sustainable management is defined as

*"managing the use, development and production of natural and physical resources in a way, or at a rate which enables people and communities to provide for their social, economic and cultural well-being, and for their health and safety while:*

*a) Sustaining the potential of natural and physical resources (excluding minerals) to meet the reasonably foreseeable needs of future generations;*

*b) Safeguarding the life-supporting capacity of air, water, soil and ecosystems; and*

*c) Avoiding, remedying or mitigating any adverse effects of activities on the environment" (section 5 (2)).*

## **1.2 Information for Resource Management**

Effective resource management relies on the acquisition and application of accurate, up-to-date information. This is not always easy to achieve. Depending on the areal extent, vegetation, and relief of the area to be managed, collection of data via field survey is usually time consuming and expensive. Furthermore, the physical format of information can be difficult to manage and link with existing databases. The West Coast of the South Island (Westland), New Zealand, typifies these difficulties. The land-area is vast, including approximately 10% of New Zealand's landmass. The population is sparse, with about 1% of New Zealand's total. The relief ranges from flat terraces to rugged mountains. The indigenous vegetation can be extremely dense and difficult to navigate, and the conditions underfoot boggy or unstable. Westland is renowned in New Zealand for its super-humid climate.

The lack of resource information in Westland was noted in a study conducted by the Greymouth Harbour Board (1982), which, after evaluating the resources of the region stated:

*"The most significant thing emanating from the study was the lack of reliable, modern resource data for the West Coast region. It also became evident as the study progressed, that what data was available was largely uncoordinated."*

Also, Norton and Leathwick (1990), in study of the indigenous vegetation of Westland stated:

*"Although some studies have been published on the ecology of lowland south Westland vegetation, many areas and communities are still poorly known."*

Remote sensing and Geographic Information System (GIS) tools have been demonstrated worldwide as methods of acquiring and managing the information required for resource management (Trotter, 1991). Remote sensing via use of aerial photography is less expensive than diverting or employing staff for field survey. Difficult terrain is easily

imaged and interpreted. Aerial photographs can be digitised and enhanced using digital image processing techniques. For larger studies, satellite imagery has been shown to be less expensive than aerial photography in terms of \$/km<sup>2</sup> (Leckie, 1990(a)). In addition, satellite imagery can provide information in the near-middle, middle and thermal infrared regions of the electromagnetic spectrum, unattainable with aerial photography.

Data storage and manipulation are fundamental aspects of a GIS. In all manner of applications where large amounts of spatial data are required, by local authorities, land management agencies and forestry agencies, a GIS is becoming an integral part of the information strategy. Furthermore, technological developments have facilitated tools to incorporate remotely-sensed images directly into a GIS database, providing a promise of a rapid, low-cost update for spatial information.

### **1.3 Research Setting**

This thesis investigates the application of remote sensing and GIS for resource management in Westland. The thesis has one aim:

To investigate how remote sensing and GIS can provide and manage the information necessary for resource management in Westland.

Westland has a vast array of natural resources and it is not practical to investigate all resource management scenarios for a region of this size in a single thesis study. Instead, research has been directed to two areas of concern identified by the Department of Conservation (DoC), Westland Conservancy: alluvial gold mining and indigenous forest management. However, the techniques demonstrated could be adapted to a number of other resource management issues. The specific objectives are:

*i)* To investigate how land-cover change due to alluvial gold mining can be identified and mapped using digital image processing of aerial photography.

*ii)* To investigate how information beneficial to management of indigenous forests can be obtained through the use of GIS and digital image processing of satellite imagery.

This thesis concentrates specifically on the use of Personal Computer (PC) digital image processing and GIS applications to attain the above objectives. PCs are used because this

is the level of computing power that is likely to be readily available to resource managers stationed in Westland.

#### **1.4 Thesis Structure**

This thesis comprises eight chapters. Chapter 1 introduces and defines the scope of the thesis. The theory and application of remote sensing, digital image processing and GIS in resource management worldwide are reviewed in Chapter 2. Chapter 3 introduces the natural resources of Westland, how the resources are managed currently, and identifies potential applications of remote sensing and GIS. Chapter 4 discusses the remote sensing and GIS techniques appropriate for resource management in Westland. Reasons for, and introductions to the experimental sites are also included in Chapter 4.

Chapters 5, 6 and 7 contain individual case studies. Chapter 5 addresses the monitoring of land-cover change in alluvial gold mining operations. Chapter 6 investigates the application of satellite imagery and digital image processing in lowland indigenous forests. Chapter 7 applies an integrated remote sensing and GIS analysis for indigenous forestry operations. The final chapter presents the general conclusions developed from the research, how well the thesis aims were satisfied, and finally makes suggestions as to where future research should be directed.

*Insert page 5 after Chapter heading*

This thesis investigates the application of PC-based digital image processing and GIS software tools for resource management in Westland. The literature review is therefore biased towards application-based research which demonstrates the use of remote sensing and GIS for natural resource management. Accordingly the review is not concerned with the in-depth theoretical aspects of digital image processing and GIS processing algorithms. Such a review would be appropriate to a thesis concerned with development of new digital image processing algorithms and spatial modelling tools to integrate digital imagery and GIS datasets. It is not the intention of this thesis to develop or evaluate new techniques or algorithms. Rather, the literature review is structured as a commentary of the underlying principles of remote sensing and digital image processing followed by a review of applications. This is followed by a review of the principles and applications of GIS to natural resource management. The final section focuses on the integration of digital imagery and GIS for resource management purposes.

Other applications of remote sensing and GIS to resource management are discussed in addition to alluvial gold mining and indigenous forestry. These other applications are included to provide the reader with an overall indication of the resource management issues and possibilities for remote sensing, digital image processing and GIS in Westland. In particular, the review concentrates on the use of aerial photography for surface mining, and SPOT and Landsat TM satellite imagery for management of indigenous forests, because these were the sources of imagery available for this study. Other sources of imagery are discussed to provide an overview of the possible sources and applications of remotely sensed imagery. By necessity, this account discusses mainly overseas applications because there are comparatively few published works reporting digital image processing and GIS for alluvial gold mining and indigenous forest management in New Zealand.

## 2: REMOTE SENSING AND GIS FOR RESOURCE MANAGEMENT

### 2.1 Remote Sensing

In 1960, remote sensing referred to the observation and measurement of an object without physical contact (Fischer, 1975). Since that date however, remote sensing has developed an application-oriented definition, generally referring to "*the use of electromagnetic radiation sensors to record images of the environment which can be interpreted to yield useful information*" (Curran, 1986).

In the early 1960's, research in remote sensing concentrated on visual interpretation of panchromatic aerial photographic prints. Further development saw the use of a wide variety of photographic emulsions and parts of the electromagnetic spectrum; black and white infrared, colour positive and false-colour infrared films. In environmental science applications, panchromatic films have remained popular because they are geometrically stable and ideal for mapping purposes (once corrected for relief displacement), are cheaper to take, process, print and purchase, have a higher spatial accuracy than colour or false-colour infrared films (Wolf, 1974; Paine, 1981). They are also the most readily available form of aerial photograph. Colour films, because of the extra spectral information contained, have been used widely in mapping and monitoring, especially in the fields of land-cover identification (Gumstrump *et al.*, 1982) and forestry (Becking, 1959). False-colour infrared photography produces distinctive colour combinations with vigorous vegetation appearing bright red due to the vegetation's high reflectance of near-infrared radiation (Harris, 1987).

In 1972, non-photographic remote sensing advanced with the launch of the Earth Resources Technology Satellite (ERTS-1), which carried a multispectral scanner (MSS). This satellite was later renamed Landsat-1, forerunner of the 'current' Landsat-5 (Landsat-6 launched in 1993 failed to reach orbit). Of the present satellite sensors, those used most frequently for terrestrial environmental monitoring applications are the Thematic Mapper (TM) on board Landsat-4 and Landsat-5, the High Resolution Visible (HRV) Range Instrument on the SPOT (Système Probatoire de l'Observation de la Terre) satellites, and the Advanced Very High Resolution Radiometer (AVHRR) on the NOAA (National Oceanic and Atmospheric Administration) satellites. Other systems such as the Shuttle Imaging Radar (SIR-B), airborne imaging spectroscopy, airborne multispectral scanners and airborne video are also used to a lesser extent.

It is the superior spatial resolution of the HRV sensor, (10 metres for the panchromatic mode and 20 metres for the multispectral (XS) mode), and the Landsat TM, (28.5 metres for the non-thermal bands), in comparison to the AVHRR's 1.1km nadir resolution, which has promoted use of Landsat TM and HRV imagery in medium scale (1:50 000) investigations. However, use of the higher spatial resolution sensors reveals a paradox. Increasing the spatial resolution decreases the number of mixed pixels which increases classification accuracy, but it also increases spectral variability which can decrease classification accuracy (Irons *et al.*, 1984). For monitoring at regional and national scales AVHRR imagery is becoming more popular due to its low cost and frequency of revisit (each day).

The spectral resolution of the HRV (XS mode) and Landsat TM sensors is summarised in Table 2.1. The spectral regions of importance to land-cover and vegetation discrimination can be summarised as: absorption by plant tissue (TM1, TM2, TM3, XS1 and XS2, where TM1 refers to Landsat TM band 1, XS1 refers to SPOT XS band 1), soil and vegetation moisture content and cloud detection (TM5 and TM7), soil and vegetation separation (TM1 and XS1), water body delineation (TM4 and XS3) and vegetative vigour and plant biomass (TM4 and XS3) (Curran, 1986).

Table 2.1: The spectral resolution of the HRV (XS mode) and Landsat TM sensors

	HRV multispectral (XS)	Thematic Mapper (TM)
Spectral Resolution	XS1 0.50-0.59 $\mu\text{m}$ (green) XS2 0.61-0.69 $\mu\text{m}$ (red) XS3 0.79-0.89 $\mu\text{m}$ (near-infrared)	TM1 0.45-0.52 $\mu\text{m}$ (blue / green) TM2 0.52-0.60 $\mu\text{m}$ (green) TM3 0.63-0.69 $\mu\text{m}$ (red) TM4 0.76-0.90 $\mu\text{m}$ (near-infrared) TM5 1.55-1.75 $\mu\text{m}$ (near-mid infrared) TM6 10.4-12.5 $\mu\text{m}$ (thermal infrared) TM7 2.08-2.35 $\mu\text{m}$ (middle infrared)

## 2.11 Digital Image Processing

A digital image is created by a non-photographic sensor such as the Landsat TM or the SPOT HRV, or by digitising an aerial photograph. A digital image is comprised of a number of individual picture elements (pixels), each of which has an intensity value and position in two-dimensional image-space. The intensity value is determined by the amount of electromagnetic energy reflected from the Earth's surface or the photographic print. Many images are recorded in an 8-bit, or 256 level, intensity range.

Digital image processing is the manipulation and enhancement of digital images. The image is usually read into the computer one pixel at a time, then manipulated through an

equation or series of equations and the result stored as a new image. The image enhancement techniques applied commonly in environmental applications are described in Table 2.2.

Table 2.2: A description of image enhancement techniques applied frequently in environmental remote sensing.

Enhancement Technique	Categories	General Description	Features
Histogram Stretch	Linear	Expands the intensity value range to the full range available	Increases contrast although the same number of levels are assigned to all intensity values.
	Non-Linear <i>e.g.</i> histogram equalisation	Assigns equal numbers of pixels to all intensity levels available	Produces maximum contrast in the most dense region of the image histogram.
Band Ratio	Simple to complex formulae	One image band or combination of image bands divided by another one or combination of bands	May discriminate subtle spectral differences and partially compensate for the effects of relief. However, totally different materials may generate the same ratio.
Filtering	Smoothing (low pass)	Emphasises the low frequency components	Smooths image texture. Banding and speckle suppression.
	Sharpening (high pass)	Emphasises the high frequency components	Sharpens image texture.
	Edge Enhancement	Enhances local contrast whilst retaining the low frequency component	Enhances either the vertical or horizontal 'edges' in image where there is a marked change in intensity values.
Principal Component Analysis (PCA) and Canonical Component Analysis.		Statistical transformation of image bands to create new images that may contain much of the variance in the original image.	Principle component 1 (PC1) and PC2 may occupy over 99% of the variance in a TM scene thus reducing data volume. PC1 can be interpreted as greenness, PC2 as brightness.

**Rectification:** To overlay images that cover the same spatial location, the images must be registered with each other. To use imagery in conjunction with map data, the pixel grid must be rectified to the map's coordinate system. The registration or rectification process

involves five steps; (1) accurately defining Ground Control Points (GCP's), (2) creating transformation functions using the GCP's, (3) creating a new, geometrically correct grid, (4) transforming old pixel locations to the new positions and (5) interpolating a new intensity value for the new pixel locations (Curran, 1986; Lillesand and Kiefer, 1987; Richards, 1986). The disadvantage of registration and rectification is that the resampling may cause a loss of the image's spectral integrity.

Precise GCP determination is critical for an accurate transformation. The coordinates for all other points in the registered or rectified image are extrapolated from the GCP's, the more uniformly dispersed the GCP's, the more reliable the transformation. If imagery is being rectified to a base map, the resolution and projection of the map should match the imagery, *e.g.* 1:25 000 base maps are suitable for rectifying Landsat TM and SPOT imagery (Smith *et al.*, 1994).

Polynomial transformations are used to convert source file coordinates to their transformed positions. The polynomial's complexity (order) is related to the distortion in the imagery, the number of GCP's used, and the spread of GCP's. A first-order polynomial is a linear transformation. It is described as

$$\begin{aligned}x_o &= a_1 + a_2x_i + a_3y_i \\y_o &= b_1 + b_2x_i + b_3y_i\end{aligned}$$

where  $x_i$  and  $y_i$  are source coordinates,  $x_o$  and  $y_o$  are registered coordinates and  $a_1, a_2, a_3, b_1, b_2$  and  $b_3$  are the transformation coefficients. A linear transformation can change location in X and/or Y, scale in X and/or Y, skew in X and/or Y and rotation. They are used to project raw imagery to a planar map projection. Transformations of order 2 or higher are non-linear transformations used for distorted data and for converting latitude/longitude data to a planar projection. Severely distorted aerial photographs, scans of warped maps and radar imagery require a third order transformation (Smith *et al.*, 1994). The minimum number of GCP's required for a polynomial of a given order is given by

$$\frac{(t+1)(t+2)}{2}$$

where  $t$  = the order of the transformation. At least three GCP's are need for a first-order transformation, six for a second-order and ten for a third-order transformation.

The transformation accuracy is assessed commonly through the rms (root mean square) error, the distance between the reference coordinate and the curve of the transformation function. However, rms error does not truly reflect the locational accuracy of all pixels in an image, it considers only GCPs. Moreover, use of a higher-order polynomial than required can produce misleading information on the transformation accuracy, *e.g.* while a high-order polynomial may give a near-perfect fit of the GCP's, it may cause added distortion in the output imagery and increase actual error at the expense of minimising rms error. A better estimate of the transformation accuracy can be obtained through ground survey with differential GPS, although this is generally too costly to implement (Lunetta *et al.*, 1991). Another procedure applied commonly is to overlay other referenced datasets, *e.g.* roads, on a rectified image to check visually for errors. In practice, the acceptable accuracy is determined by the end use of the data, the type of data used, the accuracy with which GCP's can be identified and the accuracy of any ancillary data (Smith *et al.*, 1994).

New intensity values in the transformed grids are calculated by interpolation algorithms, the nearest neighbour, bilinear interpolation and cubic convolution being the most routinely used (Table 2.3). However, how these algorithms affect the radiometric integrity of the data and its spatial appearance still needs to be more fully understood (Lunetta *et al.*, 1991).

Table 2.3: A description of pixel interpolation algorithms.

Algorithm	Description	Advantages	Disadvantages
Nearest Neighbour	Transfers the intensity value of the nearest pixel	Computationally fastest and preserves original values	Can produce a disjointed image with an offset of half a pixel
Bilinear Interpolation	Transfers a weighted average of the 4 nearest pixels	Produces a smooth, geometrically correct image	Slower than nearest neighbour and new intensity values produced
Cubic Convolution	Transfers a weighted average of the 16 nearest pixels	Produces the smoothest image of all three algorithms	The slowest of the algorithms; new intensity values produced

**Classification:** The process of categorising pixels into classes is termed image classification. The attribute commonly used is the intensity value (spectral classification) however other properties such as texture can also be applied (Gastellu-Etchegorry and Ducros-Gambart, 1991). Classification can be divided into three approaches: (1) supervised techniques where the analyst selects training data for the classes based on prior knowledge, (2) unsupervised techniques where the spectrally separable classes are determined automatically by an algorithm and (3) hybrid approaches combining both supervised and

unsupervised methods. A supervised classification requires that features to be used as classes are able to be identified easily on the image whereas an unsupervised classification can be applied where the features are not easily identified.

In a supervised classification, the selection of representative training data has more effect on the classification accuracy than the pixel-assigning algorithm applied (Hixson *et al.*, 1980). The separability of classes defined by the training data can be investigated by: (1) viewing the results of a test classification superimposed over the original image, (2) ellipse diagrams and scatterplots within feature space, (3) a confusion matrix of a classification using the training data and (4) statistical methods such as divergence, transformed divergence, and the Jeffries-Matusita distance (Swain and Davis, 1978). Of these methods, overlaying a test classification on the original image and an examination of the confusion matrix provide easily interpretable measures and show precisely how the image will be classified. In comparison, graphical plots of training data distributions and statistical measures, whilst providing valuable information, are more difficult to interpret and do not show directly how the training data will affect the classification.

The most frequently applied classification algorithms are the Minimum Distance to Mean (MDM), parallelepiped and MAX (Table 2.4). However, there has been a variety of other classification procedures and algorithms developed. Examples from the literature include combining both supervised and unsupervised techniques (Chuvieco and Congalton, 1988), using auxiliary information such as digital terrain models (Hutchinson, 1982; Cibula and Nyquist, 1987; Janssen *et al.*, 1990; Senoo *et al.*, 1990; Baker *et al.*, 1991; Congalton *et al.*, 1993); applying expert systems (Skidmore, 1989) and neural nets (Ryan *et al.*, 1991, Liu and Xiao, 1991), using non-parametric classifiers (Skidmore and Turner, 1988; Dymond, 1993), and integrating both textural and contextual information (Gastellu-Etchegorry and Ducros-Gambart, 1991; Gonzalez-Alonso and Lopez-Soria, 1991). Although many of these advanced classifiers have been shown to perform better than the MAX, MDM and parallelepiped classifiers, in practice many of the new classifiers are still in an experimental phase. Furthermore, they often require large amounts of computing power, are integrated with expensive or 'in-house' software packages and are not available to the wider remote sensing community or resource managers.

Table 2.4: A description of image classification algorithms applied frequently.

Classifier	Description	Advantages	Disadvantages
Parallelepiped	Pixel assigned on the basis of the class range	Computationally simple and fast	Rectangular 'boxes' may not fit the distribution of training data
Minimum Distance to Means (MDM)	Pixel assigned to the class with mean vector closest to pixels	Computationally simple and fast	Insensitive to variance in classes
Maximum Likelihood (MAX)	Pixel assigned to class with the highest likelihood of membership	Evaluates both variance and covariance of class	Assumes training data is normally distributed. Computationally intense

The accuracy of the classification can be represented in a confusion matrix. The accuracy of each category is described with the inclusion (commission) error and exclusion (omission) error. A confusion matrix can be used as the basis for descriptive statistics including the total accuracy, the producer's accuracy or omission error (the probability of a reference pixel being correctly classified) and user's accuracy or commission error (the total number of correct pixels in a class divided by the total number of pixels classified as that class). Other statistics calculated are those based on binomial probabilities (Curran, 1986) and the Kappa coefficient (Hudson and Ramm, 1987).

Binomial probabilities account for chance effects but do not account for errors of commission or omission (Aronoff, 1985; Dicks and Lo, 1990). The Kappa coefficient considers off-diagonal elements of the error matrix, *i.e.* errors of commission or omission, and provides a measure of the proportion of the observed agreement that is contributed by chance (Congalton *et al.*, 1983; Hudson and Ramm, 1987). The Kappa (K) is computed as:

$$K = \frac{N \sum_{i=1}^r x_{ii} - \sum_{i=1}^r (x_{i+} x_{+i})}{N^2 - \sum_{i=1}^r (x_{i+} x_{+i})}$$

where  $r$  = number of rows in the error matrix,  $x_{ii}$  = number of observations in row  $i$  and column  $i$  ( $i$ 'th diagonal element),  $x_{i+}$  = marginal totals of row  $i$ ,  $x_{+i}$  = marginal totals of column  $i$  and  $N$  = total number of observations.

## 2.12 Image Calibration

Although encountered frequently in the scientific literature, the use of raw intensity values in remote sensing applications may lead to incorrect conclusions (Robinove, 1982). For example, when ratioing bands within a single scene, the resultant values can be quantitatively incorrect due to differences in individual band calibrations (Crippen, 1988). Raw pixel intensity values are related linearly to the intensity of radiance reflected from the target. Conversion to spectral radiance provides a basis for a more normalised comparison for single scene or with multi-date imagery. Duggin and Robinove (1990) state that "*calibration of digital data to radiance units is absolutely necessary prior to the use of multi-temporal or multi-image data sets*".

However, the parameter most frequently used by researchers is the apparent reflectance, the ratio of reflected radiant energy to incident radiant energy. Apparent reflectance reduces between-scene variability by normalisation of solar irradiance but it is still affected by atmospheric absorption and scattering. Whereas atmospheric absorption reduces reflectance, atmospheric scattering generally increases reflectance. The magnitude of these effects for a particular sensor are dependant on the atmospheric conditions and the geometrical relationships between the sun, target and sensor. The methods used for atmospheric correction can be grouped into three categories (Campbell, 1987): (1) atmospheric radiative transfer models, (2) algorithms that rely on features assumed to be spectrally inert, commonly called first order correction (Caselles and Lopez-Garcia, 1989; Hill and Sturm, 1991) and (3) techniques that use a relationship between the spectral bands as well as using spectrally inert features.

First order corrections are used widely because of their simplicity and computational efficiency. They are based on the premise that the visible part of the electromagnetic spectrum is influenced strongly by scattering while the longer wavelengths remain unaffected. Richardson (1982) studied data from seven separate investigations relating Landsat MSS imagery to ground-measured bidirectional reflectance and concluded that simple linear equations could be used to account for the relationship between apparent and ground reflectance. A linear relationship has also been applied successfully in other studies (Hall *et al.*, 1987; Mukai *et al.*, 1987; Cone, 1990). However, first-order corrections make basic assumptions that in most cases are never met. These assumptions are the uniformity of haze degradation over the whole scene, the additive character and wavelength dependency of scattering and a uniform effect on all pixel intensities (Campbell, 1987).

The atmospheric parameters required for models such as LOWTRAN-7 (Kneizys *et al.*, 1988) or the 5S code (Tanré *et al.*, 1990) can be obtained from a number of sources. Examples include the satellite image itself, *e.g.* measures of atmospheric path radiance over clear water bodies (Ahern *et al.*, 1988); from mathematical modelling, *e.g.* use of a relative power law and relative scattering model to predict haze values for each band (Chavez, 1989); from ground measurement, *e.g.* sky radiance values obtained from a model with input from a vertically pointed field radiometer (Richter, 1990); or from precomputed correction functions for different standard atmospheres (Tanré *et al.*, 1990). Because of the over simplicity of first-order corrections, and the difficulty in obtaining precise atmospheric data, models that use precomputed correction functions are becoming more widely used (Frouin and Gautier, 1987; Phulpin *et al.*, 1989; Derrien *et al.*, 1992, Singh, 1992).

### 2.13 Change Detection

The algorithms applied in change detection can be grouped into two categories (Singh, 1989): (1) the simultaneous analysis of multitemporal data, *e.g.* image differencing, image ratioing, image overlay, composite classification, data transformations and regression and (2) the comparison of independently produced classifications. All of the techniques require that the images are registered precisely. The input imagery may consist of raw intensity values, processed (reflectance), transformed (vegetation indices) or raster GIS layers (Lo and Shipman, 1990). However, the procedure used can significantly affect the result. Even in the same environment, different techniques may yield different results (Colwell and Weber, 1981).

Image differencing is the most widely applied change detection algorithm (Singh, 1989). With two dates of imagery, one is subtracted from the other resulting in an image where positive and negative values represent areas of change, and zero values indicate no change. The decision on where to place the threshold between the change and no-change pixels is critical. Thresholds are often defined using fractions of the standard deviation (Jensen, 1986), *i.e.* if a difference distribution is generated for each band, it approximates a gaussian distribution with pixels of no change concentrated around the mean and pixels of change in the tails. Applications of this technique include the detection of change from forest to non-forest using Landsat MSS5 and MSS7 (Park *et al.*, 1983), the delineation of forest canopy changes due to Gypsy Moth defoliation in Pennsylvania, USA (Nelson, 1983), the detection of areas infested with Pine Bark Beetle in Japan using Landsat MSS5 and MSS6 (Mukai *et al.*, 1987) and urban spread applying texture images derived from MSS5 (Jensen, 1985).

Image ratioing is another simple and quick method of change detection. A pixel that has not changed will have a ratio of one whereas areas of change will have values either higher or lower than one. Ratio transformations tend to remain invariant to shadows and seasonal sun elevation angle differences (Lillesand and Kiefer, 1987). The selection of change thresholds is usually empirically based but, because the ratioed imagery can have a non-gaussian bimodal distribution, ratio change detection with an empirical threshold can be statistically invalid (Riordan, 1981).

Image overlay can be used for visual change detection, with areas of change shown as unique colour combinations. This method is the most appropriate in natural environments where changes are relatively subtle, however it provides the analyst with little information regarding the nature of the change (Pilon *et al.*, 1988). Changes need to be interpreted within the context of the particular spectral band or bands being used (Milne, 1988). An example is the monitoring of forest clear-cut and regeneration areas on Vancouver Island, Canada (Werle *et al.*, 1986).

Composite classification combines images collected on nearly the same day of the year but in different years. Classes where change is occurring would be expected to have statistics significantly different from where there is no change. This method is also referred to as layered spectral or temporal change classification. While this technique requires only a single classification, it is a very complex one. It also demands prior knowledge of the inter-relationships between the classes and should only be used where the user is very familiar with the study area (Jensen, 1985). Since spectral and temporal features have equal status in the combined data, they cannot easily be separated in the pattern recognition process, and as a consequence class labelling is difficult (Schowengerdt, 1983).

Imagery from two dates can also be grouped statistically in  $2n$ -dimensional space, where  $n$  is the number of input bands per image. The two transformations applied most frequently are principal component analysis and tasseled cap transformation. The exact nature of the principal components derived from multitemporal imagery is difficult to ascertain without a thorough examination of the data and inspection of the combined images and as a consequence, this analysis should never be applied as a change detection method without a thorough understanding of the study area (Fung and LeDrew, 1987). A statistical transformation was applied successfully by Ingebritsen and Lyon (1985) for detecting and monitoring vegetation change around a large open-pit uranium mine in Washington and a wetland area in Nevada.

Mathematical models can be developed to describe the correlation between two images. The algorithm is applied to each pair of spectral bands and assumes that the pixel at time two is linearly related to the same pixel at time one. This implies that the spectral properties of the majority of pixels have not changed significantly during the time interval (Vogelmann, 1988). The size of the residuals is an indicator of where change has occurred. As before, definition of threshold values for the no-change pixels is critical. Vogelmann (1988) applied a regression developed from predetermined, ground-verified sites of no change to calculate coefficients for the remainder of the image.

The independent classification approach involves classifying each image separately followed by a pixel by pixel comparison of the classified images. By properly coding the classification, a complete matrix of change is obtained, the method can be made insensitive to changes in features that are of no interest and change classes can be identified easily. Radiometric normalisation between images is not required. However, in addition to registration errors, the accuracy of the change detection is dependent on the classification error in the component images. Errors in the original images are compounded so that the results may be unsatisfactory (Howarth and Wickware, 1981).

The methods applied to minimise error are maintaining rms error to less than 0.5 pixels (Jensen, 1985) and to ensure representative areas are chosen for training data. Other research has focused on modelling error propagation (Veregin, 1992; Chrisman, 1992), or concentrated on minimising the effect of error. For example, based on the assumption that change detection errors will occur at the boundaries of changed areas, Park *et al.*, (1983) deleted 50% of the border pixels from the area mapped as changed. Allum and Dreisinger (1986) assumed that errors were evident as single, isolated pixels showing change and applied a 3x3 modal filter to remove these pixels. An estimate of the error in the change image can be made by multiplying the individual classification accuracies (Stow *et al.*, 1980).

For resource managers, the advantage of an independent classification change detection is that change detection might not have been the focus of the initial analysis. Often the analysis will be directed toward assessing the extent of present land-cover classes. This information requires classification of the image. If a subsequent change detection analysis is required, it is simpler to use the previously classified imagery rather than analyse unclassified imagery with the associated difficulties of radiometric correction, determining appropriate change thresholds and identifying the nature of the change. Also, in investigations of mining areas, there is often a low number of land-cover classes, *e.g.* bare

ground and vegetated, which can lead to high classification accuracies in the individual images (Curran, 1986).

An example of applying an individual classification approach is mapping the distribution of land-cover classes near a mining complex in Ontario, Canada (Allum and Dreisinger, 1986). Four land-cover categories were differentiated; totally vegetated, partially vegetated, unvegetated and water. An analysis of the classification change matrix identified three change classes, vegetation increase, vegetation decrease and no change. Allum and Dreisinger concluded that for their purpose, independent classifications provided a cost-effective method of monitoring major vegetation changes. A similar approach was applied in the study of forest fire impacts in the Huron National Forest, Michigan (Jakubauskas, 1989). The independent classification method is also used in vector based GIS change detection where map layers are overlaid (Welch *et al.*, 1992; Pathan *et al.*, 1993).

## 2.14 Vegetation Indices

A strong positive relationship exists between reflectance in the near-infrared and vegetative cover (Tucker, 1978), with healthy green vegetation reflecting 40 to 50% of the incident near-infrared energy (0.7 to 1.1 $\mu\text{m}$ ). The relationship is inverted for the visible region, the chlorophyll in plants absorbing 80 to 90% of the incident energy in the range from 0.4 to 0.7 $\mu\text{m}$ . This range of the electromagnetic spectrum is referred to as photosynthetically active radiation (PAR). Stressed, senescent and dead vegetation reflects a greater amount of PAR and less near-infrared energy than healthy vegetation (Curran, 1980). Linear combinations or ratios of at least one PAR band and one near-infrared band, referred to as vegetation indices or VI, may yield a higher correlation with vegetation than either band alone (Coppin, 1991).

However, ratios are dependant upon the amount of inter-band correlation, the higher the correlation, the lower the information content of the ratio. Ratio based VI's also have the advantage of reducing the environmental effects such as relief and changes in irradiance (Lillesand and Kiefer, 1987), although the ratio does not completely compensate for these problems (Ashley and Rea, 1975). Studies have suggested that ratioing may improve the signal to noise ratio (Slater, 1980), however other research has indicated that ratioing may enhance random or coherent noise (Singh, 1989).

Sellers (1985) concluded that a simple near-infrared to red ratio is a near-linear indicator of minimum canopy resistance and photosynthetic activity, while being a poor predictor of leaf area index (LAI) and biomass. Ratios of Landsat TM bands that have proven useful

in studies of vegetation are: TM4/TM3 for identifying different vegetation types (Jensen, 1986), TM2/TM4 for subtle wetland information and water identification (Jensen, 1986), TM5/TM4 and TM7/TM4 for forest damage measurement (percent foliage loss) in spruce-fir stands (Vogelmann, 1988) and TM5/TM4 and TM4/TM3 for forest decline (Khorram *et al.*, 1990).

## 2.2 Remote Sensing for Resource Management

Remotely-sensed data has generated considerable enthusiasm in natural resource management. Aldrich (1975) stated "*Even low resolution data from the Landsat MSS scanner, if combined and enhanced, will disclose 80 to 90 percent of the changes of land-use between forest and non-forest categories. In addition, such data will show 25 to 90 percent of the less distinct disturbances in the forest, depending on the category*". However, digital image processing of aerial photography and satellite imagery has not been widely accepted into the user community (Townshend, 1992). Many projects have been limited to a one-off investigation or pilot study. One reason for this is because traditional land information systems rely on ground survey and manual interpretation of aerial photography, it can be difficult to integrate new methods into the existing system (Townshend, 1992). Nevertheless, the requirement for basic resource information and monitoring change has maintained an interest in remote sensing and digital image processing techniques.

The appropriate remotely-sensed imagery to use is determined by the detail required and the extent of the study area. Satellite imagery is preferred for monitoring change over large areas, but aerial photography is more appropriate for detailed monitoring of smaller areas. However, while aerial photography provides greater spatial detail, the photography may not be available and is more expensive (\$/km<sup>2</sup>) than satellite data (Leckie, 1990(a)). Environmental research applying digital image processing of satellite imagery and aerial photography can be subdivided into various resource management issues. These include water, wetland, wildlife habitats, land-cover mapping and monitoring, and forest inventory. From the global literature, the following applications are indicative of recent research. Surface mining and forest inventory are discussed in detail because of their direct relevance to Westland.

**Water:** Water management is a key aspect of resource management. Water shortage or excess can have disastrous consequences. Equally essential is the monitoring of water quality and pollution. Haefner and Pampaloni (1992) divide water research into three areas: (1) estimation of precipitation (rainfall, hail, snow), (2) determination of soil moisture, and

(3) assessment of surface runoff. The most promising form of remote sensing to water applications is microwave sensing because it offers all weather, day-night operation with sensitivity to soil moisture even if the terrain is covered by herbaceous crops (Haefner and Pampaloni, 1992). Radar imagery has also been successful because of its ability to penetrate cloud, *e.g.* the use of SIR-B data (Shuttle Imaging Radar-B) and Landsat MSS data to map flood damage in the 1984 monsoon in the Peoples Republic of Bangladesh (Imhoff *et al.*, 1987).

In addition to microwave and radar, a variety of other sensors have been used in water management applications: Landsat TM imagery for spectral bathymetry in Western Australia (Corner and Lodwick, 1992) and shallow water mapping (up to 20m depth) in the Philippines (Creasey and Fleming, 1992); airborne imaging spectroscopy for monitoring cyanobacteria levels in eutrophic waters (Dekker *et al.*, 1992); airborne multispectral scanners for determination of chlorophyll pigments in marine environments (Hick *et al.*, 1992); GEOSAT satellite data for studies of wave height, wind speed, backscatter and swell height for the Bay of Bengal and Arabian Sea (Natesan and Subramanian, 1992) and digitised aerial photography for detecting and mapping small areas of change on the Great Barrier Reef (Catt, 1992).

Water quality monitoring is an important issue confronting resource managers in New Zealand. Pollution from factory processing, agriculture or mining operations can result in serious environmental damage. A review of remote sensing of water quality parameters is given by Alföldi (1982). Selected applications from the literature include the use of Landsat TM for monitoring the quality of both inland waters (Lathrop, 1992) and ocean water (Forster *et al.*, 1993) and AVHRR data in monitoring suspended sediment in Hangzhou Bay (Jing and Yan, 1991). In surface mining applications, colour and colour-infrared aerial photography have been used to study stream quality degradation due to mining, and to locate point sources responsible for down-stream pollution (Kenny and McCauley, 1982). More recently, narrow band multi-spectral videography has been used to successfully map acidity and iron contamination in waters affected by surface coal mining (Repic *et al.*, 1991).

**Wetland:** Wetlands contain the most diverse terrestrial ecosystems. Consequently, the identification, characterisation and detection of change in wetlands is important to resource managers. Examples of the application of remote sensing to wetlands include: the use of black and white aerial photography to identify the change in the wetland of Lake Erie (Lyon and Greene, 1992); high resolution colour infrared (1:500) aerial photography, SPOT XS, Landsat MSS and TM to detect, map and monitor the spread of Para Grass

(*Brachiaria mutica*) in coastal tropical wetland in Queensland, Australia (Catt and Thirarongnarong, 1992); SPOT panchromatic data for measurement of seasonal and yearly changes in the levels of cattails (*Typha latifolia*) and waterlilies (*Nymphaea odorata*) in South Carolina (Jensen and Mackey, 1993); Landsat MSS and TM for mapping salt-affected land along coastal environments in India (Joshi and Sahai, 1993) and aircraft MSS data to assess the change occurring in swamp forest due to thermal pollution from a nuclear reactor (Jensen *et al.*, 1987).

**Wildlife:** Much of the research in the application of remote sensing to wildlife monitoring has a common thread - to produce a map showing the location of either wildlife habitats or their food sources. A supervised classification, extrapolating data from known habitats or food sources to the remainder of the image is the method commonly used (Hodgson *et al.*, 1987; Ormsby and Lunetta, 1987; Huber and Casler, 1990; Wood *et al.*, 1991; Aspinall and Veitch, 1993; Lauver and Whistler, 1993; Herr and Queen, 1993). As in all supervised classifications, the success of this approach depends totally on how well the training data spectral signatures define the habitat or food source. In New Zealand, 1:10 000 colour-infrared photography was used to map possum (*Trichosurus vulpecula*) browsing in indigenous forest canopies (Trotter, 1994). In other studies, an unsupervised classification or clustering has been successful in identifying broad habitat types (Belward *et al.*, 1990).

**Agriculture:** Although crop discrimination is achievable with Landsat MSS imagery (Ryerson *et al.*, 1979, 1981; Zhu *et al.*, 1983), studies with Landsat MSS have been hampered by the relatively large pixel size compared to the small irregular shape of the fields. This has restricted use Landsat MSS to identifying broad agricultural classes and to mapping large homogenous areas (Lal *et al.*, 1991; Williamson and Eldridge, 1993). However, Landsat TM, SPOT and aircraft-mounted scanner imagery has resolved the pixel versus field-size problem. Classification accuracies of 90% have been achieved monitoring vegetable crops in fields as small as two hectares in New York State, USA (Williams *et al.*, 1987). Landsat TM data has also been used for predicting wheat yield in Brazil (Rudorff and Bastista, 1991) and India (Das *et al.*, 1993), for determining the extent of agricultural land in India (Ram and Kolarkar, 1993; Jadhav *et al.*, 1993), for identifying corn and soybean residue in Miami (Zhuang *et al.*, 1991) and for mapping waterlogged cereal crops in Western Australia (Wallace *et al.*, 1993).

**Surface Mining:** Periodic survey of mining operations and disturbed land is required for planning, for assessing environmental damage, and for monitoring the success of reclamation. The most widely used remote sensing technique for surface mining applications has been visual interpretation of aerial photography. Avery and Berlin (1985)

state "Most surface and some underground mining operations exhibit characteristic patterns or signatures that permit their identification on medium scale (aerial) photography" and have described the characteristic patterns of sulphur, bauxite, lead, copper, coal, petroleum and gold mines. Examples of studies that have applied manual interpretation of aerial photography are the use of colour-infrared aerial photography to identify mined and reclaimed land in Indiana (Mroczynski and Weismiller, 1982) and high altitude colour-infrared photography to identify areas of land that had proven difficult to revegetate on coal mines in Kentucky (Halverson, 1988).

Much of the research applying digital image processing to surface mining applications has focused on surface coal mining. Black-and-white aerial photography has been shown to be able to discriminate areas of bare ground, vegetation and water (Carrel *et al.*, 1978), but classification error can be caused by confusion of dark shale materials with surrounding vegetation and water. Band ratios have been shown to be of use in reducing these errors (Anderson and Schubert, 1976). In one of the earlier studies using Landsat MSS data, land disruption due to strip coal mining was mapped in east-central Ohio (Chase and Pettyjohn, 1973). Their study concluded that strip mines could be delineated easily without the need for aerial photography or maps and that standing water within the mined areas could be identified through use of bands MSS6 and MSS7. Similar results were reported by Wier *et al.*, (1973). Another early study by Alexander *et al.* (1973) identified trenched areas, backfills, acid mine drainage, new stripping and partially vegetated zones.

The higher spatial and spectral resolution of the SPOT HRV and Landsat TM sensors promised the discrimination of more classes of vegetation and types of reclamation (Legg, 1986; Parks *et al.*, 1987). However, research demonstrated that it was not the higher spatial resolution of the TM data that improved classification accuracy, rather it was the improved spectral resolution (Williams *et al.*, 1984). Many studies have used a combination of Landsat TM, SPOT and Landsat MSS imagery, *e.g.* Legg (1986) monitored open cast coal mining and reclamation in the UK by superimposing co-registered multi-temporal Landsat MSS and TM images, and Parks *et al.* (1987) used simulated SPOT, MSS and Landsat TM imagery to map vegetation and reclamation in a coal mining region of Pennsylvania. Other studies have concentrated on deriving basic vegetation change information, *e.g.* Allum and Dreisinger (1986) identified only 3 change classes: areas of vegetation gain, vegetation loss and of no change.

Other applications of relevance to mining include the detection of underground mine fires (Ellyet and Fleming, 1974; Mukherjee *et al.*, 1991), water pollution assessment (Kenny and

McCauley, 1982; Repic *et al.*, 1991) and the detection of subsidence in underground mines (Elifrits and Barr, 1982; Mechaffie and Seargent, 1985).

**Forestry:** Since 1945, aerial photography has been applied routinely in forest stand mapping, species identification, drainage, landform mapping, insect and disease survey, erosion monitoring, fire and windthrow assessment, mensuration data, communication to managers and the public, navigation in the field and the preparation of forest-use plans (Hegg and Driscoll, 1982; Harding, 1982). However, although conventional field surveys and visual interpretation of aerial photography are a major source of forest information, they have been shown to be costly and time consuming when compared to satellite imagery, specifically Landsat MSS (Walsh *et al.*, 1982). In comparison with 1:50 000 colour aerial photography, geometrically corrected Landsat TM and SPOT data has been demonstrated to be approximately half the cost (\$/km<sup>2</sup>) of aerial photography (Leckie, 1990(a)).

In 1982, Landsat MSS was recognised as having the potential for monitoring change in areas disturbed by logging, windthrow, insect attack or fire, and in broad forest classification (Hegyí and Quenet, 1982). Landsat MSS imagery has been successful in isolating forest from non-forest and broad forest-type classifications, *e.g.* deciduous versus evergreen (Klankamsorn, 1978; Williams and Miller, 1979; Barringer *et al.*, 1980; Giddings *et al.*, 1980; Pelletier and Sader, 1985; Fearnside, 1986; Woodwell *et al.*, 1987; Pradham, 1990; Kushwaha, 1990). Landsat MSS imagery has also been applied in species-based classification. A range of podocarp and hardwood classes were discriminated in the King Country of New Zealand (Benning *et al.*, 1981), as were hardwood and softwood classes in the forests of Oklahoma (Walsh *et al.*, 1982) and coniferous woodland and Calluna (*Calluna vulgaris*) classes in the forests on the island of Islay, Scotland (Belward *et al.*, 1990). However, other research in the tropical rain forest of India (Singh, 1987) and Peru (Tuomisto *et al.*, 1994) could not achieve satisfactory species discrimination.

The success of Landsat MSS imagery in species discrimination may have been due partially to the lower spatial resolution minimising the effect of small variations in canopy composition and reducing the amount of mixed pixels (Irons *et al.*, 1984; Leckie, 1990(a)). Nevertheless, Landsat MSS imagery lacked the spatial resolution to be widely accepted into the forestry community - "*satellite data (Landsat MSS) have shown a good capability for mapping broad forest types, but are not appropriate for acquiring detailed information suitable for management inventories*" (Leckie, 1990(a)).

NOAA AVHRR (1.1km nadir resolution) imagery has also been used widely in regional and national-scale forestry applications. Investigations of tropical deforestation using AVHRR imagery have been conducted in the Amazon Basin (Tucker *et al.*, 1984; Nelson and Holben, 1986; Woodwell *et al.*, 1987; Townshend *et al.*, 1987; Nelson *et al.*, 1987; Malingreau and Tucker, 1988), the Mediterranean basin (Lopez *et al.*, 1991) and in Madagascar (Nelson and Horning, 1993). AVHRR band 3 (3.5 - 3.9  $\mu\text{m}$ ) has been shown to be of use in detecting forest clearance (Tucker *et al.*, 1984; Malingreau and Tucker, 1988; Malingreau *et al.*, 1989) and forest fire, which is often an indicator of recently deforested land (Malingreau *et al.*, 1985; Matson and Holben, 1987; Riggan *et al.*, 1993). Research has also used vegetation images generated from AVHRR data for detecting areas prone to fire (Lopez *et al.*, 1991).

Studies of forestry applications have also used imagery from less widely available sources such as radar (Drieman, 1987; Sader, 1987; Ford and Casey, 1988; Hess *et al.*, 1990; Leckie, 1990(b); Hussin *et al.*, 1991; Le Toan *et al.*, 1992; Dobson *et al.*, 1992; Ahern *et al.*, 1993(a); Nezry *et al.*, 1993), high spectral resolution sensors such as airborne imaging spectrometers, airborne thematic mapper and airborne spectrographic radiometers (Danson *et al.*, 1992) and use of radar in conjunction with Landsat TM (Lozano-Garcia and Hoffer, 1993). However, radar imagery is unavailable in many countries and interpretation is complicated due to lay-over and back-scatter effects. Although the availability will be addressed with development of the RADARSAT program, potential uses of RADARSAT in forestry will be identifying clearcuts rather than providing in-depth composition and volume information (Ahern *et al.*, 1993(b)). This level of discrimination is similar to results achieved from the SIR-B data (Nezry *et al.*, 1993), Landsat MSS and NOAA AVHRR imagery.

Landsat TM and SPOT imagery have been applied at medium scale mapping (1:50 000), mapping afforestation, forest parameters, canopy alterations and more subtle forest change. Their application can be divided into two areas: (1) the discrimination of forest from other land-cover and (2) intra-forest discrimination. Identification of forest from non-forest has been very successful, 98% accuracy was achieved in a mixture of upland and lowland, hardwood and softwood forest in Wisconsin (Lillesand *et al.*, 1985) and 96% accuracy in discriminating pines, low conifers, hardwoods, grassland, water and wetland in Michigan (Karteris, 1990). The spectral resolution of Landsat TM has enabled separation of forests and vegetation classes with similar spectral responses, *e.g.* remnants of tropical rainforest in Australia were discriminated from mangroves using combinations and ratios of all TM bands (Kay *et al.*, 1990).

Intra-forest discrimination is based commonly on species, age-class or other stand parameters. The digital image processing techniques applied can be divided into three approaches: (1) supervised classification, (2) statistical techniques correlating stand parameters with imagery intensity values and (3) techniques designed to estimate class proportions or composition.

Supervised classification is applied commonly for species discrimination. In the coniferous forests of Ontario, Canada, Landsat TM data was used successfully for inventory (general cover type discrimination, age of burns and clear cuts and the age, density and species) of black spruce (*Picea mariana*), jack pine (*Pinus banksiana*), brush, hardwood, burn, clearcut and water (Horler and Ahern, 1986). An average class accuracy of 86% was obtained discriminating scotch pine (*Pinus silvestris*), red pine (*Pinus resinosa*), jack pine (*Pinus banksiana*), and hardwoods (*Acer saccharum*, *Acer rubrum*, *Fagus grandifolia*) with Landsat TM data in Michigan (Karteris, 1990) and an 88.5% average class accuracy was obtained using Landsat TM imagery to discriminate softwood and hardwood classes in the forests of Northern Carolina (Brockhaus and Khorram, 1992). Supervised classifications have also been used to detect forest understorey for various degrees of canopy closure (Stenback and Congalton, 1990).

Studies have found band ratios and vegetation indices useful enhancements for supervised classifications, e.g. a TM 4/5 ratio successfully discriminated mature and old-growth forest in Oregon and Washington State (Fiorella and Ripple, 1993). Damage caused by disease, insect pests or pollution has been detected through Landsat TM Normalised Difference Vegetation Index (NDVI) imagery (Vogelmann, 1990) and SPOT XS NDVI imagery (Chamignon and Manière, 1990). Researchers have also incorporated ancillary data (slope, aspect, elevation, roads and hydrology) to improve supervised classifications (Congalton *et al.*, 1993).

Statistical correlation techniques have been applied frequently in the estimation of forest-stand parameters, e.g. basal area, LAI, age and class structure, percent canopy cover, tree height, tree diameter and volume. SPOT XS imagery has been correlated with mean percentage canopy cover, tree density, mean tree diameter at breast height, mean tree height and the sub-compartment age for a coniferous forest in England (Danson, 1987). With the exception of mean percentage canopy cover, the correlations with XS3 were significant at the 99% confidence level. The correlations with XS1 and XS2 were lower, this attributed to a low range of intensity values in these bands. In another study, SPOT XS and panchromatic imagery were used to determine density and canopy height in *Pinus nigra* stands in even-aged coniferous forests in Belgium (De Wulf *et al.*, 1990). Stand

density and average canopy height were predicted with 65% accuracy, the panchromatic imagery yielding better results than the multispectral imagery. Similar to Danson (1987), De Wulf *et al.*, (1990) found XS3 contained more information than XS1 or XS2.

A regression of simulated TM imagery against stand basal area and biomass of coniferous forest stands composed primarily of red fir (*Abies magnifica*) indicated TM2 and TM3 to be the best predictors of basal area (TM3  $r^2 = 0.29$ ) or biomass (TM2  $r^2 = 0.30$ ) (Franklin, 1986). Other studies have shown TM4 and TM5 to be the most useful bands, *e.g.* Spanner *et al.* (1990) found an inverse relationship between LAI and TM5 ( $r = -0.8$ , ( $r^2 = 0.64$ )) and a positive relationship between LAI and TM4 ( $r = 0.5$ , ( $r^2 = 0.25$ )) in coniferous stands with greater than 89% canopy closure. In *Pinus silvestris* and *Picea abies* forests in Sweden, TM5 had the highest correlation with the field measurements of volume ( $r = -0.79$  ( $r^2 = 0.61$ )) (Ardo, 1992). Ahern *et al.*, (1991) attained an  $r^2$  of 0.8 between volume and TM4 in the spruce-fir forests of New Brunswick, Canada.

Both SPOT XS and TM were used in a study of the coniferous forests of North Carolina (Brockhaus and Khorram, 1992). XS3 had the highest correlation with basal area ( $r = -0.41$  ( $r^2 = 0.17$ )) as did TM7 ( $r = -0.48$  ( $r^2 = 0.23$ )). In discriminating age classes, TM5 had the highest correlation ( $r = -0.62$  ( $r^2 = 0.38$ )) although the largest  $r^2$  obtained with SPOT XS3 was 0.05. More significant results were obtained in a douglas fir (*Pseudotsuga menziesii*) plantation forest in Oregon correlating XS3 ( $r = -0.89$  ( $r^2 = 0.79$ )) and TM4 ( $r = -0.83$  ( $r^2 = 0.68$ )) with forest volume (Ripple *et al.*, 1991).

The  $r^2$  values reported from the literature range from 0.05 to 0.8, *i.e.*, 5 to 80% of the variation in the stand parameter is explained by the imagery. The results have depended largely on the parameter investigated and the imagery used. There is also variation in whether relationships have a positive or negative  $r$  value, making it difficult to generalise about the nature of any parameter's relationship without specific reference to the canopy architecture, the parameter and the imagery (Oza *et al.*, 1989). However, all results must be reviewed with respect to their potential application. If an even-aged, monoclonal production forest is being investigated where detailed harvest volume estimates are required, a high correlation ( $r^2 > 0.8$ ) will be necessary. In comparison, resource managers working in tropical or indigenous forestry, where there is little recorded information and movement through the forest is difficult, may tolerate a lower  $r^2$ .

The drawback of supervised classification and statistical regression techniques is that they rely on the canopy cover or stand parameter being sufficiently dense or homogenous to fill a pixel. It is important to note that the reflectance displayed by any pixel, especially those

in natural communities such as indigenous forestry, is a combination of the relative spectral combinations from all components of the ground cover. This has prompted development and use of techniques designed to estimate class proportions or botanical composition, rather than a single class label.

Linear mixture modelling (Settle and Drake, 1993) assumes that each ground cover class within a pixel contributes to the signal an amount characteristic of the ground cover and proportional to the area occupied by the ground cover. The technique relies on pixels of 'pure' ground cover for each class being identified and used to define 'endmember' spectral signatures. The position of any mixed cover pixel along this continuum indicates the percentage cover of each class. Linear mixture modelling has been applied to identify class proportions of AVHRR pixels using a higher spatial resolution sensor, *e.g.* Landsat TM. Examples from the literature using AVHRR imagery include the estimation of tropical forest cover in Ghana and Rondonia (Cross *et al.*, 1991); crop coverage in Greece (Quarmby *et al.*, 1992) and land cover (bare soil and vegetation classes) proportions in Brazil (Holben and Shimabukuro, 1993). The disadvantage of the linear mixing model is the isolation of the 'pure' pixels. In indigenous and tropical forestry, 'pure' pixels of the desired classes may not be easily identified or exist.

A second approach is the use of an additional data source to calibrate pixels in terms of ground cover parameters. Pech *et al.*, (1986) determined by field survey the percentage vegetation cover over sample plots in semi-arid rangelands of southern Australia. Statistical models were developed relating percentage vegetation cover to pixel radiance and used to generate the proportions of vegetation cover for a larger region. A similar approach was applied using Landsat TM imagery as an additional data source to determine the amount of forest cover in corresponding AVHRR pixels (Iverson *et al.*, 1989; Zhu and Evans, 1994).

Other studies have applied multivariate discriminant analysis (Afifi and Clark, 1984) to separate vegetation communities comprised of mixtures of species (Pando *et al.*, 1992) or have analysed the relationship between spectral and land-cover classes derived independently of each other. Price *et al.*, (1992) used an independent classification approach with Landsat TM imagery to monitor shrub dieback in the Great Basin of the western USA and Lewis (1994) mapped mixed land-cover classes in western Australia using spectral classes derived from Landsat MSS imagery and clustering of ground samples. Workers have also suggested that natural communities may not be amenable to discrete classification at all and have applied a 'fuzzy sets' approach to discriminate end points of vegetation continua (Foody, 1992).

### 2.3 Geographic Information Systems

There are many definitions of a 'Geographic Information System' (GIS). Maguire (1991) compiled the definitions of 11 authors. The most complete is that of Cowen (1988), defining four basic approaches: (1) the process or function oriented, (2) the application orientated, (3) the toolbox and (4) the database.

The process-oriented approach emphasises the information handling capabilities of a GIS *e.g.* "*an automated set of functions that provides professionals with advanced capabilities for the storage, retrieval, manipulation and display of geographically referenced data*" (Ozemoy *et al.*, 1981).

The application approach divides information systems on the type of data processed *e.g.* financial versus geographical. Examples are "*An information system that is designed to work with data referenced by spatial or geographic coordinates*" (Star and Estes, 1990), and "*an information technology which stores, analyzes and displays both spatial and non-spatial data*" (Parker, 1988), as well as the definition of Ozemoy *et al.*, (1981) mentioned previously.

The toolbox approach emphasises the generic aspects of GIS functions *e.g.* "*a powerful set of tools for collecting, storing, retrieving at will, transforming and displaying data from the real world*" (Burrough, 1987).

The database approach is widely used because the data storage and data manipulation capabilities of a GIS, *e.g.* "*a database system in which most of the data are spatially indexed, and upon which a set of procedures operate in order to answer queries about spatial entities in the database*" (Smith *et al.*, 1987).

In addition, GIS have been married with decision support systems *e.g.* "*a decision support system involving the integration of spatially referenced data in a problem solving environment*" (Cowen, 1988).

The development of GIS has been well documented (Marble and Peuquet, 1983; Parent and Church, 1987; Star and Estes, 1990; Coppock and Rhind, 1991). There has been debate as to whether GIS developed with progress in computing in the late 20th century, *i.e.* a tool, or whether GIS originated in mid-eighteenth century with the production of accurate base maps, manual area measurement and manual overlay techniques, *i.e.* a technique. The Collins English Dictionary (Knight, 1993) defines a 'system' as "*any assembly of*

*electronic components with interdependent functions", i.e a tool, and as "a method or complex of methods", i.e a technique. The debate is summarised effectively by Coppock and Rhind (1991); "the history of GIS is inevitably a consequence of the authors' accidental exposure to early developments and their own set of value-judgements; different views certainly exist."*

### **2.31 GIS Data Models**

Two models are used for storing GIS data: (1) the vector, historically associated with cartography, and (2) the grid cell or raster, superior for spatial modelling applications and integration of digital imagery. The vector model is based on the cartographic units of the point, line and polygon. It has two major advantages: (1) vectors operate in continuous space allowing accurate representation of length and area and (2) vector models can be structured with topology which defines spatial relationships, *i.e.* connectivity, contiguity and area definition, and allows the identification and analysis of island and neighbouring polygons (Burrough, 1987).

The raster model has the same as structure as a digital image. In GIS applications, this structure can create problems of locational precision, *i.e.*, the location of a point or a line is known only to be inside the boundaries of the cell. Although this can be resolved through the use of a small cell size in relation to the mapping scale, use of a small cell size can create large files. Compression algorithms can be used to compress large files, the degree of compression depending on the heterogeneity of the data. Many modern GIS can work with compressed data or compress and decompress data as required.

The advantages and disadvantages of the vector and raster models (Table 2.5) have been discussed in many papers and texts (Peuquet, 1984; Burrough, 1987; Maffini, 1987). However, with technological advances, the vector vs raster debate has dwindled. Many of the GIS available in 1995 can process both vector and raster data or include the appropriate conversion routines. Nevertheless Maffini (1987) suggested that the advantages and disadvantages of the respective models means that neither structure is likely to completely disappear in the foreseeable future. This is still applicable in 1995.

Table 2.5: A comparison of raster and vector data models, (adapted from Burrough, 1987)

<b>VECTOR</b>	
<b>Advantages</b>	<ul style="list-style-type: none"> <li>Good representation of phenomenological data structure</li> <li>Compact data structure</li> <li>Topology with network analysis possible</li> <li>Accurate, aesthetically pleasing graphics</li> <li>Retrieval, updating and generalisation of graphics and attributes possible</li> </ul>
<b>Disadvantages</b>	<ul style="list-style-type: none"> <li>Complex data structure</li> <li>Polygon overlay problems can be difficult</li> <li>Simulation exercises are difficult</li> <li>Display and output technologies are usually expensive</li> <li>Analysis and filtering within polygons is impossible</li> </ul>
<b>RASTER</b>	
<b>Advantages</b>	<ul style="list-style-type: none"> <li>Simple data structure</li> <li>Overlay and combination with remote sensing data is simple</li> <li>Variety of spatial analysis and simulation problems handled easily</li> <li>Technology is inexpensive</li> </ul>
<b>Disadvantages</b>	<ul style="list-style-type: none"> <li>Large file sizes</li> <li>Recognisable shapes can be lost, with a loss in information</li> <li>Graphic output are often not aesthetically pleasing</li> <li>Network linkage analysis hard to establish</li> </ul>

### 2.32 GIS Analysis

The capability to analyse spatial data separates a GIS from computer aided design (CAD) and computer aided mapping (CAM) software. Spatial analyses such as overlay, buffering, modelling and network analysis are normally included as part of standard GIS software.

Overlay analysis combines two data layers to create a new layer and is reliant on the boolean algebra operators AND, OR, XOR and NOT. The overlay procedure can be divided into two general categories, point operations and neighbourhood operations. Point operations are equivalent to image processing techniques. Neighbourhood or region operations relate a point to its immediate neighbours or to a larger region and involve topology.

Buffering is an extension of overlay analysis creating a boundary of known width around a feature. A point buffer may be a zone around a waste disposal site or the

area around a nesting site of an endangered species. A linear or polygon buffer may be used to delineate an area around a stream where logging is prohibited.

Modelling operations involve simulating outcomes using a combination of spatial and non-spatial information. Data layers are combined with weightings prioritising important factors.

Network analysis identifies the path of an object. It is of use in hydrological, transport and other disciplines which study flow. Possible applications of network analysis are identification of point-source pollution in streams and rivers, and modelling of erosion effects in catchments.

Advanced analyses, *e.g.* spatial autocorrelation modelling, spatial econometric modelling, spatial general linear modelling and spatial interaction modelling (Bailey, 1994) may require the integration of GIS and specific analytical software. However, development of statistical relationships in a GIS requires adherence to the basic assumptions associated with the statistical model, *e.g.* linear regression assumes that sample statistics are independent and errors are constant over the measurement space (Montgomery and Peck, 1982). These assumptions are often violated in earth science data due to spatial autocorrelation in the independent variables.

Spatial autocorrelation occurs when the presence, absence or degree of a certain characteristic affects the presence, absence or degree of the same characteristic in neighbouring units (Cliff and Ord, 1973). Positive spatial autocorrelation (non-random clustering) causes variance to be underestimated whereas negative autocorrelation (non-random dispersion) increases variance (Lowell, 1991). Work by Congalton (1988) on Landsat MSS data from three areas of varying spatial diversity *i.e.* agricultural, rangelands and forest sites, indicated there may be a positive influence as far as 30 pixels away.

### **2.33 Error in GIS**

The error in GIS data may be divided into three groups: (1) user error (data age, scale, coverage and relevance), (2) measurement error (instrument error, field error and natural variation) and (3) processing error (precision, interpolation, generalisation, conversion, digitisation) (Burrough, 1987). Errors may also be grouped as to whether they arise from primary methods of data collection (geodesy, photogrammetry and surveying) or from secondary methods (data collected from existing documents) (Thapa and Bossler, 1992). The error arising from primary methods of data collection are identical to those described

by Burrough (1987) as measurement error. Secondary methods of data collection include all error contained in the primary methods and include the following errors (Thapa and Bossler, 1992).

Plotting control: The error ranges from 0.17mm to 0.32mm RMS for coordinatographs attached to photogrammetric plotters. Error is negligible if using GPS (Thapa and Bossler, 1992).

Compilation: The error introduced is  $e = ke'$ . (Maling, 1989). The value of  $e$  ranges between 0.30mm and 0.32mm where  $e'$  is the error in the detail survey. The value of  $e'$  ranges from 5m to 7.5m if the map is collected by a photogrammetric method at 1:25 000. Normally, point features can be compiled more accurately than line features.

Drawing: The error is quoted (Maling, 1989) as ranging from 0.06mm to 0.18mm.

Map generalisation: This is difficult to quantify as it is dependant on the type of feature and its complexity. Error in feature displacement (features cannot be displayed in their proper position without overlapping) is dependant on the mapping scale and the proximity of the features (Thapa and Bossler, 1992).

Map reproduction: The error in map reproduction varies between 0.1mm and 0.2mm (Maling, 1989).

Colour registration: The error for printing plate alignment varies between 0.17mm and 0.30mm (Maling, 1989).

Deformation of material: The error induced during printing (1.25 percent in length, 2.5 percent in width) and by humidity variation (1.6 percent at room temperature) (Maling, 1989).

The wrong use of scale: For example, when using the Lambert conformal projection, the principal scale (scale quoted in a map) is true only along standard parallels. Therefore the scale is too small between the parallels and too large outside the parallels. This requires the use of a scale factor correlation when digitising a map (Thapa and Bossler, 1992).

Uncertainty in feature definition: This is related to natural features that do not have a clear-cut boundary *e.g.* a river bed, therefore introducing uncertainty into the feature's true position.

Feature exaggeration: The error may be substantial depending on the scale and the type of feature involved *e.g.* a road marked as an 0.5mm line on a 1:250 000 scale map covers 125m on the ground.

Digitising or scanning: The error depends on the width of the feature, the skill of the operator, the feature's complexity, the digitiser resolution and the density of features. Petrie (1990) quotes the digitisation error as 0.25mm. Line following techniques and scanners may introduce fewer planimetric errors, but errors in feature tagging may be higher in the case of scanning (Thapa and Bossler, 1992).

It is difficult to assess total error as the functional relationships between individual errors are unknown. Assuming that a linear relationship exists between total error and individual error, the total error may be calculated using the law of error propagation (Drummond, 1990). This results in a worst case scenario of 0.81mm and a best case scenario of 0.5mm at each map scale (Table 2.6). In addition there may also be factual error and error due to computer precision. Factual error can be attributed to mislabelling errors, misclassification errors and feature-coding errors. Factual information is either right or wrong, and is able to be verified by checking field notes and other compilation material. Precision error is introduced through data manipulation, *e.g.* many computers use 8 or 16 decimal digits of precision for each coordinate. On the Earth, 8 decimal digits resolves positions to the nearest 10cm, which is far more precise than typical global data.

Table 2.6: The total error at different map scales

Map scale	Worst Case Error (m)	Best Case Error (m)
1:10 000	8.1	5.0
1:25 000	20.3	12.5
1:50 000	40.5	25.0
1:250 000	202.5	125.0

If data is manipulated or modelled, an alternative to calculating the amount of error is to calculate the effect error has on the result. This is termed sensitivity analysis, *i.e.*, how sensitive are results to variation in input data. Whereas many image processing and quantitative GIS error analyses compare results with an independent measure of truth, sensitivity analysis compares the initial result with alternative results derived from data perturbed in a controlled, systematic way (Lodwick *et al.*, 1990). Recent examples of

sensitivity analysis include testing the effects of classification error (Lyon *et al.*, 1987), grid cell size (Lyon *et al.*, 1987; Turner *et al.*, 1989), the number of classes (Lyon *et al.*, 1987), subjective weighting factors (Heinen and Lyon, 1989) and uncertainty in input data (Stoms *et al.*, 1992).

Formal error analysis has not been readily accepted into the GIS community. Openshaw (1992) listed six reasons for this: (1) current use of spatial data is a continuation of the past even though we are using more precise tools than before, (2) there is a lack of techniques for measuring uncertainty in spatial data and outputs, (3) the seriousness of the problem is unknown, (4) there is a lack of consensus on data quality and accuracy, (5) there is a lack of established rules for dealing with error and (6) there is a lack of established methods for modelling error. Although the lack of established techniques and procedures has been addressed (Goodchild, 1992), the other reasons listed by Openshaw (1992) are still relevant in 1995.

## 2.4 GIS for Resource Management

The potential applications of a GIS in resource management have been quickly realised. Issues of "ARC News", a newsletter distributed by ESRI (Environmental Systems Research Institute) to all users of the ARC/INFO GIS package, features numerous applications of a GIS. A selection of these are: petrochemical exploration (recording well locations, lease and seismic data) in Venezuela, traffic management systems and earthquake and fire recovery in California, and military battle simulation, toxic chemical spills in Florida (ESRI, 1994); forest fire response in California and biodiversity and conservation mapping in Idaho, (ESRI, 1993); and world-wide deforestation, marine oil spills in Alaska, municipal wastewater and sewer management in Hawaii, water resource management in Oman, coal mine management in Missouri, cadastral data management in Slovenia and agricultural crop feasibility studies in Peru (ESRI, 1992).

Applications have also been reported in scientific GIS journals. In this section, work that focuses on the integration of remotely-sensed imagery is excluded. These applications will be discussed in a following section dedicated to the integration of remote sensing and GIS.

**Water:** A selection of GIS applications for water resource management include: modelling point-source pollution, soils and geological data to assess groundwater contamination from fuel storage tanks at Vandenberg Air Force Base, USA (Leipnik, 1993); using land-use and water quality models to calculate pollutant loadings in sewer outfalls in Wisconsin (Kim and Ventura, 1993); creating response plans for areas of ecological damage following a

potential marine oil spill in Florida (Friel *et al.*, 1993); targeting areas requiring action in the Chesapeake Bay Program by creating an "agricultural non-point pollution potential" map from watersheds, slope, soils, land use and animal loading layers (Mertz, 1993) and modelling the spread of pollutants in the Gulf of Mexico (Rifai *et al.*, 1993).

**Wildlife:** A GIS provides an efficient means for describing habitats and modelling species and habitat distribution. Investigations have included the analysis of grizzly bear sightings in the Northern Cascades (Agee *et al.*, 1989); modelling cattail and water lily spread on water reservoirs in Southern Carolina (Jensen *et al.*, 1992) and integrating data on manatee distribution, mortality and migration in Florida (Ward and Weigle, 1993). In other studies, habitat modelling has been extended to produce information of biological diversity in the ecosystem (Davis *et al.*, 1990; Stoms, 1992).

**Land-cover:** Applications that map land-cover but that exclude remotely-sensed imagery are uncommon. GIS specific applications have focused usually on managing existing information, *e.g.* development of an 'Environmental Impact Statement' for a gold mining company in Nevada (Rodbell, 1993), evaluating coal reserves and managing leases and ownership arrangements in West Virginia and Kentucky (Wilson, 1993) and investigating differing land-uses in North Carolina (Whitley *et al.*, 1993). Similar to the research in remote sensing, the analysis of land-use change has been a major application of GIS. In many cases, where raster GIS is used, there is no difference between the techniques used for change detection via GIS and those applied in image processing. Examples from the literature include the analysis of vegetation change caused by forest fires (Jakubauskas, 1989), land-use change in Nepal (Jampoler and Haack, 1989) and the analysis of urban land-use change in Hong Kong (Lo and Shipman, 1990).

**Forestry:** The production and revision of forest inventory maps are major management tasks that can be simplified with a GIS. Additionally, a GIS can be used to perform planning and modelling analyses. Applications reported in the literature have seen the integration of soils and topographic information to assess site-index (Price, 1986); the design and positioning of forest roads (Martin, 1985; Susilawati and Weir, 1990); and the management of timber harvesting operations (Dunningham and Thompson, 1989). Modelling operations include evaluating the outcome of differing management scenarios on visual quality, landscape ecology, wind management and timber production (Johnston, 1987); the management of forest fire response (Gronland *et al.*, 1994); the effects of widespread logging on wildlife habitats (Chang *et al.*, 1994) and the evaluation of forest pest and disease management strategies (Morse, 1986; Rowland, 1986; White, 1986; Jordan and Vietinghoff, 1987).

## 2.5 Integrated Remote Sensing and GIS

The integration of remote sensing and GIS has received widespread enthusiasm. It has been referred to as "*an unrealized potential*" (Shelton and Estes, 1981) and "*a necessary evolution*" (Ehlers *et al.*, 1989). Barker (1988) referred to remote sensing as the "*unheralded component of Geographic Information Systems*" and Goodenough (1986) stated that "*The integration of remote sensing and geographic information systems is essential for effective resource management*". In addition, the integration of remote sensing and GIS is one of the 12 major GIS research initiatives proposed by the National Centre of Geographic Information and Analysis (NCGIA) (Star *et al.*, 1991). The reason for the enthusiasm is because although GIS was becoming rapidly accepted as a resource management tool, the cost of acquiring and interpreting data, was and still is, the major impediment (Blakeman, 1987; Barker, 1988; Congalton and Green, 1992). Remote sensing has potential to lower the cost of acquiring the current, comprehensive data necessary for a GIS.

In this thesis, a distinction is drawn between the process of integrating remotely-sensed imagery into a GIS and the development of "integrated remote sensing and GIS" (IGIS). IGIS facilitates more than basic data transfer between separate systems or screen overlay functions (Ehlers, 1990). It must address issues of handling large spatial databases, designing of user interfaces, data processing and computing environments, in addition to resolving the underlying differences in vector and raster data (Ehlers *et al.*, 1991). An example of IGIS was presented by Piwowar and LeDrew (1990), who proposed the idea of a multiformat GIS that did not require conversion of all data to a common format upon entry, rather the system would convert formats when required. However, such systems are not generally available, and the development of the hardware and software requirements for IGIS is the realm of programmers, not resource managers.

Although the process of integrating remotely-sensed data with a GIS can be thought of as a simple data conversion exercise, it is by no means trivial. There are the technical aspects of raster to vector conversion, and the theoretical aspects of integrating data which are representations of the world at two different levels of generalisation (Ehlers *et al.*, 1989). Furthermore, aerial photographs can have considerable errors due to distortion and displacement which can render the data useless in GIS applications (Trotter, 1994). The potential sources of error which can affect a remote sensing-GIS data flow are illustrated in Figure 2.1. In theory, the error entering the system at each step can be estimated, although in practice this is not always the case (Lunetta *et al.*, 1991).

The algorithms for raster and vector conversion are well documented (Pavlidis, 1982; Peuquet, 1981(a); Peuquet, 1981(b); Clarke, 1985; Burrough, 1987; Piwowar *et al.*, 1990). While there is no loss in positional accuracy when converting from raster to vector (lines are drawn where cell values change), the same is not true when converting from vector to raster. Polygon borders do not coincide normally with raster cell boundaries. The error and loss of information arising from the conversion are additional to those from inputting data into the GIS and will dominate errors arising from data input (van der Knaap, 1992).

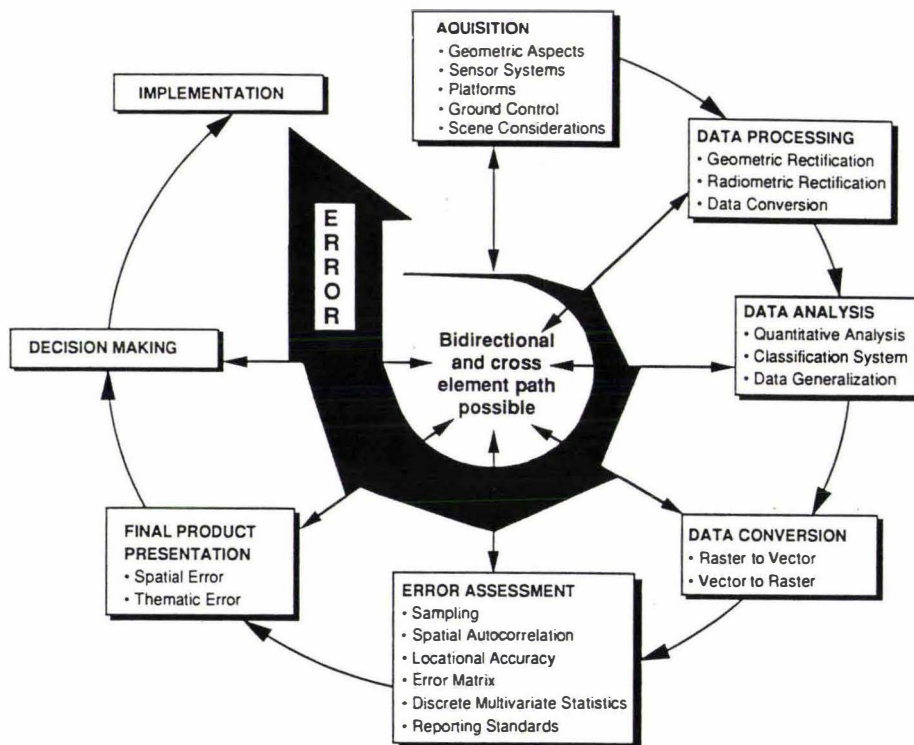


Figure 2.1: The accumulation of error in a typical remote sensing through GIS data flow (From Lunetta *et al.*, 1991).

In testing eight GIS software applications for vector to raster conversion, van der Knaap, (1992) found that each GIS gave results that differed both in number and location of assigned raster cells. Results were dependent totally on the GIS used, the way in which the vector data are organised and options chosen within the system. Furthermore, most GIS do not include options for influencing the conversion and the documentation gives little information about the process or results expected. A technique to reduce error is to use as small a cell as possible or to create a raster pattern and superimpose this over the vector data, manually assigning values to raster cells. Although this may be time consuming, it

ensures a consistent raster pattern provided the analyst does not make any errors (van der Knaap, 1992).

Aside from the technical aspects, a fundamental problem arises in the incorporation of remotely-sensed imagery into a GIS. It relates to the generalisation of imagery to the mapping scales found in GIS (Trotter, 1991). Digital imagery from Landsat TM or SPOT HRV (multispectral mode) sensors have spatial resolutions of 30 metres and 20 metres respectively. To integrate this imagery into a vector GIS, the imagery must be generalized to homogenous areas that cover an area sufficient for the mapping scale, *i.e.* 100 or more pixels at a scale of 1:50 000. While this is not a problem when the features can be uniquely identified and cover large areas, it is increasingly important as features become smaller.

## **2.6 Integrated Remote Sensing and GIS for Resource Management**

The pressure for up-to-date information has seen many resource management agencies around the world explore or implement integrated remote sensing and GIS. The potential levels of integration can be grouped as: (1) remotely-sensing imagery as a backdrop to GIS layers, (2) remotely-sensed imagery to update GIS information, (3) GIS to improve the accuracy of digital image classification, and (4) combining remotely-sensed imagery and GIS for spatio-temporal modelling.

The simplest level of integration is the use of digital imagery as a backdrop to GIS thematic layers. This operation is a standard feature in many GIS or image processing systems. Examples from the literature include Ahearn *et al.*, (1990) who used this approach in a pilot study of a conservation-oriented GIS in Nepal, and Logan (1993), who used a digital orthophoto as a base for a wetland mapping project in Maryland.

A further development is the use of on-screen digitising or the conversion of classified imagery into a GIS. The process of extending a GIS to handle image data routinely has been described by Derenyi and Pollock (1990). Examples of applications include the integration of aerial photography, SPOT imagery, and GIS layers of farm boundaries and land resources, to assess the temporary and long term damage cause by landsliding (Trotter *et al.*, 1989); incorporating a classified SPOT image into a GIS to update the irrigation status of agricultural fields (Eckhardt *et al.*, 1990); integrating Landsat TM derived maps of geology, structure and geomorphology with other GIS layers to provide information on ground water potential in India (Venkatachalam *et al.*, 1991); classifying Landsat MSS and Landsat TM imagery to produce vector layers of urban land-use and identify change (Pathan *et al.*, 1993); using classified Landsat TM and NOAA AVHRR to update forest

cover maps (Zhu and Evans, 1992), and incorporating large-scale aerial photography (1:1200) in a database of forest sample sites (Biggs and Green, 1992).

GIS layers can also be used as auxiliary data sources for digital image classification. Examples include the use of topographic data to modify a Landsat TM classification of land use (Janssen *et al.*, 1990); using layers of known habitat to classify the remainder of the satellite image for potential habitats (Aspinall and Veitch, 1993); applying elevation, soils and geology to classify an AVHRR image for deforestation in the tropical forest of Sumatra (Gastellu-Etchegorry *et al.*, 1993); and integrating data from the New Zealand Land Resource Inventory database to improve the accuracy of a Landsat TM derived vegetation map (Dymond *et al.*, in press).

The most complex level of integration is the combination of remotely-sensed imagery and GIS in spatio-temporal modelling. This may be viewed as a superset of the three previous levels of integration. An early application was the generation of buffer zones on a classified Landsat TM image to create a map of potential food availability for whitetail deer (*Odocoileus virginia*) (Ormsby and Lunetta, 1987). A similar approach was used by Buck and co-workers (Buck *et al.*, 1992) in mapping preferred habitat trees for Koala in Australia and by Chewings *et al.* (1992) who combined vegetative cover information from land-system mapping and Landsat MSS images to monitor grazing impact in the arid rangelands of Australia.

Other work has applied AVHRR imagery and GIS layers of land-use to forecast periods of severe feed deficits and drought-related land degradation in Australia (Brook *et al.*, 1992). Reed (1993) followed a similar methodology in Kansas, using NDVI imagery to investigate the effects of a potential drought. On a larger scale, Preston (1993) integrated meteorological satellite imagery with ocean current models and ice stress data to forecast sea-ice motion. Spatio-temporal models have been used to produce alternative management plans for coastal mixed-eucalypt forest and alpine woodlands in Victoria, Australia (Woodgate and Ritman, 1992) and to generate multiple land use scenarios for the dry tussock grasslands of the Mackenzie Basin in New Zealand (Wardle *et al.*, 1993).

However, with sophisticated data manipulation there is a corresponding requirement for computer processing power, *e.g.* the FERIS (Forest Environment and Resource Information System) (Preston, 1992) which integrates remotely-sensed imagery, DTMs, climatological data and site attributes requires a high performance Hewlett Packard 433S Unix Workstation. In general, the potential of such computing power being available to field-based resource managers in the near future is limited.

### 3: NATURAL RESOURCE MANAGEMENT IN WESTLAND

#### 3.1 Westland

Westland, the West Coast of New Zealand's South Island, extends from Kahurangi Point in the north to the Awarua River in the south (Figure 3.1). To the west it is bounded by the Tasman Sea, to the east, by the Southern Alps. The total length is 515 km with an average width of 50 km.

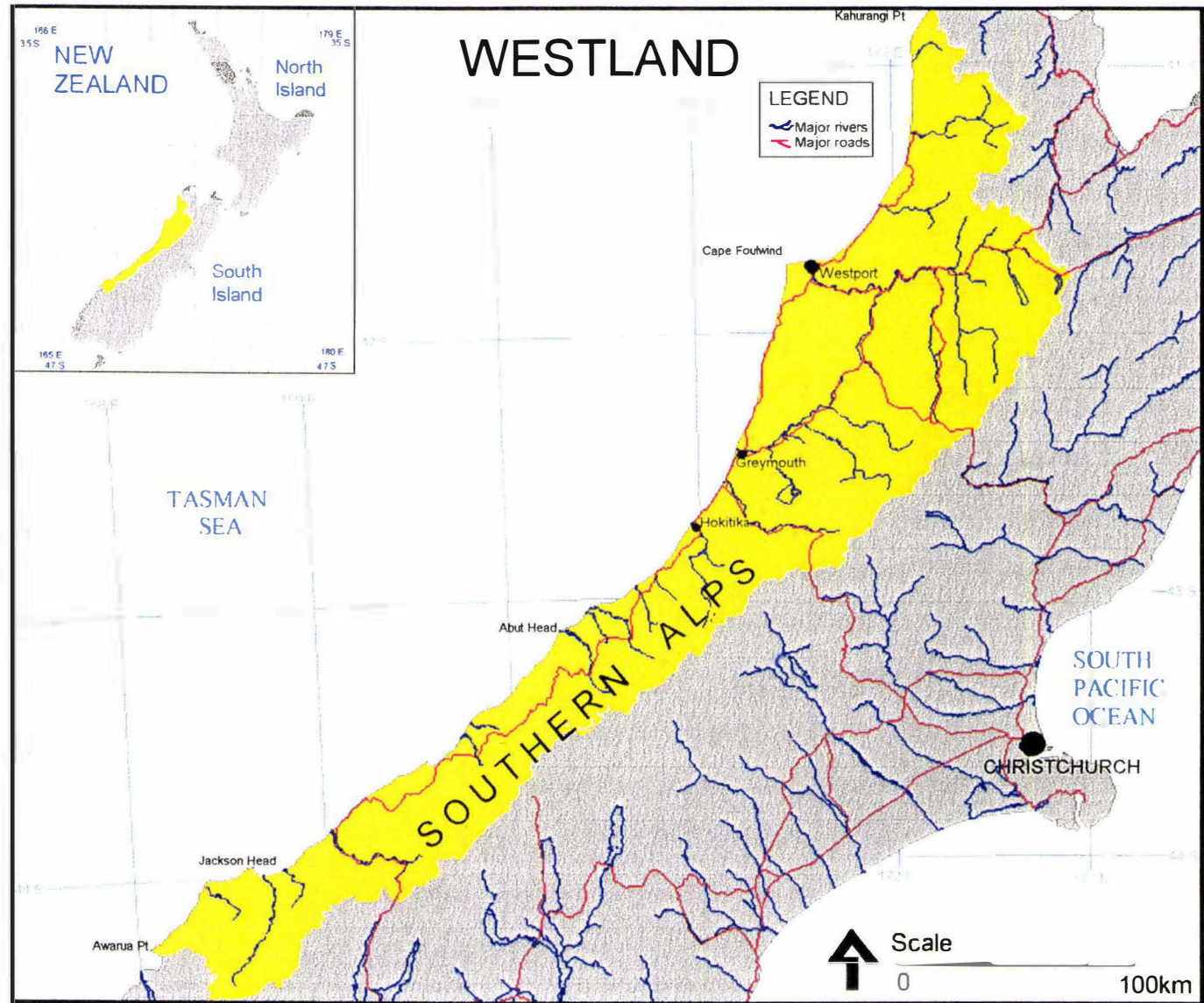
Westland is bisected by the Alpine Fault, which separates the schists and Mesozoic greywacke of the Main Divide from Pre-Cambrian greywacke in the west. To the west of the Fault, Pre-Cambrian greywacke crop out in the Paparoa, Victoria and Brunner Ranges. Elsewhere, they have been overlain with moraines and outwash gravels of Quaternary age which has created a topography characterised by low mountains divided by numerous river valleys. To the east of the Fault, the land rises steeply to the Main Divide.

The climate of Westland is renowned in New Zealand for its high rainfall. Moisture-laden winds from the Tasman Sea are forced to rise over the Southern Alps, causing orographic rain that varies from 2000mm/year in coastal locations to over 8000mm/year towards the Main Divide. Rainfall is evenly distributed throughout the year and is notable for its high intensity, with falls of 200 to 250mm in twenty four hours being recorded. When the number of days of rain is taken into account, the magnitude of these downpours is evident, *e.g.* Hokitika has an average rainfall of 2940mm and 167 rain days, compared with Auckland's 1268mm annual rainfall and 140 rain days.

The soils of Westland can be divided into five main groups: (1) recent soils found on river floodplains throughout the region; (2) yellow-brown sands which are confined to a narrow belt of sand dune country along the coast; (3) soils of the terrace, rolling and hilly lands *i.e.* yellow-brown earths (widespread in the central and northern areas), gley soils (of limited extent), gley podzols (extensive in swampy terraces throughout Westland) and podzols (of limited extent); (4) organic soils which are of minor extent and (5) the skeletal soils which occupy more than 70% of the land area, covering all of the steep mountainous country. The majority of the lowland is covered by terrace soils which are notable for their high degree of leaching and infertility.

Westland is noted for its outstanding scenery. The conservation and scientific values of the biota are of international significance with few forests in the world having such ancient evolutionary origins. Many plant communities that are severely depleted elsewhere in New Zealand are well represented in Westland. Foremost amongst these are the dense podocarp

Figure 3.1: Westland - the West Coast of New Zealand's South Island.



forests of rimu (*Dacrydium cupressinum*) and kahikatea (*Dacrycarpus dacrydiodes*) and the extensive natural freshwater wetlands.

### 3.2 Resource Management in Westland

Westland contains broad expanses of indigenous lowland forest (up to 400m a.s.l.) and undisturbed freshwater wetland. The lowland forests often run into the hill country and terminate in subalpine grasslands, providing a contiguous habitat from the mountains to the sea. It is in these lowland forests where the soils are generally more fertile and the climate is less extreme, that the most abundant wildlife is found. It is also where the majority of conflicts arise between conservation and other land uses.

**Wetland:** The extensive wetlands of Westland can be divided into two broad types: (1) fertile wetland, where water movement maintains nutrient inputs, and (2) infertile wetland or 'pakihi' which develop generally in basins or older alluvial terraces. Pakihi vegetation is characterised by the presence by shrubs and stunted forest but may also contain rarer species such as silver pine (*Lagarostrobos colensoi*), yellow silver pine (*Dacrydium intermedium*), pink pine (*Dacrydium biforme*) and bog pine (*Dacrydium bidwillii*).

**Mining:** Westland's geology provides a rich source of minerals but because of fluctuating world prices, topographic difficulties and a heavy bush cover, there is comparatively little prospecting activity. The metallic minerals extracted include gold, ilmenite, chromite, nickel and scheelite, but gold is the only one to have seen major mining. Non metallic minerals are asbestos, limestone, greenstone (nephrite) and coal.

Westland's coal resources are estimated at approximately 3 billion tonnes, excluding coal in seams of less than one metre thickness and some areas of poorly described geology. Only 5% of this is potential resource is classified as identified. Approximately 50% of the coal is located within the Paparoa Coal Measures of the Greymouth Coal Field (Greymouth Harbour Board, 1982). The resource blocks of these coalfields are relatively small, and this has substantially affected the pattern of mining in the past, most production coming from several medium-size mines. Coal mining in the future will depend on the implementation of highly productive technology adapted to the small, structurally complex resource blocks. In addition, coal exploration must continue to ensure that resources are sufficiently well known for long-term planning. It is expected that future coal exploration will move into areas regarded as inaccessible previously. Mining in such areas will be sensitive to transport and shipping costs as well as conservation resource management issues.

Gold was discovered in Westland in 1864. Most of the gold is either associated directly with the Pre-Cambrian sedimentary rocks of the Greenland and Waiuta Groups, or has been derived from these rocks through weathering and erosion (Williams, 1965). The eroded material has been deposited as alluvial gold or beach sand deposits. Only minor contributions are thought to have come from the Haast Schist and Toulasse rocks to the east of the Alpine Fault (Williams, 1965). Initially the gold was very easy to win, over 0.5 million ounces in 1867. However, after this gold was worked out, the level of mining has fluctuated depending on the price of gold. A steady drop in the gold price between 1940 and 1960 saw only the Kaniere dredge survive. To date, approximately 10 million ounces of gold have been won (Cumberland, 1981).

Gold mining in Westland has been exploitive. In early gold rushes, little or no attention was paid to environmental issues, particularly attempts to rehabilitate mined land to a productive, conservation or amenity land use. Dredges generally produced coarse, bare tailings that were left to revegetate naturally. In the 1960's and 1970's, the NZ Government revegetated large areas of tailings with *Pinus radiata* production forestry. Other sites were converted to pasture, but significant areas still remain as derelict scrubland or unvegetated boulders.

It is estimated that in 1990, up to 400 hectares per year were being worked or turned over in alluvial gold mining operations (Metcalf and Godfrey, 1990). These operations range in scale from land-based screening plants processing 6-15m<sup>3</sup> of alluvium per hour to large floating plants handling 100-150m<sup>3</sup>/hour. However, the majority of the turnover is not due to the large operations, but to smaller operations turning over 40-60 m<sup>3</sup>/hour. Most of the present day small scale mining comprises 70-80 operations concentrated in the area between Greymouth and Hokitika. Although many of the deposits in this area were extensively dredged for gold in the 1940's but are now being reworked - a rule of thumb in mining is that previously worked areas are more likely to contain mineable ore than mineralised areas with no history of mining. The pressure on resource use is dependant on the price of gold. Each time a new price level is reached, previously marginal gold deposits will become sufficiently valuable to permit economic working, and renewed effort will be put into the search for unlocated deposits.

Mining activities are controlled by a licensing system with applications reviewed by the Department of Conservation. The sites of proposed mining activities are surveyed and draughted onto halftones derived from aerial photography. Any changes to existing licenses must also draughted and approved.

**Forestry:** Westland National Park and the Saltwater Ecological Area are the major areas of protected undisturbed lowland forest remaining in New Zealand today. Apart from a few scenic reserves and some upland forest areas in Mt Aspiring National Park, there are no legally protected natural reserves south of the Cook River. Complete mosaics of forest, shrubland and wetland plant communities are the key feature. Because of logging and forest clearance elsewhere, the South Westland beech-podocarp ecotone is the only example in New Zealand where the process of forest readjustment after glaciation is represented.

The New Zealand rain-forest is composed generally of podocarp-broadleaf rain-forest and southern beech forests. When the early settlers arrived, about half of the total forest was in each type. A large part of the beech forest still remains today but the greater part of the podocarp-broadleaf forests have been cleared for agriculture (Poole and Johns, 1992). A general description of a podocarp-broadleaf forest in Westland is as follows. Dense rimu forest occurs on the infertile soils of poorly-drained glacial terraces and on older portions of alluvial flood plains. On the more fertile hill country soils, the rimu are more scattered with a dense understorey of southern rata (*Metrosideros umbellata*), kamahi (*Weinmannia racemosa*) and quintinia (*Quintinia acutifolia*). Dense clumps of kiekie (*Freycinetia banksii*) occur in lowland coastal forest. The kahikatea is the dominant species on recent alluvial soils. Mature kahikatea swamp forest also occurs on deep, wet, organic soils away from the river floodplain. On older areas of floodplains, the kahikatea forest merges into mixed kahikatea-rimu stands, e.g. on the Poerua River floodplain bordering Saltwater Forest and Saltwater Ecological Area.

Logging these lowland podocarp-broadleaf forests is difficult. The logging equipment compresses the soil and elevates the water table on soils that are already difficult to drain and constantly wet. Different logging techniques such as selective logging have been investigated, but in the long run any logging is detrimental to the remaining trees and regeneration (Poole and Johns, 1992). The growing conditions are poor and the growth rates are too low for management as a commercial enterprise. In addition, the slow growth rates have made interpretation of trial results difficult, e.g. at the end of 25 years, one rotation of *Pinus radiata*, rimu saplings, even when grown under nursery conditions are only 3-4m high and have a 2.5-3cm diameter.

The most promising technique for management of the Westland rimu forests is sustained yield management, whereby "*only those trees near the end of their natural lifespan in senescent stands and recently windthrown trees should be harvested. Conventional logging machinery causes an unacceptable amount of damage to rimu forests. The use of bush*

*milling and heavy-lift helicopters minimises the damage to the residual forest and allows the use of a wider range of silvicultural techniques" (James, 1987). However, even sustained yield forestry is in direct conflict with the forest bird resource. O'Donnell and Dilks (1986) state that "... our results indicate a potential conflict between logging and the maintenance of kaka and parakeet populations. Large podocarps, especially the rimu and kahikatea, are usually the target of timber extraction. These two threatened bird species would be at risk if removal of a significant proportion of such trees, which are the preferred food plants took place; or the removal of "senescent" trees, which are used for feeding and breeding. Thus the use of helicopters and portable chainsaw mills to extract selected trees, or the management of even-aged forest stands on short term rotation which precludes natural ageing, would probably not be compatible with conservation of these parrots."*

In 1989, legislation was passed halting the destruction of indigenous forests and if any logging was to continue it must be on a sustainable basis. The amount of timber removed annually must equate to the annual increment of the forest, keeping the forest intact and stable so that natural regeneration and growth are not compromised. Quotas were imposed on the logging of state owned beech forests and for the more difficult question of rimu forest management, proposed forestry was confined to 11,000 hectares in two State forests, the Saltwater Forest and the North Okarito Forest.

Management of the indigenous forests requires a detailed, up-to-date forest inventory. With much indigenous forestry, reliance has been placed on the data collected on the 1946-1955 National Forest Survey (Masters *et al.*, 1957) which concentrated on the lowland and intermediate altitude forests where there were known or probable resources of timber. Since 1955, deficiencies in the survey, notably in montane forest, have been addressed and a number of studies have gathered more specific and detailed information (Allen and McLennan, 1983). The most complete record is for Westland National Park, where Wardle (1975, 1977) described the plant communities and aspects of the ecology (Wardle, 1974, 1978, 1980). Other studies have investigated vegetation and soil development on different aged surfaces (Smith and Lee, 1984; Wardle, 1980; Sowden, 1986), flood plain forests (Foweraker, 1929; Wardle, 1974; McSweeney, 1982), rimu dominated forests (Hutchinson, 1932; Poole, 1937; Six Dijkstra *et al.*, 1985, James, 1987) and forest-mire ecotones (Mark and Smith, 1975; Norton, 1989).

The techniques used for forest inventory comprise typically a grid of sample plots (0.4-2ha) or transect lines (Allen and McLennan, 1983) throughout the forest. Additional plots may be added in areas of in the heavier timber. The stockings (densities) of all tree species at

different diameters at breast height (d.b.h.) are recorded for each plot. Full details of the field procedures used in the National Forest Survey are given in the project report (Masters *et al.*, 1957). Aerial photography is used commonly as a mapping base for identifying lines of plots, checking topography and extrapolating plot data to stand-based information. The extrapolation is subjective, based usually on visual interpretation and user knowledge.

**Fishing:** Westland's coastline fronts a fishing ground of approximately 192,000 km<sup>2</sup>. The catch composition is vast, hake, hoki, barracuda, jack mackerel, squid, tuna (southern blue fin, skipjack and albacore) and has attracted interest from foreign vessels. This potential resource is only beginning to be realised, especially in the harvesting of deep water species (hake and hoki). In 1992, Greymouth had the highest catch in New Zealand for albacore and southern blue fin tuna, Westport ranked second (White, 1992). Marine fishing is regulated through a quota system under Government control.

An estimated 30 tonnes of eels were taken from Westland in 1989. Although this tonnage represents only about 1.5% of the New Zealand catch, the industry is of local importance. The main constraint to the expansion of the eel industry is the limited water available, with fishing prohibited in many lakes within National Parks and scenic reserves. The whitebait fishery of Westland is the largest in New Zealand, providing additional income for both local people and visitors. The whitebait resource not only has high commercial value, but also high recreational and tourist value due to its uniqueness. It is recognised that the current whitebait catch is not sustainable and this is being addressed through consultation with local people and fishing industry personnel (Ministry for the Environment, 1987).

**Sphagnum moss:** Sphagnum moss is used mainly as a horticultural product in flower baskets. The sphagnum industry has grown from an output of 7 tonne/year in 1978 to about 500 tonnes/year (van Beek, 1987). Studies in central Westland (Deene, 1983) have suggested that sphagnum occurs mainly on land cleared from forest. Swamp areas support scattered sphagnum, with the greatest concentrations occurring at the forest margin. However, the state of the resource is unknown (Ministry for the Environment, 1987) and although research has been devoted to the methods used to harvest sphagnum (De Goldi, 1984; Chant, 1987), the long term effects of harvesting upon sustainability are undetermined (Levack and Hinton, 1987).

Sphagnum harvesting is based on a licensing system, with licenses ranging in term. The Ministry for the Environment review (1987) calls for licenses to promote sustained-yield which requires that the long-term licenses have a provision for a review of management practices as experience indicates the factors which promote sustained-yield management.

**Agriculture:** Agriculture employs 12% of Westland's workforce (White, 1992). Sheep, beef-cattle and dairy farming are the main agricultural enterprises. A study commissioned by the Greymouth Harbour Board (1982) noted considerable potential for further development of farming enterprises with only 47% of the area identified as suitable for farming being used. A feature of farming in Westland is the low number of freehold farms. The economic viability of the lease farms depends on the secure access to the land. Over the years, the length of tenure of grazing privileges has generally declined. State forest grazing licenses range from one to nine years and have set stocking rates. If rents under lease agreements are set too high, there is a likelihood that farmers will increase stocking rates and cause damage to the surrounding forest.

Overgrazing of river valleys is a major problem. Fencing the floodable river flats from the bush is not always practical because of the expense and difficulty in maintaining stock-proof barriers across tributary streams and rivers. A good reason not to fence is to allow the stock to move to higher ground in flood conditions. Resource managers are keen to promote low stocking rates, as there is less pressure for stock to damage the adjacent bush or forest. It is also in the best interests of farmers to avoid over-stocking the valleys as this may cause problems such as a reduction in calving rate and deterioration in animal condition.

**Wildlife:** Wildlife is abundant in Westland. Noted wildlife habitats extend from alpine tussock lands, through mountain and hill forests, lowland podocarp-broadleaved forests, grasslands and riverbeds, wetland to the coast. The New Zealand Wildlife Service rated the greater part of the region as having habitats of "high" or "outstanding" value (Ministry for the Environment, 1987). The influences affecting the long term survival of species in these habitats include, habitat destruction, the effects of predators (stoats, rats), the effects of browsing animals on forest structure and composition, competition between introduced and native species, forest clearance, modification of waterways/catchments, swamp drainage and the loss of complex habitat mosaics.

Red deer (*Cervus elaphus*) are present in all forested land south of the Cook River. At some stages the red deer population has caused severe over-browsing of both forest and grassland. After hunting, the population has been reduced and red deer are now in low to moderate numbers throughout South Westland. The hunting effort has to be maintained to ensure that numbers do not rise. However, if aerial hunting pressure was reduced, there may be a return of the deer to the alpine grasslands and river flats, thus reducing forest browsing.

The possum (*Trichosurus vulpecula*) is in an "eruptive" phase in many areas of Westland and is spreading. The possum causes widespread canopy dieback in rata, kamahi, totara and kaikawaka forest types. Possums compete with native birds for food and may be contributing to species decline. They are carriers of bovine tuberculosis (TB) and could cause widespread damage to cattle and deer farming should TB be introduced to the area. The minor presence of goats and pigs is not considered a problem at the present time in that localised operations control them.

**Archaeological sites:** Evidence indicates that Māori were using the Westland stone resources as early as the 13th century (Ministry for the Environment, 1987). Artifacts and occupation sites occur at many places along the coast. Sites at Jackson Bay and Barn Bay are of national significance providing information on early use of nephrite (greenstone). Other sites have been identified at Hunts Beach, Jacobs River, Mahi Tahī, Paringa River, Waiatoto River and Neils Beach to name a few. Reserves have been created at these sites.

European settlement started with the sealing era around 1800 and black-sand gold mining from the late 1860's. There are no known remains of the sealing era. Gold mining remains are of local significance although the Jackson Bay Special Settlement of 1875 is of regional importance. The remains of a large number of beach mining activities have been destroyed by coastal and river mouth erosion, for example in Bruce Bay, erosion has been calculated at 200m since 1866 (Ministry for the Environment, 1987). The remaining sites have a high tourism value especially where they coincide with other recreational values.

### **3.3 Remote Sensing and GIS for Resource Management in Westland**

There is a wealth of historical resource management information available in Westland. Many organisations and individuals have access to comprehensive photographic archives, map data and textual records. There is also the prospect of using satellite imagery from the SPOT HRV, Landsat TM and NOAA AVHRR sensors to update the information. However, with regard to the implementation of remote sensing and GIS technologies in resource management, Euan Nicol, formerly of the Science and Research Division of DoC, noted that "*Implementation of these new information management tools (remote sensing and GIS) in the Department (of Conservation) has been limited to date by financial and operational constraints, and a small base of staff familiar with them. In addition, in contrast to word processing...advocates of remote sensing, imaging and GIS have not so far been able to convince senior management of the values of these tools in managerial decision making*". Nicol also states that one reason for the non-adoption of this technology is that "*technical specialists need to start listening to the needs of managers and planners and seeing how*

*new technologies might assist meeting those needs*" (Nicol, 1993). The following section discusses the potential application of remote sensing, digital image processing and GIS for resource management in Westland.

**Mining:** Remote sensing and GIS are of use in the planning and restoration of surface coal and gold mines. With digitised, rectified aerial photography as a backdrop, GIS layers of existing and potential mining licences, roading and other spatial data, *e.g.* archaeological sites, can be superimposed quickly and simply. Hard-copy prints can be produced on a standard laser printer at a cost of a few cents per copy. The digitised aerial photographs may be processed to thematic (single factor) maps, quantifying the area and location of the actively mined land. Through digital change detection techniques, any change in the area of land mined, or surrounding vegetation, can be identified and quantified, providing a perspective of historical resource use.

**Forestry:** Manual interpretation of aerial photography for inventory of exotic and indigenous forest is well developed in New Zealand. However, much less work has been reported on the inventory of indigenous forestry using satellite imagery, digital image processing, GIS, and integrated remote sensing/GIS analyses. There is a potential for application of these techniques to provide detailed inventory information for large tracts of indigenous forest and to identify change at the forest margin or within the forest.

Conversion of existing forest inventory information into a GIS can enable both spatial and aspatial database queries and modelling analyses to be undertaken. Many of the data manipulation requirements for queries would be unfeasible without a GIS. For example, to produce a map indicating the distribution of a species or size-class would have involved manually locating all records which fit the search criteria and identifying these on a map. If digital imagery, either a scanned aerial photograph or satellite image was available, the sample-plot locations could be superimposed on the image backdrop, enabling easier, quicker navigation when revisiting plots. Furthermore, relationships may be established between the imagery and inventory, which would enable an objective extrapolation of the inventory to the remainder of the forest.

**Fishing:** Remotely-sensed imagery can be used effectively to monitor water quality (sediment loads) in the coastal fishing grounds. When combined with tidal and weather models in a GIS environment, there is the possibility for spatio-temporal modelling, *e.g.* predicting the development of algal blooms. Satellite imagery could also be of use for determining and identifying foreign ships fishing inside New Zealand's Exclusive Economic Zone.

**Sphagnum moss:** Remote sensing and GIS could be used to identify pockets of land, either areas recently cleared from forest or swamp areas at the forest margin, that would be suitable for the growth of sphagnum. In existing moss harvesting areas, digital change detection techniques based on aerial photography, may be able to determine whether a change in vegetative composition is occurring in the surrounding ecotone as a result of the moss harvesting. There is the possibility of storing licensing and volume extraction information in a GIS. Integrating this GIS information with digital imagery may allow changes in ecotones to be correlated with sphagnum harvesting and provide information on the sustainability of the current licensing provisions.

**Agriculture:** Vegetation indices derived from aerial photography or satellite imagery may be able to identify the biomass or photosynthetic activity of pasture on the river flats. Over time, change in the biomass or photosynthetic activity may provide an indication of change in the land's productivity. Digital change detection could also be used to identify where stock are being forced to graze the forest margins. At the farm level, a low-cost, PC-based GIS could be applied in monitoring stock movement, fence and track condition, and water system planning.

**Wildlife:** Aerial photography can be used to assess the effects and distribution of possum browsing. Although the current generation of multispectral satellite imagery is not of sufficient resolution to detect the effects on individual tree crowns, the imagery may be of use in detecting more widespread damage. Possum occurrence data from traps or information on the location of poison baits could be stored in a GIS. There is the possibility of establishing a link between the effects seen in the remotely-sensed imagery and the occurrence data. This information could be of use in understanding the relationship between possum density and damage to indigenous forest types.

**Archaeological sites:** Archaeological information for all sites could be managed in a centralised GIS database. This database could integrate all of the spatial and attribute information associated with that site and provide further understanding of the relationships that existed. Image enhancement techniques applied to aerial photography or satellite imagery may be able to locate new areas on existing sites or provide information in support of potential sites.

## 4: METHODOLOGY AND EXPERIMENTAL SITES

### 4.1 Remote Sensing and GIS Methods to be Analysed

Natural resource management requires accurate, up-to-date information on the condition and reserves of resources, whether change in resource use is occurring and how any change impacts on the resource and ecosystem. Remote sensing, digital image analysis and GIS are tools that may help resource managers in Westland obtain and manage this information. In this thesis, these tools are evaluated for monitoring alluvial gold mining and management of indigenous forests, topics identified by DoC Westland Conservancy as examples of current resource management issues in Westland.

*Alluvial Gold Mining:* Plans showing the location of mining operations, quantitative data on the amount of mined land, and information indicating the position of current mining compared with previous workings are examples of the type of information required for monitoring alluvial gold mining. The requirement for quantitative land-cover information dictates that any remotely-sensed imagery must be classified. Given the availability of classified imagery, an appropriate change detection procedure to apply is a post-classification (or independent change detection) (Singh, 1989). Although this technique suffers from classification errors in the independent classifications being compounded in the change detection (Howarth and Wickware, 1981), the fact that the classified imagery is potentially available may override these error considerations.

Furthermore, in surface mining applications it may be possible to achieve high classification accuracies in the individual images. If information on the area of mined versus vegetated land is all that is required, only these two land-cover classes will need to be discriminated. In addition, change detection techniques that use unclassified imagery, *e.g.* image differencing or composite classification, may require radiometric correction of imagery, determination of an appropriate change vs no-change threshold (Jensen, 1985; Jensen, 1986; Riordan, 1981) and considerable skill in interpreting the nature of any change (Pilon *et al.*, 1988). An independent change detection does not require determination of change thresholds, simplifies the interpretation of change and removes the need for radiometric correction of individual images.

*Indigenous Forest Management:* Forest inventory, based on species, age-class discrimination or a number of other compositional parameters is a key factor in successful management of the forest. However, the research reported in the literature for intra-forest discrimination has been conducted largely in the coniferous and production forests of the

USA and Canada (Horler and Ahern, 1986, Brockhaus and Khorram, 1992). The results have varied, depending on the forest parameter or compositional classes investigated. Compared to the New Zealand rainforest, these coniferous forests occupy vast areas, are often nearly monoclonal, even-aged and have a homogenous canopy. The New Zealand rainforest is notable for the abundance of different species and age classes present. Research is required to determine how digital image processing, aerial photography and satellite imagery can be applied to yield species, age-class, and other compositional information beneficial in management of these indigenous forests.

A GIS may be used to store and manipulate a forest inventory database (Dunningham and Thompson, 1989). In addition, the inventory database may be integrated with digital remotely-sensed imagery and relationships developed to extrapolate the inventory information to other unsampled areas of the forest (Zhu and Evans, 1992). Alternatively, the forest inventory may be used to aid classification of remotely-sensed imagery (Dymond *et al.*, in press).

#### **4.2 A PC Approach**

The decision between a PC-based approach (I refer to a PC as running typically either the DOS, OS2™, Microsoft Windows™ or Macintosh™ operating system with 1 to 16 megabytes of RAM (Random Access Memory) and hundreds of megabytes (MB) of hard disk storage) and a workstation (here I refer to a workstation as running typically the UNIX® operating system with tens to hundreds of megabytes of RAM and gigabytes of hard disk storage) is principally a price versus performance decision. The hardware (screen, memory, processor, disk storage) of a PC is less expensive, approximately by a factor of 10, than a workstation. Correspondingly, the PC provides a lower level of computing 'power' and for digital image processing and GIS applications, PC software may provide a lower level of functionality compared to workstation software.

The increased computing power of the workstation must be weighed against the extra financial expense. In many cases, a workstation will be required, *e.g.* manipulating an entire Landsat TM image occupying some 230MB, or managing a city's roading and utilities database. Although the boundary between PC and workstation power is being eroded steadily, in 1995, PC technology has not yet developed to a state where these types of large applications can be handled efficiently. However, for smaller applications and where the software is sufficient, a PC system will be appropriate.

The user skill level, the ease of integration with existing systems (Townshend, 1992), and the support available for hardware and software will also affect the choice of system. The majority of resource managers are not image processing or GIS specialists. The functionality provided by a comprehensive PC-based image processing package or GIS is likely to meet their needs. In addition, many resource managers are exposed to DOS based PC's in other aspects of their work, whereas they may have little or no experience with UNIX<sup>®</sup>. It is also unlikely for a field station budget to support workstation technology or have the staff to install and maintain UNIX<sup>®</sup> workstations. However, this does not imply that workstation-based image processing or GIS will not be available to a resource manager in Westland. These computer intensive tasks could be directed to a central facility or outsourced as required.

#### **4.3 Approaches to Methodology based on Computing Environment and Needs**

The work in this thesis was based on the application of a PC-based GIS and digital image processing system. The reasons for this are: (1) it is unlikely that resource management field offices in Westland will afford the capital expense, have the necessary computing support or user skill level to operate a workstation platform. Large regional or national datasets requiring workstation power are more likely to be stored and managed at a central facility outside of Westland, and (2) Massey University's Department of Soil Science provides PC technology for remote sensing and GIS study. The image processing and GIS software provided is DRAGON, PC ARC/INFO and EPPL7.

In surface mining applications, where discrimination of mined land from bare fields or a detailed vegetation classification is required, it is preferable to use a multispectral data source, *e.g.* colour-infrared aerial photography (Carrel *et al.*, 1978, Halverson, 1988). However in this thesis, the imagery used was black-and-white aerial photography. This imagery was used because DoC Westland Conservancy, who provided the images for the study and maintain an archive of aerial photography, have traditionally used black-and-white photography to create halftones of mining licenses.

The remotely-sensed imagery used in the indigenous forestry studies was SPOT XS and Landsat TM satellite imagery. A SPOT XS image was used because DoC Westland Conservancy had purchased an image prior to commencement of the thesis and were interested to learn what relevant resource management information could be extracted. A Landsat TM image was obtained from EOSAT through the student data grant scheme. Funding was not available to purchase additional satellite imagery or aerial photography during this project.

#### 4.4 Choice of Experimental Sites

The alluvial mining study area is Tuckers Flat, an area typical of the small alluvial gold mining claims located between Greymouth and Hokitika. The studies of indigenous forestry are centred on Saltwater Forest, a predominantly rimu forest under consideration for sustained yield logging, and Saltwater Ecological Area, an virgin ecotone. These areas were chosen because they are both examples of current resource management issues in Westland. Furthermore, remotely-sensed data for both sites was freely available, other research had been undertaken in Saltwater Forest and Saltwater Ecological Area (James 1978; Six Dijkstra *et al.*, 1985; Almond 1986; Norton and Leathwick, 1990) and given the rugged terrain and isolation of many areas of Westland, both sites were readily accessible.

## 5: ALLUVIAL GOLD MINING

### 5.1 Study Objective

One of the objectives of this study was to investigate how change in land-cover due to alluvial gold mining operations can be identified and mapped on a PC-based digital image processing system using black-and-white aerial photography.

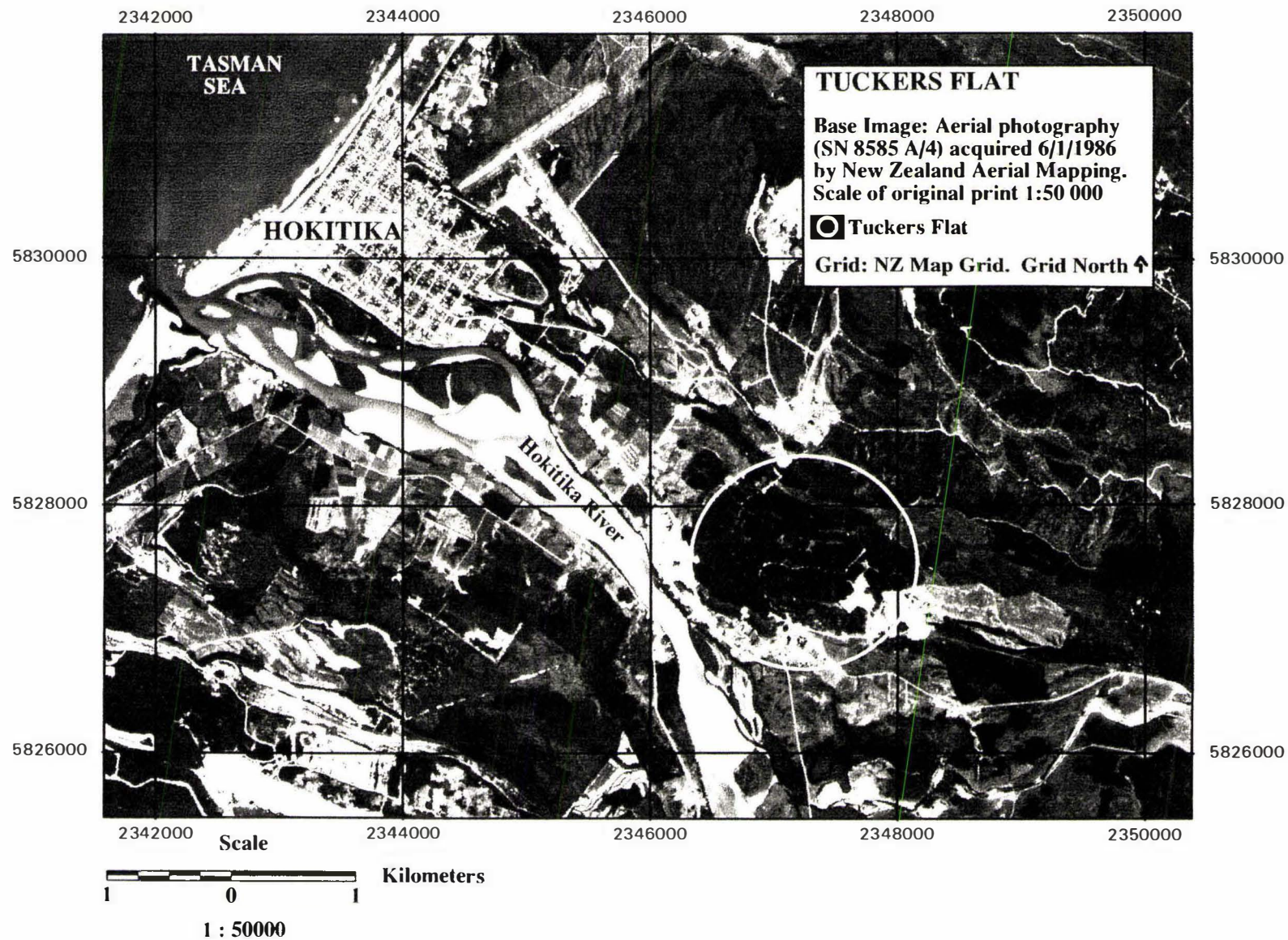
### 5.2 Site Description

Tuckers Flat is located on alluvial deposits produced during the Kumara-3 glacial advance (Soons, 1982). These deposits were mined extensively for gold in the 1940s which has created a landscape characterised by large piles of stony tailings and areas of *Pinus radiata* state forest. The forests are part of rehabilitation efforts by the New Zealand Government. In the late 1980s, there was a renewed interest in gold mining in this area, due largely to a rise in the real price of gold and the use of hydraulic excavators and rotary screening plants (Figure 5.1). These machines could process more material, and extract more gold from a given amount of alluvium than the old dredging systems and made it economical to rework old tailings. The site is located 5 km southeast of Hokitika (Figures 3.1 and 5.2) at approximately 171°E, 42°45'S (NZ Map Grid 2347000 5827500).



Figure 5.1: A hydraulic excavator and rotary screening plant working at a mining claim within Tuckers Flat (photo L. J. Brown)

Figure 5.2: The location of Tuckers Flat - an area of alluvial gold mining.



### 5.3 Methodology

**Imagery:** This study used five black-and-white aerial photographs from DoC Westland Conservancy archives (Table 5.1) (Figures 5.3 to 5.7). All except the 1988 photograph (taken by the New Zealand Forest Service) were taken by NZ Aerial Mapping Ltd. The photographs were all vertical and all prints were of high quality.

Table 5.1: The black and white aerial photography used in the Tuckers Flat study

Survey	Date	Focal length	Format	FOV	Scale
SN 827/12	4/5/1943	209.5 mm	220x162mm	±33°	1:15 000
SN 2977 G1/5	28/9/1976	209.5 mm	230x230mm	±38°	1:15 000
SN 5312 S/5	17/1/1979	209.5 mm	230x230mm	±38°	1:10 000
SN 8585 A/4	6/1/1986	152.7 mm	230x230mm	±47°	1:50 000
Forest Service	8/11/1988	not recorded	copied print	-	1:10 000

**Relief Displacement:** The relief displacement in the aerial photographs over the Tuckers Flat area was calculated using the equation:

$$displacement = h.tan\theta$$

where  $h$  = height of the object of interest above a datum and  $\theta$  = view angle, measured from vertical. Elevations were estimated from a 1:10 000 contour plan obtained from DoC, Westland Conservancy. A 30m datum was assumed.

**Digitising:** The photographic prints were digitised through a SONY 8-bit frame-grabber at Massey University's Image Analysis Unit. The area of the photograph digitised was adjusted for the scale of print. For the larger scale prints (1:10 000 and 1:15 000) nearly the whole photograph was digitised, whereas on the 1986 print (1:50 000), only the area surrounding Tuckers Flat was captured. The frame grabber's spatial resolution was 512x512 pixels, which, based on the area captured, created ground resolutions of 6.8m on the 1943 and 1976 images, 4.8m on the 1979 and 1986 images and 3.6m on the 1988 image.

**Registration:** The 1976 image was used as the base-image for registering the imagery. This image was at the largest-scale to give complete coverage of the Tuckers Flat area. Ground control points, chosen at road intersections and other easily recognised features, e.g. sharp bends in streams, were distributed as widely as possible across the Tuckers Flat area (Figure 5.8). A first-order transformation was used to calculate the registered pixel locations. The new pixel values were interpolated with a bilinear algorithm.



Figure 5.3: The 1943 aerial photograph. The location of the Tuckers Flat area is indicated by the yellow box. Scale as printed in thesis 1:34 000.

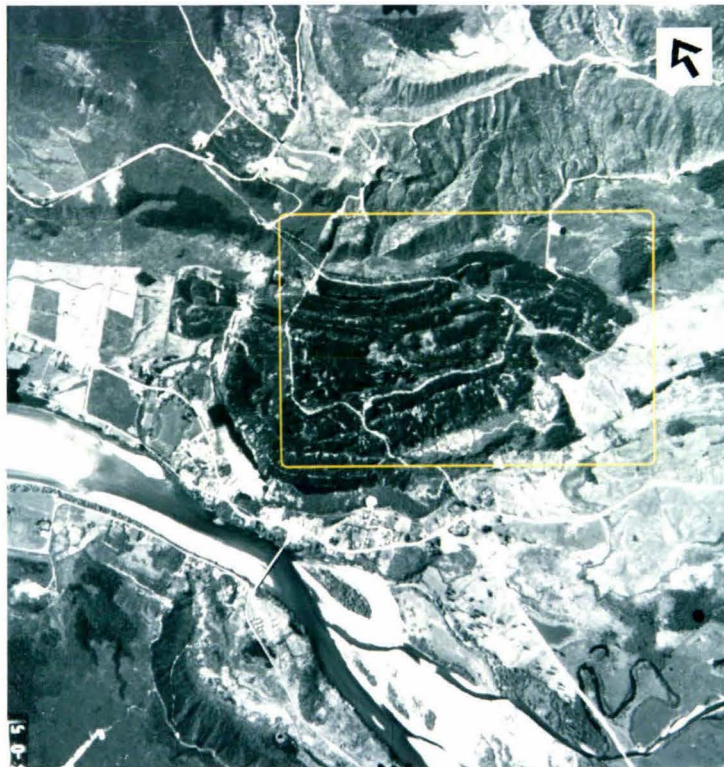


Figure 5.4: The 1976 aerial photograph. The location of the Tuckers Flat area is indicated by the yellow box. Scale as printed in thesis 1:34 000.

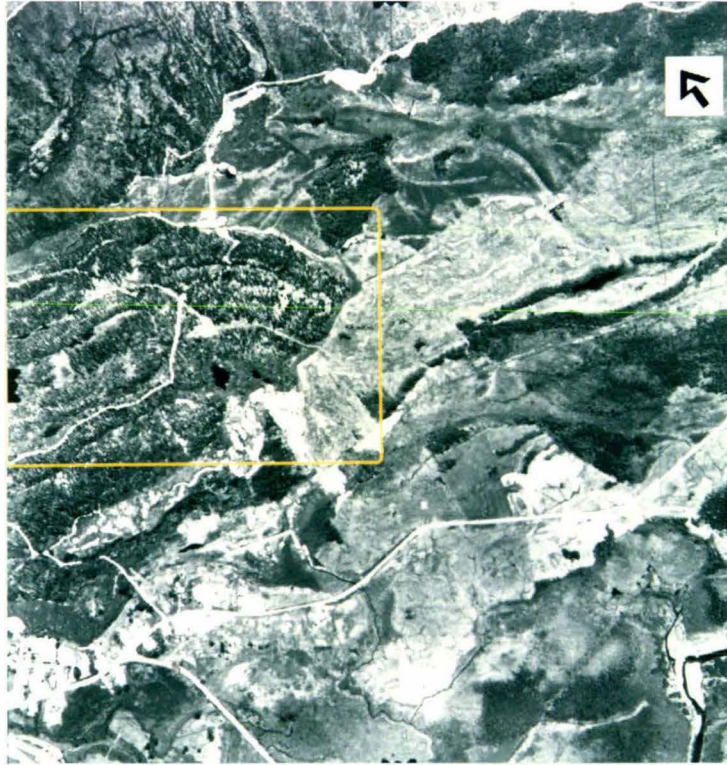


Figure 5.5: The 1979 aerial photograph. The location of the Tuckers Flat area is indicated by the yellow box. Scale as printed in thesis 1:22 000.



Figure 5.6: The 1986 aerial photograph. The location of the Tuckers Flat area is indicated by the yellow box. Scale as printed in thesis 1:110 000.

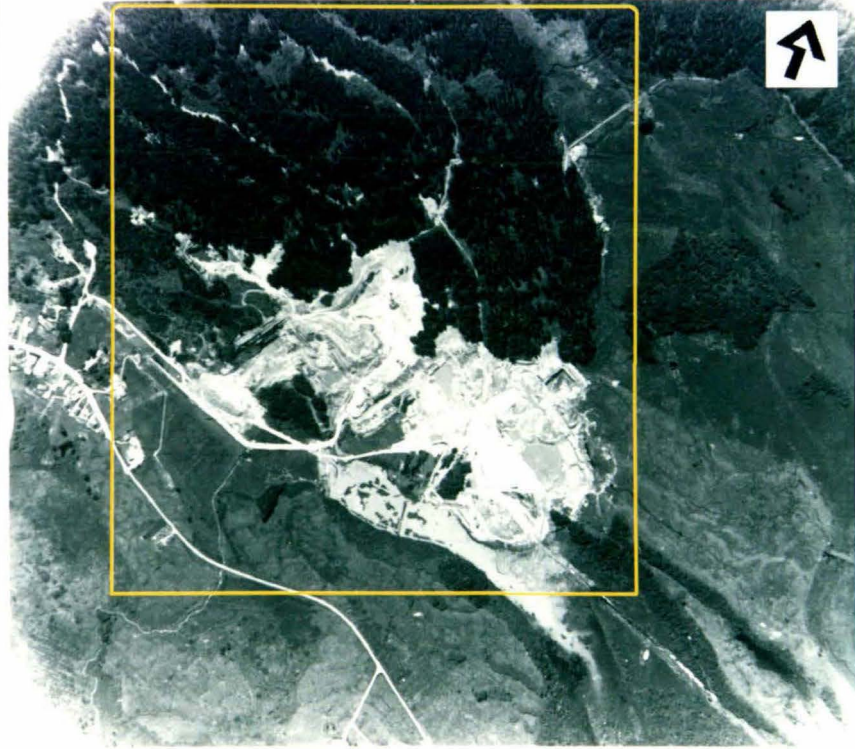


Figure 5.7: The 1988 aerial photograph. The location of the Tuckers Flat area is indicated by the yellow box. Scale as printed in thesis 1:15 000.

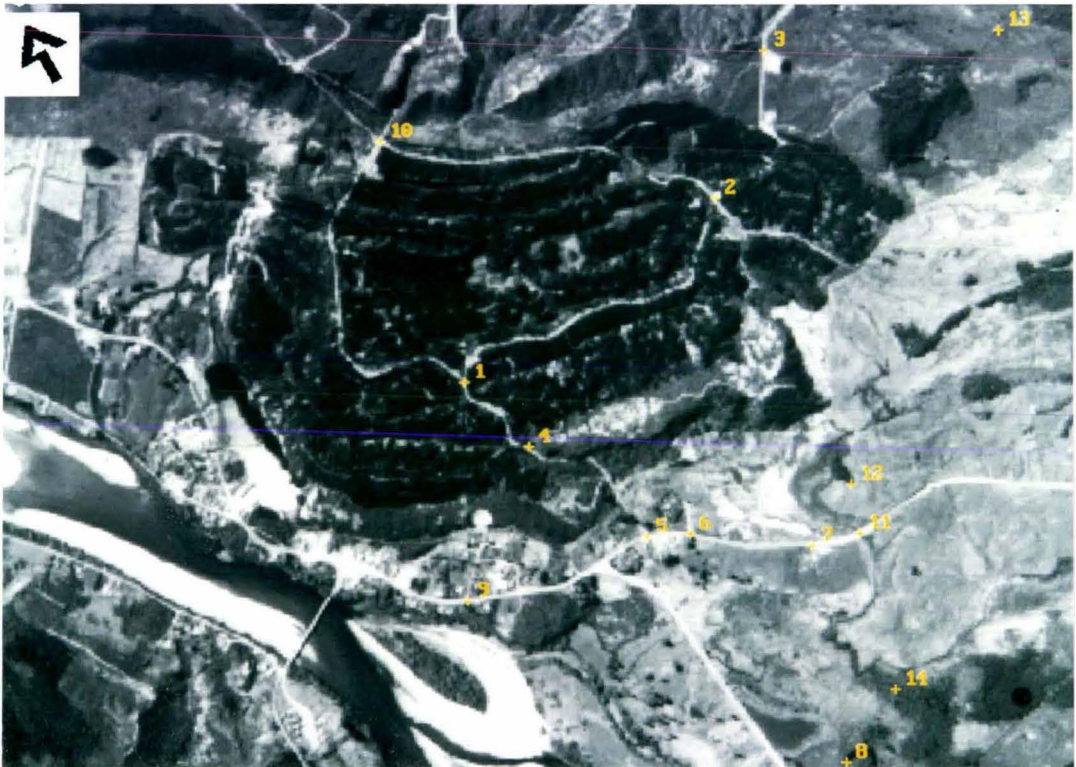


Figure 5.8: The 14 GCPs used in the registration superimposed on the 1976 image. Only a selection of GCPs were used to register a particular image. Scale as printed in thesis 1:11 000.

**GIS information:** The cadastral information for Tuckers Flat was obtained from a plan provided by DoC Westland Conservancy (Figure 5.9). The plan indicated 4 land parcels within the general Tuckers Flat area; State Forest 2106, State Forest 2149, Rural Section 4668 and Gravel Reserve DP 1305. The boundaries for these land tenure parcels were digitised manually into PC ARC/INFO version 3.3. During the digitising, the digitiser transformation error was maintained below the suggested 0.003 rms tolerance (ESRI, 1993(a)). The digitised lines were built into polygon features and each polygon assigned an identification number. To enable individual land tenure parcels to be extracted from the digital images, the cadastral information was rasterised to a 512x512 grid with the ARC/INFO *polygrid* command. The cadastral grid was registered to the 1976 image with a first-order transformation.

It was evident when the gridded cadastral data was superimposed on the 1976 image, that the shape and location of many roads on the cadastral plan were a simplification of the actual road network. In the case of Tuckers Flat road, there was considerable error even allowing for subsequent road realignment (Figure 5.10). These errors made GCP definition at precise road intersections difficult. To compensate for the errors, the transformation was iteratively adjusted to achieve the best fit to the most accurately drawn roads. A new, more accurate Tuckers Flat Road was digitised directly off the image into the cadastral grid after registration (Figure 5.11).

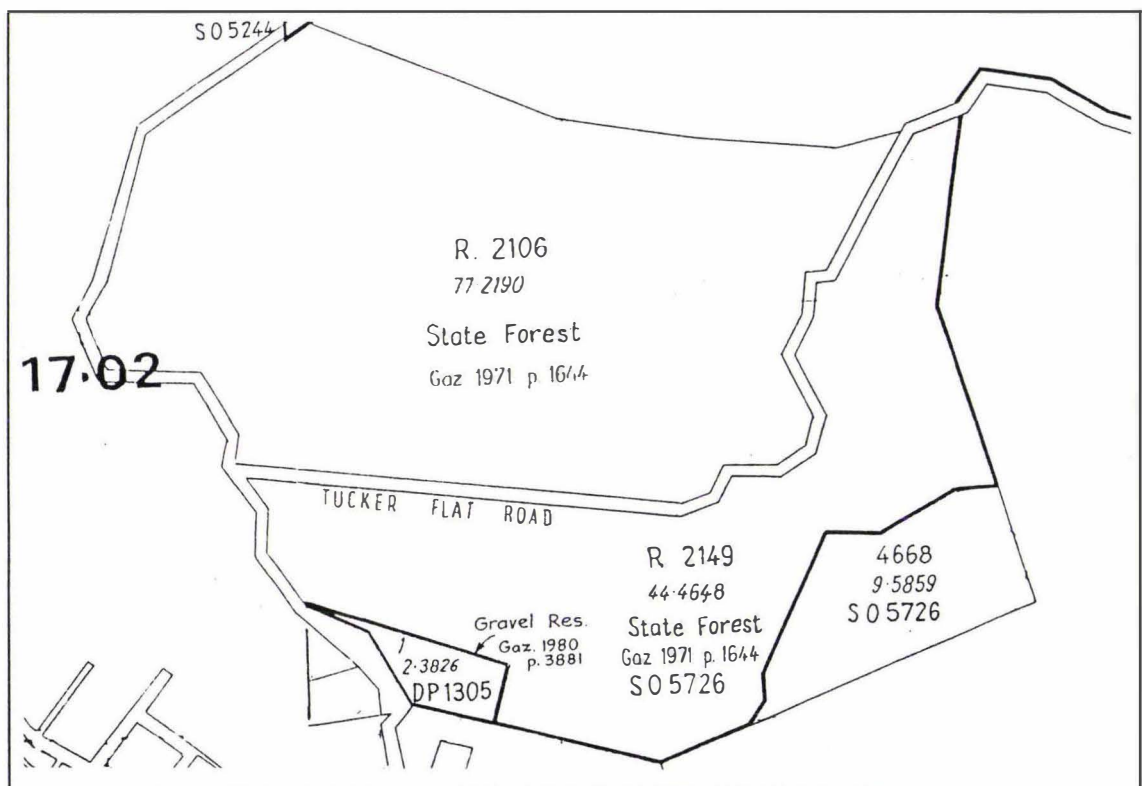


Figure 5.9: The DoC cadastral plan used to obtain the land parcel boundaries for the Tuckers Flat area. The parcels used in this study are State Forest R.2106, State Forest R.2149, Rural Section 4668 and Gravel Reserve DP 1305. Scale as printed in thesis 1:12 500.

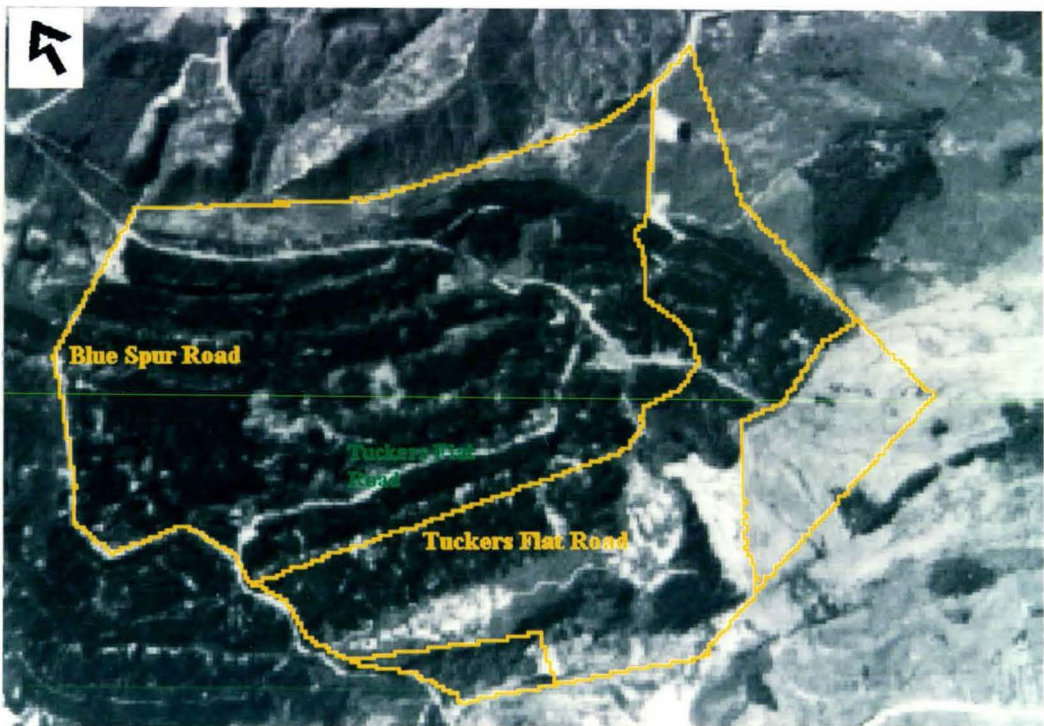


Figure 5.10: The cadastral information derived from the DoC plan superimposed on the 1976 image. This image shows the misplacement of Tuckers Flat Road as drawn on the cadastral plan. Scale as printed in thesis 1:10 000.

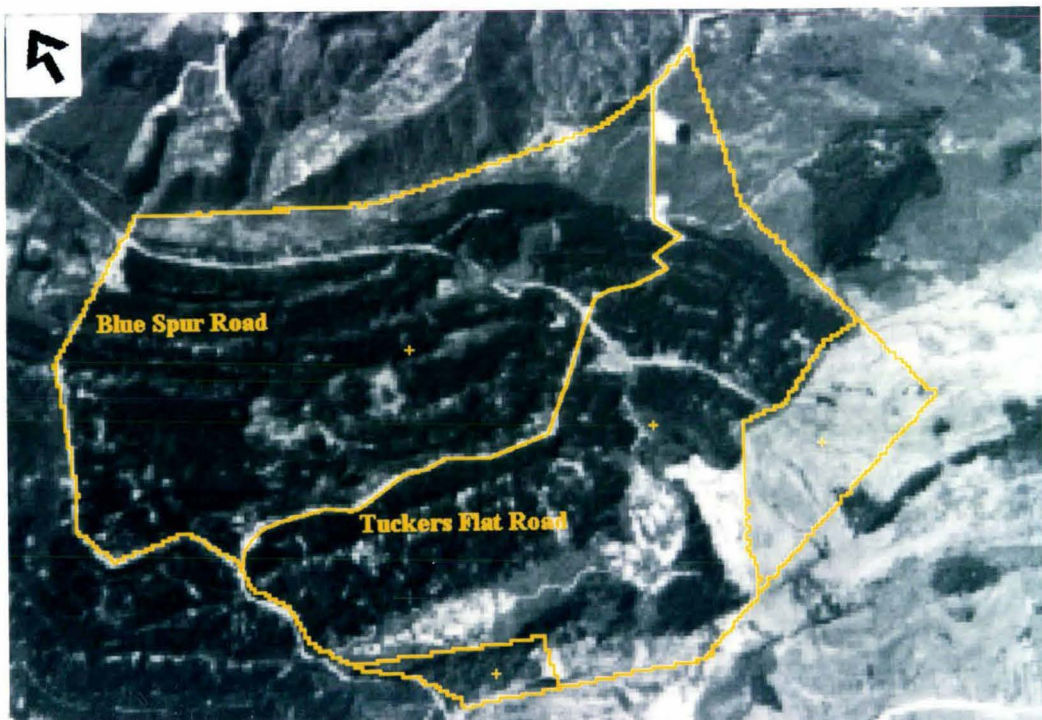


Figure 5.11: The cadastral information derived from the DoC plan superimposed on the 1976 image with the new Tuckers Flat Road that was digitised off the computer screen directly. Scale as printed in thesis 1:10 000.

**Image segmentation:** The rasterised cadastral information was used to extract the area encompassing the Tuckers Flat land tenure parcels from the digital images. A masking procedure was used, whereby all image pixels inside a mask defined by the cadastral data were retained and all outside the mask set to zero. The same procedure was later used to isolate individual land parcels such as Rural Section 4668 or State Forest 2106 (Figure 5.9). The masking procedure applied a conditional statement in the EPPL7 *evaluate* command, *i.e.*,

Let old-image1 = gridded cadastral information (*the land parcels within the Tuckers Flat boundary are represented as unique codes e.g. 250*)

Let old-image2 = image derived from an aerial photograph.

If old-image1 = 250 or old-image1 = 251 or.... then (*selects the pixels of all land parcels within the Tuckers Flat Area*)

then new-image1 = old-image2 (*clips out the land parcels from the digital image*)

else new-image1 = 0 (*surrounds the area of Tuckers Flat with 0 values*)

**Classification:** The purpose of classification was to determine quantitative information on the area of land being mined at each date of photography. In the Tuckers Flat area, alluvial gold mining operations are directly associated with bare ground, implying that only two land-cover classes, bare ground and vegetated, need to be discriminated. On advice from DoC Westland Conservancy staff it was decided to investigate whether information on the amount of land being cleared from native forest and the amount of scrub being afforested could also be determined. Therefore, three land-cover classes were chosen: (1) bare ground (synonymous with mined land), (2) trees (*Pinus radiata* in the revegetated tailings area and native species in undeveloped areas) and (3) land covered by scrub.

These land-cover classes were easily recognised on the unclassified digital imagery; bare ground was evident as light grey to white tones (higher intensity values), and trees as dark grey tones (lower intensity values). Scrub was intermediate between the bare ground and tree classes (Figures 5.3 - 5.7). Circular training areas representative of each class were selected on each image. The study attempted to maximise the correct classification of bare ground in areas of known mining activity, and trees in known areas of *Pinus radiata* forest by iteratively adjusting class limits and reclassifying the imagery. The classified imagery was visually compared with the original images after each iteration. The intensity value limits of the scrub class were adjusted to fill the range between the trees and bare ground classes (Table 5.2).

Table 5.2: The range of pixel intensity values used to define each land-cover class.

Image	Pine	Scrub	Bare Ground
1943	45-78	79-137	138-225
1976	32-63	64-179	180-199
1979	32-80	81-155	156-234
1986	26-47	48-177	178-221
1988	30-62	63-93	94-208

A density slice or level slice was used to classify each image. This procedure defines an upper and lower limit of intensity values for a particular class (Table 5.2). All pixels with intensity values that fall within a class's range are assigned to that class. The classification procedure can be visualised as drawing vertical lines through an image histogram. The accuracy of the classification was assessed by recording values from 100 points selected at random on the classified imagery and comparing these with the class interpreted manually from the unclassified digital imagery. Sample pixel locations were located exactly on the classified and unclassified imagery. The results were tabulated in error matrices and the Kappa coefficient of agreement calculated (Hudson and Ramm, 1987).

**Change detection:** The change in location of land-cover classes between images was identified using an independent-classification change detection (Singh, 1989). This procedure uses a pixel-by-pixel comparison of two classified images to identify change. Prior to the change detection, the codes assigned to the land-cover classes were modified to ensure that the nature of any change could be interpreted easily, *e.g.* if the classes bare ground, trees and scrub have values 1, 2 and 3 respectively, a code of 23 on the change detection image shows an area that is tree-covered in the later image, but was covered by scrub at the previous date. A conditional statement was used to perform the change detection *i.e.*

Let old-image1 = date1

Let old-image2 = date2

If old-image1 = 3 and old-image2 = 2 then

new image1 = 23 (*a unique code to identify each type of change*)

elseif old-image1 = 1 and old-image2 = 2 then

new-image1 = 21

elseif ...

The change detection images were filtered with a 3x3 modal filter to remove the single, isolated pixels showing change (Allum and Dreisinger, 1986). The 3x3 modal filter evaluates the pixel values occurring in a 9-cell window and assigns the most commonly

occurring value to the central cell, before moving to the next window. These isolated pixels showing change were assumed to indicate areas of spurious change.

#### 5.4 Results and Discussion

**Computer hardware and software:** All the image processing was handled in the PC environment. The image size (512x512 pixels, 256 kbytes) was manipulated and stored efficiently by the PC hardware. The functionality provided by the digital image processing software was in excess of the requirements for this study. In addition, the continuing rapid development of the PC (Anthony, 1994), will ensure that any processing power and storage constraints diminish as time progresses.

**Relief displacement:** The relief displacement over Tuckers Flat is presented in Table 5.3. The displacement was calculated at the farthest boundary of the land tenure parcels at Tuckers Flat from each photograph's fiducial point. To minimise relief displacement to less than 1 pixel at the farthest boundary, the maximum GCP elevations above a 30m datum are 11.3m, 14.2m, 8.3m and 14.5m for the 1943, 1976, 1979 and 1986 images respectively. Given that the elevation of the tailings varies between 3 to 16m above datum, in the large-scale aerial photographs, GCPs sited on tailings at the edge of the Tuckers Flat study area should be avoided as displacement may exceed one pixel. However, GCPs sited on tailings inside the Tuckers Flat area will probably be displaced by less than one pixel, depending on the image.

The highest point in Tuckers Flat is a hill, 32m above datum, in State Forest Reserve 2149. If relief displacements are calculated for the crest of the hill, the effects can be greater than one pixel, *e.g.* assuming that the hill is present in the 1943 photograph, the crest is displaced 11.4m from its true location relative to the 30m datum. Similarly, the displacement is 5.1m, 9.7m and 7.5m for the 1976, 1979 and 1986 images. These displacements are in the order of 1-2 pixels in all except the 1976 image. Selection of GCP's in this area should be avoided.

In this study, many of the GCPs used were located on road and stream intersections (Figure 5.8). If it is assumed that roads and streams usually run through areas of lower local elevation, *i.e.*, roads usually go around the base of hills and streams around major obstacles, then any relief displacement present would have been minimised. Some GCPs were also selected outside the Tuckers Flat Area. These may have been subject to more severe relief displacement but elevation data was not available for these sites.

Table 5.3: The relief displacement present in the aerial photographs over Tuckers Flat.

Date of Photography	Maximum Distance from Fiducial Point	Relief Displacement
1943	125mm	0.60m per 1m vertical
1976	80mm	0.38m per 1m vertical
1979	122mm	0.58m per 1m vertical
1986	50mm	0.33m per 1m vertical

There was no calculation of relief displacement for the 1988 image as no camera focal-length or aircraft flying altitude information could be obtained.

**Registration:** In this study, two aspects of registration accuracy must be considered; (1) the absolute error between cadastral data and imagery and (2) the relative error between individual images. The accurate assessment of the area covered by a land-cover class within a cadastral boundary is dependant on the registration of cadastral data to the individual image. In this study, no rms error assessment was made for the registration of the cadastral information to the 1976 base-image. This was because the draughted roads, not being an accurate representation of the real road network, prevented selection of accurate GCPs. However, the procedure of iteratively adjusting the transformation to visually align the road network with the imagery ensured that an accurate registration was obtained (Figures 5.10 and 5.11).

The accuracy of change detection is dependent on the registration error between images, *i.e.*, the reliability of viewing precisely the same area from both images, regardless of whether the area extracted is an accurate representation of the cadastral boundaries. For the image-to-image registration, calculation of the relative error indicated that the rms error across all images was 0.51 pixels or less (Table 5.4 and Appendix 1). However, the validity of rms error as a measure of registration accuracy is dependant on the number of GCPs used. When only four or five GCPs are used in a linear transformation, the calculation of error is limited to one or two points respectively. A complementary approach is to assess registration accuracy visually, by superimposing features, *e.g.* roads, from one image to the next. This procedure can be used to assess the effect of error across the whole image and identify areas where the registration is better or worse (Figures 5.12 to 5.16). This analysis confirmed that the image-to-image registration was sufficiently accurate to allow the same land parcel to be extracted from each image.

Table 5.4: The rms error between the 1943, 1979, 1986 and 1988 images and the 1976 base-image.

Date	Rms Error to 1976 Image	# GCP's
1943	0.44	5
1979	0.51	10
1986	0.36	8
1988	0.44	7

The simplification of the road network draughted on the cadastral data impeded the integration of the cadastral plan with the imagery. Although an image-to-image registration minimises error between images, in practice it would be preferable to rectify the imagery to a base map rather than another image. This would enable other rectified datasets, *e.g.* protected area boundaries or habitat surveys, to be included in the analysis. However, an image-to-map rectification requires an accurate, well-defined base map, *i.e.*, cadastral information plus locational references, at a scale similar to the proposed remote sensing data source (Smith *et al.*, 1994).

Nevertheless, it would have been difficult to register even an accurately draughted cadastral plan with the 1943 image because of insufficient GCP's. Often roads are the only feature drawn on plans to provide locational information and in many areas of Westland there is either little roading development, roads are not distributed across the imagery, or they have become disused and overgrown. Furthermore, considerable change can occur between the imagery being taken and preparation of a plan. In the case of the 1943 photograph, this was in excess of 30 years. Where gross change in land-cover has occurred, it will always be necessary to use an image-to-image registration.

A possible solution is to use the global positioning system (GPS) (van Diggelen, 1994). A GPS unit is able to retrieve coordinates for any location, thus not requiring the existence of a detailed map or cultural features, and is capable of positioning coordinates to sub-metre accuracy (van Diggelen, 1994). Many GPS units also provide elevation information which could be used in assessing relief displacement on GCPs. The drawback in a field station operation is cost, although this will decrease over time and suitable instruments with sub-metre accuracy can be purchased in 1995 for \$NZ6 000 - \$NZ26 000. A GPS unit was not available for use during this thesis.

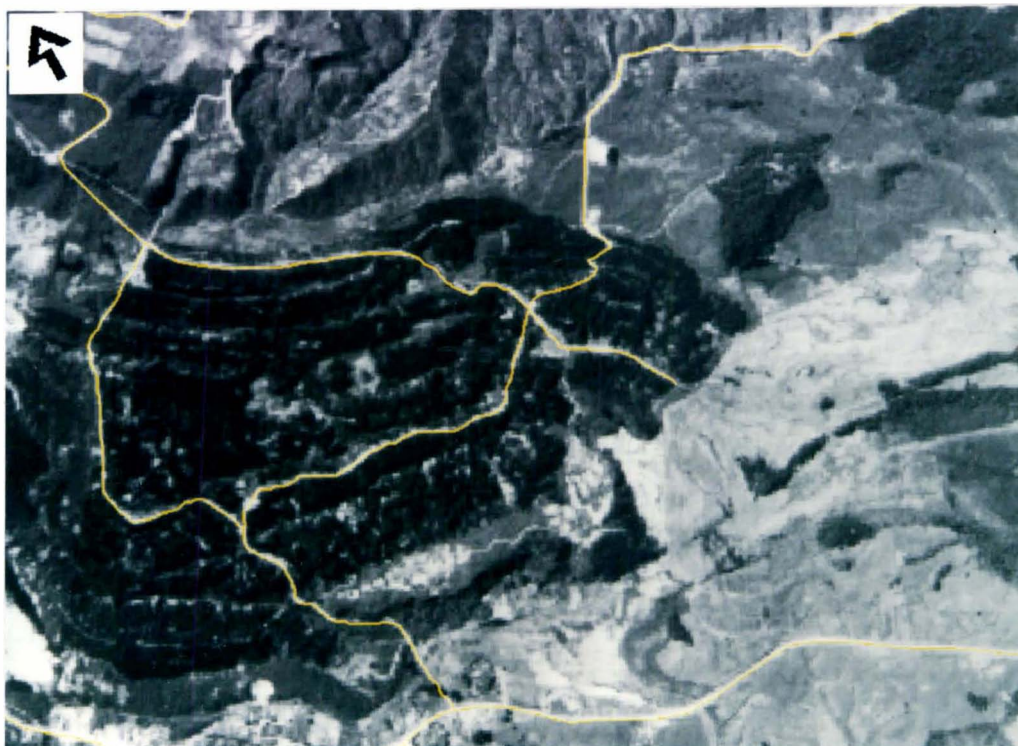


Figure 5.12: The 1976 image showing the roads (yellow) that were used to highlight errors in the image-to-image registration. Scale as printed in thesis 1:17 000.

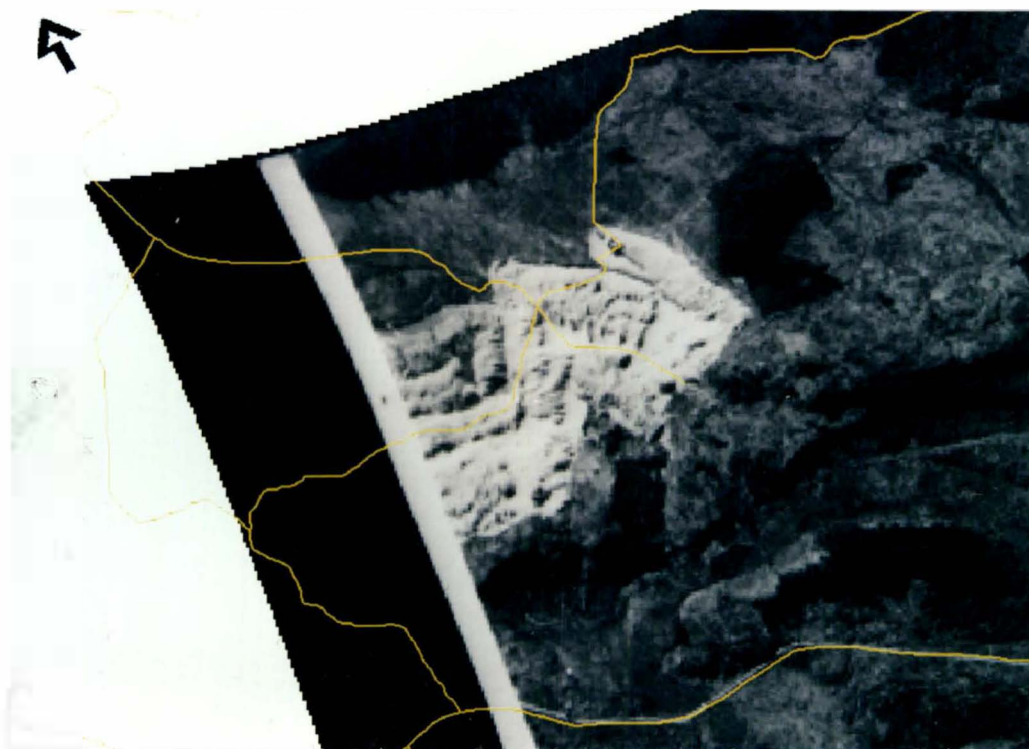


Figure 5.13: A test of the image-to-image registration accuracy - the 1943 image with roads from the 1976 base-image superimposed. Scale as printed in thesis 1:17 000.

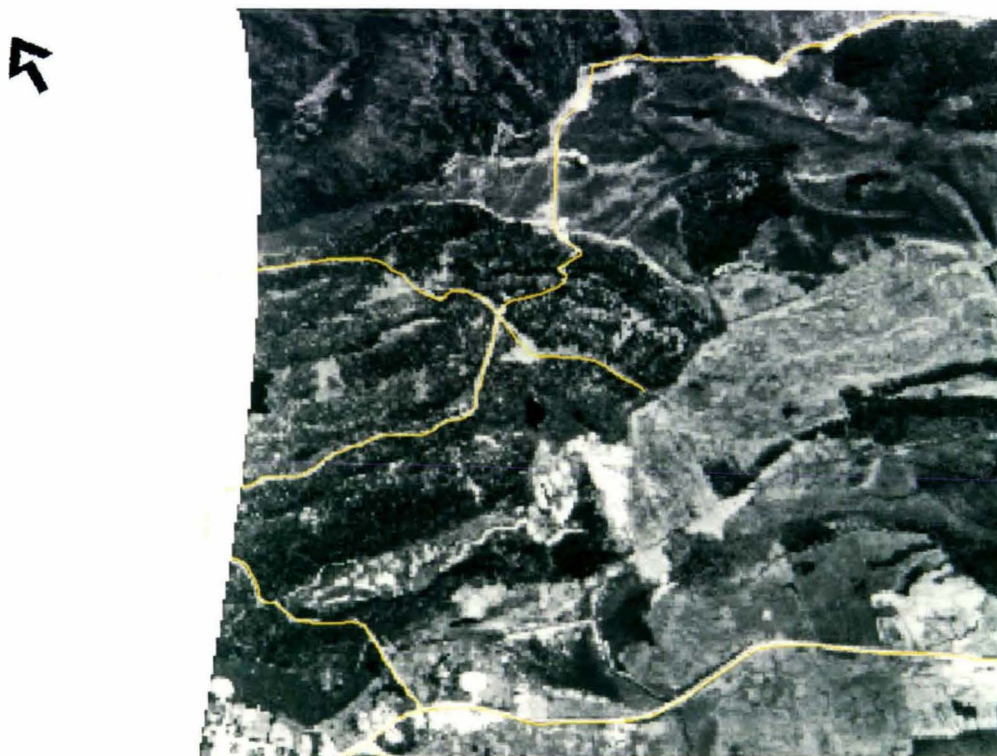


Figure 5.14: A test of the image-to-image registration accuracy - the 1979 image with roads from the 1976 base-image superimposed. Scale as printed in thesis 1:17 000.

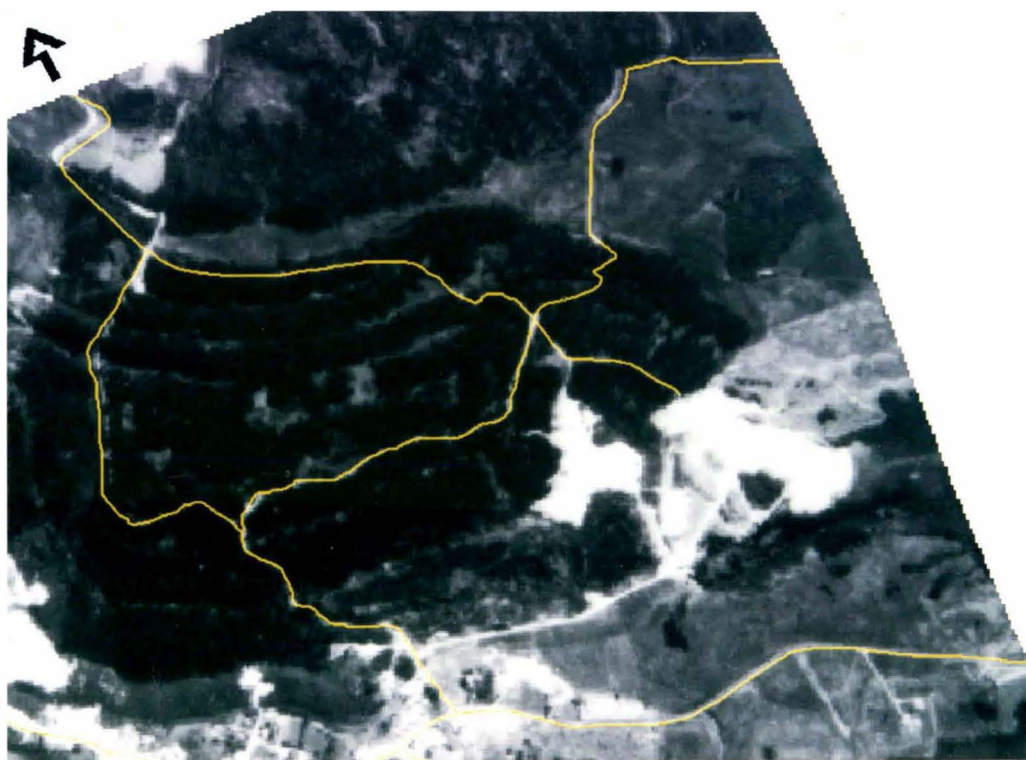


Figure 5.15: A test of the image-to-image registration accuracy - the 1986 image with roads from the 1976 base-image superimposed. Scale as printed in thesis 1:17 000.

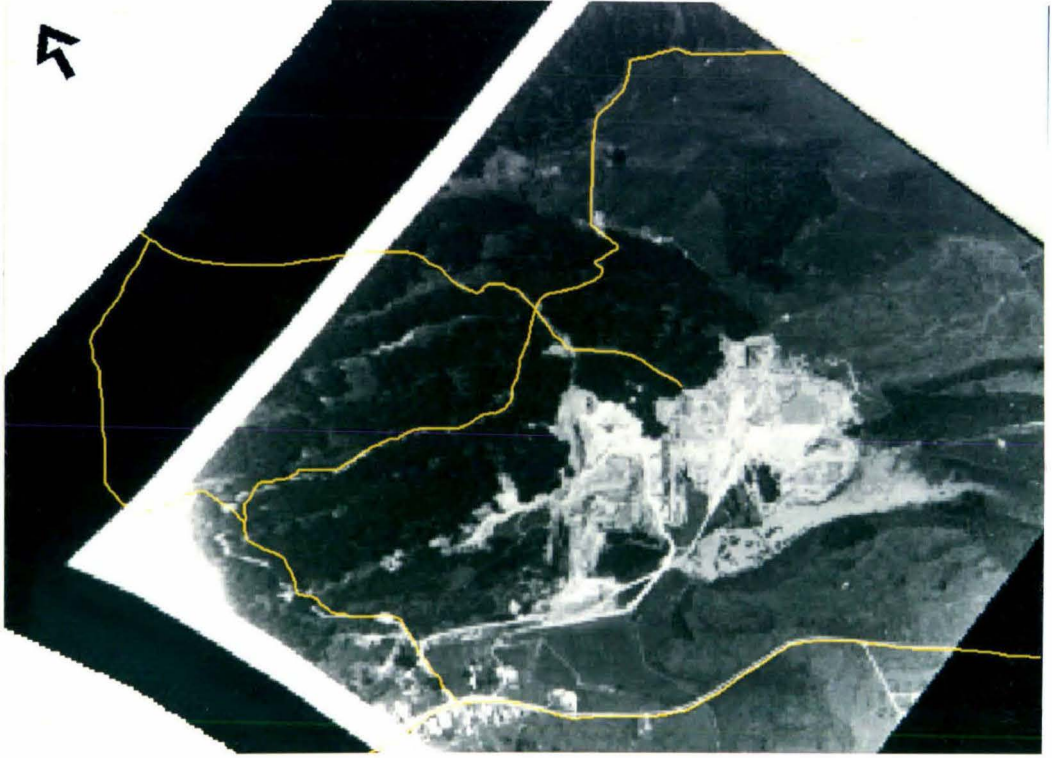


Figure 5.16: A test of the image-to-image registration accuracy - the 1988 image with roads from the 1976 base-image superimposed. Scale as printed in thesis 1:17 000.

**Classification:** The classified images for each date of photography are shown in Figures 5.17 to 5.21. An examination of the classified imagery and the quantitative information extracted shows that there has been a marked change between the amounts of the three land-cover classes in all land parcels (Table 5.5). Rural Section 4668 was the only parcel to be included entirely in all dates of photography. The areas shown in Table 5.5 have been rounded to the nearest tenth of a hectare.

Table 5.5: The area (ha) classified in each land-cover class for each year.

	Date of photography				
	1943	1976	1979	1986	1988
<b>State Forest Reserve 2106</b>					
Bare ground	10.3	0.0	2.5	0.0	1.9
Tree	0.3	60.4	26.3	67.6	25.9
Scrubland	26.1	29.9	22.4	22.7	21.1
<b>Total</b>	<b>36.7</b>	<b>90.3</b>	<b>51.2</b>	<b>90.3</b>	<b>48.9</b>
<b>State Forest Reserve 2149</b>					
Bare ground	33.0	2.6	9.0	5.6	17.0
Tree	6.9	38.6	40.4	43.2	40.3
Scrubland	21.0	38.1	29.0	30.5	22.0
<b>Total</b>	<b>60.9</b>	<b>79.3</b>	<b>78.4</b>	<b>79.3</b>	<b>79.3</b>
<b>Rural Section 4668</b>					
Bare ground	0.7	0.1	1.3	6.2	11.7
Tree	0.6	0.2	0.6	0.1	0.4
Scrubland	12.1	13.1	11.5	7.1	1.3
<b>Total</b>	<b>13.4</b>	<b>13.4</b>	<b>13.4</b>	<b>13.4</b>	<b>13.4</b>
<b>Gravel Reserve DP 1305</b>					
Bare ground	0.0	0.0	0.1	0.0	0.0
Tree	0.3	1.3	2.5	0.4	0.8
Scrubland	0.3	2.6	1.3	3.5	3.1
<b>Total</b>	<b>0.6</b>	<b>3.9</b>	<b>3.9</b>	<b>3.9</b>	<b>3.9</b>

*State Forest Reserve 2106:* It is evident in Figure 5.17 (1943) that there is extensive bare ground as a result of 1940's mining. In Figures 5.18 - 5.21, much of this area has been rehabilitated to *Pinus radiata* production forest through Government planting in the 1960's. Because of the spatial coverage of the photography, only the 1976 and 1986 images include all of State Forest 2106 with the other images showing approximately half the total area.

In the 1976 and 1986 images, no land was classified as bare ground. However, in the 1979 and 1988 images (Figure 5.19 and 5.21 respectively) approximately 2ha of land was identified as bare. This difference is attributed to the range of intensity values used to define each land-cover class on each image. The focus on classifying known areas of mined land accurately caused some features, especially roads, that were on the edge of the bare ground vs scrub discrimination to fluctuate between classes depending on the particular image. Also, small pockets of scrub that occupied intensity values inside the lower limit of the bare ground class could have been classified incorrectly as bare ground. Because State Forest 2106 is far away from the area of active mining in the post-1940s imagery, there was less emphasis applied to correctly distinguishing scrub from bare ground in this parcel.

There is a decrease in the amount of land classified as tree in the 1979 image (Figure 5.19). In addition, the distribution of the tree class is not as contiguous as for other years. This decrease is attributed to the silvicultural practice of thinning a production forest where the lower branches and some of the trees are removed. Because the thinned canopy is less dense, the land under the canopy is affecting the pixel's spectral signature, causing the pixel to be classified as scrub. The larger scale of the 1979 photograph (1:10 000) and therefore its ability to resolve more detail on the ground also contributes to this effect. However, a visual comparison with the unclassified 1976 photograph indicated that the decrease is probably caused by thinning more than a finer spatial resolution. This was confirmed verbally during visits to DoCs Westland Conservancy office. A resource manager familiar with the site could resolve issues such as this easily and could use the data to provide information on the degree of thinning.

*State Forest Reserve 2149:* This area also has a significant covering of *Pinus radiata* forest covering tailings from earlier mining. The discussion of the effects of silvicultural thinning operations in State Forest 2106 is also applicable here. The amount of bare ground decreased to 2.6ha in the 1976 image, but increased again to 17ha in 1988. Given the location of the bare ground around areas of previous mining, it is clear that the increased bare ground is attributable to mining activities.

*Rural Section 4668:* This parcel has been the subject of most of the present-day mining activities. It is the only area to be covered completely in each image. There has been an increase in the amount of bare ground from 0.7 ha in 1943 to 11.7 ha in 1988. Notably the majority of the increase occurred between 1986 and 1988, which supports a recorded increase in gold mining activity in the late 1980s (Metcalf and Godfrey, 1990). The amount of tree cover (probably native vegetation) has remained relatively the same, but the

amount of scrubland has decreased dramatically, *i.e.* from 1943 there has been a 10.8ha decrease in the area of scrub which represents 90% of the area classified in 1943. This change indicates a conversion of scrub into mined areas.

*Gravel Reserve DP 1305:* This parcel was the smallest in size at 3.9ha. The imagery shows that the areas of scrub and tree vary through the years. However visual inspection of the unclassified imagery shows that the change is attributable to small variations in an individual image's classification rather than a real change. For an area designated as a gravel reserve, it is notable that only in the 1979 image was a significant amount of land classified as bare ground (0.1 ha).

**Classification accuracy:** A confusion matrix for each classified image is presented in Tables 5.6 through 5.10. All classifications achieved overall accuracies above 85%, with the 1943, 1986 and 1988 classifications scoring above 90%. The Kappa coefficients signify that the results are 87.5%, 74.7%, 75.4%, 90.4% and 85.0% better than what would be expected if the pixels were assigned randomly to the classes.

Errors in the classification are attributed to the difficulty of maintaining representative class thresholds across the whole image. The training statistics for the bare ground class were developed from sites in known areas of mining. However, the statistics were not representative over the entire image, causing pockets of scrub in other parts of the image to be included with the bare ground class. In addition, on the left margin, and in the corners of the 1988 photograph (Figure 5.7), a general increase in the overall brightness can be observed. The effect, which occurred probably during development of the photographic film, caused some trees in State Forest 2106 to be classified as scrub.

Possible approaches for a resource manager to minimise classification error are to partition the image into a number of smaller images where the intensity value range for a class is well-defined, *e.g.* land tenure boundaries. Because the classification is restricted to a defined parcel, this will remove the errors caused by focusing on the correct classification of bare ground in other parcels. This technique may also be sufficient to remove the effect of silvicultural thinning. However, partitioning may not remove the errors completely and, depending on the degree of subdivision, may require too many classifications to make it a practical option. An alternative is to use manual classification and digitise class boundaries off the screen directly. The limitation of this approach is that boundary definition is subjective and only as reliable as the operator's patience and mouse control.

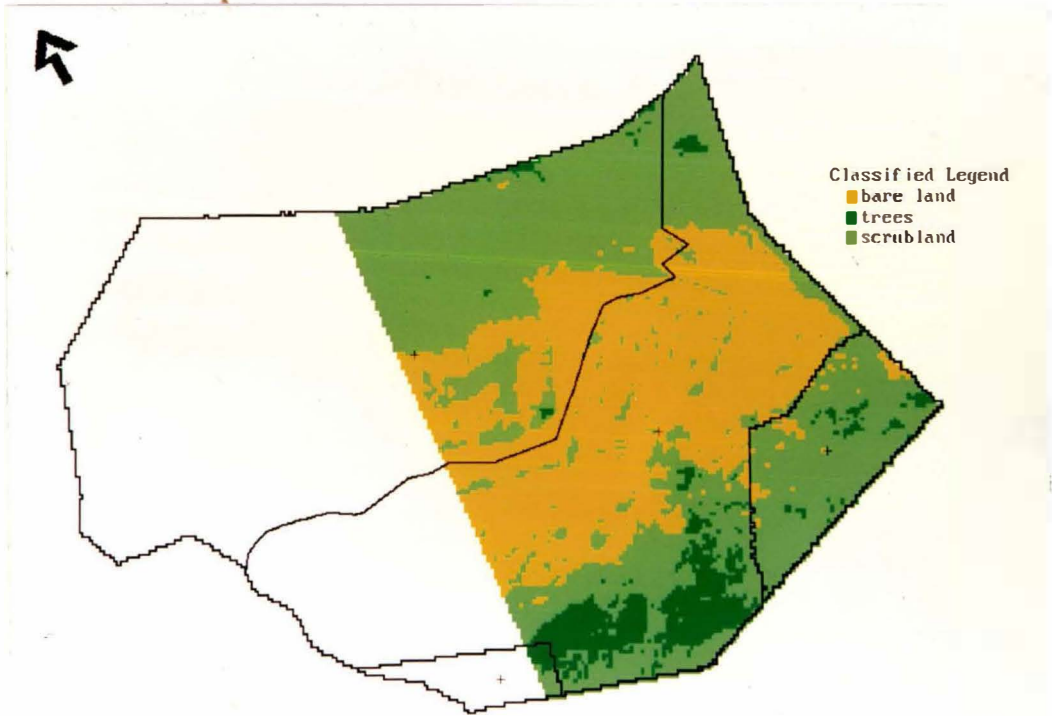


Figure 5.17: The classified image derived from the 1943 photograph showing the location of the bare land, tree and scrub classes. Scale as printed in thesis 1:15 000.

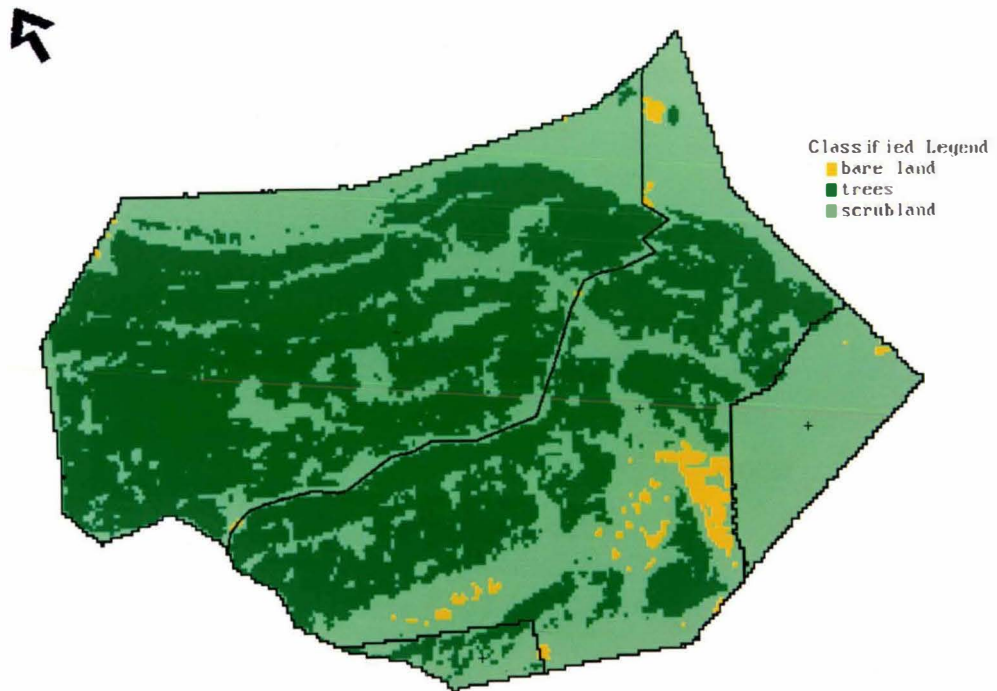


Figure 5.18: The classified image derived from the 1976 photograph showing the location of the bare land, tree and scrub classes. Scale as printed in thesis 1:15 000.

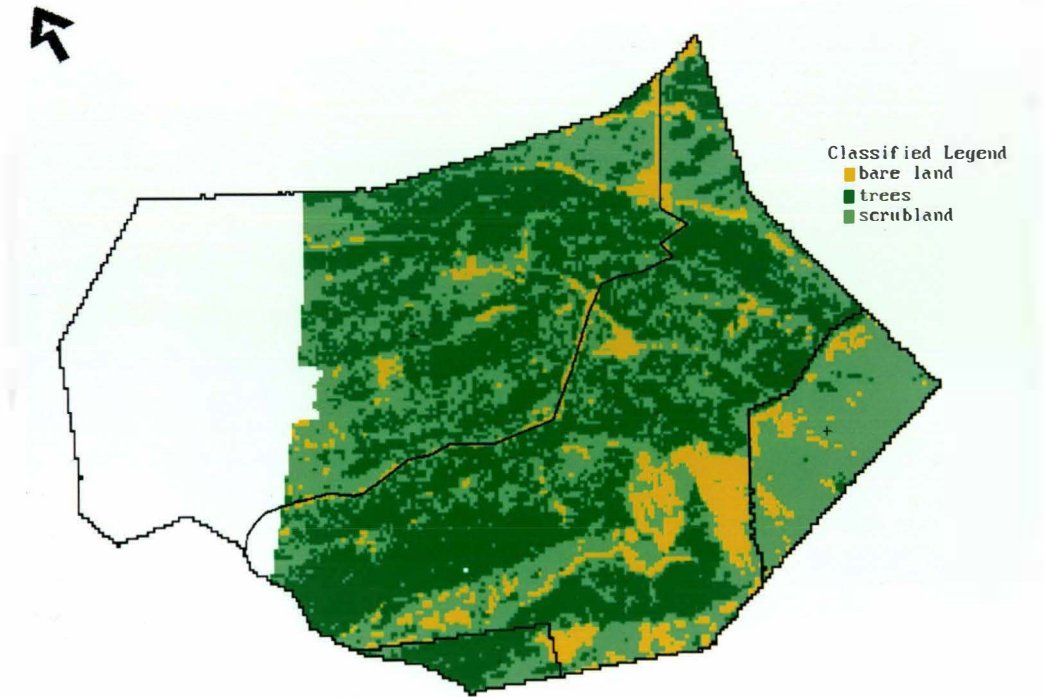


Figure 5.19: The classified image derived from the 1979 photograph showing the location of the bare land, tree and scrub classes. Scale as printed in thesis 1:15 000.

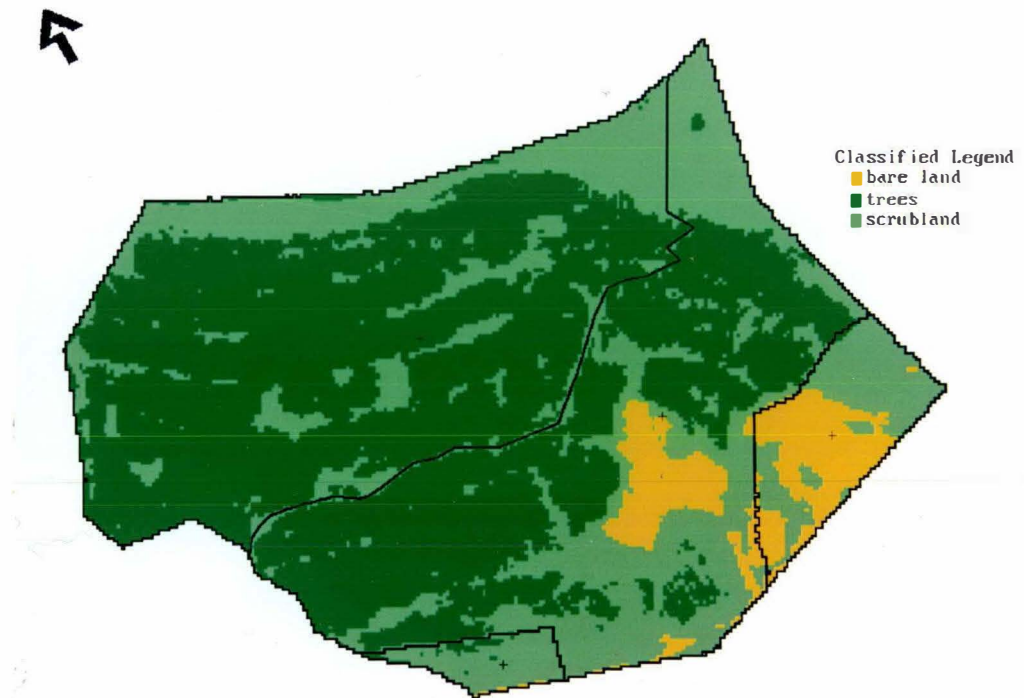


Figure 5.20: The classified image derived from the 1986 photograph showing the location of the bare land, tree and scrub classes. Scale as printed in thesis 1:15 000.

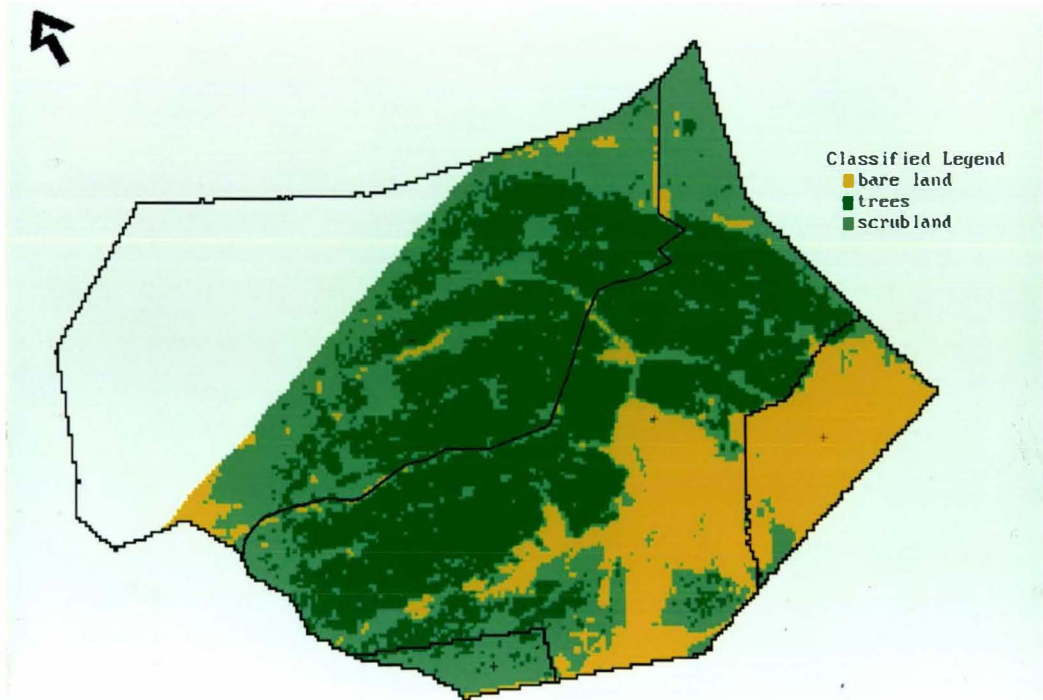


Figure 5.21: The classified image derived from the 1988 photograph showing the location of the bare land, tree and scrub classes. Scale as printed in thesis 1:15 000.

Table 5.6: A confusion matrix showing the number of pixels classified as each class for the 1943 classified image. The diagonal represents correct classifications.

Image Class	Reference Class			
	Bare	Trees	Scrub	Total
Bare	38	0	6	44
Trees	0	7	0	7
Scrub	1	0	48	49
Total	39	7	54	100

Overall accuracy = 93 %: Kappa = 0.875

Table 5.7: A confusion matrix showing the number of pixels classified as each class for the 1976 classified image. The diagonal represents correct classifications.

Image Class	Reference Class			
	Bare	Trees	Scrub	Total
Bare	1	0	0	1
Trees	0	51	2	53
Scrub	4	7	35	46
Total	5	58	37	100

Overall accuracy = 87 %: Kappa = 0.747

Table 5.8: A confusion matrix showing the number of pixels classified as each class for 1979 classified image. The diagonal represents correct classifications.

Image Class	Reference Class				
		Bare	Trees	Scrub	Total
Bare		9	0	0	9
Trees		0	46	2	48
Scrub		3	9	31	43
Total		12	55	33	100

Overall accuracy = 86 %: Kappa = 0.754

Table 5.9: A confusion matrix showing the number of pixels classified as each class for the 1986 classified image. The diagonal represents correct classifications.

Image Class	Reference Class				
		Bare	Trees	Scrub	Total
Bare		6	0	0	6
Trees		0	59	0	59
Scrub		1	4	30	35
Total		7	63	30	100

Overall accuracy = 95 %: Kappa = 0.904

Table 5.10: A confusion matrix showing the number of pixels classified as each class for the 1988 classified image. The diagonal represents correct classifications.

Image Class	Reference Class				
		Bare	Trees	Scrub	Total
Bare		29	0	0	29
Trees		0	35	0	35
Scrub		0	10	26	36
Total		29	45	26	100

Overall accuracy = 90 %: Kappa = 0.850

*Change detection:* The images resulting from the independent-classification change detection are shown in Figures 5.22 through 5.25.

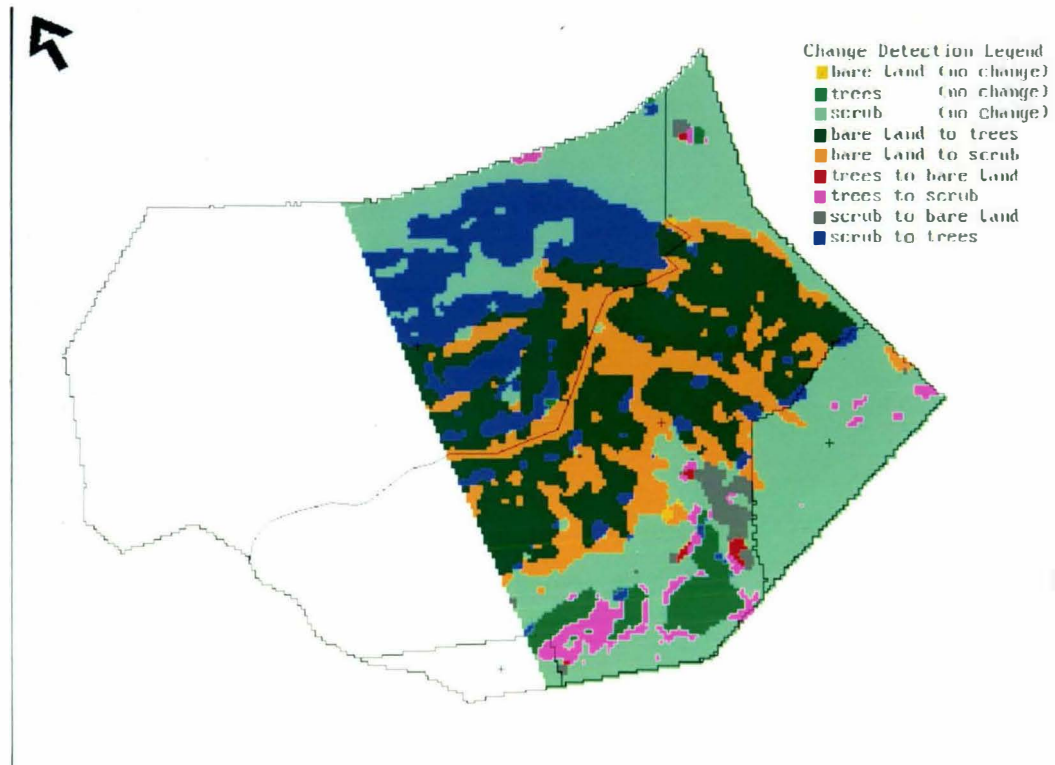


Figure 5.22: An image showing the change in location of the bare ground, tree and scrub classes between the 1943 and 1976 classified images. Scale as printed in thesis 1:15 000.

*1943 to 1976 (Figure 5.22):* This image shows that little of the land classified as bare ground in 1943 remains in 1976. Much of this area had been revegetated either as *Pinus radiata* production forest or as scrub. There are also large areas where the scrub has been converted into forest as part of the Government planting. Without referring to the unclassified imagery and site knowledge, it is impossible to distinguish whether change from trees to scrub is a result of native forest clearance or due to the different classifications in each year.

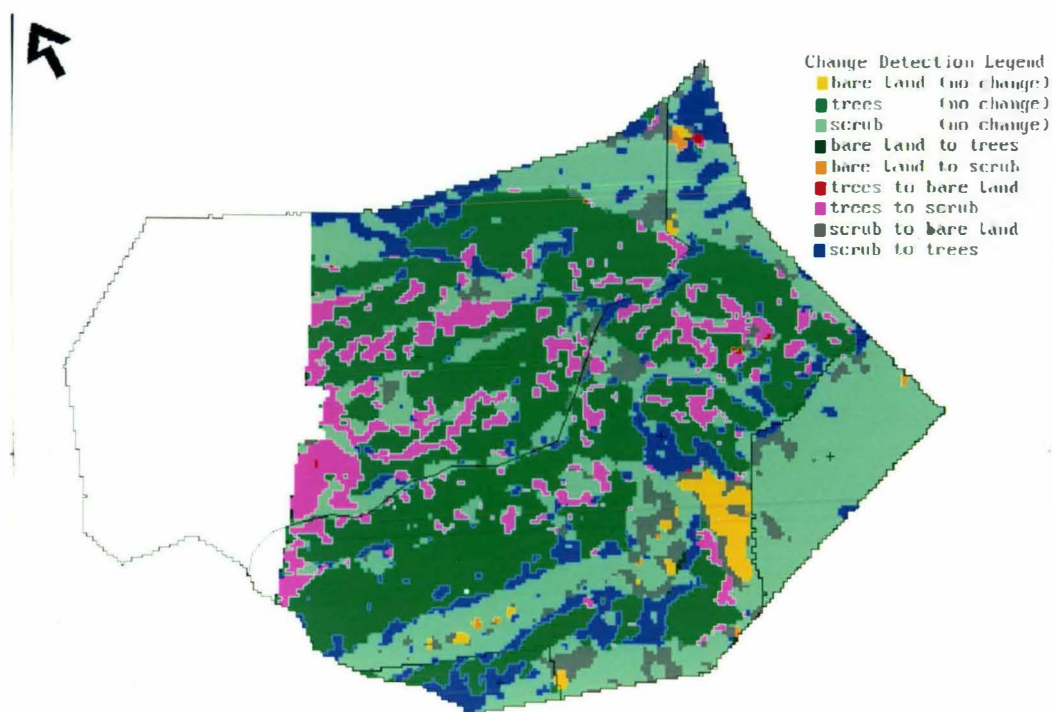


Figure 5.23: An image showing the change in location of the bare ground, tree and scrub classes between the 1976 and 1979 classified images. Scale as printed in thesis 1:15 000.

*1976 to 1979 (Figure 5.23):* The dominant feature in this image is the change from trees to scrub interspersed with areas of no change in the tree class. This shows the effects of silvicultural thinning in the production forest. There is also a change from scrub to trees in many areas which coincide with the tree to scrub change of Figure 5.22. This information indicates that the change identified in Figure 5.22 was probably not a real change in land-cover but a result of different classifications in each image. There are also areas which indicate a change from scrub to bare land. However, this change must be interpreted in relationship to where the change is occurring. For example, if the change occurs on a road, it is likely to be a result of different classifications, but in an area of active mining, it may well represent a real change in land-cover.

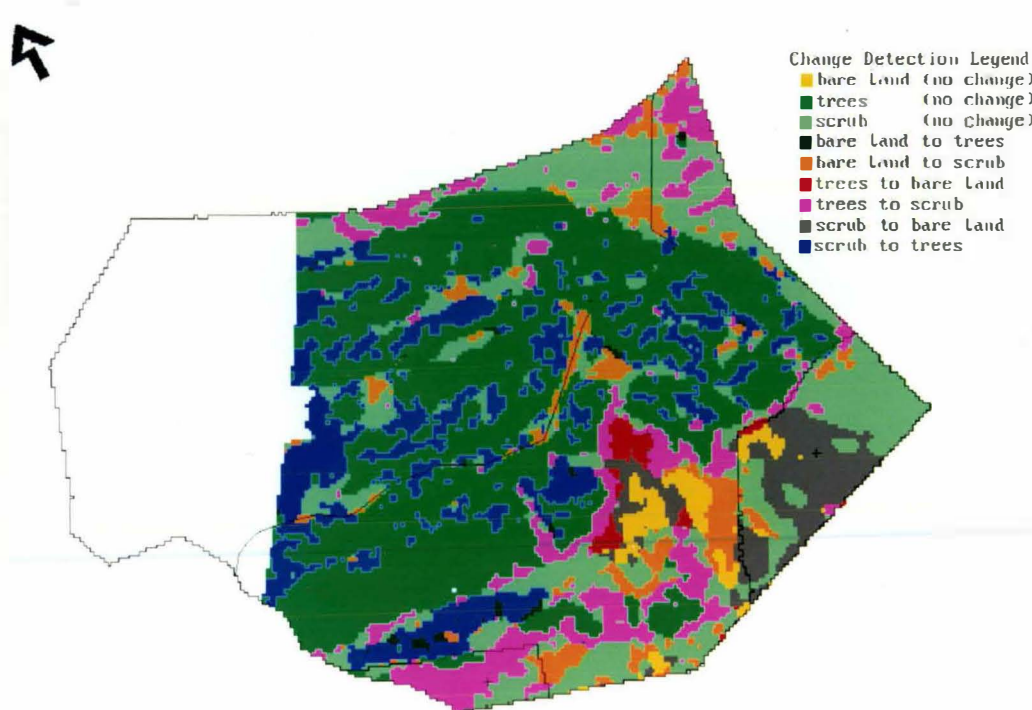


Figure 5.24: An image showing the change in location of the bare ground, tree and scrub classes between the 1979 and 1986 classified images. Scale as printed in thesis 1:15 000.

*1979 to 1986 (Figure 5.24):* In the area of the production forest, much of the change from trees to scrub in the previous image is replaced by change from scrub to trees. While this may indicate a land-cover change, another reason is a thickening of the forest canopy after thinning. The effect of the original photograph scale, 1:10 000 for the 1979 print, and 1:50 000 for the 1986 print would also contribute to this result, with the smaller areas of scrub between the trees not being resolved on the 1986 image. The image shows an area of scrub to bare ground change in Rural Section 4668 which is related to an increase of mining in the mid-1980's.

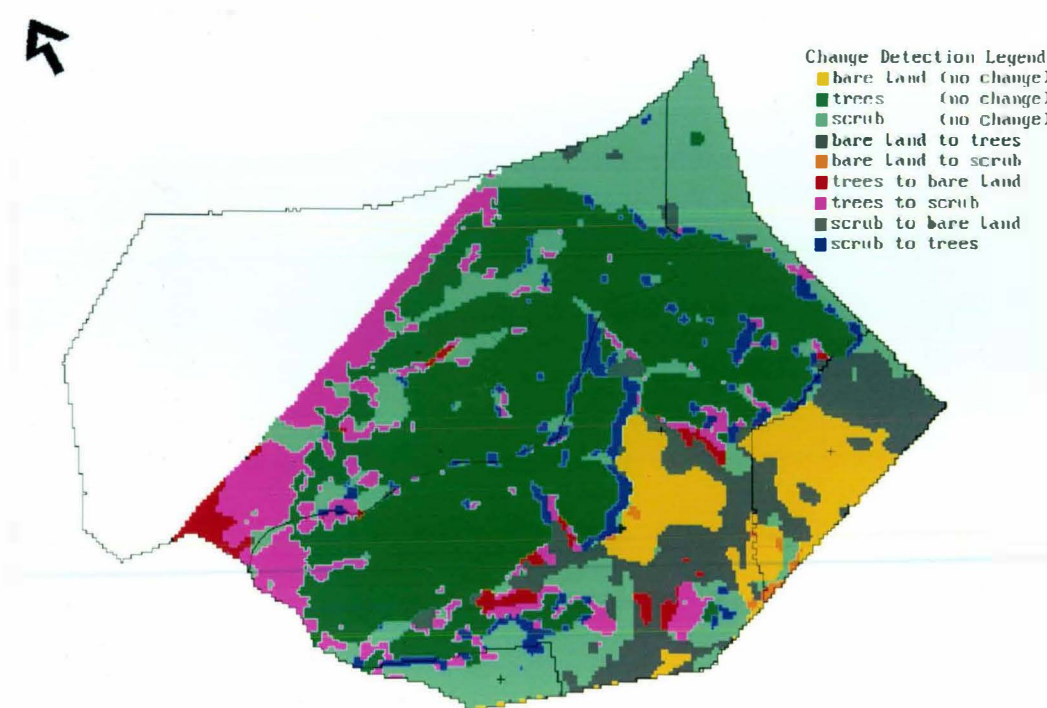


Figure 5.25: An image showing the change in location of the bare ground, tree and scrub classes between the 1986 and 1988 classified images. Scale as printed in thesis 1:15 000.

*1986 to 1988 (Figure 5.25):* This image is notable for the large homogenous areas compared with the other change detection images. There is a large increase in the area of bare land in the lower half of the image, especially in Rural Section 4668, which can be attributed to an increase of mining in this area.

While not affecting the classification accuracy of the 1988 image significantly, the effect of a general increase in intensity values on the left side of the 1988 photograph is evident in the change image. The classification error has been propagated through the change detection and is evident as areas of spurious change, *i.e.* a false change from trees to scrub and trees to bare land. This image demonstrates again how site knowledge is a necessity for sensible interpretation of change detection imagery.

**Change detection accuracy:** The accuracy of an independent-classification change detection is reliant on the registration accuracy and the accuracy of the independent classifications. An estimate of the accuracy of the change detection images was obtained by multiplying the individual classification accuracies (Stow *et al.*, 1980) (Table 5.11). It

is difficult to say whether the accuracies achieved are acceptable, as this will depend on the purpose of the analysis and the resource manager involved.

Table 5.11: An estimate of the overall change detection accuracy. The fourth column is the result of multiplying the two classification accuracy columns.

Image	Classification accuracy date 1	Classification accuracy date 2	Accuracy of the change image
1943 - 1976	93%	87%	81%
1976 - 1979	87%	86%	75%
1979 - 1986	86%	95%	82%
1986 - 1988	95%	90%	86%

The study has indicated how possible areas of spurious change can be identified by examining subsequent change detection images. Spurious change may be evident as areas of land which alternate between opposing change categories, *i.e.* an area is shown as change from tree to scrub in image 1 and scrub to tree in image 2. However, there is also the possibility that an alternating change over a long time represents a real change in land-cover, *e.g.* scrub has been cleared to bare ground and has subsequently reverted back to scrub. This confirms the need for in-depth site knowledge if classified imagery and change detection images are to be interpreted sensibly (Jensen, 1985; Fung and LeDrew, 1987). Once possible areas have been identified and verified with the original photography, they could be removed and a new change-image created, leaving only those areas which showed a consistent and logical change. The comprehensive photographic archives available to resource managers in DoC, Westland Conservancy means that this would be a practical technique to apply in historical resource management studies.

**Presentation to resource managers:** A presentation of image processing software and the study of Tuckers Flat was made to resource managers in the Draughting Office of DoC Westland Conservancy. A formal survey of opinion was not instigated, but from a series of informal discussions, the staff showed a keen interest in the capabilities of a digital image processing system and could see many other immediate applications. However, they could also see problems in implementing such a system because; (1) they lacked basic PC hardware to perform many other tasks let alone image processing, (2) they did not feel that senior management were supportive of the funding required to purchase the necessary software and hardware (Nicol, 1993), (3) many did not feel confident with the level of computing or image processing knowledge required and (4) they would have to make time to learn new skills when there were already large amounts of work to be done.

## 5.5 Summary

The application of a PC-based digital image processing system to provide resource management information for alluvial gold mining operations was investigated. The study used black-and-white aerial photography which was digitised and processed to create classified images showing the area of bare ground, scrub and trees. Cadastral boundaries of land tenure parcels within Tuckers Flat were digitised from a DoC plan, registered with the photography and used to extract specific land tenure parcels from the digital images. The area of each land-cover class in each parcel was obtained from the classified imagery. The classified images were processed in an independent-classification change detection analysis to indicate where there had been changes in land-cover between dates of photography.

Registration of the cadastral information to imagery and the selection of representative training data for image classification require further attention. The cadastral data was difficult to register to the imagery simply because the roads drawn on the plan did not represent the real shape and position of the road network. Although this may not be representative of other cadastral plans held by DoC, it is of concern because in many remote sensing applications, roads are the only feature in common between the imagery and base data, and are therefore the only features suitable for using as GCPs. While a level of abstraction may be acceptable for schematic plans, it is not if the data is to be used in a digital image processing or GIS analysis. In future, thought must be given to this at compilation of the cadastral plan.

For an individual land-cover class, it was difficult to select a range of intensity values that was representative over the whole image. This was because the classification was focused on determining the area of bare ground, *i.e.*, mined land in areas of known mining. Additionally there were errors caused by silvicultural thinning of the forests, and the effects of film processing. To reduce classification error, the resource manager may use simple techniques such as partitioning the image into a number of smaller areas prior to classification, or digitise class boundaries directly off the screen, although each of these approaches has limitations. The manager may also rely on site knowledge to explain the effects caused by thinning operations.

Although the extent of error in the individual classifications was not obvious in the confusion matrices or classified images, the errors were recognisable in the change detection imagery. Examination of subsequent change detection images demonstrated how possible areas of spurious change could be identified as areas of land alternating between

opposing change classes. This makes a second change-detection image a valuable tool to rapidly identifying possible areas of spurious change and confirms the need for in-depth site knowledge if classified imagery and change detection images are to be interpreted sensibly.

The requirement for detailed site knowledge compels that the image processing specialist works closely with the resource manager or that the resource manager performs a portion of the image processing themselves. In a field-office environment in Westland, it is unlikely that the funding to employ a full-time image processing specialist will be available. This dictates that resource managers must either contract specialist remote sensing agencies or become conversant with digital image processing. From visits to the DoC Westland Conservancy office, the feedback suggested that resource managers were enthusiastic about digital image processing and could see many immediate applications. However, organisational difficulties due to funding, skill shortages and staff workloads made implementing in-house image processing systems, even those based on low-cost PC hardware unlikely at the present time.

## 6: INDIGENOUS FORESTRY: SALTWATER ECOLOGICAL AREA

### 6.1 Study Objective

An objective of this thesis was to investigate how information beneficial to management of indigenous forest resources can be obtained through the use of GIS and digital image processing of satellite imagery. This study, in the Saltwater area near Harihari, was prompted by DoC to investigate how digital image processing of satellite imagery could be used in updating vegetation maps.

### 6.2 Site Description

The study area is sited in the Saltwater Forest and Saltwater Ecological Area (SEA) located approximately 60 km south of Hokitika, at approximately 170°28'E and 43°05'S (NZ Map Grid 2295000 5785000) (Figures 3.1 and 6.1). In this study, only SEA was investigated, however the following physical description relates to both SEA and Saltwater Forest.

The elevation ranges from approximately 50 to 200 metres a.s.l. The climate is damp with a mean annual precipitation at the nearest climate station (Lower Whataroa) of 3564mm. The landscape is dominated by a post-glacial alluvial plain between the Poerua and Hinatua Rivers and older glacial moraines and outwash surfaces to the south. Although the exact ages of these landforms are unknown, some moraine features are likely to pre-date the last major period of valley glacier expansion (Norton and Leathwick, 1990). Soils typical of this area are imperfectly drained yellow-brown earths on better drained slopes that become increasing gleyed with lower angles of slope. Podzols are present on levees and terraces, with poorly drained organic and peaty gley soils occurring in the backswamps (Almond, 1986). There are 4 mires which have formed in depressions in the plain between the Poerua and Hinatua rivers.

The vegetation is characterised as a podocarp-broadleaved forest (McKelvey, 1984; Poole and Johns, 1992) (Figure 6.2). The predominant species include rimu (*Dacrydium cupressinum*), kamahi (*Weinmannia racemosa*) and silver pine (*Lagarostrobos colensoi*). There are also patches of kahikatea (*Dacrocarpus dacrydioides*) on the floodplain of the Poerua River. The relative dominance of the different species depends on the soil drainage conditions and the age of the surface. The sedge/fern/restiad communities typical of the mires are similar to other infertile surfaces in Westland (Norton, 1989). The mires are known locally as pakihi (Figure 6.3)

Figure 6.1: A location map of Saltwater Ecological Area and Saltwater Forest.

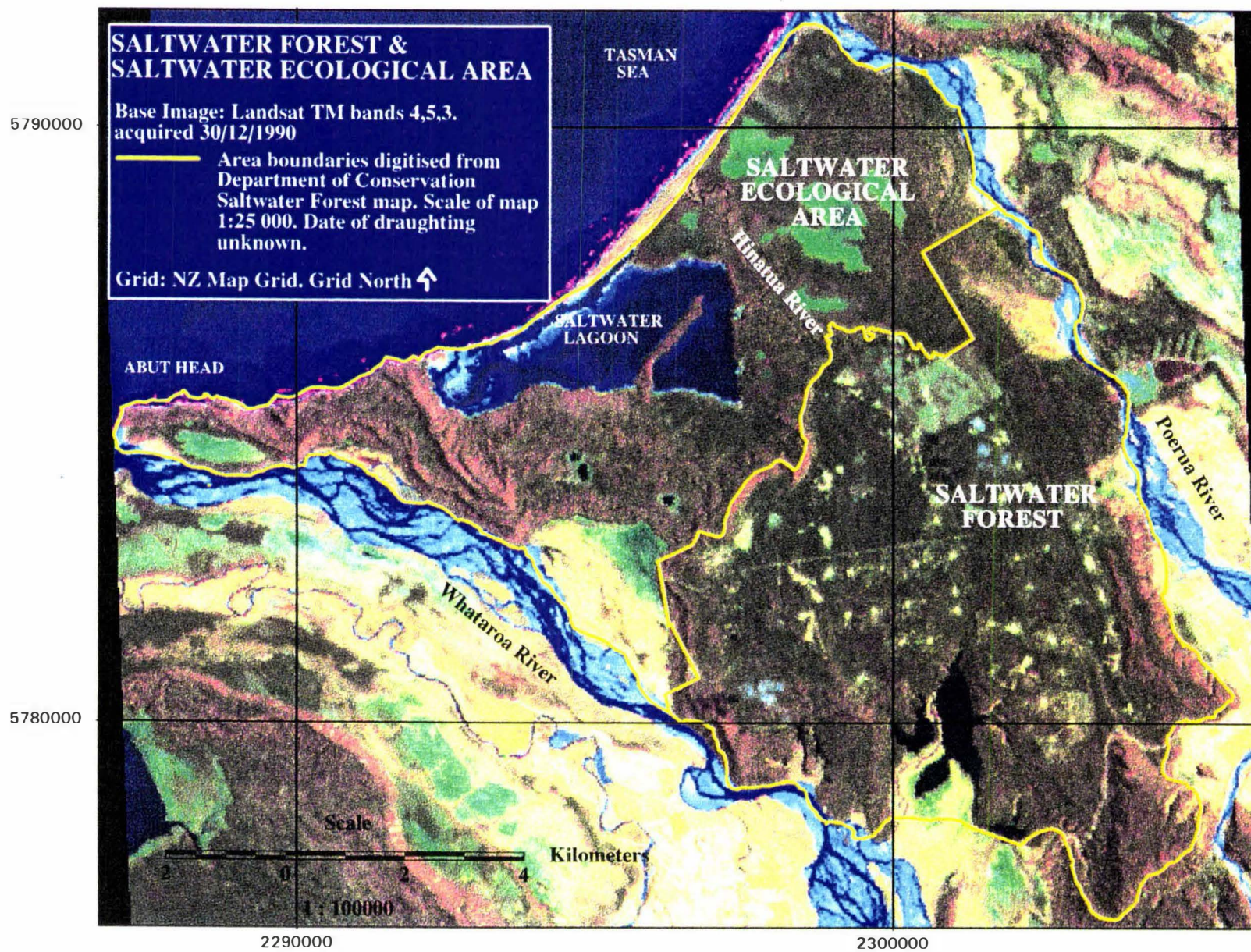




Figure 6.2: A road leading into Saltwater Ecological Area through Saltwater Forest. The road runs right through the dense, predominantly rimu, forest on either side (photo L. J. Brown)



Figure 6.3: One of the pakihi areas in Saltwater Ecological Area. Wire rush (*Empodisma minus*) is dominant in the foreground. The pakihi is bordered by forest where manuka (*Leptospermum scoparium*) is the dominant canopy species. This changes to rimu-dominated forest further from the pakihi (photo L. J. Brown).

### 6.3 Methodology

**Imagery:** The study used both SPOT XS and Landsat TM imagery. The SPOT XS image used had been acquired on August 1, 1988 at 10:30am New Zealand time (Figure 6.4). The sun elevation angle at the time of image acquisition was 22°. The 60x60 km extent of the image included from the Wanganui River in the north, to the Waiho River in the south, and from the coast inland to the Southern Alps.

The Landsat TM image used had been acquired on December 30, 1990 (Figure 6.5). The sun elevation angle at the time of image acquisition was 59°. The extent of this image covered from the Taramakau River in the north, to the Paringa River in the south, and from the west coast across the Southern Alps to Lakes Tekapo and Heron.

**Map Data:** A vegetation community map of SEA prepared by Norton and Leathwick (1990) was used as ground data (Figure 6.6). The map was derived from a field survey of 127 plots in the summer of 1984/1985. The plots were 500m<sup>2</sup> in area, located at 457 metre intervals along east-west transects 914 metres apart. Cover abundance was recorded for all plant species up to six height strata. The major species present included rimu, kahikatea, kamahi, silver pine, mountain toatoa (*Phyllocladus alpinus*) and manuka (*Leptospermum scoparium*). Wire rush (*Empodisma minus*), *Dracophyllum* and tangle fern (*Gleichenia dicarpa*) were dominant species in the pakihi.

Norton and Leathwick (1990) applied a polythetic divisive technique of indicator species analysis (Hill *et al.*, 1975) to classify the plots into vegetation communities. Indirect ordination of plots and species was performed simultaneously using detrended correspondence analysis (Hill and Gauch, 1980). This generated ten communities, the naming of which follows the system proposed by Atkinson (1985). The following description of the communities is summarised from Norton and Leathwick (1990). The number of each community is referred to in Figure 6.6.

1: Kahikatea is the dominant emergent conifer, with occasional matai (*Prumnopitys taxifolia*) present. Kamahi is the dominant subcanopy species. This community is dominant on the recent alluvial surfaces close to the Poerua River. There are frequent areas of standing water.

2: Scattered tall emergent kahikatea over a diverse shrub layer. This community is also found on the recent alluvial soils close to the Poerua River.

3: Dense canopy dominated by kamahi with rimu and miro occurring as scattered trees (less than 10%). This community is most common in the southern part of the study area where the terrain is hilly and there is good drainage.

4: Canopy dominated by kamahi. More rimu present compared with community 3 and in contrast to community 3 is found on generally flat terrain mainly between the Poerua and Hinatua Rivers.

5: Canopy dominated by rimu with a subcanopy dominated by kamahi. This community is mainly found on a glacial outwash surface between the Hinatua River and the Saltwater Lagoon.

6: Canopy of silver pine and mountain toatoa with scattered emergent rimu. This community is mainly found in the poorly-drained sites on the edge of pakihi.

7: Canopy dominated by manuka with scattered kahikatea above. This community was found in poorly drained areas.

8: Manuka is the dominant canopy species with scattered rimu above. The community occurs marginal to the large pakihi where there is poor drainage.

9: Scattered to dense scrub cover of manuka, wire rush and tangle fern. This community occurs around the edge of the pakihi, adjacent to open water.

10: Dense sward of wire rush and tangle fern is common. The community is dominant on the open areas of the pakihi.

Norton and Leathwick (1990) omitted communities 6 and 7 from the map due to them being of small areal extent or dispersed within other communities.

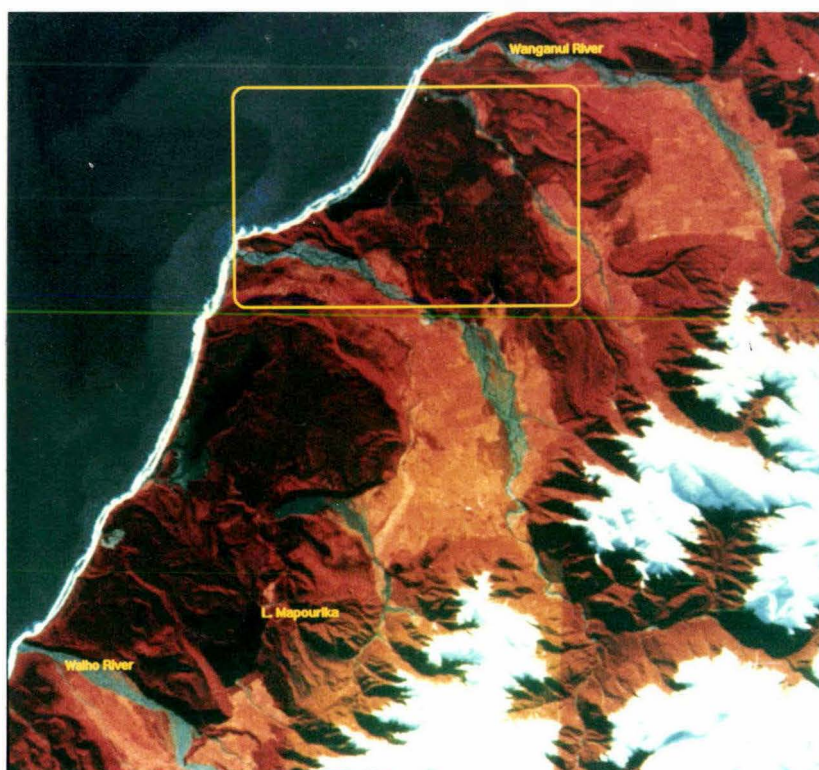
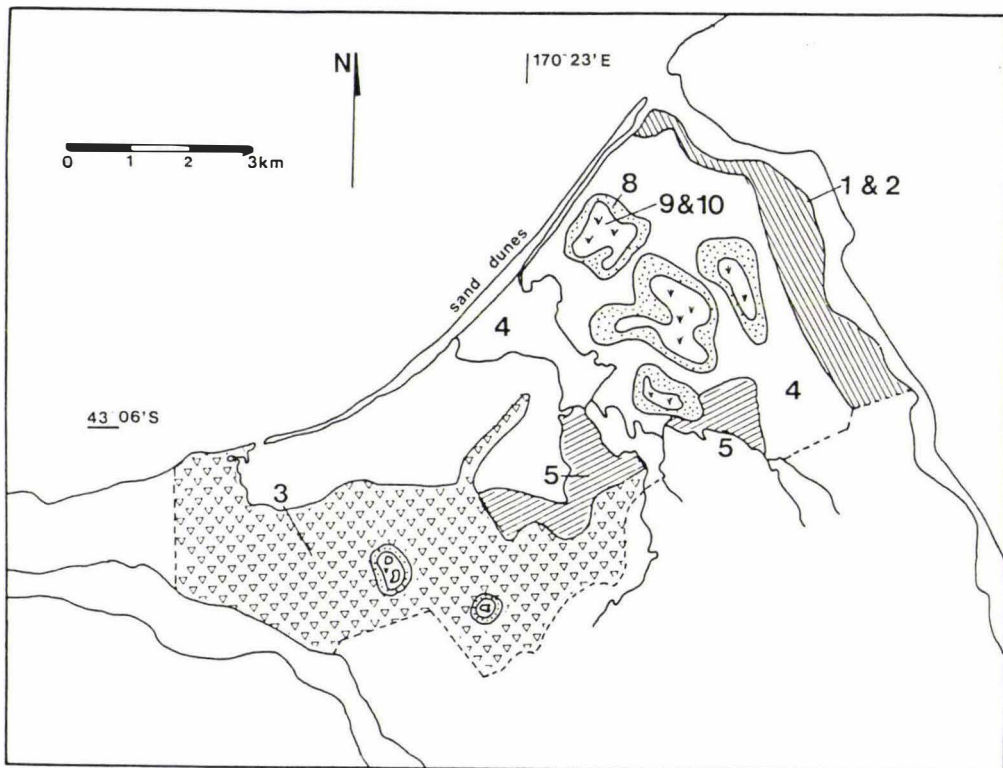


Figure 6.4: A band 3,2,1 (RGB) composite of the SPOT XS image. The location of Saltwater Forest and Saltwater Ecological Area is shown by the yellow rectangle. Scale as printed in thesis 1:450 000.



Figure 6.5: A band 3,2,1 (RGB) composite of the Landsat TM image. The location of Saltwater Forest and Saltwater Ecological Area is shown by in the yellow rectangle. Scale as printed in thesis 1:1 100 000.



Abbreviated legend of the dominant species in each community: 1=kahikatea, 2=scattered kahikatea, 3=dense kamahi, 4=kamahi/rimu, 5=rimu, 6=silver pine/mountain toatoa, 7=manuka/kahikatea, 8=manuka/rimu, 9=manuka/wire rush/tangle fern, 10=wire rush/tangle fern.

Figure 6.6: Norton and Leathwick's (1990) vegetation map of Saltwater Ecological Area.

**Image Classification:** Only the communities portrayed separately on the vegetation map were used in the image classification. Communities 1 and 2 were aggregated as were communities 9 and 10 because they had similar vegetation composition and occupied the same area on the map. Although communities 3 and 4 both had a canopy dominated by kamahi they were included as separate classes to determine if there was sufficient rimu in the canopy of community 4 for it to be discriminated. In this study, each community on the map, except communities 6 and 7, is referred to by the predominant canopy species, *i.e.* kahikatea (1,2), kamahi (3), kamahi/rimu (4), rimu (5), manuka (8) and wire rush (9,10).

For each image, training data sample sites were located where areas that corresponded to the mapped vegetation communities could be observed. Within these areas, the sample sites were located where the imagery appeared relatively homogenous. Several small samples were distributed within each area (Figures 6.7 and 6.8). The same training sites were not used for each image. This approach was taken to achieve the highest possible mapping accuracy for the individual images. The separability of the classes was assessed through a trial classification (Smith *et al.*, 1994) using the training data as the reference.

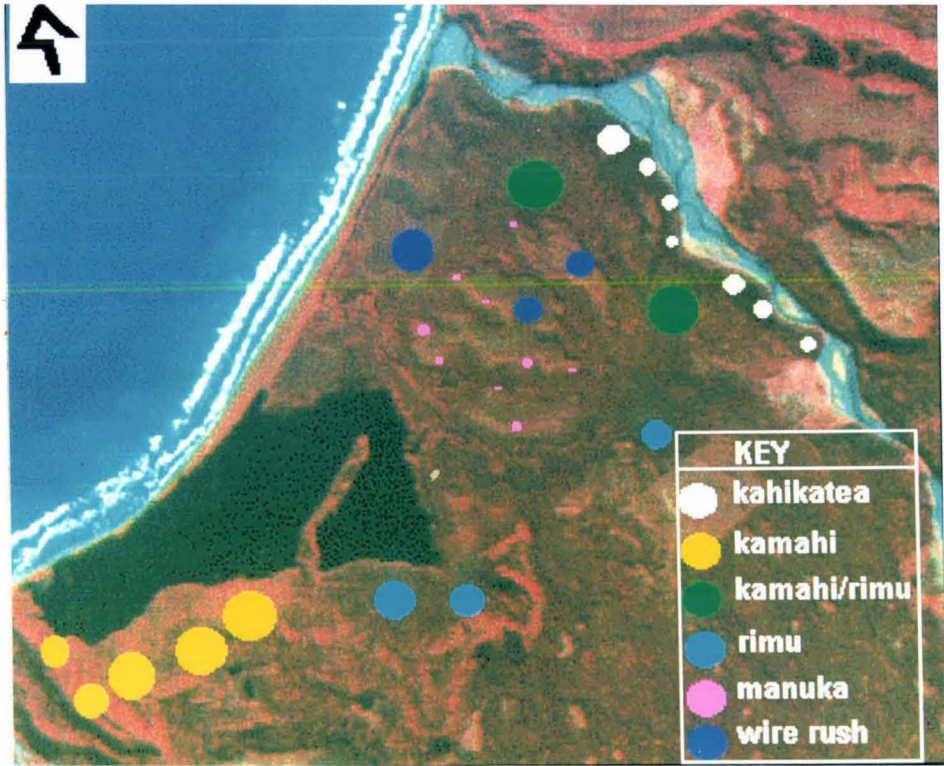


Figure 6.7: The sample sites used to collect training data for classification of the SPOT XS image. Scale as printed in thesis 1:100 000.

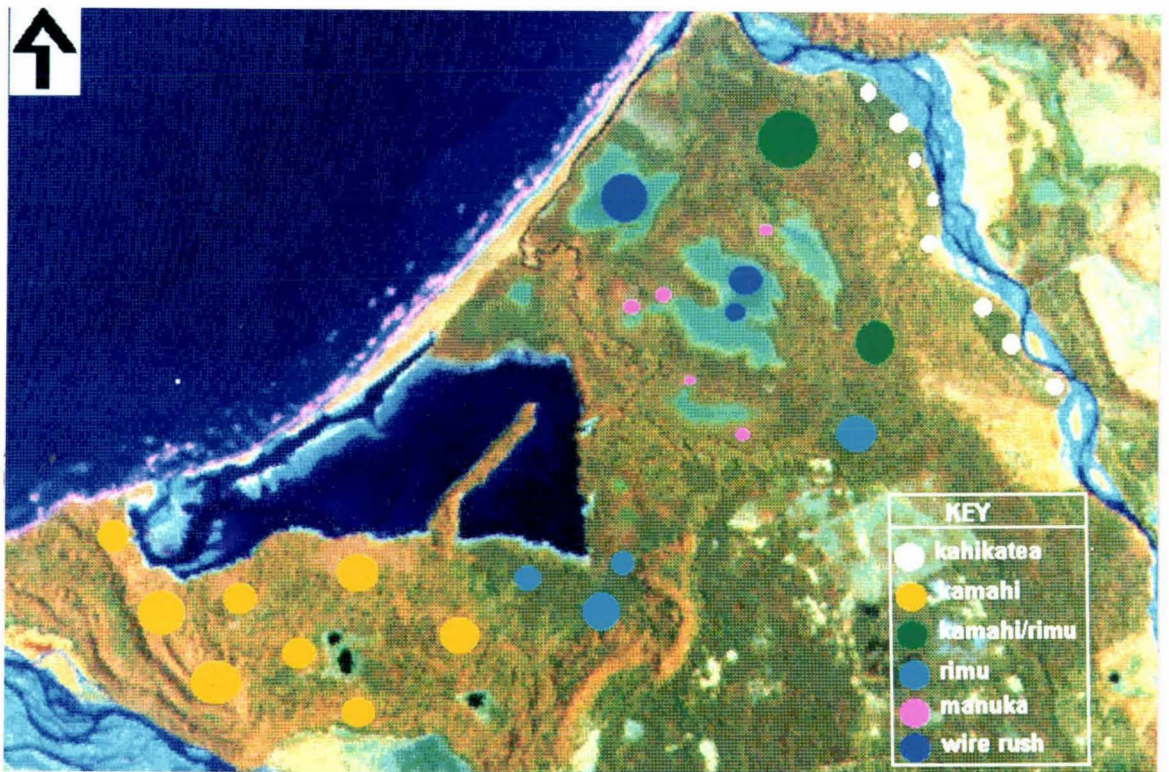


Figure 6.8: The sample sites used to collect training data for classification of the Landsat TM (4,5,3 composite) image. Scale as printed in thesis 1:100 000.

A maximum likelihood algorithm was used to classify each image. Assuming that a class's spectral response approximates a Gaussian distribution, the maximum likelihood classifier uses a mean vector and covariance matrix to describe the distribution of intensity values. The statistical probability of a given pixel being a member of a particular land-cover class can be calculated and the pixel assigned to the most likely class (the highest probability value), or labelled "unknown" if the probability values are all below a threshold set by the analyst. The disadvantage of the maximum likelihood classifier is the large number of computations required to classify each pixel.

## 6.4 Results and Discussion

**Hardware and Software:** In 1990 - 1991 when this study was performed, it was necessary to use a VAX minicomputer to store the full images. This was because the physical storage requirement of 48MB and 230MB for the SPOT XS and Landsat TM images respectively was beyond the capabilities of a PC system - a large hard disk was considered to be 100 MB and disk partitions were limited to 32MB. External high capacity devices, *e.g.* 8mm tape, were too expensive to be included in low-cost PC-based image processing systems. In addition, the PC image processing software available (DRAGON v2.1) could not process a full image because of RAM and software limitations. The resolution of the display was limited to 320x200 pixels in 256 colours.

In 1995, PC software and hardware have developed to a stage where it would no longer be necessary to store the satellite images on a minicomputer or workstation. There has been a progression to optical disk storage (600MB capacity) and devices for reading optical disks are commonplace on home PCS. Advances in 32-bit operating systems such as OS2™ and WINDOWS'95™ have removed the 640Kb RAM limit. The capability of PC graphics has improved enabling true colour images can be displayed for only a cost of a few hundred dollars. These technological advances combine to mean that a resource manager at a field station could have the capability to process full SPOT and Landsat TM images on their own desk for under \$4000 NZ.

**Image Classification: SPOT XS:** The spectral signatures obtained from the SPOT XS training data demonstrate the low range of intensity values in XS1 and XS2, the green and red bands (Figure 6.9). In XS1, intensity values ranged from 13 to 17, with 94% of pixels in values 14 and 15. In XS2, intensity values ranged from 6 to 11, with 99% in values 7, 8 and 9. In comparison the range in XS3 was 6 to 31, with 98% of values in the range 7 to 20. The results from the test classification are presented in Tables 6.1 and 6.2.

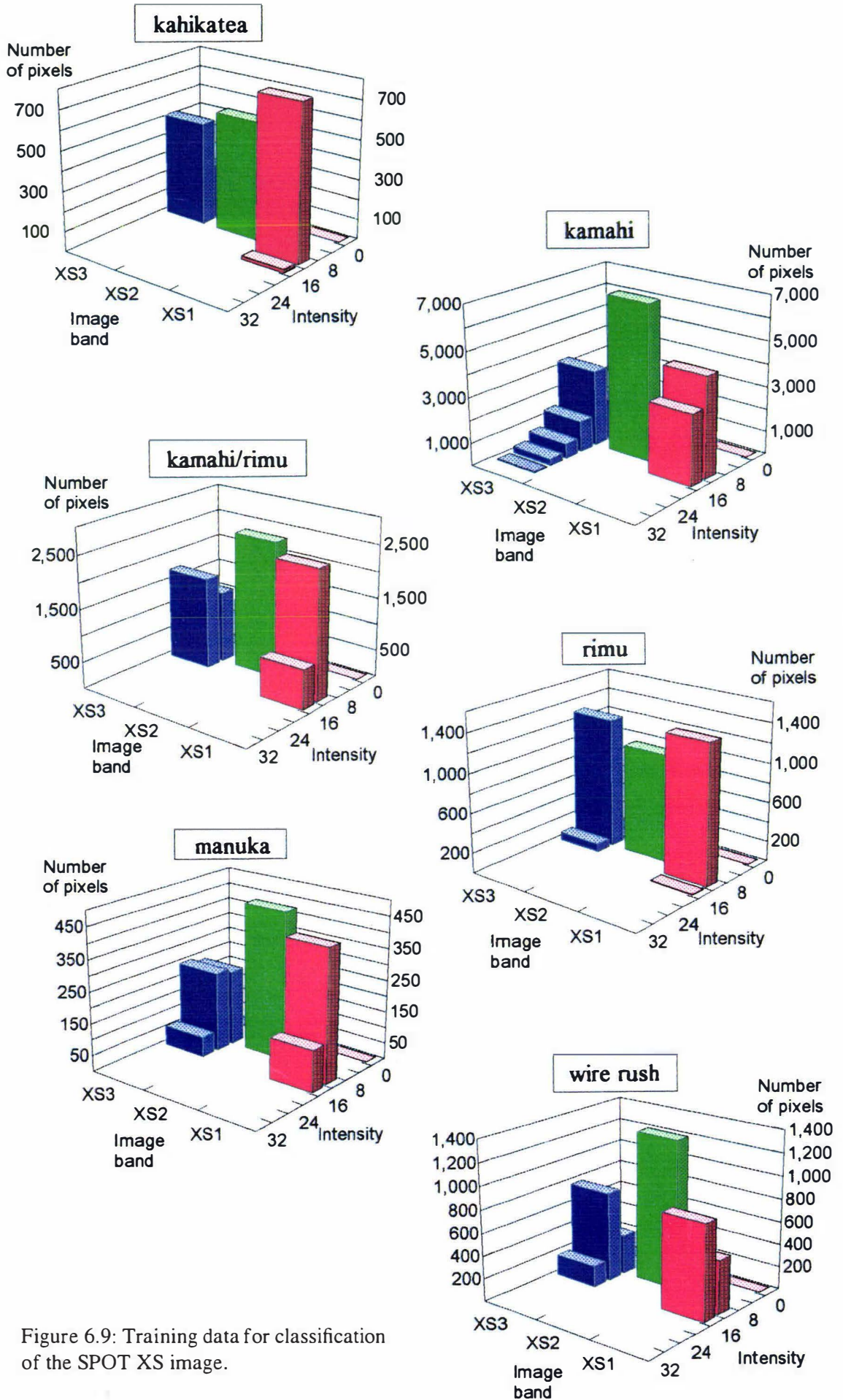


Figure 6.9: Training data for classification of the SPOT XS image.

Table 6.1: The confusion matrix for the test classification of the SPOT XS image. The table shows the number of pixels classified from the image into each class as defined by the training data. The diagonal represents correct classifications.

Image class	Reference class							Total
		kahik-atea	kamahi	kamahi/rimu	rimu	manuka	wire rush	
kahikatea	589	15	68	109	31	140	952	
kamahi	53	5735	617	204	75	230	6914	
kamahi/rimu	93	1143	1755	630	93	484	4198	
rimu	71	202	577	351	137	140	1478	
manuka	0	260	90	10	0	22	382	
wire rush	0	245	90	109	214	301	959	
Total	806	7600	3197	1413	550	1317	14883	

Table 6.2: A summary of the results of the SPOT XS classification. The omission error shows for each reference class, the pixels that were classified as another class. The commission error shows the pixels classified incorrectly into a given image class.

Class	% correct	% omission error	% commission error
kahikatea	73	27	38
kamahi	75	25	17
kamahi/rimu	55	45	58
rimu	25	75	76
manuka	0	100	100
wire rush	23	77	69

Average class correct: 42%; Overall accuracy of all pixels 58%; Kappa coefficient of agreement 0.39.

The kahikatea and kamahi classes obtained the highest classification accuracies. These classes were at opposite ends of the XS3 training data spectra and at opposite ends of SEA. However, it appeared that the separability of the kamahi-dominant canopy in the southwest region of SEA may be attributable partially to the effect of the low sun angle and increased local variation in relief. All slopes facing north-east recorded higher intensities in XS3 than areas of low relief or slopes facing southwest. This effect is also noticeable in other areas to the north of SEA (Figure 6.4).

The pakihi areas were able to be discriminated visually in XS3 (Figure 6.4), however they could not be differentiated from the other classes by their spectral signature, recording almost the same signature as the kamahi/rimu class. The visual difference is due to the smooth texture of the pakihi in XS3 compared with the roughness of the forest canopy. The pakihi areas may have been able to be separated automatically using a textural classifier, however the image processing software available (DRAGON v2.1) did not include the facility to generate textural images.

The test classification identified that the six vegetation communities could not be discriminated to the 85% overall accuracy level suggested by Anderson *et al.* (1976) as the minimum for remotely-sensed data. The six classes were combined into four hybrid classes (Table 6.3) based on the similarities in vegetative composition and the overlap identified in the test classification, and the classification repeated (Figure 6.10, Tables 6.4 and 6.5). The pakihi were classified manually and are therefore omitted from the confusion matrix.

Table 6.3: The hybrid vegetation classes used for the SPOT XS classification.

Initial vegetation class	Hybrid class
kahikatea	kahikatea.
kamahi	kamahi. Kamahi-dominated canopy found on north-east facing slopes in areas of greater relief.
kamahi/rimu	kamahi/rimu. Mixed kamahi/rimu forest with varying amounts of kamahi and rimu in the canopy/sub canopy. This class is found on generally flat terrain.
rimu	
manuka	manuka-wire rush-tangle fern. Scattered to dense scrub cover of manuka with dense areas of wire-rush.
wire rush/tangle fern	

Table 6.4: A confusion matrix for the SPOT XS classification applying the hybrid vegetation classes. The table shows the number of pixels classified from the image into each class as defined from the training data. The diagonal represents correct classifications.

Image class	Reference class				Total
		kahikatea	kamahi	kamahi/rimu	
kahikatea		589	0	53	642
kamahi		34	5735	44	5813
kamahi/rimu		183	1865	4513	6561
Total		806	7600	4610	13016

Table 6.5: A summary for the SPOT XS classification using the hybrid vegetation classes. The omission error shows for each reference class the pixels that were classified as another class. The commission error shows the pixels that were classified incorrectly into a given image class.

Class	% correct	% omission error	% commission error
kahikatea	73	27	8
kamahi	75	25	2
kamahi/rimu	98	2	31

Average class correct:82 %; Overall accuracy of all pixels 83%; Kappa 0.70.

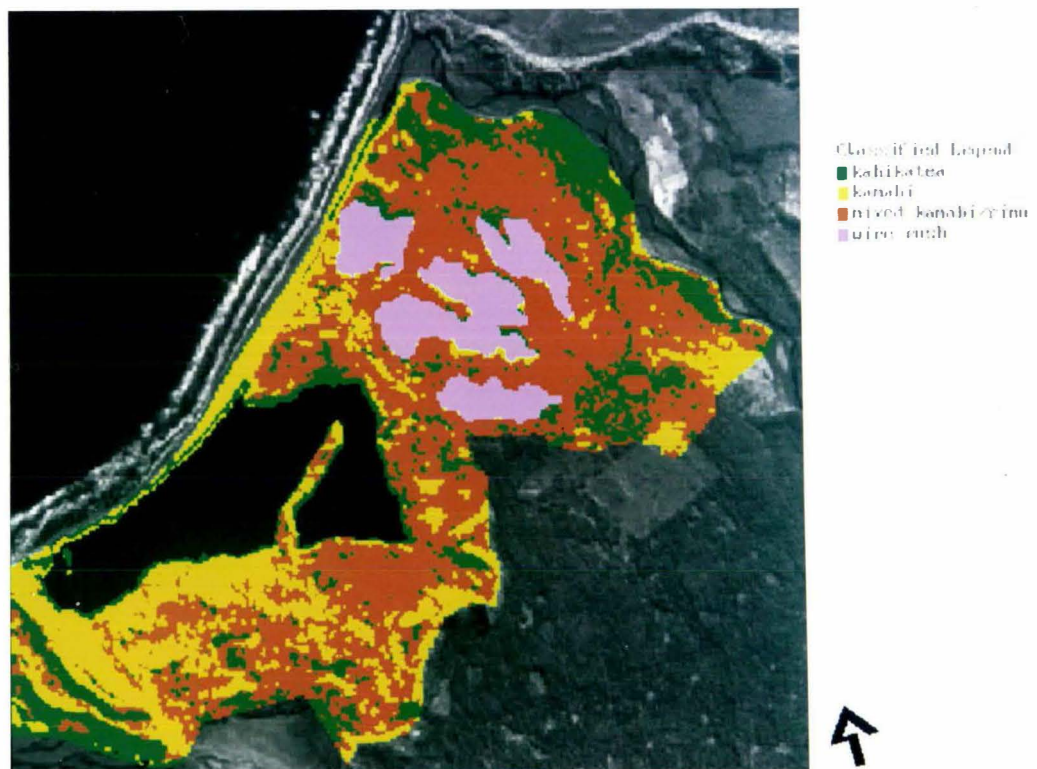


Figure 6.10: The classified image showing the vegetation of Saltwater Ecological Area derived from the SPOT XS image using the hybrid vegetation classes. Scale as printed in thesis 1:115 000

*Landsat TM:* The spectral signatures obtained from the Landsat TM image demonstrated an increased range of intensity values (Figure 6.11). All six of the vegetation communities were able to be discriminated visually with a TM4,5,3 composite; kahikatea as dark green, kamahi identifiable as light brown, kamahi/rimu as a greener-brown, rimu as a darker green, manuka as a khaki and wire rush as a lime green (Figure 6.8). This band combination was used because of its general superiority for vegetation discrimination in New Zealand. The results from the test classification supported the improved visual discrimination. (Tables 6.6 and 6.7).

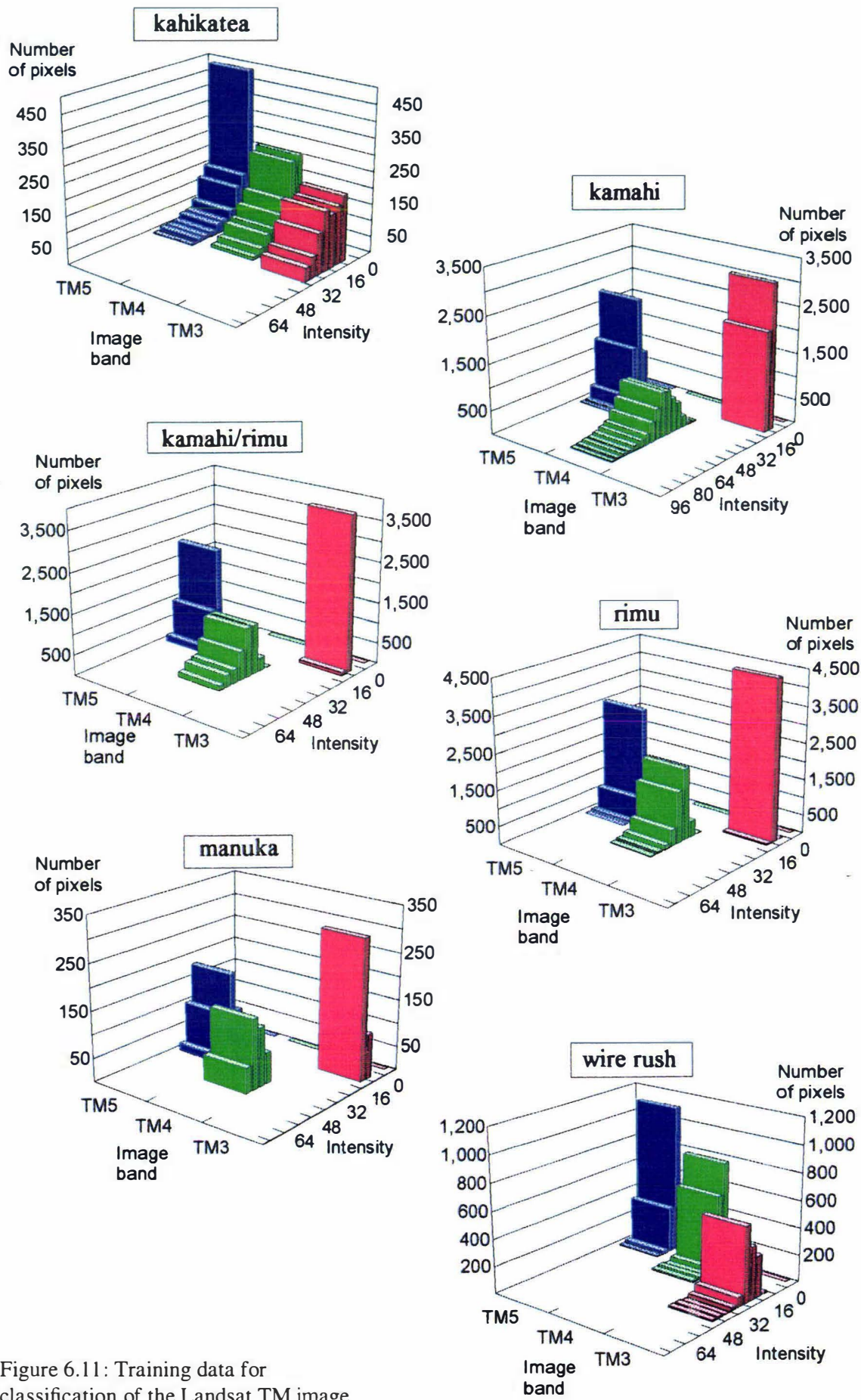


Figure 6.11: Training data for classification of the Landsat TM image

Table 6.6: A confusion matrix for Landsat the TM classification using the 6 vegetation classes. The table shows the number of pixels classified from the image into each class as defined by the training data. The diagonal represents correct classifications.

Image class	Reference class							Total
	kahik-atea	kamahi	kamahi/rimu	rimu	manuka	wire rush		
kahikatea	560	64	109	351	51	1	1136	
kamahi	14	4159	161	18	20	0	4372	
kamahi/rimu	37	788	2743	903	13	0	4484	
rimu	205	133	846	3154	2	0	4340	
manuka	109	102	45	68	310	0	634	
wire rush	0	0	0	0	2	1489	1491	
Total	925	5246	3904	4494	398	1490	16457	

Table 6.7: A summary of the Landsat TM classification using 6 vegetation classes. The omission error shows for each reference class, the pixels that were classified as another class. The commission error shows the pixels that were classified incorrectly into a given image class.

Class	% correct	% omission error	% commission error
kahikatea	61	39	51
kamahi	79	21	5
kamahi/rimu	70	30	39
rimu	70	30	27
manuka	78	22	51
wire rush	100	0	0

Average class correct: 76 %; Overall accuracy of all pixels 75%; Kappa 0.68

Although the Landsat TM results did not achieve the 85% overall classification accuracy (Anderson *et al.*, 1976), a visual inspection of the classified image (Figure 6.12), indicated that the original six classes could be discriminated without a need to merge classes as in the SPOT XS classification.

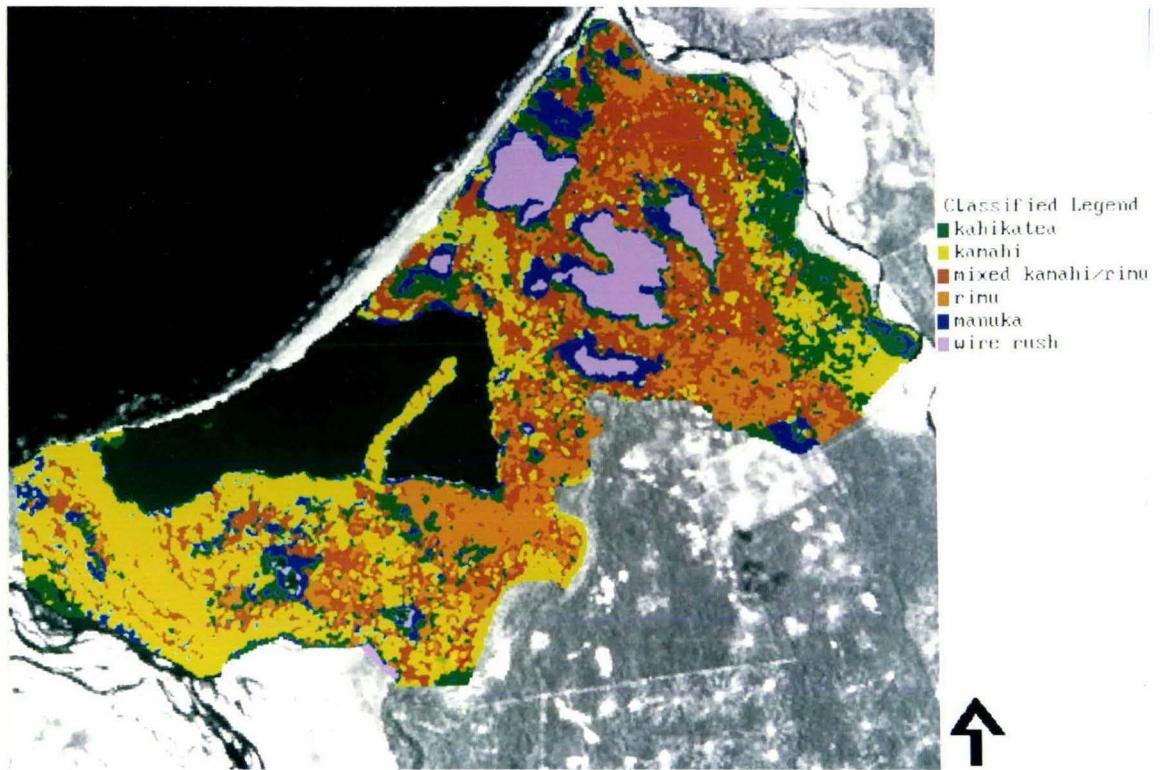


Figure 6.12: The classified image of the Saltwater Ecological Area vegetation derived from the Landsat TM image. The image shows the 6 vegetation types based on the vegetation communities identified from an existing vegetation map (Figure 6.6) (Norton and Leathwick, 1990). Scale as printed in thesis 1:110 000.

**General discussion:** The overall classification accuracy obtained using all six communities in the SPOT XS image was 58%. This error is intuitively too high for making quantitative cover-type assessments and resource management decisions. The amalgamation to three hybrid classes increased the accuracy to 83%, but with a corresponding reduction in information content. The majority of SEA was classified as mixed kamahi/rimu forest, which is only a general description of Westland indigenous forest (Poole and Johns, 1992, McKelvey, 1984) and provides little information in this resource management application.

In comparison, classification of the Landsat TM image using all six classes achieved an overall accuracy of 75%. The average class accuracy was 76%, which is superior to the 69% achieved by Benning *et al.* (1981) who used Landsat MSS to map tawa (*Beilschmiedia tawa*), kamahi and podocarps (rimu, matai, miro and kahikatea) in the King Country, New Zealand. However this was still below the 85% level (Anderson *et al.*, 1976) regarded as the minimum acceptable from remotely-sensed data.

The spectral information in the SPOT XS image was dominated by the reflectance in XS3. However, much of the variation in XS3 may be attributed to the interaction of a low sun elevation angle and local relief rather than vegetative differences. This was evident on the north-easterly facing slopes of large moraines (50m high) and on much smaller features, e.g. around the edge of the pakihi (Figure 6.4). Although studies have shown that the effects of relief may be minimised by band ratioing (Lillesand and Kiefer, 1987) or using DTM's (Janssen *et al.*, 1990; Senoo *et al.*, 1990), neither of these solutions were applicable in this study because; (a) the low dynamic range evident in XS1 and XS2 negated any benefit from ratioing these bands with XS3 and (b) a DTM of SEA was not available.

Photogrammetric methods of DTM generation are not generally applicable in a heavily forested area such as SEA because the photogrammetric technique tends to record forest canopy height rather than underlying relief. Field-based methods, e.g. barometric survey, are also difficult to apply. The author and other workers attempted a barometric survey in 1991 but this proved a very arduous exercise because of the dense indigenous vegetation hindering progress and making it impossible to retain precise locational information. A GPS was not available during this study.

Although this study was designed to optimise the classification of each image with respect to the vegetation map and not as a comparison of SPOT XS and Landsat TM imagery, visually, there was a noticeable difference in the vegetative information content in the imagery. This difference may be attributed to three causes: (1) sun-angle differences at the time of image acquisition, (2) differences in the TM and SPOT HRV sensors' spectral resolution and (3) seasonal differences in vegetation.

The low sun elevation angle (22°) of the SPOT XS image, because of the winter morning acquisition time, contributed to relief effects influencing the reflectance in XS3. Sun angle effects may also have contributed to the small range of intensity values recorded in XS1 and XS2 although low dynamic ranges in XS1 and XS2 have also been noted by Danson (1987) and De Wulf *et al.* (1990) in studies of coniferous forests in England and Belgium respectively. De Wulf *et al.* (1990) suggested that all forests in temperate regions have low albedo values in XS1 and XS2 and that future SPOT HRV sensors may need to be provided with variable gain facilities to improve their utility in forest monitoring.

Screen displays generated from a Landsat TM 4,5,3 (RGB) composite highlighted the vegetation information contained in these particular bands. The benefit of the near and mid-infrared bands has also been noted in a number of other land-cover mapping and forest species discrimination studies (Tucker, 1978; Horler and Ahern, 1986). Moreover, previous

studies comparing the information content of Landsat TM and SPOT XS have found Landsat TM to be superior because of the inclusion of the mid-infrared bands, TM5 and TM7 (Chamignon and Manière, 1990; Karteris, 1990; Brockhaus and Khorram, 1992).

Discrimination of the pakihi may have been affected by seasonal differences in vegetation between the winter and summer acquisition dates of the images. The pakihi were unable to be discriminated spectrally from other areas of rimu/kamaha forest in the SPOT XS image whereas in the Landsat TM image, a 100% class classification accuracy was achieved. A possible explanation may be the pakihi remaining damp throughout summer, increasing the spectral differentiation from forested areas. The discrimination of the kahikatea-dominant community may also have been affected by seasonal differences. Here, the intensity values recorded in XS3 were low compared to those recorded in the dense forest. As the XS3 wavelength (0.79 to 0.89 $\mu\text{m}$ ) is absorbed by water, damp ground conditions in winter may have affected the spectral response in this community. Supporting this interpretation is the community's generally open canopy structure and its location on the floodplain of the Poerua River where there may be frequent areas of standing water (Norton and Leathwick, 1990).

Although satellite imagery has been shown to be a less expensive method to map land-cover than field work and aerial photography (Benning *et al.*, 1981, Leckie, 1990(a)), if resource managers are tempted to use satellite imagery and digital image processing as tools to update vegetation maps, they must also be aware of the accuracy of the original map and the nature of the image versus map comparison. The comparison of a classified image to another map provides a measure of classification accuracy with respect to the map - not to the ground conditions. When using maps derived from field data and photo-interpretation, the extrapolation of point data to community boundaries is an obvious source of error. Land-cover mapping is a subjective assessment made by the mapper and interpretations may vary considerably between mappers (Biging and Congalton, 1991).

However, regardless of the accuracy of the map, the process of comparing classified imagery to existing vegetation maps may not be a valid operation (Biging and Congalton, 1991). The two products are different because the two methods of mapping are different. Berry (1993) suggested that the classified image itself is an outdated product and that it may be time to move toward a pixel structure for maps. While this approach has definite advantages to the application of remote sensing, it must be tempered with the need to integrate all of the existing data sources into easily understandable and useable resource management information. Even though a GIS can integrate different data layers and data models, in most GIS, one mapping system has to be accepted as the base (Ehlers, 1990).

At present, the default is chloropleth maps. In addition, there is strong support for chloropleth mapping within the resource management community because the maps are a familiar format to managers and they provide the categorized, quantitative information required for reports and resource consents.

A more appropriate application of digital image processing and satellite imagery in the indigenous forests of Westland may be in temporal monitoring, changing the focus from image classification to change detection. For example, using a detailed vegetation map, every pixel on a rectified image can be assigned a vegetative community purely from its spatial location. Therefore in-depth information of a pixel's vegetation composition is already known and it may not be necessary to classify the image. When sequential satellite images of either raw pixel values or vegetation indices (Vogelmann, 1990; Chamignon and Manière, 1990) are compared in an image differencing or other change detection technique, the pixels showing change may be quickly identified. However, setting of the change thresholds will require study and experience. A resource manager may be able to explain possible causes of the change by referring to the existing vegetation maps. The scope and expense of field survey can be minimised by focusing on the areas identified through the change detection analysis.

## 6.5 Summary

This study investigated the application of SPOT XS and Landsat TM imagery for providing resource management information in an area of virgin indigenous forest. The study focused on how digital image processing of the satellite imagery could be used to update existing vegetation maps. Classes derived from an existing vegetation map based on a field survey were used to define and test the results of a supervised digital image classification.

The study found that neither image could achieve the 85% accuracy level suggested as the minimum for classified imagery (Anderson *et al.*, 1976). Including six of the vegetation classes in the SPOT image classification resulted in a 53% overall classification accuracy whereas amalgamating the six classes to three hybrid classes obtained an overall accuracy of 83%. However, associated with the reduction in classes was a decrease in information obtained, *i.e.* the majority of SEA was classified as mixed kamahi/rimu forest which is only a general description of the podocarp-hardwood forest of Westland (Poole and Johns, 1992). In comparison, classification of the Landsat TM into six vegetation classes achieved an overall classification accuracy of 75%.

Although the study was not designed as a comparison of the SPOT XS and Landsat TM imagery, with respect to the vegetation map, the Landsat TM image provided more information on the vegetative composition than the SPOT XS image. This was attributed to (1) the SPOT XS image being acquired with a low sun elevation angle which exaggerated the effect of relief rather than differences in vegetative composition, (2) the differing spectral resolutions of the sensors, specifically in the information contained in the near and mid-infrared bands (Landsat TM4 and TM5) and (3) seasonal differences in the date of acquisition, the SPOT in winter (1 August) and the Landsat TM in summer (30 December).

Based on the classification accuracies obtained, it was noted that comparison of the classified imagery to an existing map may not have been the correct application of digital image processing and satellite imagery. The two products are different because the two methods of mapping are different and they should not necessarily be compared (Biging and Congalton, 1991). Given that in indigenous forest management, the detailed vegetation information provided by field survey is fundamental, a more appropriate application of satellite imagery in Westland's forests may have been in change detection. Pixels that have changed in successive images can be identified rapidly and the possible causes of the change explained by resource managers using a detailed vegetation survey. The application of change detection techniques would minimise the time and personnel costs associated with field survey by focussing teams on the areas identified in the imagery.

## 7: INDIGENOUS FORESTRY: SALTWATER FOREST

### 7.1 Study Objective

One of the objectives in this thesis was to investigate how information beneficial to management of indigenous forests can be obtained through the application of GIS analyses and digital image processing of satellite imagery. This study applied these techniques in the Saltwater Forest, an indigenous forest designated for sustained-yield forestry. A proposal for logging Saltwater Forest, based on the extraction of large rimu trees by helicopter and chainsaw milling of windthrown trees, is currently under negotiation with Timberlands New Zealand Ltd.

### 7.2 Site Description

The physical site description of Saltwater Forest is similar to that given for Saltwater Ecological Area (Chapter 6). The terraces support a podocarp-hardwood forest composed mainly of rimu, miro, and kahikatea with a shrub-hardwood understorey. Stands appear as a mosaic of even-aged groups on the flat terraces with “semi even-aged, mixed-aged groups” on steeper land (Six Dijkstra *et al.*, 1985). In the mature forest, rimu comprises 76-93% of the trees greater than 30cm diameter at breast height (d.b.h) (Chavasse, 1964) and often forms a continuous upper canopy between 40m and 25m in height (Wardle, 1977). Below the upper canopy (25m to 9m) there is a second layer comprised mainly of kamahi, quintinia (*Quintinia acutifolia*), miro, thin-barked (Hall's) totara (*Podocarpus hallii*) and silver pine. Other subcanopy species in abundance include pokaka (*Elaeocarpus bookerianus*), lancewood (*Pseudopanax crassifolium*), broadleaf (*Griselinia littoralis*), pigeonwood (*Hedycarya arborea*), pepper tree (*Pseudowintera colorata*), *Ascarina lucida*, *Coprosma lucida*, *Cyathea smithii*, *Dicksonia squarrosa*, *Myrsine australis* and *Neomyrtus pedunculata* (Six Dijkstra *et al.*, 1985).

Saltwater Forest comprises both logged areas and stands of virgin forest. The logging technique applied previously was selective logging whereby 30% of the timber was removed. Trees were felled and the logs hauled across the forest floor to sites where they were loaded onto trucks. This logging compressed the soil and elevated the water table on soils that were already difficult to drain and constantly wet (Poole and Johns, 1992). The 'wheel spokes' leading to the hauler sites (Figure 7.1) are evident in the satellite imagery (Figures 7.2 and 7.3). The remainder of Saltwater Forest is virgin indigenous forest. In 1989, legislation was passed to protect the remainder of this and other podocarp-hardwood forests whereby future logging must be performed on a sustainable basis and not damage the remainder of the forest. Saltwater Forest was one of two forests selected for sustained-yield forestry.



Figure 7.1: The centre of a hauler site used for selective logging of Saltwater Forest. The breaks in forest canopy indicate tracks where the logs were dragged across the forest floor before being loaded onto trucks (photo L. J. Brown).

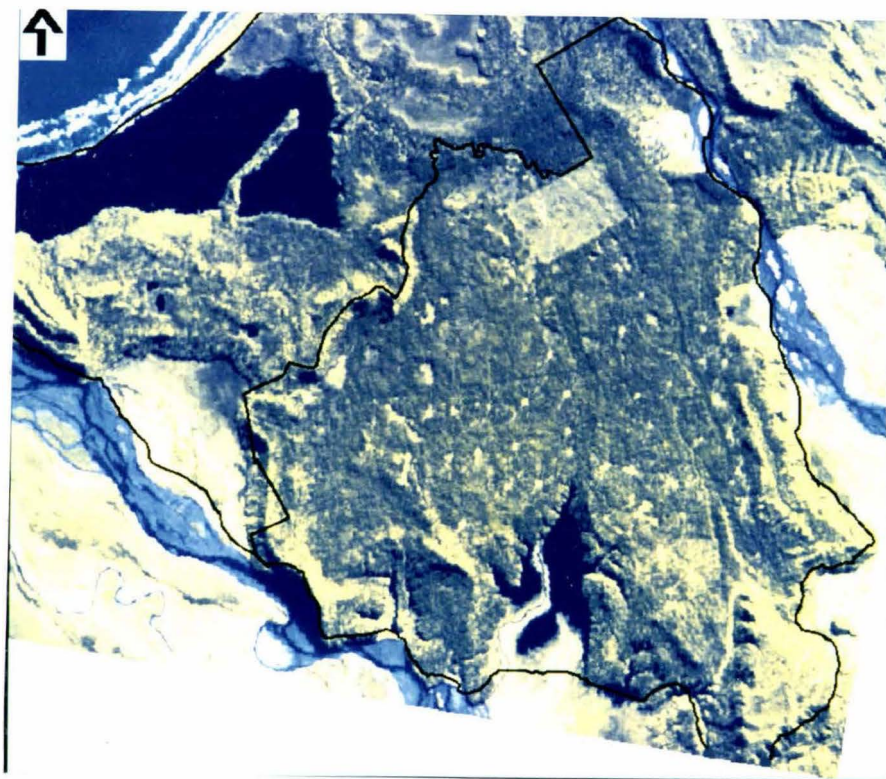


Figure 7.2: Saltwater Forest in the SPOT XS (bands 3,3,1 (RGB) composite) image. This combination of bands provided the most visual discrimination within Saltwater Forest. The black line, digitised from a 1:25 000 forest map, indicates the extent of Saltwater Forest. Saltwater Ecological Area is to the west. Scale as printed in thesis 1:115 000.

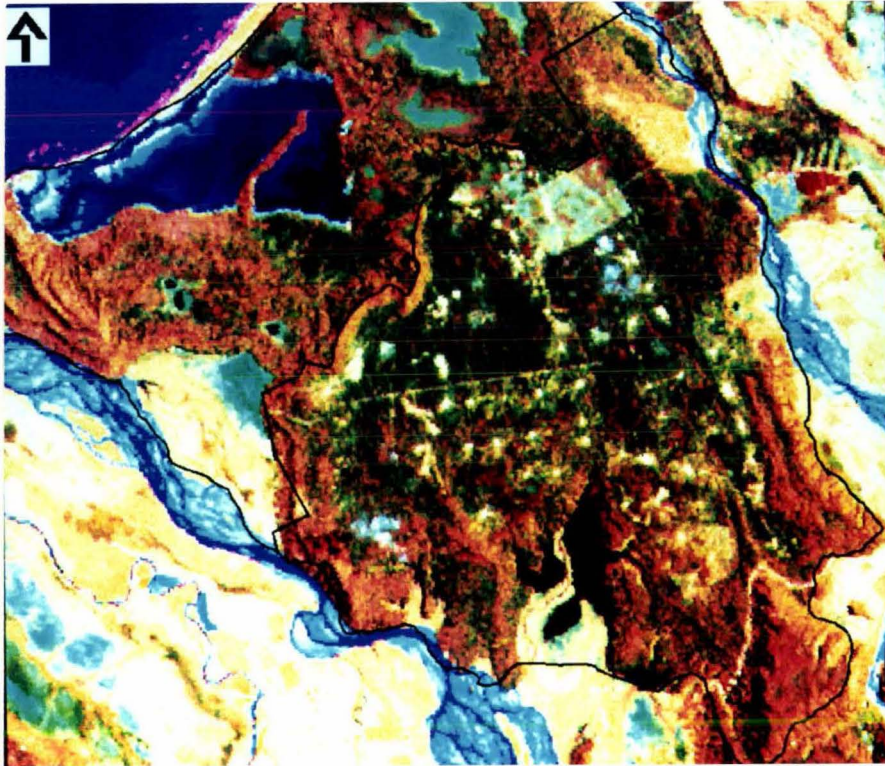


Figure 7.3: Saltwater Forest in the Landsat TM (bands 4,5,3 (RGB) composite) image. The contrast and brightness of the image have been stretched to reveal the spectral variation within Saltwater Forest. The black line, digitised from a 1:25 000 forest map, indicates the extent of Saltwater Forest. Scale as printed in thesis 1:115 000.

### 7.3 Methodology

**Imagery:** The study used the same SPOT XS and Landsat TM imagery as in the Saltwater Ecological Area study (Figures 7.2 and 7.3).

**GIS Processing:** This study used a field-plot based inventory of Saltwater Forest. The inventory was completed in 1986 by Gernot and Gisela Uhlig and a team of field personnel working for the New Zealand Forest Service. The survey technique comprised 325 plots distributed throughout Saltwater Forest (Figure 7.4). Each plot was circular, approximately 0.2ha in area (26m radius). Plot locations were recorded on field sheets as bearings and distances from landmarks such as track junctions. These were subsequently draughted onto a 1:10 000 scale map. The information recorded for each plot comprised the major species present and a classification of the trees into 12 size classes based on the stem diameter at breast height (d.b.h.) (Table 7.1).

The plot locations as shown on the map were digitised manually into PC ARC/INFO. In all digitising sessions, the digitiser transformation error was maintained below 0.003 (ESRI, 1993(a)). Each plot was entered as a point feature with the plot number recorded

as the user identification number. To represent the area of an individual plot, the points were converted to polygon features using a 26m radius buffer around each point. The location of the digitised plots was checked against the original map by superimposing a print of the GIS data on the original map. The plot layer was aligned to the NZ Map Grid using tic coordinates obtained from a 1:25 000 scale forest map. The roads, streams and boundary of Saltwater Forest were also digitised manually from the 1:25 000 forest map.

For this study, the plot attributes were entered into the dBASE IV database. Each plot number was entered as a record, and the composition data stored as fields, *e.g.* the field 'mi\_a\_cw' represented the miro in size class 'a' that was damaged (cw). The integrity of the dataset was verified by locating plots with no attributes, and attributes with no plots. The discrepancies were discussed with Gernot Uhlig and the GIS dataset modified where necessary. This reduced the number of plots to 316.

Table 7.1: A typical plot record from the Saltwater Forest inventory

Plot Number 245	Class A 0-0.09m		Class B 0.1- 0.19m		Class C 0.2- 0.29m		Class D 0.3- 0.39m		Class E 0.4- 0.49m		Class F 0.5- 0.59m	
	'	'	sl <sup>3</sup>	cw <sup>3</sup>	sl	cw	sl	cw	sl	cw	sl	cw
miro		66	2	14	2	12	4	10	2	2	0	0
rimu		56	2	16	0	2	0	8	0	8	4	0
silver pine		0	0	0	0	0	0	0	0	0	0	0
others <sup>2</sup>		14	0	0	0	0	0	0	0	0	0	0
	Class G 0.6- 0.69m		Class H 0.7- 0.79m		Class I 0.8- 0.89m		Class J 0.9- 0.99m		Class K 1.0- 1.09m		Class L >1.1m	
	sl	cw	sl	cw	sl	cw	sl	cw	sl	cw	sl	cw
miro	0	0	0	0	0	0	0	0	0	0	0	0
rimu	0	4	2	0	6	0	0	0	0	0	0	2
silver pine	0	0	0	0	0	0	0	0	0	0	0	0
others <sup>2</sup>	0	0	0	0	0	0	0	0	0	0	0	0

<sup>1</sup> 'sl' and 'cw' divisions not recorded for this class.

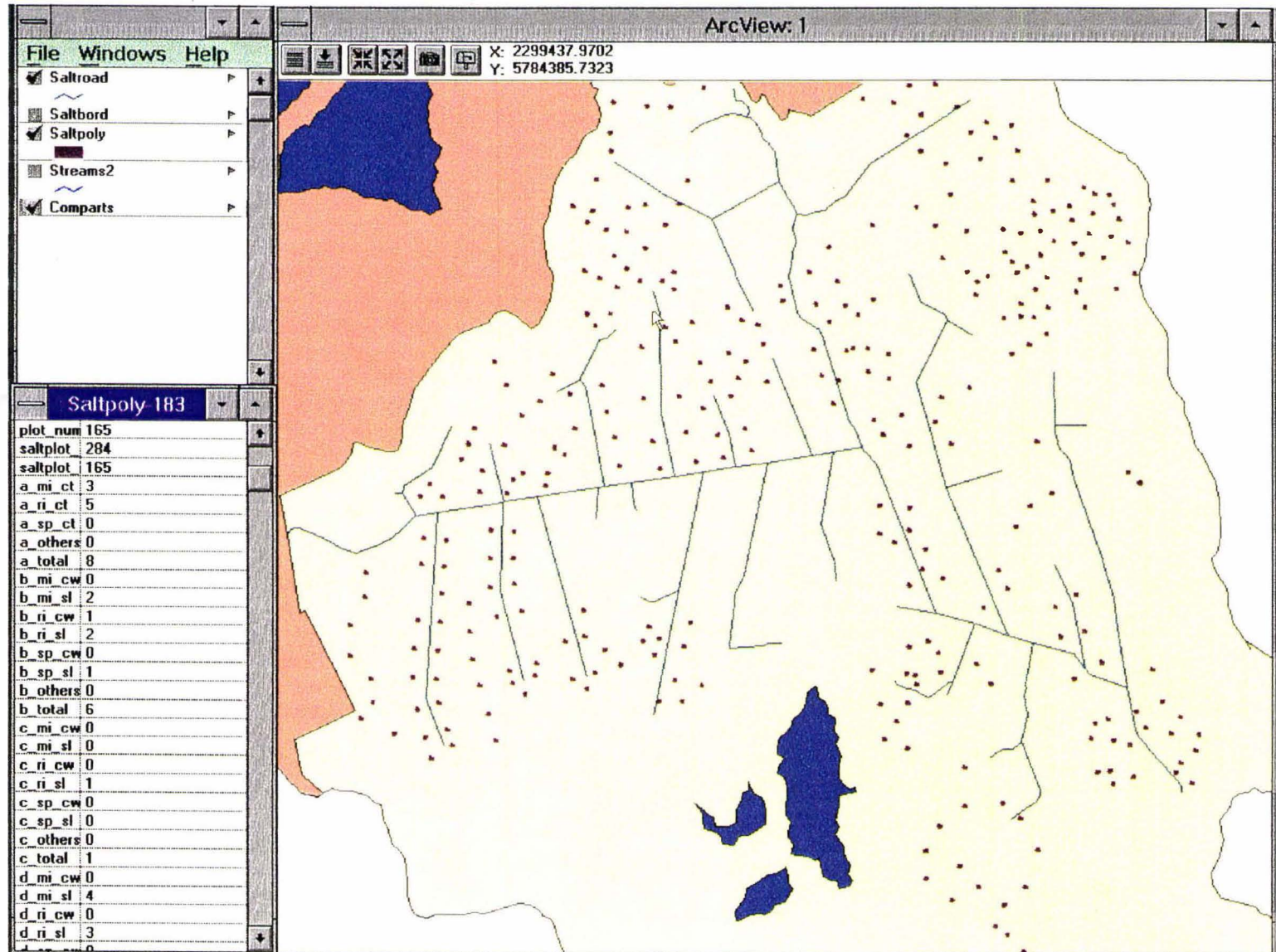
<sup>2</sup> The major species in this class is kahikatea.

<sup>3</sup> 'sl' refers to a 'saw log', 'cw' to damaged timber.

Figure 7.4: A sample screen from the ArcView desktop mapping software. The 'theme' window (top left) indicates the layers of the database shown in the 'display' window (right). Only those layers with a tick in their check box are displayed. The 'display' window shows the distribution of the forest inventory plots and the roads of Saltwater Forest. The 'database' window (lower left) shows the result of clicking the mouse pointer on one of the plots.

Scale 1:56 000

1 km



**Transformation of intensity value to apparent reflectance:** For both the SPOT XS and Landsat TM image, the intensity value for each pixel was transformed to apparent reflectance using the method described by Price (1987). This calibration is necessary prior to calculating vegetation indices and to enable comparison with imagery acquired from different sensors and with different sun-satellite geometry (Robinove, 1982). The term 'apparent' reflectance signifies that the reflectance has not been corrected for atmospheric absorption and scattering. The variables used in the transformation are tabulated in Table 7.2. The apparent reflectance is calculated:

$$R = \frac{\pi(\alpha_i DN_i + \beta_i)}{\theta_s E_i}$$

where  $R$  is the apparent reflectance,  $\alpha_i$  and  $\beta_i$  are calibration coefficients for band $_i$ ,  $DN_i$  is the digital number in band $_i$ ,  $E_i$  is the total irradiance in band $_i$ , and  $\theta_s$  is the cosine of the solar zenith angle (0.857 for the Landsat TM and 0.375 for the SPOT XS) (Price, 1987). Reflectance values (0-1) were linearly scaled to a 256 level image for display in the PC image processing software. In the remainder of this study, the term 'pixel value' refers to the transformed value of the apparent reflectance.

Table 7.2: The variables used in transformation of intensity values to apparent reflectance.  $\alpha$  and  $\beta$  are calibration coefficients and  $E$  is the total irradiance for each band (from Price, 1987).

Image Band	$\alpha$ (gain)	$\beta$ (offset)	$E$ ( $Wm^{-2}\mu m^{-1}$ )
XS1	1.2214	0	1850
XS2	1.3175	0	1627
XS3	1.0767	0	1087
TM1	0.602	-1.5	1948
TM2	1.17	-2.8	1813
TM3	0.806	-1.2	1548
TM4	0.815	-1.5	1043
TM5	0.108	-0.37	211
TM7	0.0570	-0.15	77

**Rectification:** Both images were rectified to the New Zealand Map Grid. Ground control points, obtained from a 1:25 000 forest map, were chosen at road intersections distributed throughout Saltwater Forest. A first-order transformation was used to calculate new pixel positions. To retain the original pixel values, a nearest neighbour algorithm was used for interpolation.

**Vegetation Indices:** A Normalised Difference Vegetation Index (NDVI) image was created from the Landsat TM image. A NDVI image was not calculated from the SPOT XS image because of the lack of variation within the forest in XS2. The Landsat TM NDVI image was calculated as:

$$NDVI_{TM} = \frac{TM4 - TM3}{TM4 + TM3}$$

where  $NDVI_{TM}$  is the NDVI value calculated from the near-infrared and red wavelength bands  $TM4$  and  $TM3$ . NDVI values were linearly scaled to a 256 level image for display.

**Remote sensing and GIS analysis:** For each plot, a pixel value was obtained from each image band by overlaying a raster version of the inventory dataset on the imagery (Figure 7.5). To reduce positioning and assignment error, both the imagery and inventory datasets were resampled to 5m cells prior to overlay (van der Knaap, 1992). The pixel value that occupied greater than 50% of the plot area was recorded as the representative value for that plot. In the case of no single pixel value occupying greater than 50% of the area, the median value of all pixels occurring within the plot was used.

Analysis of the relationship between the image and inventory datasets was divided into two sections. The first analysis investigated the use of satellite imagery to discriminate vegetation clusters derived from the forest inventory. The second analysis reversed the procedure and identified the classes on the image that could be differentiated spectrally. The botanical composition of each spectral class was interpreted from the forest inventory.

**Satellite imagery to discriminate forest inventory clusters:** The inventory variables were grouped into three size classes to aid interpretation of the dataset. The size classes were chosen to represent canopy layers; layer 1 represents an upper canopy layer comprising larger trees, mainly rimu > 60cm d.b.h., layer 2 represents a subcanopy layer comprised of mainly of rimu, miro and silver pine between 20cm and 60cm d.b.h. and layer 3 represents a layer of shrubs and small trees < 20cm d.b.h.

The number of trees in each layer was used as the variable to identify clusters of plots in the inventory. A Kmeans procedure (SYSTAT, 1992) was used to generate the clusters. Kmeans is a form of partitioned clustering where cases are assigned to non-overlapping clusters. The algorithm identifies a 'seed' case for each cluster which is spread from the centre of all cases as much as possible. Cases are reassigned iteratively to clusters to

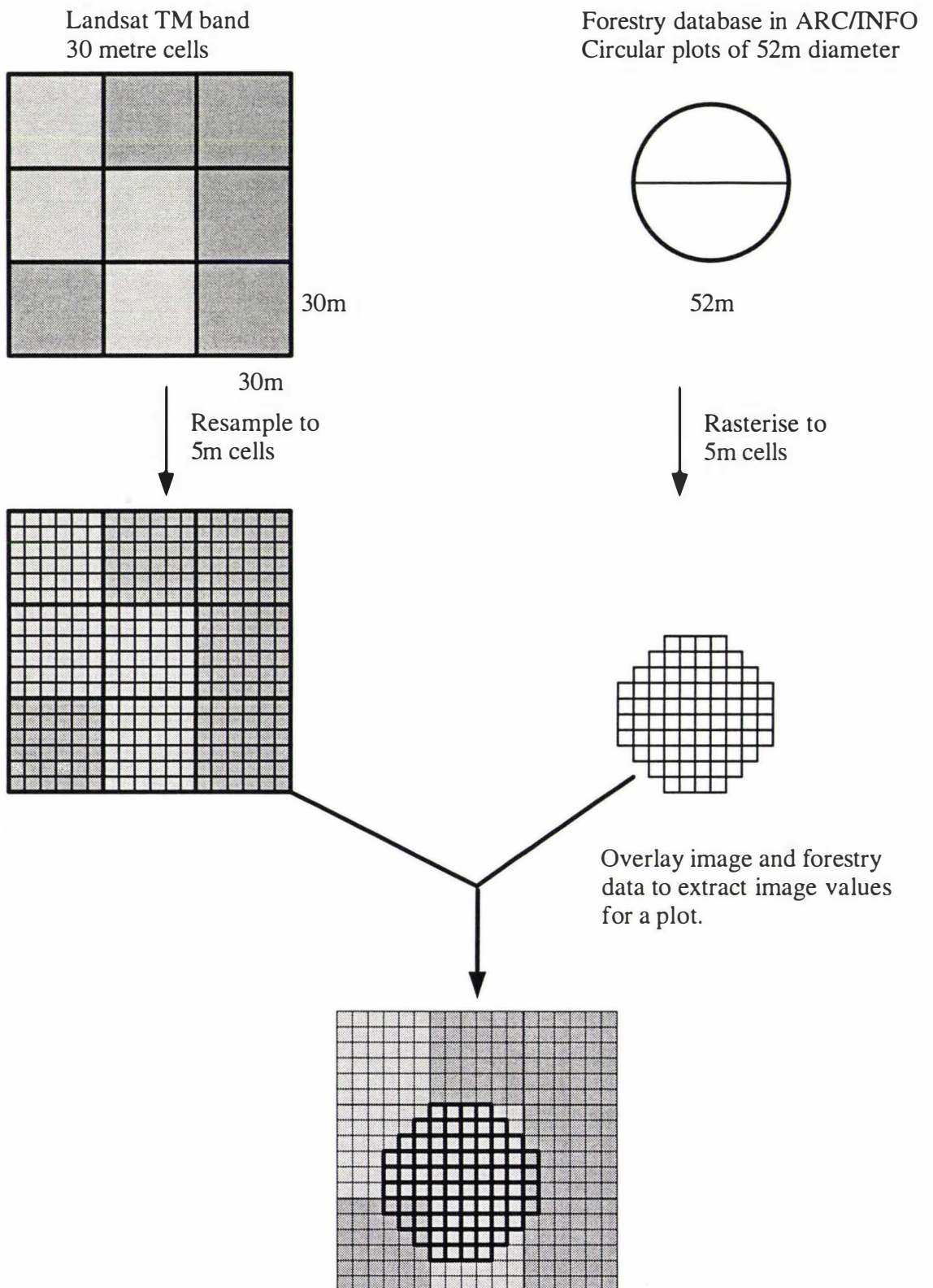


Figure 7.5: A flow-chart indicating the method used to extract a pixel value for each plot from each image band.

maximise the between-cluster relative to within-cluster variation. The number of clusters chosen is arbitrary. In this study, five clusters were chosen following the results of Six Dijkstra *et al.*, (1985) who, in a study of the forest architecture of Saltwater Forest, identified 5 distinct 'growth phases'.

Discriminant analysis, a statistical technique used to classify individuals into two or more groups (Klecka, 1980), was used to determine whether the spectral information in the satellite imagery could discriminate between the inventory clusters. This method is applied commonly in the social sciences (Afifi and Clark, 1984) and has also been used in remote sensing as a replacement for the maximum likelihood classifier (Tom and Miller, 1984). Discriminant analysis has four functions; (1) to find linear composites (discriminant functions) of  $n$  independent variables which maximise the ratio of among-groups to within-groups variance, (2) to test whether the group centroids of  $k$  dependant groups are different, (3) to determine which of the  $n$  independent variables contribute the most information to group discrimination and (4) to classify observations to one of  $k$  groups. This study focused on the classification function. The classification evaluates cluster membership based on the location of clusters in discriminant space. The closer a case is to a particular cluster's location, the more likely it is that it belongs to that cluster. In this study, the Mahalanobis distance was used to calculate the distance between cases and clusters.

*Forest variables to interpret image spectral classes:* The spectrally separable classes on each image were generated using an unsupervised classification. An iterative isodata procedure was used (Smith *et al.*, 1994). This algorithm bases initial class centres on the distribution of pixel values within each band. Each pixel is assigned to a class via a minimum distance to mean classification, a new mean is calculated and the classification is repeated. Over multiple iterations the classes converge which reduces the number of pixels changing class.

As in Kmeans clustering, the number of classes chosen is arbitrary. In this study, the number of classes was based on visual interpretation of the imagery. Each image was enhanced with contrast and brightness stretches on the individual image bands. Only SPOT XS3 was used to generate classes from the SPOT image because it was the only band to show significant variation within the forest. Three classes were identified in the SPOT XS3 image. For the Landsat TM image, four classes were distinguished using a TM4,5,3 composite. Both of the classified images were smoothed with a 3x3 modal filter prior to extracting a class membership for each plot (Figure 7.5). The class value that occupied the majority of the plot area was used as the representative value. The vegetative composition of the classes was investigated using the forest inventory.

## 7.4 Results and Discussion

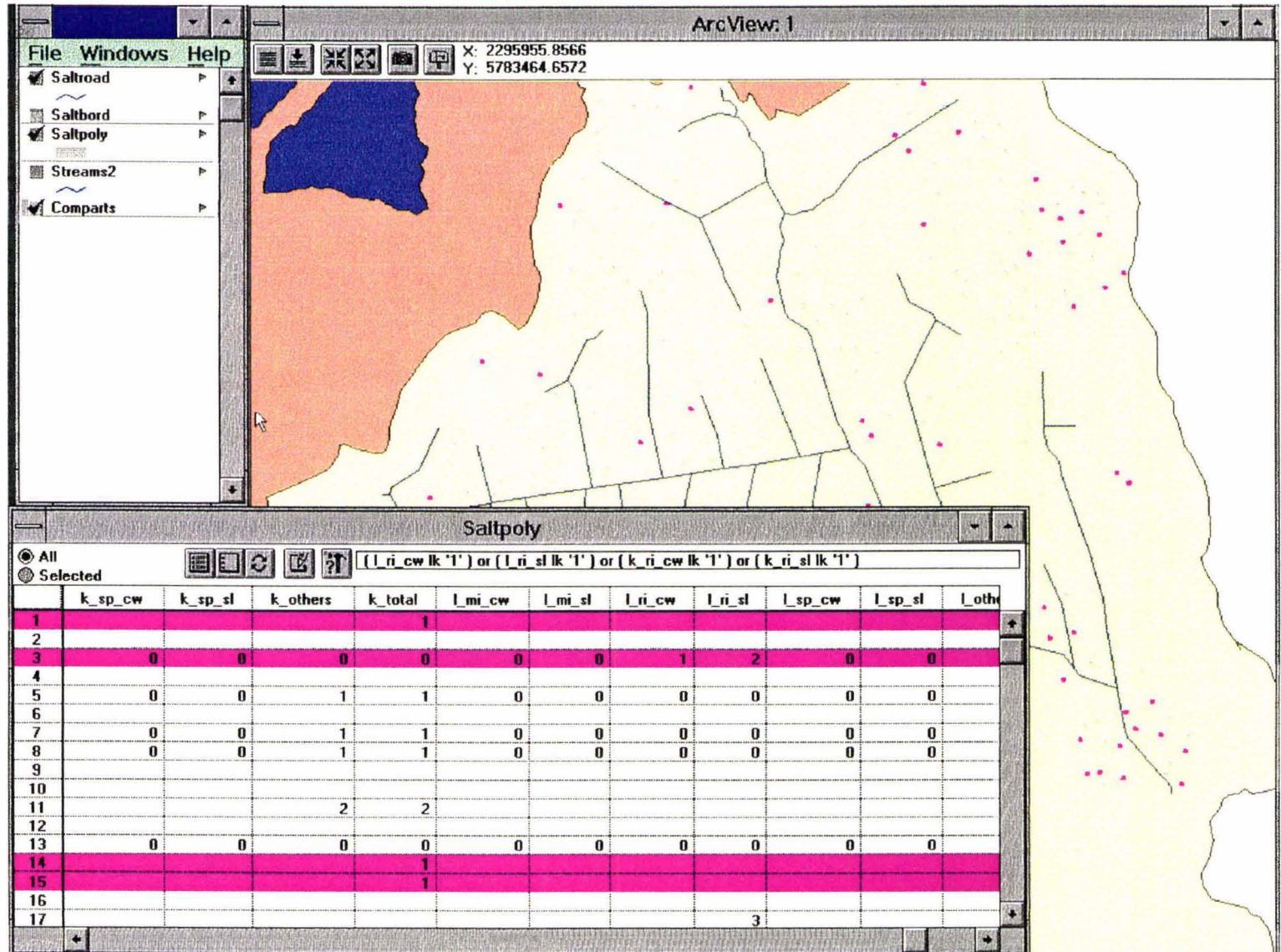
**GIS processing:** In 1986, the forest inventory database used in this study was stored on the New Zealand Forest Service computer. However, the computer files were lost during the dissolution of the Forest Service. All that remained was one private copy of a printout from the database, and one copy of the map showing the plot locations. The massive amount of data had never been analysed by the New Zealand Forest Service or its successors, the Department of Conservation and Timberlands New Zealand Ltd. Entering the inventory in a GIS created a new, permanent copy of the inventory and added the capability of linking the inventory data with other digital survey information. In addition, copies of digital data can be provided to a number of resource managers and researchers with minimal expense compared to distributing the paper versions.

Correlating the information in the inventory and map whilst in a paper form was a daunting task. For example, the identification of plots containing large senescent rimu, the type sought for harvesting in sustained-yield forestry, involved manually searching the printout to identify the plots which matched the criteria, locating the plots on the map and possibly draughting a new map. A GIS can process a simple query such as this in a fraction of the time. Maps can be printed at a size convenient to take into the field with the coordinates of individual plots shown if a GPS unit is being used. The analyses can be performed easily by a resource manager familiar with a GIS package. Moreover, the whole analysis and map production process can be automated through the use of GIS macro languages or the use of user-friendly desktop-mapping software (Figure 7.6).

The error, or effect of error, in GIS datasets must be considered. The locations of plots drawn on the original map is an obvious source of primary error (Thapa and Bossler, 1992). Plot locations were recorded as a distance and bearing from landmarks. Given the dense undergrowth in Saltwater Forest, error in distance measurement could be substantial, but impossible to measure. Without access to the original field sheets, the error in map compilation is also impossible to calculate. Other sources of error particularly relevant to this map include uncertainty in feature definition, *i.e.* undefined stream and track boundaries, and the error due to feature exaggeration, *i.e.* a 0.5mm line representing a track on a 1:10 000 map covers 5m on the ground (Thapa and Bossler, 1992). Errors would also arise from digitising the map, but given the care taken to digitise the map accurately and the visual overlay check performed, these would be insignificant compared to the errors on the original map.

Figure 7.6: A sample screen from the ArcView desktop mapping software. The 'display' window (right) shows the result of querying the forestry database to select all inventory plots that have rimu with a d.b.h greater than 1m present. The 'database' window (bottom left) shows the inventory database with all plots matching the search criteria coloured in magenta

Scale 1:56 000  
 \_\_\_\_\_ 1km



If the original field sheets had been available, plots could have been positioned directly using the original bearings and distances. This would remove map composition and digitising error but error due to feature definition and feature exaggeration would remain. Re-visiting survey plots and digitising plot locations directly with a GPS system, would remove feature definition and feature exaggeration error. However, satellite reception will probably be difficult under the dense forest canopy. The error in plot attributes is also open to measurement error and subjective assessments made by the field teams. Entering the attribute data into the original computer database and then retyping into the GIS database, although checked thoroughly, is another source of attribute error.

However, in contrast to GIS applications that require features to be defined precisely, *e.g.* routing electrical cables or cadastral mapping, the New Zealand rainforest is a natural community where there are no distinct compositional boundaries. Indigenous forests do not divide neatly into classes but occur as gradients with classes showing a certain amount of overlap (James, 1978). It is therefore unlikely that the extent of any positional error the inventory dataset would cause sufficiently large differences in vegetation composition to affect indigenous forestry operations. In addition, a forester must go into the forest and locate visually the trees to be harvested. Only an approximate location of where the particular trees are located is required, 10m error will not make a difference. Error in plot attributes could, however, send a forester to a completely wrong location.

**Image rectification:** Four GCP's were used to rectify each image. The rms error calculated from the GCP's was 0.34 pixels for the Landsat TM image and 0.21 pixels for the SPOT XS image. However, the use of 4 GCP's makes the rms an inappropriate method for assessing rectification accuracy because the error is calculated as the deviation of one point from the transformation function. A superior method is to superimpose a digital dataset, *e.g.* a road network, onto the registered imagery and observe the error visually. Overlaying the road network digitised from the 1: 25 000 map on the SPOT XS and Landsat TM imagery indicated a 'good fit' within the area of Saltwater Forest (Figures 7.7 and 7.8). A close inspection of the overlain roads indicated the rectification error on the main access roads within Saltwater Forest was within a pixel. At the far end of some minor roads leading off the main access road, the rectification error was 2 or 3 pixels. Given the lack of distinct compositional boundaries in the New Zealand rainforest (James, 1978), this error is not expected to influence the results of the analysis significantly.

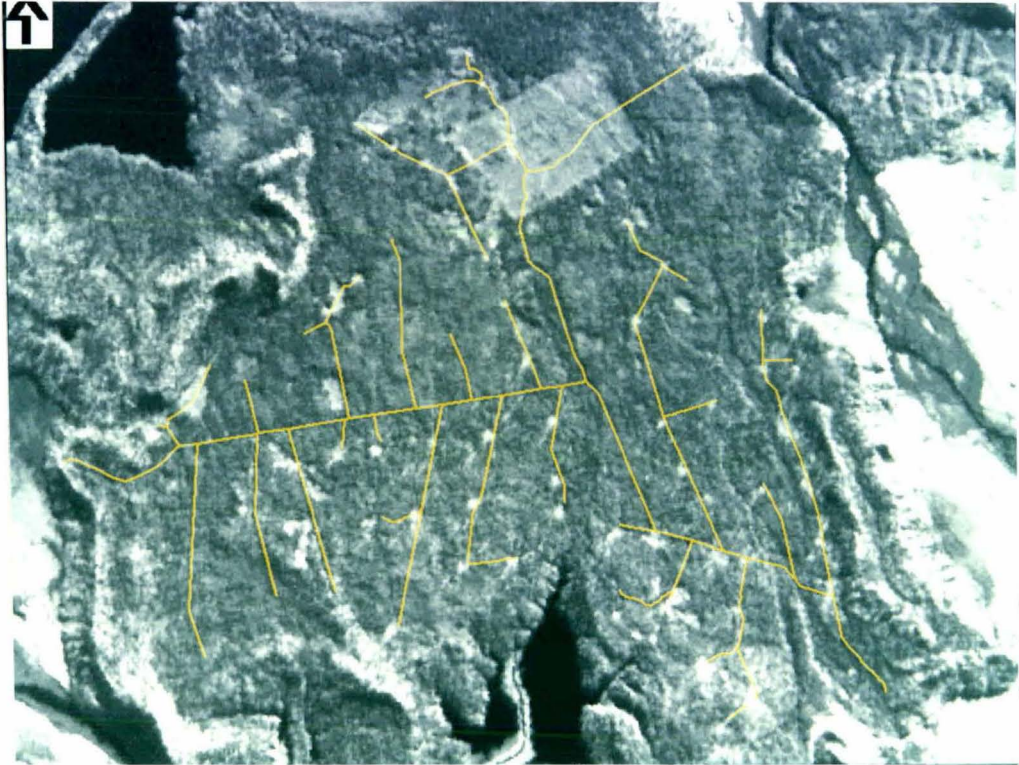


Figure 7.7: The rectified SPOT XS3 image with the roads digitised from the 1:25 000 forest map superimposed in yellow. Scale as printed in thesis 1:80 000.

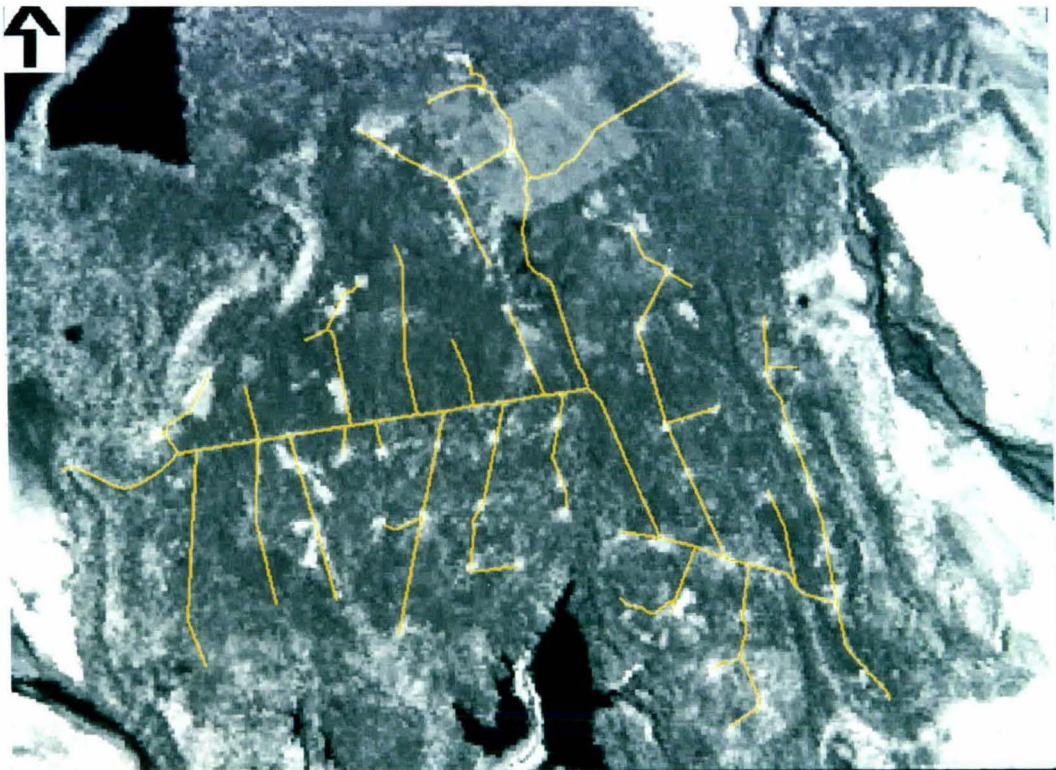


Figure 7.8: The rectified Landsat TM image with the roads digitised from the 1:25 000 forest map superimposed in yellow. Scale as printed in thesis 1:80 000.

*Integrated remote sensing and GIS analysis:* Overlaying the inventory plots on the imagery revealed there was variation in pixel values within the area occupied by a single plot. This is an example of a fundamental problem in integrating vector and raster information. In all but the most homogenous land-cover, variability will be evident and it is necessary to generalise the image data prior to integration with a GIS (Ehlers *et al.*, 1989). The variation observed within plots as a proportion of the range across all plots is graphed in Figure 7.9. In bands XS1 and XS2, the intra-plot variation was up to 50% of the total inter-plot variation because the range of XS1 and XS2 was only four pixel values across all plots. However in the TM bands, which showed increased variation across all plots, there was relatively little within-plot variation. This supports the argument that slight positional error in the GIS dataset and rectification error in the imagery were unlikely to affect the spectral signature extracted for each plot. In addition, most of the plots were comprised of over 50% of one pixel value (Figure 7.10).

The procedure of recording the pixel value that occupied the largest area, and the median value where one pixel value is not dominant, as the representative value for a plot is effectively the same as using modal and median filters on the satellite imagery. The value extracted for each plot in each image band is shown in Figures 7.11 and 7.12. The graphs indicate that the near-infrared bands, XS3 and TM4, exhibited the greatest variation between plots.

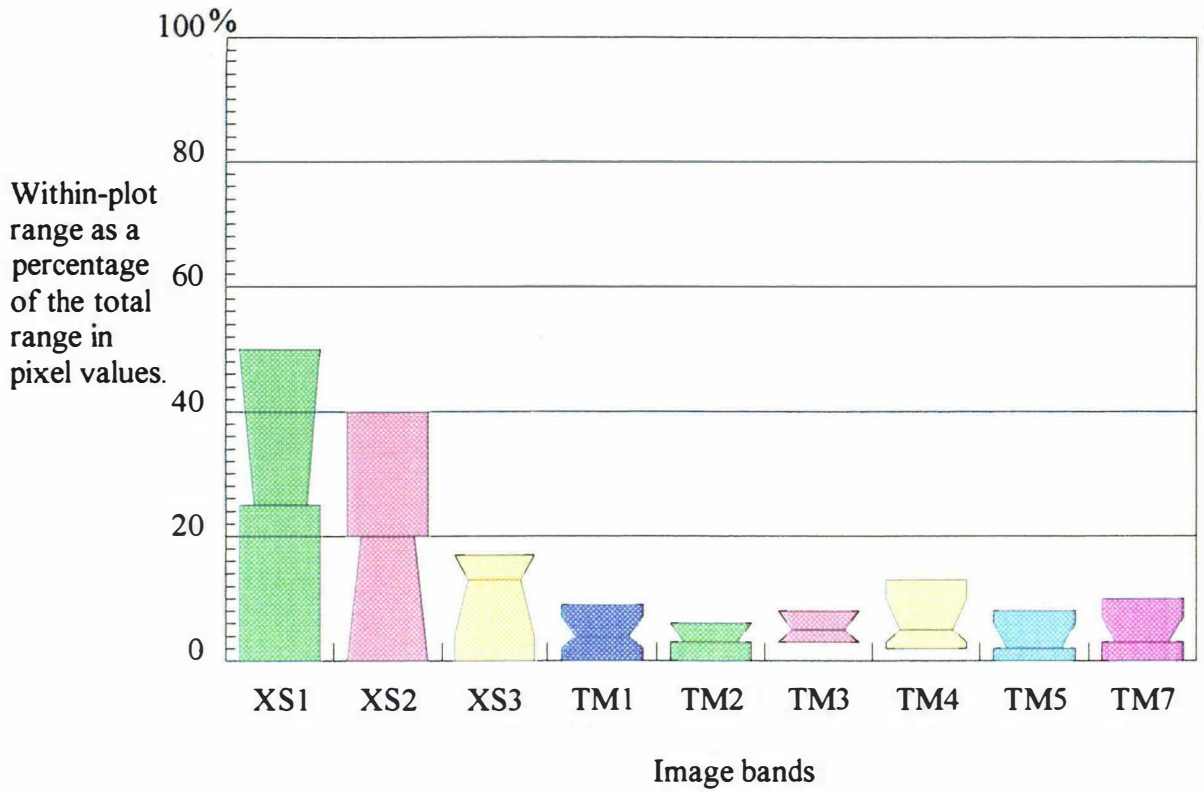


Figure 7.9: A box plot of the range of pixel values occurring within a plot as a percentage of the range across all plots. The colour of the box indicates the wavelength of light associated with the image band (yellow, cyan and magenta were chosen to represent the infrared bands). The line within each box is the mean. The boxes divide the data into quartiles.

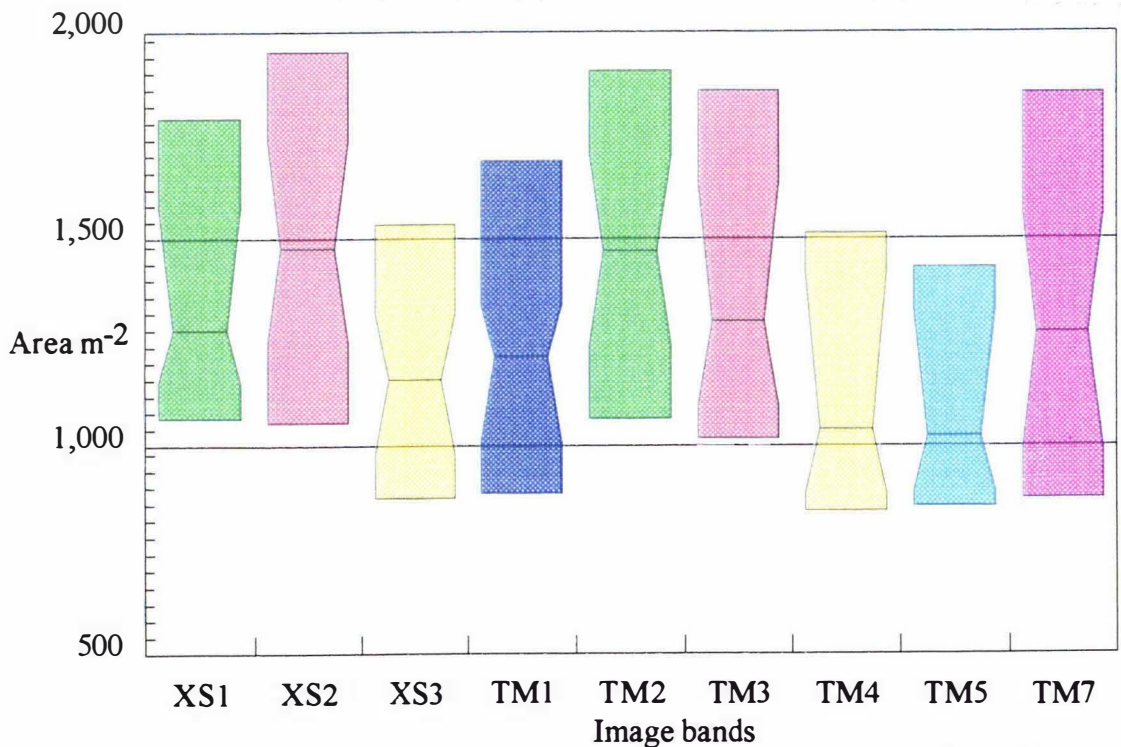


Figure 7.10: The area occupied by the pixel value taken as representative for a particular plot. Total plot area is 2,000m<sup>2</sup>. The colour of the box indicates the wavelength of light associated with the image band (yellow, cyan and magenta were chosen to represent the infrared bands). The line within each box is the mean. The boxes divide the data into quartiles.

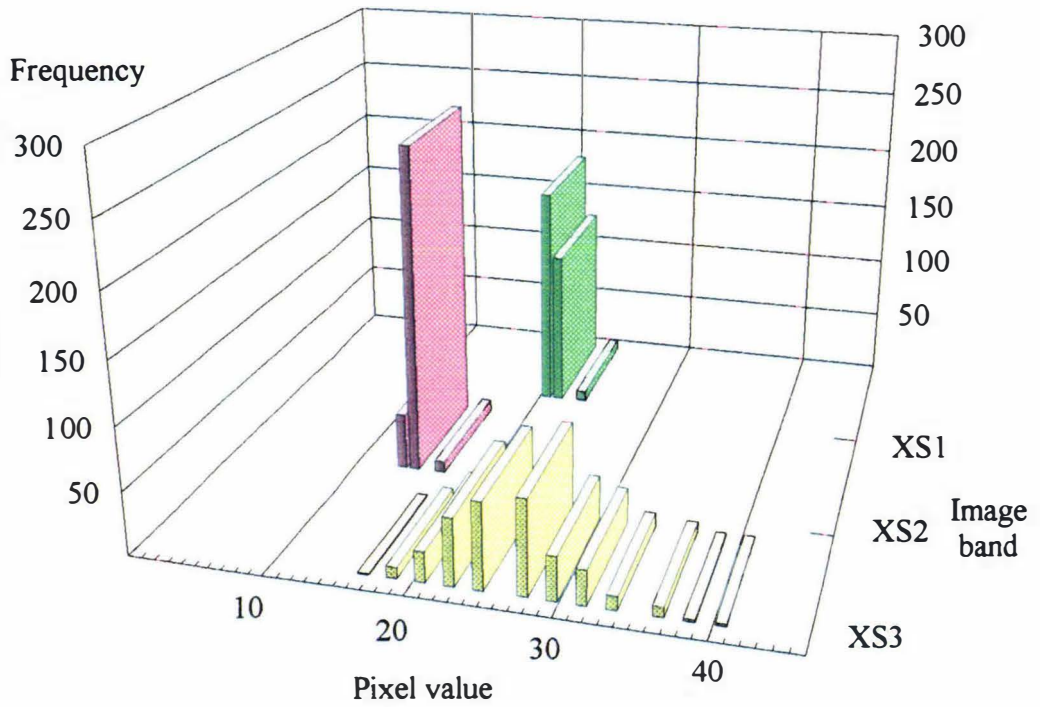


Figure 7.11: The range of pixel values observed within plots on the SPOT XS image. XS3 shows the greatest variation between plots. The colour of the box indicates the wavelength of light associated with the image band (yellow was chosen to represent the near-infrared band).

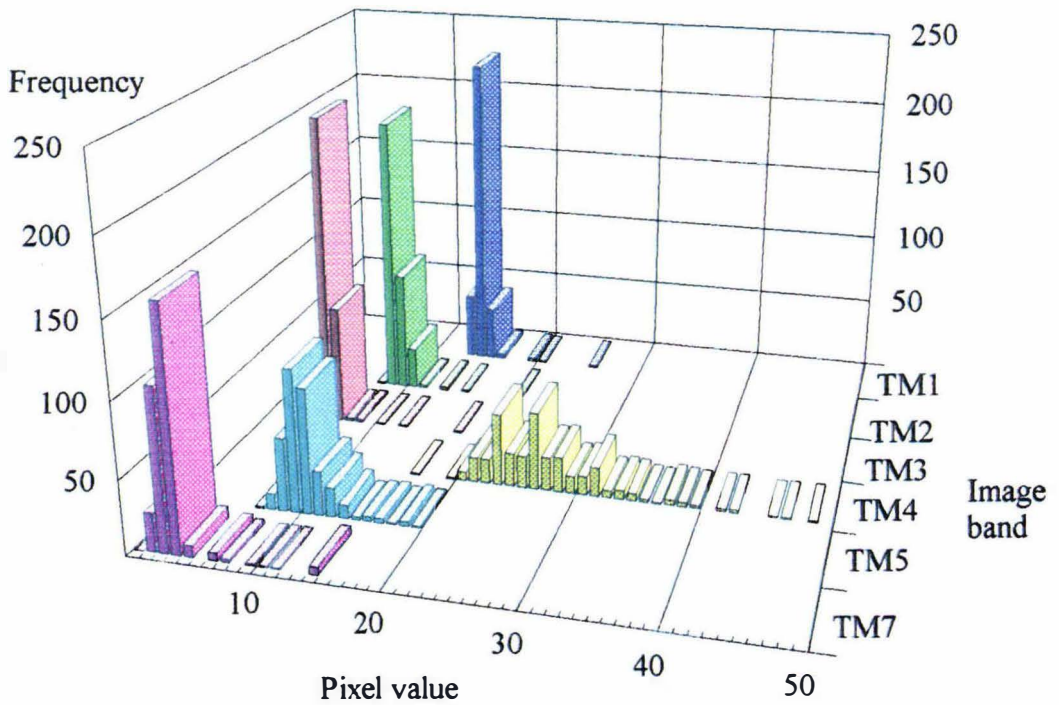


Figure 7.12: The range of pixel values observed within plots for the Landsat TM image. TM4 (near-infrared) shows the greatest variation between plots. The colour of the box indicates the wavelength of light associated with the image band (yellow, cyan and magenta were chosen to represent the infrared bands).

*Satellite imagery to discriminate forest inventory clusters:* The mean number of trees in each forest inventory cluster is shown in Table 7.3.

Table 7.3: The forest inventory clusters generated using the number of trees in each layer as the clustering variable.

Cluster	Number of plots	layer 3 (shrubs and small trees)	layer 2 subcanopy (rimu, miro and silver pine)	layer 1 canopy (rimu)
1	133	40	10	5
2	12	1300	20	6
3	77	55	40	6
4	7	60	75	20
5	87	32	20	14

In this study, these clusters were interpreted as:

1. Young saplings of rimu and silver pine with a broken canopy of scattered tall rimu trees. There are low number of trees in the subcanopy layer. This cluster has a similar composition to the 'senility/regeneration' growth phase of Six Dijkstra *et al.*, (1985).
2. High numbers of regeneration (silver pine), with a broken canopy of tall rimu. This cluster is usually found in boggy conditions (Six Dijkstra *et al.*, 1985) and is differentiated from cluster 1 in that the plots have high (1000 - 2000) numbers of regenerating silver pine. It is also similar to the 'senility/regeneration' growth phase of Six Dijkstra *et al.*, (1985).
3. Young saplings of rimu, miro and silver pine under a broken canopy of rimu. This cluster differs from cluster 1 in that the subcanopy layer is more dense. It is similar to the 'early competition growth phase' of Six Dijkstra *et al.*, (1985).
4. Mature forest with a dense canopy of heavily crowned rimu trees. Underneath this there is a well developed subcanopy of miro and silver pine. The cluster is similar to the 'competition growth phase' of Six Dijkstra *et al.*, (1985).
5. Mature forest forming a dense canopy of rimu with a subcanopy of rimu, miro and silver pine. This cluster has a less dense canopy and subcanopy than cluster 4 and is similar to the 'homeostatic growth phase' of Six Dijkstra *et al.*, (1985).

Confusion matrices derived from the discriminant analysis classification are shown in Tables 7.4 through 7.7. The matrices indicate that the spectral information contained in both the Landsat TM and SPOT XS images was unable to discriminate between the inventory clusters. Although class 1 had the highest percentage of correct classifications, 91% and 77% for the Landsat TM and SPOT images respectively, the result was not a true indication of class 1's separability because the majority of all plots, 244 for SPOT XS and 247 for Landsat TM were classified as class 1. It is best shown in the commission error, 58% for SPOT XS and 51% for Landsat TM.

Table 7.4: The confusion matrix derived from classification of the SPOT XS imagery. The table shows the number of pixels classified from the image as each inventory cluster. The diagonal indicates correct classifications.

Predicted Forest cluster	True forest cluster						
		1	2	3	4	5	total
1	103	10	56	5	70	244	
2	0	0	0	0	0	0	
3	26	1	20	2	16	65	
4	0	0	0	0	0	0	
5	4	1	1	0	1	7	
total	133	12	77	7	87	316	

Table 7.5: A summary of the SPOT XS classification results. The omission error shows for each cluster the pixels that were classified as another cluster. The commission error shows the pixels that were classified incorrectly into a given cluster.

Cluster	% correct	% omission error	% commission error
1	77	23	58
2	0	100	no pixels
3	26	74	69
4	0	100	no pixels
5	1	99	86

Average class correct: 21%. Overall accuracy of all pixels 39%.

Table 7.6: The confusion matrix derived from classification of the Landsat TM imagery. The table shows the number of pixels classified from the image as each inventory cluster. The diagonal indicates correct classifications.

Predicted Forest cluster	True forest cluster						
		1	2	3	4	5	total
1	121	11	46	3	66	247	
2	0	0	0	0	0	0	
3	7	1	27	4	16	55	
4	0	0	0	0	0	0	
5	5	0	4	0	5	14	
total	133	12	77	7	87	316	

Table 7.7: A summary of the Landsat TM classification results. The omission error shows for each cluster the pixels that were classified as another cluster. The commission error shows the pixels that were classified incorrectly into a given cluster.

Cluster	% correct	% omission error	% commission error
1	91	9	51
2	0	100	no pixels
3	35	65	51
4	0	100	no pixels
5	6	94	64

Average class correct: 26%. Overall accuracy of all pixels 48%.

It is notable that cluster 2 containing high numbers of regenerating trees (> 1000) and damp soil conditions was unable to be distinguished from cluster 1. A possible explanation for this lack of discrimination may be due partially to cluster 2 comprising only 12 plots which gives a 4% prior probability of classification. Similarly, cluster 4 which comprised 7 plots with the most dense canopy was classified as clusters 3 and 5. Cluster 5 (87 plots), was classified mainly as cluster 1. An analysis of the NDVI imagery indicated there was considerable overlap in NDVI between each inventory cluster (Figure 7.13).

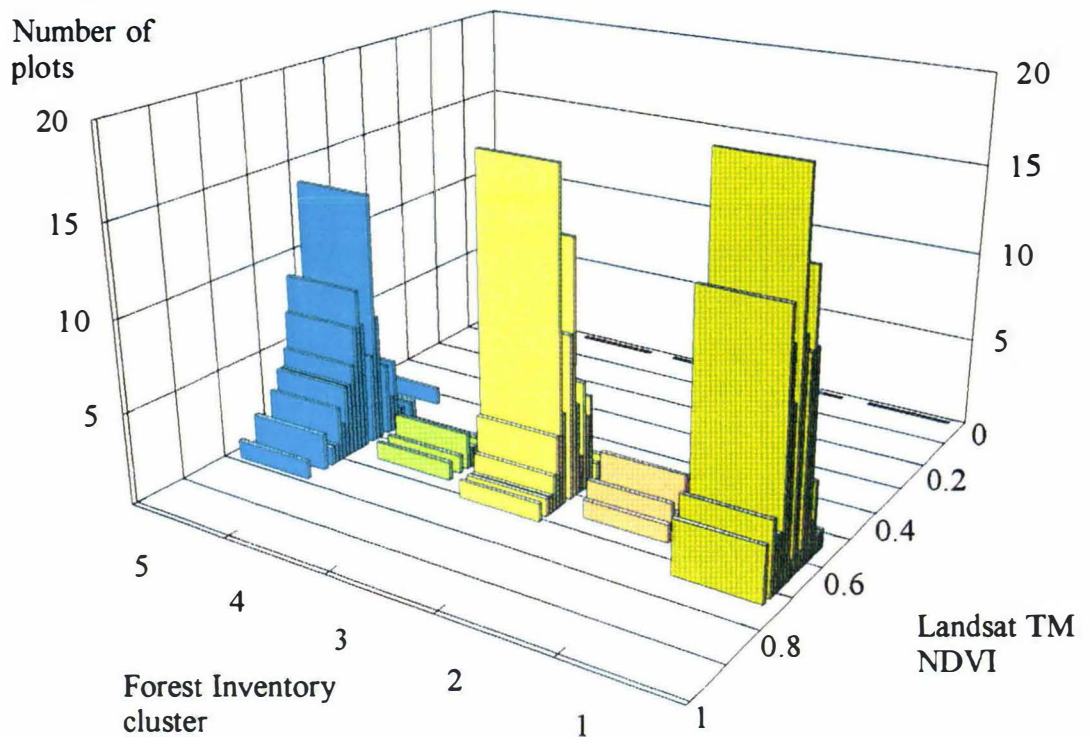


Figure 7.13: The Landsat TM NDVI values for each forest cluster. There is considerable overlap present in the range of NDVI recorded by the clusters.

It is surprising that clusters 1 and 5 cannot be distinguished through the Landsat TM and SPOT XS imagery as they represent two very different forest compositions. Cluster 1 is regenerating forest with a broken canopy of rimu, whereas cluster 5 is mature rimu forest with a dense canopy. The result demonstrates the spectral similarity that may be evident between dissimilar vegetative clusters in natural environments (Lewis, 1994) and highlights the difference between classification of remotely-sensed imagery and the clustering or extrapolation of field data (Biging and Congalton, 1991). Any clustering or extrapolation of point data is a subjective assessment made by the interpreter, and the clusters may vary considerably between interpreters (Biging and Congalton, 1991). Failure to discriminate the inventory clusters does not mean that satellite imagery has failed in providing information beneficial for resource management. Rather, it means that the particular clusters applied in this study were inappropriate for use with this satellite imagery. A multitude of other useful groupings could have been applied, one of which may have been discriminated successfully. The clusters that were able to be identified from the imagery are discussed in the next section of this thesis.

*Forest variables to interpret image spectral classes:* The classes derived from the unsupervised classification of the SPOT XS3 and Landsat TM images are shown in Figures 7.14 and 7.15.

Figure 7.14: The image classes derived from an unsupervised classification of the SPOT XS band 3 image. Three classes were chosen from visual inspection of the unclassified imagery. The roads of Saltwater Forest are superimposed.

Scale 1:85 000  
—— 1km

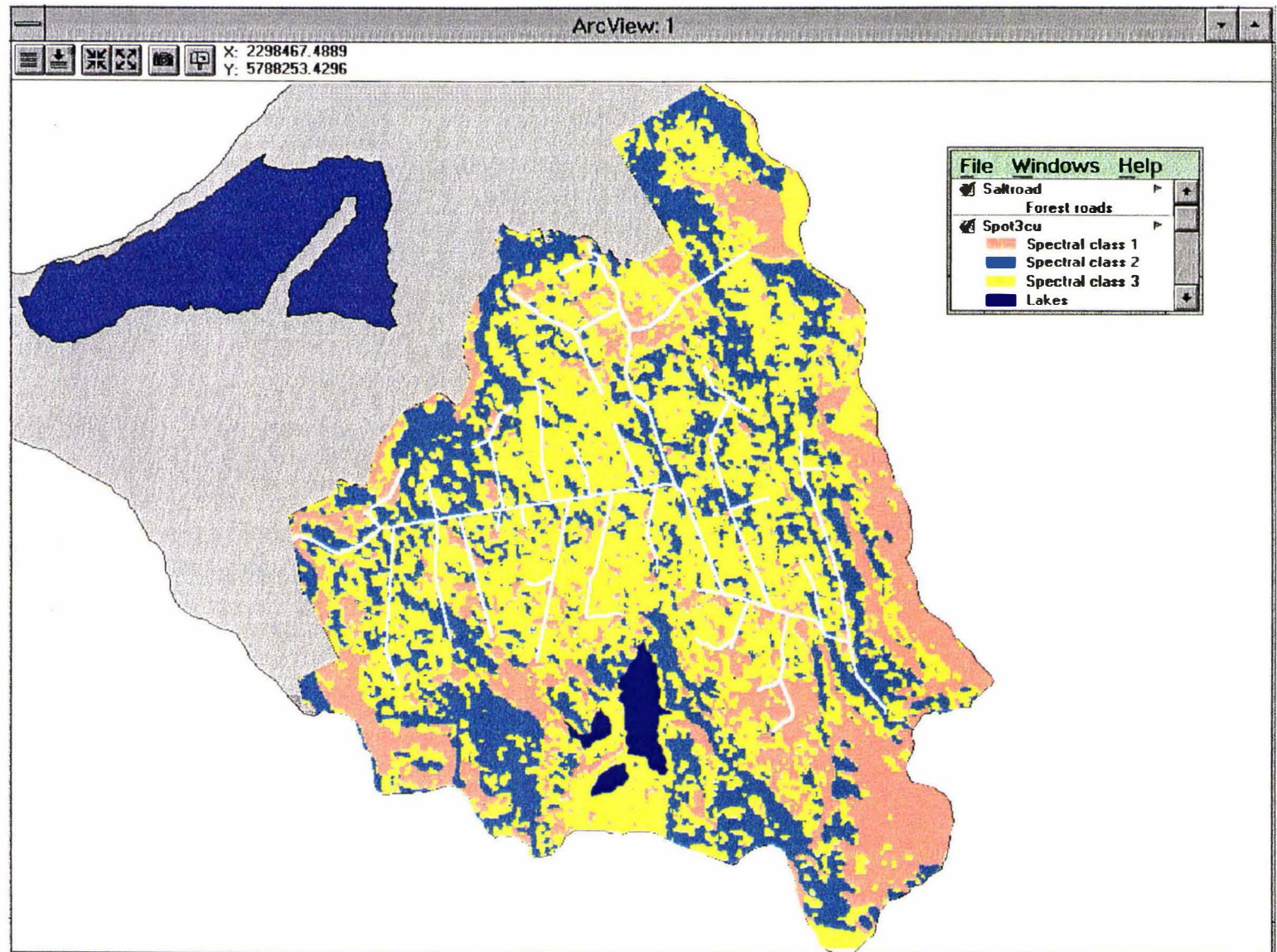
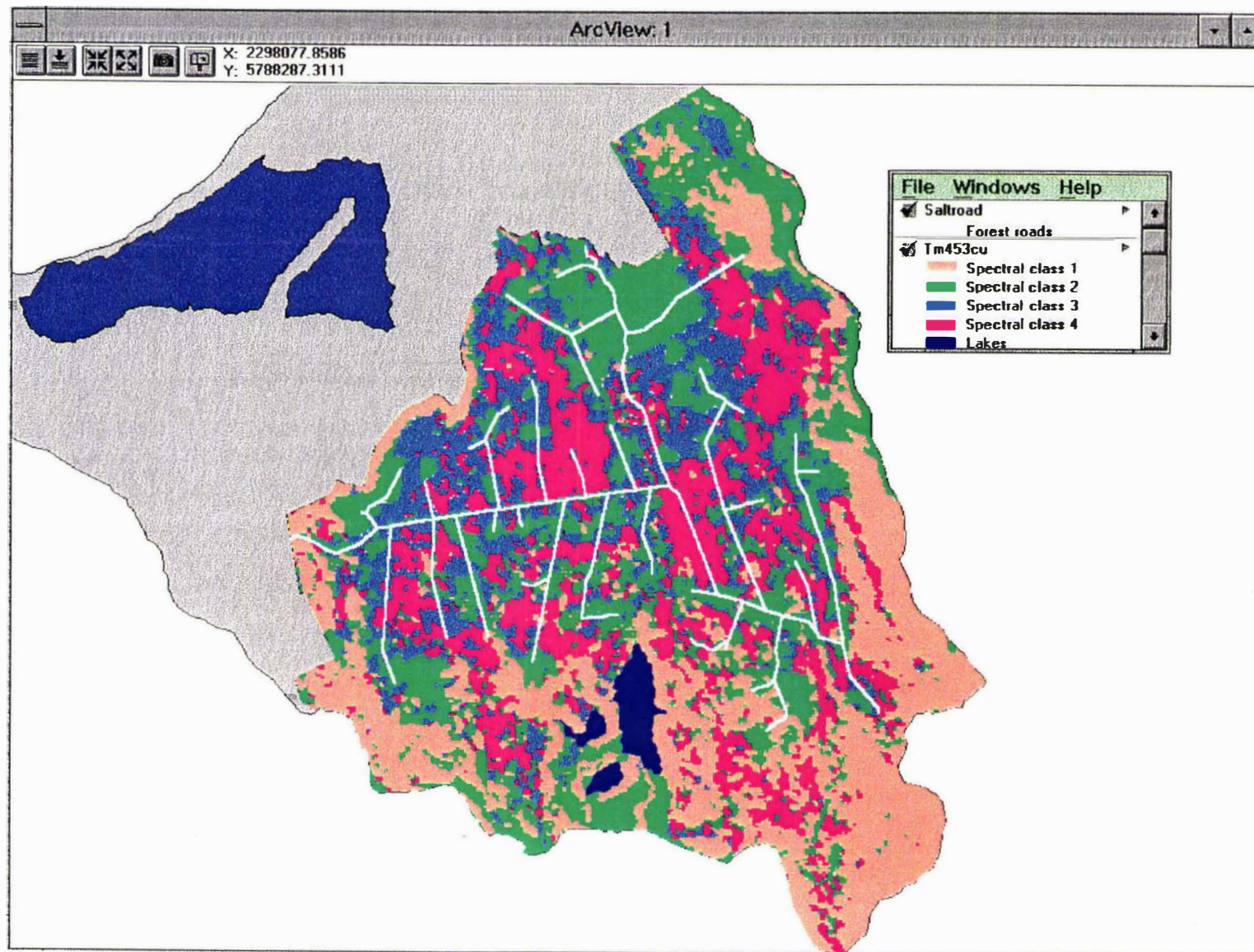


Figure 7.15: The image classes derived from an unsupervised classification of the Landsat TM4,5,3 image. Four classes were chosen from visual inspection of the unclassified imagery. The roads of Saltwater Forest are superimposed.

Scale 1:85 000  
1km



The classified imagery was filtered with a 3x3 modal filter prior to extracting a spectral class for each plot. While generalisation reduces the spatial variability of the image, previous work in tropical forests demonstrated that spatial filtering with a 3x3 mean filter increased class separability by reducing intra-class variance (Hill and Foody, 1994). An alternative to generalising the imagery is to use techniques such as linear mixing modelling (Quarmby *et al.*, 1992) whereby plots are attributed a certain percentage of each pixel value occurring within the plot boundary. However, whereas spatial filtering increases tolerance of errors in image rectification and plot positioning, linear mixture modelling requires that the datasets are rectified precisely, otherwise the class proportions are meaningless.

Both the SPOT XS3 and Landsat TM spectral classes exhibited high variation in the number of trees present within each layer (Tables 7.8 and 7.9). In the regenerating trees/shrub layer, the range included plots with no trees to some plots with more than 2000 trees. The high end of the range was due to plots with high numbers of regenerating trees not being discriminated as a separate class as in the previous analysis. The relationships between the median number of trees in each forest layer for each image class are graphed in Figures 7.16 and 7.17. The median was calculated as the centre of the distribution because it is resistant to the influence of the outliers *e.g.* plots with 0 or more than 2000 trees. The layers have been subdivided into their species components.

Both graphs exhibit a similar pattern. The majority of the variation between image classes was contained in the total number of trees in the size classes c through f (0.2 - 0.59m d.b.h), *i.e.* layer 2, the subcanopy layer. Within this grouping, the major influence was from the number of rimu trees. However, conclusions based on species differences must be made with caution because the variation may be due simply to their being large numbers of rimu present compared with other species. The number of trees in the regenerating layer also varied between classes but the distinctions evident in the inventory data, *i.e.* plots greater than 2000 stems, were not reflected in the spectral classification.

The larger forest size classes (> 0.6m d.b.h) demonstrated little variation across all image classes. However, it is notable that the number of trees in the large size classes was not the discriminating factor even when some plots had over 20 mature rimu trees in a 2000m<sup>2</sup> area. This highlights how in natural environments a spectral signature is a mixture of the different components in the pixel, the canopy, sub-canopy, ground cover and ground conditions (Spanner *et al.*, 1990) and that simplification to classes based on canopy composition may not always be appropriate (Foody, 1992). The small difference in species contribution between image clusters agrees with the work of Lewis (1994) who noted that spectrally distinct vegetation groups are often defined by difference in vegetation cover and vertical structure, with species differences playing a subordinate role.

Table 7.8: The median, minimum and maximum number of trees occurring in each spectral class generated from the SPOT XS image.

Image Class	Forest layer	Minimum	Median	Maximum
1 (19 plots)	1	0	8	1147
	2	0	5	102
	3	0	4	21
2 (110 plots)	1	0	23	2023
	2	0	24	123
	3	0	7	30
3 (187 plots)	1	0	20	1999
	2	0	30	141
	3	0	7	26

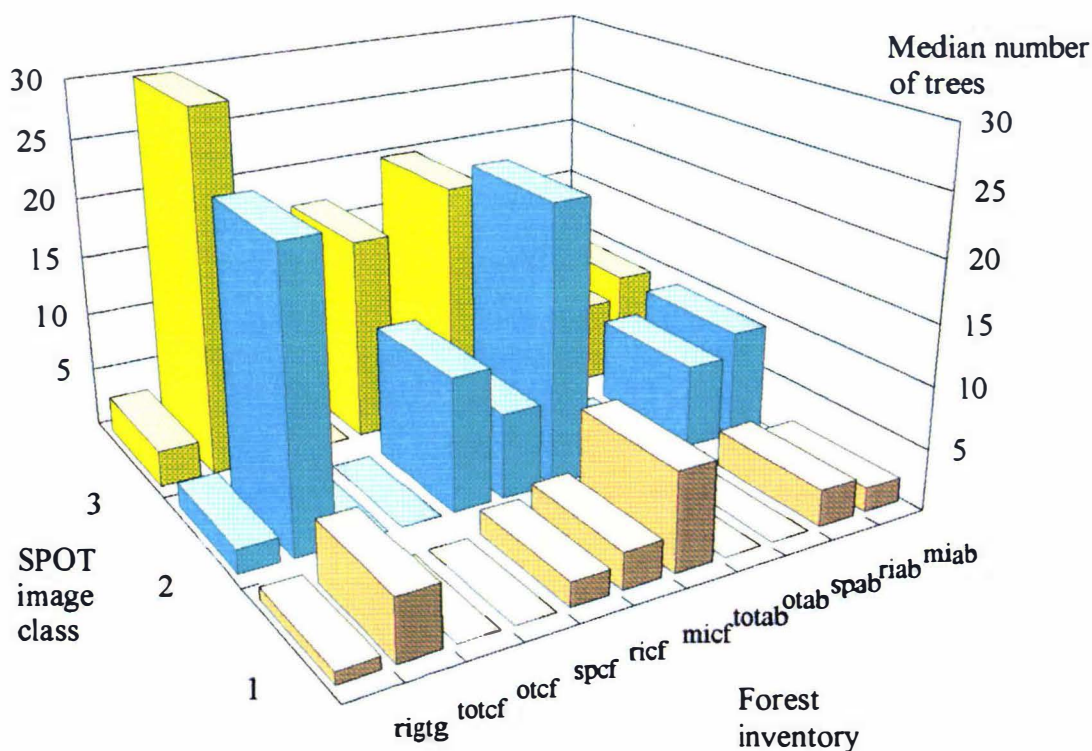


Figure 7.16: The forest composition of the SPOT XS image classes. The number of trees refers to the median number of trees found in each grouping. The forest inventory axis shows the species ('mi' (miro), 'ri' (rimu), 'sp' (silver pine), 'ot' (others)) within each layer ('ab' (layer 1), ('cf' (layer 2), 'gtg' (layer 3)) e.g. 'riab' is the rimu in layer 1. 'Tot' refers to the total number of trees within a layer. Rimu was the only species present in layer 3.

Table 7.9: The median, minimum and maximum number of trees occurring in each spectral class generated from the Landsat TM image.

Image Class	Forest layer	Minimum	Median	Maximum
1 (34 plots)	1	0	15	130
	2	0	5	42
	3	0	4	20
2 (36 plots)	1	0	14	1147
	2	0	13	67
	3	0	7	19
3 (89 plots)	1	0	24	2021
	2	0	24	141
	3	0	7	23
4 (157 plots)	1	0	18	2023
	2	0	36	123
	3	0	7	30

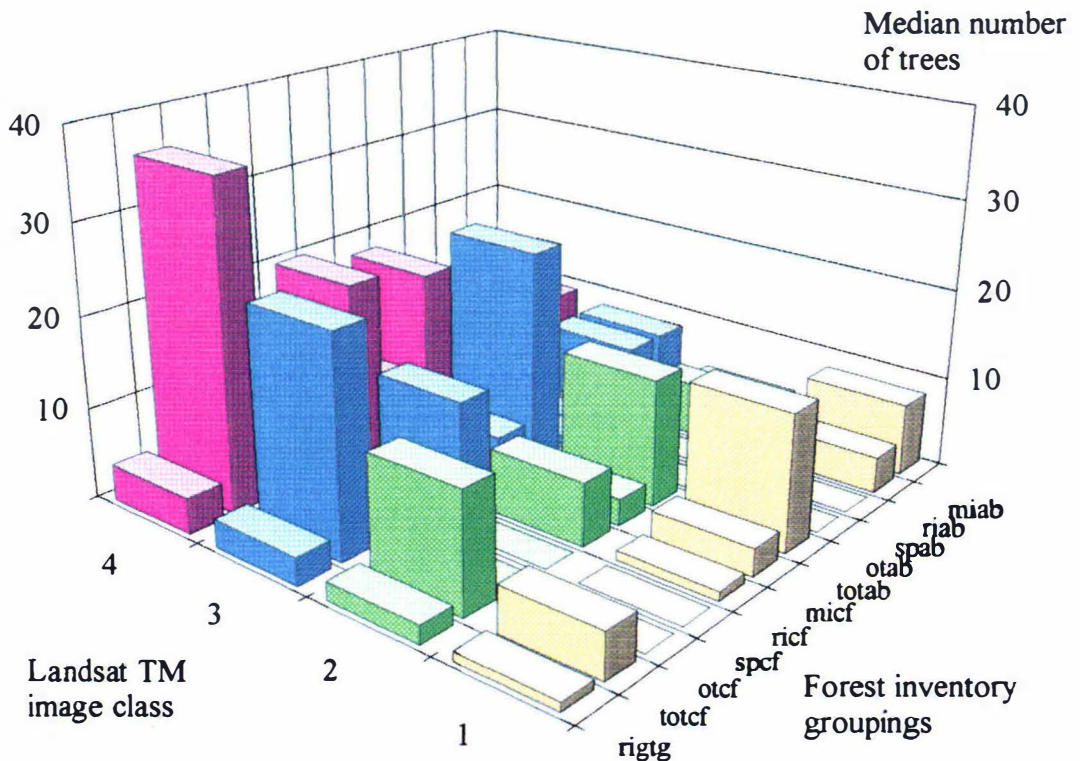


Figure 7.17: The forest composition of the Landsat TM image classes. The number of trees refers to the median number of trees found in each grouping. The forest inventory axis shows the species ('mi' (miro), 'ri' (rimu), 'sp' (silver pine), 'ot' (others)) within each layer ('ab' (layer 1), 'cf' (layer 2), 'gtg' (layer 3)) e.g. 'riab' is the rimu in layer 1. 'Tot' refers to the total number of trees within a layer. Rimu was the only species present in layer 3.

***Application to resource management:*** The implementation of the remote sensing and GIS tools and techniques demonstrated in this study requires the appropriate computer hardware and software, digital data, and experience in image processing/GIS integration. All of these require additional capital and operating funding which must be supported by senior management. This study has shown how the application of a GIS could return immediate benefit for resource management in indigenous forests, reducing the time and expense involved in data management and field operations for both ecological monitoring and sustained-yield logging operations.

The practical application of the two remote sensing and GIS methodologies applied in this study is open to debate. The supervised image classification was not able to discriminate the different vegetative clusters inherent in the inventory data. This may cause satellite imagery to be construed by some resource managers as an ineffectual technique for providing the information they require. In contrast, relating an unsupervised classification to field plots produced an objective, up-to-date view of the forest composition. Although the composition of the image classes may not be the same that is intuitive from analysis of inventory data, this information could not be obtained from field survey without considerable financial expense.

The unsupervised classification technique could also be used to identify forest types that have been under-represented in previous field surveys. For example, in the Landsat TM spectral classification, classes 3 and 4 contained 78% of the plots (Table 7.9). These classes were shown to contain more trees in the subcanopy and canopy layers than classes 1 or 2, which may indicate a bias in the positioning of the plots for timber extraction purposes. To generate a more balanced view of the forest, additional field plots could be targeted to the areas indicated by classes 1 and 2.

## **7.5 Summary**

This study investigated the application of GIS to indigenous forest management and examined strategies for relating field survey data with SPOT XS and Landsat TM imagery. A GIS was used to analyse a forest inventory database which recorded species and size class information for 316 circular 0.2ha plots. The study demonstrated how a resource manager could use the GIS to perform spatial queries on the inventory database, locating trees suitable for harvesting in sustained yield logging operations.

Two distinct integrated remote sensing/GIS strategies were investigated. The first approach clustered the inventory data to generate the natural communities inherent in the inventory.

Five clusters, comprising various degrees of canopy cover, subcanopy and smaller trees and shrubs, were identified. Discriminant analysis was applied to determine whether the inventory clusters could be differentiated with the spectral information in the SPOT XS and Landsat TM imagery. Confusion matrices indicated that this was not possible with overall classification accuracies of 39% and 48% for the SPOT XS and Landsat TM images respectively.

A second analysis applied an unsupervised classification to generate the spectrally separable classes from the satellite imagery. The number of classes was determined from visual analysis of the imagery. Each inventory plot was assigned to a class and the vegetative composition of the classes investigated by examining the number and species of trees occurring within each class. Examination revealed that it was the subcanopy density that varied the most between classes. There was also variation in the shrub/regeneration layer but this was small compared to the variation observed in the subcanopy layer. Little variation was observed in the canopy layer.

The study illustrated the difficulty of relating ground-based classifications with classifications from satellite imagery. Because the inventory clusters could not be observed in the imagery, results from studies attempting to map ground-based classes from satellite imagery may undermine the utility of satellite imagery in the eyes of resource managers. In contrast, the application of an unsupervised image classification produces an objective, up-to-date view of the entire forest. The limitation is that the vegetative composition of the spectral classes may not coincide with classes generated from field data.

## 8: CONCLUSIONS & RECOMMENDATIONS

Management of natural resources is an issue that effects all New Zealand citizens. The exploitation of resources can result in severe environmental, economic and social problems. Effective natural resource management is reliant on appropriate decisions made from accurate, up-to-date information. However field survey, the method used commonly to gather natural resource information, can be expensive, time consuming, and is hampered by difficult terrain and dense vegetation. These physical conditions are typified in Westland, the West Coast of New Zealand's South Island. A superhumid climate, dense indigenous vegetation, rugged relief and low population density combine to create an environment in which it is difficult to retain up-to-date resource information.

Remote sensing, digital image processing and GIS are examples of information sources and tools that have been demonstrated to aid in acquiring and managing the information necessary for resource management (Trotter, 1991). This thesis was initiated to investigate the application of remote sensing, digital image processing and GIS for resource management in Westland. From the multitude of potential applications, research was directed toward two issues identified by DoC Westland Conservancy, namely alluvial gold mining and indigenous forestry.

A case study investigated the application of digital image processing in monitoring alluvial gold mining operations. Alluvial gold mining is a major land use in Westland with the majority of the production coming from 70-80 small sites distributed throughout the Greymouth and Hokitika region (Metcalf and Godfrey, 1990). Although many land-cover monitoring applications require use of a multispectral data source, *e.g.* colour-infrared aerial photography (Carrel *et al.*, 1978, Halverson, 1988), this study investigated the application of black-and-white aerial photography. This type was used because DoC have historically used black-and-white photography to create halftones for mining license applications. In addition, black-and-white photography is less expensive than colour-infrared photography (Avery and Berlin, 1985) and digital image processing of black-and-white photography requires only a third of disk storage and processing as colour-infrared photography.

The study demonstrated how a supervised classification of digitised black-and-white aerial photography could provide the quantitative and spatial land-cover information required for monitoring alluvial gold mining. However, given that the image registration and classification techniques applied in the study were straightforward, that DoC has access to a comprehensive archive of aerial photography and that the digital image processing was

performed on inexpensive PC hardware and software, this begs the question "Why has a digital image processing system not been installed in an operational environment previously?"

A possible explanation is given by Nicol (1993) who noted that in DoC, advocates of remote sensing and GIS have been unable to convince senior management of the value of these tools in decision making. Other explanations may be that it is simply too difficult to integrate new methods with the traditional system (Townshend, 1992), that resource managers do not have access to the necessary computer hardware, or that resource managers are already overworked and do not have sufficient time to experiment with or implement new techniques. While issues surrounding the access to suitable computing hardware are likely to disappear with the decreasing price/performance ratio of PCs (Anthony, 1994), other issues such as the difficulty integrating digital image processing into the existing systems will require substantial effort.

An example of the difficulty integrating digital image processing with the existing system was evident in the alluvial gold mining study. On a cadastral plan obtained from DoC, the roads did not represent the actual shape and position of the road network. Although this error may not be representative of other cadastral plans held by DoC, it is of concern because in many remote sensing applications, roads are often the only feature visible in both the imagery and base map data, and are therefore the only features suitable for use as GCPs. While a level of abstraction may be acceptable for schematic plans, it is not acceptable if the data is to be used in a digital image processing or GIS database. Thought must be given to this at compilation of such plans.

Although quantitative information on the area of each land-cover class could be extracted quickly and easily from the classified images, caution must be exercised in the application of digital change detection procedures. Whereas change detection techniques such as composite classification can make identification and interpretation of change difficult (Pilon *et al.*, 1988), the independent-classification change detection as applied in this study, may suffer from being able to identify change too easily, making it tempting for resource managers to rush in and produce pretty pictures, but erroneous data. The extent of classification error in the individual images was not obvious in the confusion matrices or classified images, however the error was propagated through into the change detection imagery. Examination of subsequent change detection images demonstrated how possible areas of spurious change could be identified as land alternating between different change classes. This indicated how a second subsequent change detection image can be used as a tool in rapidly identifying areas where change may be an artifact of the independent classifications.

A further two case studies investigated the application of digital image processing of satellite imagery (SPOT XS and Landsat TM) to provide information beneficial to management of the New Zealand rainforest. SPOT XS and Landsat TM images were used because they were the only multispectral imagery available. DoC had purchased the SPOT XS image prior to commencement of this thesis, and the Landsat TM image was acquired for the studies under EOSAT's student data grant scheme. The study in the Saltwater Ecological Area, examined how digital image processing of satellite imagery could be used as a method to update vegetation maps. The study concluded that a supervised spectral classification of either image type was unable to provide the detailed information required to update the existing map. Including six vegetation classes in classification of the SPOT XS image resulted in a 53% overall classification accuracy. Amalgamating the six classes to three hybrid classes resulted in an overall accuracy of 83%, but with an associated reduction in information content, *i.e.* the majority of the forest was classified as mixed kamahi/rimu forest which is only a general description of the podocarp-hardwood forest of Westland (Poole and Johns, 1992) and of no use in this resource management application. In comparison, classification of the Landsat TM into six vegetation classes achieved an overall classification accuracy of 75%.

Although the study was not designed as a comparison of the SPOT XS and Landsat TM imagery, examination of the images revealed that with respect to the vegetation map, the Landsat TM image provided more information on the vegetative composition than the SPOT XS image. Whereas a strict comparison of Landsat TM and SPOT XS would have to apply imagery acquired at the same time of year under similar geometrical conditions, the study indicates how selection of appropriate imagery is critical to the information obtained and impressions formed. Had only the SPOT XS image been available, conclusions from this study would have been based solely on the poor results obtained from the SPOT XS image. At a cost of approximately \$NZ8000 per Landsat TM scene, it may be difficult for resource managers to justify funding for further satellite imagery once an image has been purchased and found unsatisfactory.

The poor classification accuracies obtained in the study indicated that comparison of classified imagery to an existing map may not have been the correct application of satellite imagery in indigenous forestry. For resource management applications in indigenous forests it is probable that the present satellite-borne sensors and image interpretation techniques cannot provide the information required to update existing maps. While GIS visionaries have suggested that the choropleth map is now a redundant form of mapping (Berry, 1993), the requirement for quantitative information in resource reports and natural resource management consents, and the familiarity of resource managers with choropleth

mapping means that image classification procedures will have to remain the focus of many remote sensing analyses in the near future.

A more appropriate application of satellite imagery and digital image processing in indigenous forests may be in detecting change. Once images have been radiometrically, atmospherically and geometrically corrected, pixels that have changed in successive images could be identified quickly by a number of change detection techniques that do not require image classification. The possible causes of the change may be explained by resource managers using the existing detailed vegetation survey and knowledge of the land management practices applied in the area. Application of this technique would minimise time and personnel costs associated with field survey by focussing teams on the areas identified in the imagery.

The second study of indigenous forestry in the Saltwater Forest investigated how a GIS can be used to aid manipulation and analysis of forest inventory databases and examined methodologies for integrating the inventory database with SPOT XS and Landsat TM imagery. Manipulation of the inventory database with a GIS demonstrated immediate benefits to sustained-yield logging operations. Large rimu trees, the type suitable for timber extraction, could be identified simply and rapidly with desktop mapping software, saving both time and money for forest managers. Furthermore, this type of information could not have been extracted practically without a GIS. For sustained-yield logging operations a detailed forest inventory is a necessity, as is a GIS to interpret and manipulate the data into useful information.

The two integrated remote sensing/GIS methodologies applied in the second forestry study approached integration of the imagery and inventory database from different directions. The first approach clustered the forest inventory data to generate the clusters inherent in the inventory. Five clusters, comprising various degrees of canopy cover, subcanopy and smaller trees and shrubs, were identified. Overall classification accuracies of 39% and 48% for the SPOT XS and Landsat TM images respectively, indicated how replication of the inventory classes was not feasible with the spectral information in the imagery. The lack of discrimination demonstrated the spectral similarity that may be apparent between dissimilar vegetative clusters in natural environments (Lewis, 1994).

The second approach applied unsupervised clustering to the satellite imagery. Analysis of the vegetative composition of the classes revealed that it was the subcanopy density that varied the most between classes. This highlighted how in natural environments, a spectral signature is a mixture of the different components in the pixel (Spanner *et al.*, 1990) and that simplification to classes based on canopy composition may not always be appropriate

(Foody, 1992). The small difference in species contribution between classes agreed with the work of Lewis (1994) who noted how spectrally distinct vegetation groups are often defined by difference in vegetation cover and vertical structure, with species differences playing a subordinate role.

Both of these studies in indigenous forestry have strong messages for resource managers intending to use satellite imagery and digital image processing to remap forest classifications derived from ground data. The case studies showed that this was not the appropriate application of satellite imagery in indigenous forestry, and trying to use it for this purpose would probably lead to disappointing results. An unsupervised classification could be used to generate an objective classification of the entire forest, however it may fail to identify the vegetative classes inherent in the inventory. Although the classes identified may have application in future resource management applications, the fact that the detailed ground-based classifications, the type of information used traditionally by resource managers, could not be observed in the imagery, will only impede the adoption of digital image processing and satellite imagery in detailed indigenous forest applications.

General conclusions about the application of remote sensing and GIS to resource management outside the areas of the case studies are not appropriate. The studies were only two out of many potential applications in Westland, each of which may have returned different results and conclusions. Similarly, aerial photography, SPOT XS and Landsat TM imagery are only three of many possible sources of remotely-sensed data. Because of the hardware and software restrictions imposed in the execution of this thesis, the digital image processing techniques applied were restricted to those found in the available PC software. In the studies of indigenous forests, more complex procedures and more powerful algorithms may have provided more detailed and useful information for resource management. However the installation and operation of these systems in the resource management centres of Westland is unlikely due to the funding and operator skills required. It must also be noted that the thesis focused the application of digital image processing and satellite imagery on one small, but highly important aspect of resource management in Westland, but did not investigate the capability of satellite imagery for less detailed, regional monitoring for which more success could have been expected.

With respect to alluvial gold mining and indigenous forestry, this thesis has succeeded in its aim to investigate how remote sensing and GIS can provide and manage the information necessary for resource management in Westland. Nevertheless, a major limitation of the thesis, and the cause of many of the problems preventing the adoption of remote sensing and GIS in resource management agencies (Nicol, 1993), is that the studies were not performed on site in a resource management centre. Rather, all of the digital image

processing and GIS analysis occurred at Massey University. It was evident from the visits made to Westland that many resource managers were keen to see the adoption of new technology - if time permitted. However, pilot projects must have the funding to be completed in-house. Only when resource management agencies are prepared to invest in studies whereby resource managers can experiment with digital image processing and GIS technology, in their workplaces, will the true potential of satellite imagery, digital image processing and GIS for resource management be realised.

The subject of the application of remote sensing and GIS for natural resource management in Westland is far from completely examined. It is recommended that additional efforts be expended on:

*Change detection in indigenous forestry:* Indigenous forests are under threat from pests, such as the possum, which cause severe damage to forest vegetation. The degree of forest damage that must occur before change can be identified in remotely-sensed imagery, both varying scales of aerial photography and satellite imagery, needs to be investigated. Associated with this is the determination of the appropriate image transformations, e.g. band ratios or the tasselled-cap transformation, which may be applied to identify damage, and the integration of atmospheric correction and image normalisation procedures.

*Knowledge-based techniques to interpret imagery:* To provide information applicable in resource management, images must be interpreted and the nature of any change must be identified. This requires work on knowledge-based techniques integrating existing sources of vegetation information with change detection analyses and raw imagery.

*Integration of image-based and ground-based classifications:* In remote sensing, the procedures for spectral classification are well established as are those for vegetation classification in the disciplines of ecology, botany and forestry. The two classification systems could be integrated, incorporating both data sources to improve the accuracy and application of information derived from land-cover mapping. Incorporation of the ground-based classifications, can focus a remote sensing analysis on identifying the classes of interest to resource managers, while still providing an encompassing, synoptic view.

## REFERENCES

- Afifi, A.A. and Clark, V. (1984). Computer Aided Multivariate Analysis. Lifetime Learning Publications, Belmont, California.
- Agee, J. K., Stitt, S. C. F., Nyquist, M., & Root, R. (1989). A geographic analysis of historical grizzly bear sightings in the North Cascades. Photogrammetric Engineering and Remote Sensing, 55, 1637-1642.
- Ahearn, S. C., Smith, J. L. D., & Wee, C. (1990). Framework for a Geographically Referenced Conservation Database: Case Study in Nepal. Photogrammetric Engineering and Remote Sensing, 56, 1477-1481.
- Ahern, F. J., Brown, R. J., Cihlar, J., Gauthier, R., Murphy, J., Neville, R. A., & Teillet, P. M. (1988). Radiometric correction of visible and infrared remote sensing data at the Canada Centre of Remote Sensing. In A. Cracknell & L. Hayes (Eds.), Remote Sensing Yearbook (pp. 101-127). Taylor and Francis, New York.
- Ahern, F. J., Erdle, T., Maclean, D. A., & Knepeck, I. D. (1991). A quantitative relationship between forest growth rates and Thematic Mapper reflectance measurements. International Journal of Remote Sensing, 12, 387-400.
- Ahern, F. J., Leckie, D. G., & Drieman, J. A. (1993(a)). Seasonal changes in relative C-Band backscatter of Northern forest cover types. IEEE Transactions on Geoscience and Remote Sensing, 31, 668-680.
- Ahern, F. J., Leckie, D. G., & Werle, D. (1993(b)). Applications of RADARSAT SAR data in forested environments. Canadian Journal of Remote Sensing, 19, 330-337.
- Aldrich, R. C. (1975). Detecting disturbance in a forest environment. Photogrammetric Engineering and Remote Sensing, 41, 39-48.
- Alexander, S. S., Dein, J., & Gold, D. P. (1973). The use of ERTS-1 MSS data for mapping strip mines and acid mine drainage in Pennsylvania. Quoted in Rathore, C.S. and Wright, R. (1993) Monitoring environmental impacts of surface coal mining. International Journal of Remote Sensing, 14, 1021-1042.
- Alföldi, T. T. (1982). Remote Sensing for water quality monitoring. In C. J. Johannsen & J. L. Sanders (Eds.), Remote Sensing for Resource Management (pp. 317-328). Soil Conservation Society of America.
- Allen, R. B., & McLennan, M. J. (1983). Indigenous Forest Survey Manual: Two Inventory Methods (Bulletin No. 40). Forest Research Institute.
- Allum, J. A., & Dreisinger, B. R. (1986). Remote sensing of vegetation change near Inco's Sudbury mining complexes. International Journal of Remote Sensing, 8, 399-416.
- Almond, P. (1986). Soils of the Saltwater State Forest. Quoted in Norton, D.A. and Leathwick, J.R. (1990). The lowland vegetation pattern, south Westland, New Zealand 1. Saltwater Ecological Area. New Zealand Journal of Botany, 28, 41-51.

- Anderson, A. T., & Schubert, J. (1976). ERTS-1 data applied to strip mining. Photogrammetric Engineering and Remote Sensing, *42*, 211-219.
- Anderson, A. T., Schultz, D., Buchman, N., & Nock, H. M. (1977). Landsat imagery for surface mine inventory. Photogrammetric Engineering and Remote Sensing, *43*, 1027-1036.
- Anderson, J. R., Hardy, E. E., Roach, J. T., & Witmer, R. E. (1976). A Land Use and Land Cover Classification System for use with Remote Sensor Data (Professional Paper No. 964). United States Geological Survey.
- Anthony, R. S. (1994). Unleashing the Power of the Pentium. PC Magazine, *April 12, 1994*, 114-180.
- Ardo, J. (1992). Volume quantification of coniferous forest compartments using spectral radiance recorded by Landsat Thematic Mapper. International Journal of Remote Sensing, *13*, 1779-1786.
- Aronoff, S. (1985). The minimum accuracy value as an index of classification accuracy. Photogrammetric Engineering and Remote Sensing, *51*, 593-600.
- Ashley, M. D., & Rea, J. (1975). Seasonal vegetation differences from ERTS imagery. Photogrammetric Engineering and Remote Sensing, *41*, 713-719.
- Aspinall, R., & Veitch, N. (1993). Habitat Mapping from Satellite Imagery and Wildlife Survey Data Using a Bayesian Modelling Procedure in a GIS. Photogrammetric Engineering and Remote Sensing, *59*, 537-543.
- Atkinson, I. A. E. (1985). Derivation of vegetation mapping units for an ecological survey of Tongariro National Park, North Island, New Zealand. New Zealand Journal of Botany, *23*, 361-378.
- Avery, T. E., & Berlin, G. L. (1985). Interpretation of Aerial Photographs. Burgess Publishing Company, Minneapolis, USA.
- Bailey, T. C. (1994). A Review of Statistical Spatial Analysis in Geographical Information Systems. In S. Fotheringham & P. Rogerson (Eds.), Spatial Analysis and GIS (pp. 13-45). Taylor and Francis.
- Baker, J. R., Briggs, S. A., Gordon, V., Jones, A. R., Settle, J. J., Townshend, J. R. G., & Wyatt, B. K. (1991). Advances in classification for land cover mapping using SPOT HRV imagery. International Journal of Remote Sensing, *12*, 1071-1085.
- Barker, G. R. (1988). Remote Sensing: the unheralded component of geographic information systems. Photogrammetric Engineering and Remote Sensing, *54*, 195-199.
- Barringer, T. H., Robinson, V. B., Coiner, J. C., & Bruce, R. C. (1980). Landsat analysis of tropical forest succession employing a terrain model. In 14th International Symposium on Remote Sensing of Environment, *3* (pp. 1691-1700). San Jose, Costa Rica.

- Becking, R.W. (1959). Forestry applications of aerial colour photography. Photogrammetric Engineering, 25, 559-565.
- Belward, A. S., Taylor, J. C., Stuttard, M. J., Bignal, E., Mathews, J., & Curtis, D. (1990). An unsupervised approach to the classification of semi-natural vegetation from Landsat Thematic Mapper data: A pilot study on Islay. International Journal of Remote Sensing, 11, 429-445.
- Benning, V. M., Ching, N. P., Bennetts, R. L., Thomas, I. L., & Beach, D. W. (1981). King Country Resources from Satellite Imagery. New Zealand Cartographic Journal, 11(2), 20-29.
- Berry, J. K. (1993). Beyond Mapping Concepts, Algorithms and Issues in GIS. GIS World Books, GIS World Inc, Colorado, USA. 246p.
- Biggs, P. H., & Green, M. A. (1992). Forest Resource Information from Large-Scale Aerial Photography and GIS. In 6th Australasian Remote Sensing Conference, 1 (pp. 338-344). Wellington, New Zealand: Committee of the 6th Australasian Remote Sensing Conference.
- Biging, G. S., & Congalton, R. G. (1991). A Comparison of Photointerpretation and Ground measurements of Forest Structure. In Proceedings from the ACSM-ASPRS Annual Convention, 3 (pp. 7-15). Baltimore, Maryland, USA: ACSM-ASPRS.
- Blakeman, D. A. (1987). Some thoughts about GIS data entry. In GIS '87, (pp. 226-233). San Francisco: American Society for Photogrammetry and Remote Sensing - American Congress on Surveying and Mapping.
- Brockhaus, J. A., & Khorram, S. (1992). A comparison of SPOT and Landsat TM data for use in conducting inventories of forestry resources. International Journal of Remote Sensing, 13, 3055-3043.
- Brook, K. D., Carter, J. O., Danaher, T. J., McKeon, G. M., Flood, N. R., & Peacock, A. (1992). The Use of Spatial Modelling and Remote Sensing for Monitoring and Forecasting of Drought-Related Land Degradation Events in Queensland. In 6th Australasian Remote Sensing Conference, 1 (pp. 140-149). 2-6 November 1992, Wellington, New Zealand: Committee of the 6th Australasian Remote Sensing Conference.
- Buck, R. G., Pahl, L., & Preston, R. A. (1992). Predictive Mapping of Preferred Koala Habitat Trees in South East Queensland, Australia. In 6th Australasian Remote Sensing Conference, 1 (pp. 249-260). Wellington, New Zealand: Committee of the 6th Australasian Remote Sensing Conference.
- Burrough, P. A. (1987). Principles of Geographical Information Systems for Land Resources Assessment. Clarendon, Oxford.
- Campbell, J. B. (1987). Introduction to Remote Sensing. New York: The Guilford Press.

- Carrel, J. E., Johannsen, T. W., Barney, T. W., & McFarland, W. (1978). Remote Measurements of vegetative cover in surface mines. In Twelfth International Symposium on Remote Sensing of the Environment, (pp. 1653-1664). Centre for Remote Sensing Information and Analysis, Environmental Research Institute of Michigan. Ann Arbor, Michigan, USA.
- Caselles, V., & Lopez-Garcia, M. J. (1989). An alternative simple approach to estimate atmospheric correction in multitemporal studies. International Journal of Remote Sensing, 10 (1127-1134).
- Catt, P. (1992). Digitised Aerial Photography for High Resolution Studies on Coral Reefs. In 6th Australasian Remote Sensing Conference, 1 (pp. 366-369). Wellington, New Zealand.: Committee of the 6th Australasian Remote Sensing Conference.
- Catt, P., & Thirarongnarong, K. (1992). An evaluation of remote sensing techniques for the detection, mapping and monitoring of an invasive plant species in coastal wetlands: A case study of Para Grass (*Bracharia mutica*). In 6th Australasian Remote Sensing Conference, 1 (pp. 200-204). Wellington, New Zealand.: Committee of the 6th Australasian Remote Sensing Conference.
- Chamignon, C., & Manière, R. (1990). Forest cover type mapping and damage assessment of *Zeiraphira diniana* by SPOT 1 HRV data in the Mercantour National Park. International Journal of Remote Sensing, 11, 1439-1450.
- Chang, K., Verbyla, D. L., Yeo, J. L., & Zhao-xing, L. (1994). GIS-Based Program Aids Wildlife Habitat and Timber Management. GIS World, 7(1), 40-43.
- Chant, L. (1987). Letter to Secretary for the Environment 23.6.87. Quoted in Ministry for the Environment (1987) South Westland South of the Cook River Resource Management Study, Public Discussion Document, 6 November 1987. Ministry for the Environment. 88pp.
- Chase, P. E., & Pettyjohn, W. (1973). ERTS-1 investigation of ecological effects of strip mining from eastern Ohio. Quoted in Rathore, C.S. and Wright, R. (1993) Monitoring environmental impacts of surface coal mining. International Journal of Remote Sensing, 14, 1021-1042.
- Chavasse, C. G. R. (1964). Guide to the Forest Types of Westland. New Zealand Forest Service. Wellington.
- Chavez, P.S. (1989). Radiometric calibration of Landsat Thematic Mapper multispectral images. Photogrammetric Engineering and Remote Sensing, 55, 1285-1294.
- Chewings, V. H., Bastin, G. N., & Pickup, G. (1992). Remote Sensing Models for Determining Grazing Impact in Arid Rangelands. In 6th Australasian Remote Sensing Conference, 1 (pp. 169-178). Wellington, New Zealand.: Committee of the 6th Australasian Remote Sensing Conference.

- Chuvieco, E., & Congalton, R. G. (1988). Using cluster analysis to improve the selection of training statistics in classifying remotely sensed data. Photogrammetric Engineering and Remote Sensing, 54, 1275-1281.
- Chrisman, N. R. (1992). Modelling error in overlaid categorical maps. In M. Goodchild & S. Gopal (Eds) Accuracy of Spatial Databases, (pp 21-34). Taylor & Francis.
- Cibula, W. G., & Nyquist, M. O. (1987). Use of topographic and climatological models in a geographic database to improve Landsat MSS classification for Olympic National Park. Photogrammetric Engineering and Remote Sensing, 53, 67-75.
- Clarke, K. C. (1985). A comparative analysis of polygon to raster interpolation methods. Photogrammetric Engineering and Remote Sensing, 51, 575-582.
- Cliff, A. D., & Ord, J. K. (1973). Spatial Autocorrelation. Pion Limited, London.
- Colwell, J. E., & Weber, F. P. (1981). Forest change detection. In 15th International Symposium on Remote Sensing of Environment, (pp. 839-852). Ann Arbor, Michigan, USA.
- Cone, J. E. (1990). Determination of surface reflectance and estimates of atmospheric optical depth and single scattering albedo from Landsat Thematic Mapper data. International Journal of Remote Sensing, 11, 783-828.
- Congalton, R. G. (1988). Using Spatial Autocorrelation Analysis to Explore Errors in Maps Generated from Remotely Sensed Data. Photogrammetric Engineering and Remote Sensing, 54, 587-592.
- Congalton, R. G., & Green, K. (1992). The ABCs of GIS. Journal of Forestry, Geographic Information Systems. Part 1. November 1992., 13-20.
- Congalton, R. G., Green, K., & Teply, J. (1993). Mapping Old Growth Forests on National Forest and Park Lands in the Pacific Northwest from Remotely Sensed Data. Photogrammetric Engineering and Remote Sensing, 59, 529-535.
- Congalton, R. G., Oderwald, R. G., & Mead, R. A. (1983). Assessing Landsat Classification Accuracy Using Discrete Multivariate Statistical Techniques. Photogrammetric Engineering and Remote Sensing, 49, 1671-1678.
- Coppin, P. R., (1991). The change component in multitemporal Landsat TM Images: Its potential for forest inventory and management. Ph.D. Thesis, University of Minnesota.
- Coppock, J. T., & Rhind, D. W. (1991). The History of GIS. In D. J. Maguire, M. F. Goodchild, & D. W. Rhind (Eds.), Geographic Information Systems. Volume 1: Principles (pp. 8-19). Longman Scientific and Technical.
- Corner, R. J., & Lodwick, G. D. (1992). Spectral Bathymetry Using Landsat Thematic Mapper Data in Cockburn Sound, WA. In 6th Australasian Remote Sensing Conference, 1 (pp. 180-191). Wellington, New Zealand: Committee of the 6th Australasian Remote Sensing Conference.

- Cowen, D. J. (1988). GIS versus CAD versus DBMS: What are the differences. Photogrammetric Engineering and Remote Sensing, 54, 1551-1559.
- Creasey, J. W., & Fleming, C. (1992). Shallow Water Mapping in the Philippines Using Landsat TM Imagery. In 6th Australasian Remote Sensing Conference, 1 (pp. 191-199). Wellington, New Zealand: Committee of the 6th Australasian Remote Sensing Conference.
- Crippen, R. E. (1988). The dangers of underestimating the importance of data adjustments in band ratioing. International Journal of Remote Sensing, 9, 767-776.
- Cross, A. M., Settle, J. J., Drake, N. A., & Paivinen, R. T. M. (1991). Subpixel measurement of tropical forest cover using AVHRR data. International Journal of Remote Sensing, 12, 1119-1129.
- Cumberland, K. G. (1981). Landmarks. Readers Digest Services Pty Ltd.
- Curran, P. J. (1980). Multispectral sensing of vegetation amount. Progress in Physical Geography, 4, 315-341.
- Curran, P. J. (1986). Principles of Remote Sensing. Longman Scientific and Technical.
- Danson, F. M. (1987). Preliminary evaluation of the relationships between SPOT-1 HRV data and forest stand parameters. International Journal of Remote Sensing, 8, 1571-1577.
- Danson, F. M., Curran, P. J., & Plummer, S. E. (1992). Remotely-sensed inputs to a forest ecosystem model. In 6th Australasian Remote Sensing Conference, 1 (pp. 130-139). Wellington, New Zealand.: Committee of the 6th Australasian Remote Sensing Conference.
- Das, D. K., Mishra, K. K., & Kalra, N. (1993). Assessing growth and yield of wheat using remotely-sensed canopy temperature and spectral indices. International Journal of Remote Sensing, 14, 3081-3092.
- Davis, F. W., Stoms, D. M., Estes, J. E., Scepan, J., & Scott, J. M. (1990). An information systems approach to the preservation of biological diversity. International Journal of Geographic Information Systems, 4, 55-78.
- De Goldi, J. A. (1984). The Sphagnum moss industry on the West Coast. Quoted in Ministry for the Environment (1987) South Westland South of the Cook River Resource Management Study, Public Discussion Document, 6 November 1987. Ministry for the Environment. 88pp.
- De Wulf, R. R., Goossens, R. E., De Roover, B. P., & Borry, F. C. (1990). Extraction of forest stand parameters from panchromatic and multispectral SPOT-1 data. International Journal of Remote Sensing, 11, 1571-1588.
- Deene, T. (1983). Sphagnum on the West Coast, South Island. N.Z. Centre for Resource Management, Lincoln College.

- Dekker, A. G., Malthus, T. J., & Goddijn, L. M. (1992). Monitoring Cyanobacteria in Eutrophic Waters Using Airborne Imaging Spectroscopy and Multispectral Remote Sensing Systems. In 6th Australasian Remote Sensing Conference, 1 (pp. 204-214). Wellington, New Zealand: Committee of the 6th Australasian Remote Sensing Conference.
- Derenyi, E., & Pollock, R. (1990). Extending a GIS to Support Image-Based Map Revision. Photogrammetric Engineering and Remote Sensing, 56, 1493-1496.
- Derrien, M., Farki, B., Legleau, H., & Sairouni, A. (1992). Vegetation cover mapping over France using NOAA-11 AVHRR. International Journal of Remote Sensing, 13, 1787-1795.
- Dicks, S. E., & Lo, T. H. C. (1990). Evaluation of Thematic Map Accuracy in a Land Use and Land Cover Mapping Program. Photogrammetric Engineering and Remote Sensing, 56, 1247-1252.
- Dobson, M. C., Ulaby, F. T., Le Toan, T., Beaubien, A., Kasiscke, E. S., & Christensen, N. (1992). Dependence of Radar Backscatter on Coniferous Forest Biomass. IEEE Transactions on Geoscience and Remote Sensing, 30, 412-415.
- Drieman, J. A. (1987). Evaluation of SIR-B Imagery for Monitoring Forest Depletion and Regeneration in Western Alberta. Canadian Journal of Remote Sensing, 13, 19-25.
- Drummond, J. (1990). A framework for handling error in Geographic Data manipulation. In Fundamentals of Geographic Information Systems: A Compendium (pp. 109-118). ASPRS.
- Duggin, M. J., & Robinove, C. J. (1990). Assumptions implicit in remote sensor data acquisition and analysis. International Journal of Remote Sensing, 11, 1669-1694.
- Dunningham, A., & Thompson, S. (1989). Use of Geographic Information Systems in New Zealand Forestry Applications. Commonwealth Forestry Review, 68(3), 203-213.
- Dymond, J. R. (1993). An improved Skidmore/Turner classifier. Photogrammetric Engineering and Remote Sensing, 59, 623-626.
- Dymond, J. R., Page, M. J., & Brown, L. J. (in press). Large area vegetation mapping in the Gisborne district, New Zealand, from Landsat TM. International Journal of Remote Sensing.
- Eckhardt, D. W., Verdin, J. P., & Lyford, G. R. (1990). Automated Update of an Irrigated Lands GIS Using SPOT HRV Imagery. Photogrammetric Engineering and Remote Sensing, 56, 1515-1522.
- Ehlers, M. (1990). Remote Sensing and Geographic Information Systems: Towards Integrated Spatial Information Processing. IEEE Transactions on Geoscience and Remote Sensing, 28(4), 763-766.
- Ehlers, M., Edwards, G., & Bedard, Y. (1989). Integration of Remote Sensing with Geographic Information Systems: A necessary evolution. Photogrammetric Engineering and Remote Sensing, 55, 1619-1627.

- Ehlers, M., Greenlee, D., Smith, T., & Star, J. (1991). Integration of Remote Sensing and GIS: Data and Data Access. Photogrammetric Engineering and Remote Sensing, 57, 669-675.
- Elifrits, D. C., & Barr, D. J. (1982). Application of remote sensing to subsidence detection at a room-and-pillar coal mine. In C. J. Johannsen & J. L. Sanders (Eds.), Remote Sensing for Resource Management (pp. 347-361). Soil Conservation Society of America.
- Ellyet, C. D., & Fleming, F. W. (1974). Thermal infrared imagery of the Burning Mountain coal fire. Remote Sensing of Environment, 3, 79-86.
- ESRI (1992). In ARC News, 14(1-4). Environmental Systems Research Institute, Redlands, CA, USA.
- ESRI (1993). In ARC News, 15(1-4). Environmental Systems Research Institute, Redlands, CA, USA.
- ESRI (1993(a)). In PC ARC/INFO Starter Kit Manual. Environmental Systems Research Institute, Redlands, CA, USA.
- ESRI (1994). In ARC News, 16(1-4). Environmental Systems Research Institute, Redlands, CA, USA.
- Fearnside, P. M. (1986). Spatial Concentration in the Amazon Basin. Ambio, 15, 74-81.
- Fiorella, M., & Ripple, W. J. (1993). Determining Successional Stage of Temperate Coniferous Forests with Landsat Satellite Data. Photogrammetric Engineering and Remote Sensing, 59, 239-246.
- Fischer, W. A. (1975). History of Remote Sensing. In R. G. Reeves (Eds.), Manual of Remote Sensing (pp. 27-50). Falls Church, Virginia, USA: American Society of Photogrammetry.
- Foody, G. M. (1992) A fuzzy sets approach to the representation of vegetation continua from remotely sensed data: an example from lowland heath. Photogrammetric Engineering and Remote Sensing, 58, 2, 221-225.
- Ford, J. P., & Casey, D. J. (1988). Shuttle Radar Mapping with diverse incident angles in the rainforest of Borneo. International Journal of Remote Sensing, 9, 927-943.
- Forster, B. C., Xingwei, S., & Baide, X. (1993). Remote sensing of sea water quality parameters using Landsat TM. International Journal of Remote Sensing, 14, 2759-2772.
- Foweraker, C. E. (1929). The podocarp rain forests of Westland, New Zealand. 2. Kahikatea and totara forests and their relationship to silting. Te kura ngahere, 2(4), 6-12.
- Franklin, J. (1986). Thematic mapper analysis of coniferous forest structure and composition. International Journal of Remote Sensing, 7, 1287-1301.
- Friel, C., Leary, T., Norris, H., Warford, R., & Sargent, B. (1993). GIS Tackles Oil Spill in Tampa Bay. GIS World, 6(11), 30-33.

- Frouin, R., & Gautier, C. (1987). Calibration of NOAA-7 AVHRR, GOES-5 and GOES-6 VISSR/VAS Solar Channels. Remote Sensing of Environment, 22, 73-101.
- Fung, T., & LeDrew, E. (1987). Application of principal components analysis to change detection. Photogrammetric Engineering and Remote Sensing, 53, 1649-1658.
- Gastellu-Etchegorry, J. P., & Ducros-Gambart, D. (1991). Computer-assisted land cover mapping with SPOT in Indonesia. International Journal of Remote Sensing, 12, 1493-1507.
- Gastellu-Etchegorry, J. P., Estreguil, C., Mougin, E., & Laumonier, Y. (1993). A GIS based methodology for small scale monitoring of tropical forests- a case study in Sumatra. International Journal of Remote Sensing, 14, 2349-2368.
- Giddings, L. E., Soto, M., Angulo, M. J., Larios, H., & Ramirez, A. M. (1980). The use of Landsat data in mapping tropical vegetation. In 14th International Symposium on Remote Sensing of Environment, 3 (pp. 1691-1700). San Jose, Costa Rica.
- Gonzalez-Alonso, F., & Lopez-Soria, S. (1991). Using contextual information to improve land use classification of satellite images in central Spain. International Journal of Remote Sensing, 12, 2227-2235.
- Goodchild, M. F. (1992). Modelling error in objects and fields. In M. Goodchild & S. Gopal (Eds.), Accuracy of Spatial Databases (pp. 263-276). Taylor and Francis, London.
- Goodenough, D. G. (1986). The integration of remote sensing and geographic information systems. In Symposium on Remote Sensing for Resources Development and Environmental Management, (pp. 1015-1028). Enshede, August 1986.
- Greymouth Harbour Board, (1982). A Choice for the Future: A Resource Evaluation of the West Coast Region. James Printing Service, 119pp
- Gronland, A. G., Xiang, W., & Sox, J. (1994). GIS, Expert System Technologies Improve Forest Fire Management Techniques. GIS World, 7(2), 32-36.
- Gumstrump, P., Meyer, P., Gustafson, R. & Hendrikson, E. (1982). Aerial photographic measurement of transmission line structure impact on agricultural crop production. Photogrammetric Engineering and Remote Sensing, 48, 1313-1317.
- Haefner, H., & Pampaloni, P. (1992). Water Resources. International Journal of Remote Sensing, 13(6 & 7), 1277-1303.
- Hall, F. G., Strebel, J. E., Goetz, S. J., Woods, K. D., & Botkin, D. B. (1987). Landscape pattern and successional dynamics in the boreal forest. In 7th IGARSS Symposium, (pp. 165-168). Washington DC, USA.
- Halverson, H. G. (1988). High altitude photography to evaluate coal-mine reclamation. In Second Forest Service Remote Sensing Applications Conference, (pp. 360-365). Slidell, Louisiana and NSTL Mississippi, USA: American Society of Photogrammetry and Remote Sensing.

- Harding, R. A. (1982). Remote sensing as a tool for forest management. In C. J. Johannsen & J. L. Sanders (Eds.), Remote Sensing for Resource Management (pp. 448-453). Soil Conservation Society of America.
- Harris, R. (1987). Satellite Remote Sensing - An Introduction. Routledge and Kegan Paul Publishers, London and New York.
- Hegg, K. M., & Driscoll, R. S. (1982). Remote sensing applications to national forest inventories. In C. J. Johansen & J. L. Sanders (Eds.), Remote Sensing for Resource Management (pp. 512-518). Soil Conservation Society of America.
- Hegyí, F., & Quenet, R. V. (1982). Updating the forest inventory database in British Columbia. In C. J. Johannsen & J. L. Sanders (Eds.), Remote Sensing for Resource Management (pp. 512-518). Soil Conservation Society of America.
- Heinen, J. T., & Lyon, J. G. (1989). The effects of changing weighting factors on wildlife habitat index values: A sensitivity analysis. Photogrammetric Engineering and Remote Sensing, 55, 1445-1447.
- Herr, A. M., & Queen, L. P. (1993). Crane Habitat Evaluation Using GIS and Remote Sensing. Photogrammetric Engineering and Remote Sensing, 59, 1531-1538.
- Hess, L. E., Simonett, D. S., & Sun, G. (1990). Radar Detection of Flooding beneath the forest canopy: A review. International Journal of Remote Sensing, 11, 1313-1325.
- Hick, P., Pattiaratchi, C., & Wyllie, A. (1992). A Comparison of Two Airborne Multispectral Scanners for Determination of Chlorophyll Pigments in Riverine, Lacustrine, Estuarine and Oceanic Environments. In 6th Australasian Remote Sensing Conference, 1 (pp. 215-224). Wellington, New Zealand: Committee of the 6th Australasian Remote Sensing Conference.
- Hill, J., & Sturm, B. (1991). Radiometric correction of multitemporal Thematic Mapper data for use in agricultural land cover classification and vegetation monitoring. International Journal of Remote Sensing, 12, 1471-1491.
- Hill, M. O., Bunce, R. G. H., & Shaw, M. W. (1975). Indicator species analysis, a divisive polythetic method of classification and its application to a survey of native pinewoods in Scotland. Journal of Ecology, 63, 597-613.
- Hill, M. O., & Gauch, H. G. (1980). Detrended correspondence analysis: an improved ordination technique. Vegetation, 42, (47-58).
- Hill, R. A., & Foody, G. M. (1994). Separability of tropical rain-forest types in the Tambopata-Candamo Reserved Zone, Peru. International Journal of Remote Sensing, 15, 2687-2693.
- Hixson, M., Schulz, D., Fuhs, N., & Akiyama, T. (1980). Evaluation of several schemes for the classification of remotely sensed data. Photogrammetric Engineering and Remote Sensing, 46, 1547-1554.

- Hodgson, M. E., Jensen, J. R., Mackey, H. E., & Coulter, M. C. (1987). Remote Sensing of Wetland Habitat: A Wood Stork Example. Photogrammetric Engineering and Remote Sensing, 53, 1075-1080.
- Holben, B. N., & Shimabukuro, Y. E. (1993). Linear mixing model applied to coarse spatial resolution data from multispectral satellite sensors. International Journal of Remote Sensing, 14, 2231-2240.
- Horler, D. N. H., & Ahern, F. J. (1986). Forestry information content of Thematic Mapper data. International Journal of Remote Sensing, 7, 405-428.
- Howarth, P. J., & Wickware, G. M. (1981). Procedures for change detection using Landsat. International Journal of Remote Sensing, 2, 277-291.
- Huber, T. P., & Casler, K. E. (1990). Initial analysis of Landsat TM data for elk habitat mapping. International Journal of Remote Sensing, 11, 907-912.
- Hudson, W. D., & Ramm, C. W. (1987). Correct formulation of the Kappa Coefficient of Agreement. Photogrammetric Engineering and Remote Sensing, 53, 421-422.
- Hussin, Y. A., Reich, R. M., & Hoffer, R. M. (1991). Estimating Slash Pine Biomass Using Radar Backscatter. IEEE Transactions on Geoscience and Remote Sensing, 29, 427-431.
- Hutchinson, C. F. (1982). Techniques for combining Landsat and auxiliary data for digital classification improvement. Photogrammetric Engineering and Remote Sensing, 48, 123-130.
- Hutchinson, F. E. (1932). The life history of the Westland rimu stands. Te kura ngahere, 3, 54-61.
- Imhoff, M. L., Vermillion, C., Story, M. H., Choudhury, A. M., Gafoor, A., & Polcyn, F. (1987). Monsoon Flood Boundary Delineation and Damage Assessment Using Space Borne Imaging Radar and Landsat Data. Photogrammetric Engineering and Remote Sensing, 53, 405-413.
- Ingebritsen, S. E., & Lyon, R. J. (1985). Principal components analysis of multitemporal image pairs. International Journal of Remote Sensing, 6, 687-696.
- Irons, J. R., Markham, B. L., Nelson, R. F., Toll, D. F., & Williams, D. L. (1984). The effect of spatial resolution on the classification of Thematic Mapper data. International Journal of Remote Sensing, 6, 1385-1403.
- Iverson, L. R., Cook, E. A., & Graham, R. L. (1989). A technique for extrapolating and validating forest cover across large regions: Calibrating AVHRR with TM data. International Journal of Remote Sensing, 10, 1805-1812.
- Jadhav, R. N., Kimothi, M. M., & Kandya, A. K. (1993). Grassland mapping / monitoring of Banni, Kachchh (Gujarat) using remotely-sensed data. International Journal of Remote Sensing, 14, 3093-3103.

- Jakubauskas, M. E. (1989). Utilising a geographic information system for vegetation change detection. In Technical Papers of the 1989 ASPRS/ACSM Convention, 4 (pp. 56-64). Baltimore, Maryland, USA.
- James, I. L. (1978). Silvicultural Plan - Compartments 14 and 16 of Saltwater Forest. New Zealand Forest Service Report.
- James, I. L. (1987). Silvicultural management of the rimu forests of South Westland. Forest Research Institute Bulletin 121.
- Jampoler, S. M., & Haack, B. N. (1989). Use of GIS to Identify Land Use Change: Kathmandu, Nepal. In Technical Papers of the 1989 ASPRS/ACSM Convention, 3 (pp. 77-83). Baltimore, Maryland, USA.
- Janssen, L. L. F., Jaarsma, M. N., & van der Linden, E. T. M. (1990). Integrating Topographic Data with Remote Sensing for Land-Cover Classification. Photogrammetric Engineering and Remote Sensing, 56, 1503-1506.
- Jensen, J. R. (1985). Urban change detection mapping using Landsat digital data. In R. K. Holz (Eds.), The Surveillant Science: Remote Sensing of the Environment (pp. 310-325). New York: John Wiley and Sons.
- Jensen, J. R. (1986). Introductory Digital Image Processing. Prentice-Hall, Englewood Cliffs, New Jersey.
- Jensen, J. R., & Mackey, H. E. J. (1993). Measurement of Seasonal and Yearly Cattail and Waterlily Changes Using Multidate SPOT Panchromatic Data. Photogrammetric Engineering and Remote Sensing, 59, 519-525.
- Jensen, J. R., Narumalani, S., Weatherbee, O., Morris, K. S. J., & Mackey, H. E. J. (1992). Predictive Modelling of Cattail and Waterlily Distribution in a South Carolina Reservoir using GIS. Photogrammetric Engineering and Remote Sensing, 58, 1561-1568.
- Jensen, J. R., Ramsey, E. W., Mackey, H. E., Christensen, E. J., & Sharitz, R. R. (1987). Inland Wetland Change Detection Using Aircraft MSS Data. Photogrammetric Engineering and Remote Sensing, 53, 521-529.
- Jing, L., & Yan, L. (1991). The Use of AVHRR data and GIS to Study Quantitatively the Suspended Sediment in Hangzhou Bay. Asian-Pacific Remote Sensing Journal, 3, 75-77.
- Johnston, K. M. (1987). Natural Resource Modelling in the Geographic Information System Environment. Photogrammetric Engineering and Remote Sensing, 53, 1411-1415.
- Jordan, G., & Vietinghoff, L. (1987). Fighting Spruce Budworm with a GIS. In AutoCarto 8, (pp. 492-499).
- Joshi, M. D., & Sahai, B. (1993). Mapping of salt-affected land in Saurashtra coast using Landsat satellite data. International Journal of Remote Sensing, 14, 1919-1929.

*Insert page 148 after Lal, J.B.....*

Lambert, N.J., Ardö, J., Rock, B.N. and Vogelmann, J.E. (1995) Spectral characterization and regression-based classification of forest damage in Norway spruce stands in the Czech Republic using Landsat Thematic Mapper data. International Journal of Remote Sensing, 16, 1261-1287.

- Karteris, M. (1990). The utility of Thematic Mapper data for natural resources classification. International Journal of Remote Sensing, *11*, 1589-1598.
- Kay, R. J., Hick, P., & Houghton, H. J. (1990). Mapping Tropical Rain Forests using Multiscene and Multitemporal Landsat Thematic Mapper Data. Asian-Pacific Remote Sensing Journal, *3*, 23-29.
- Kenny, J. F. & McCauley, R. (1982). Remote Sensing Investigations in the coal fields of southeastern Kansas. In C. J. Johannsen & J. L. Saunders (Eds.) Remote Sensing for Resource Management (pp 338-346). Soil Conservation Society of America.
- Khorram, S., Brockhaus, J. A., Bruck, R. I., & Campbell, M. V. (1990). Modelling and multitemporal evaluation of forest decline with Landsat TM digital data. IEEE Transactions on Geoscience and Remote Sensing, *28*, 746-648.
- Kim, K., & Ventura, S. (1993). Large-Scale Modelling of Urban Nonpoint Source Pollution using a Geographic Information System. Photogrammetric Engineering and Remote Sensing, *59*, 1539-1544.
- Klankamsorn, B. (1978). Use of satellite imagery to assess forest deterioration in East Thailand. In 12th International Symposium on Remote Sensing of Environment, *2* (pp. 1299-1306). April 20-26, Manila, Philippines: Environmental Research Institute of Michigan.
- Klecka, W.R. (1980). Discriminant Analysis. Beverly Hills: Sage, 71p.
- Kneizys, F. X., Shettle, E. P., Abnreu, L. W., Chetwynd, J. H., Anderson, G. P., Gallery, W. O., Selby, J. E. A., & Clough, S. A. (1988). Users Guide to LOWTRAN-7. No. AFGL-TR-88-0177). Air Force Geophysics Laboratory Hanscom AFB, Massachusetts.
- Knight, L. (1993). Collins English Dictionary. HarperCollins Publishers.
- Kushwaha, S. P. S. (1990). Forest type mapping and change detection from satellite imagery. ISPRS Journal of Photogrammetry and Remote Sensing, *45*, 464-483.
- Lal, J. B., Gulati, A. K., & Bist, M. S. (1991). Satellite mapping of alpine pastures in the Himalayas. International Journal of Remote Sensing, *12*, 435-443.
- Lathrop, R. G. (1992). Landsat Thematic Mapper Monitoring of Turbid Inland Water quality. Photogrammetric Engineering and Remote Sensing, *58*, 1355-1360.
- Lauver, C. L., & Whistler, J. L. (1993). A Hierarchical Classification of Landsat TM Imagery to Identify Natural Grassland Areas and Rare Species Habitat. Photogrammetric Engineering and Remote Sensing, *59*, 627-634.
- Le Toan, T., Beaubien, A., Riom, J., & Guyon, D. (1992). Relating Forest Biomass to SAR data. IEEE Transactions on Geoscience and Remote Sensing, *30*, 403-411.
- Leckie, D. G. (1990(a)). Advances in remote sensing technologies for forest survey and management. Canadian Journal of Forestry Research, *20*, 464-483.

- Leckie, D. G. (1990(b)). Synergism of Synthetic Aperture Radar and Visible Infrared data for Forest Type Discrimination. Photogrammetric Engineering and Remote Sensing, 56, 1237-1246.
- Legg, C. A. (1986). Monitoring of open cast mining and reclamation works in the United Kingdom using MSS and Landsat TM imagery. In 20th International Symposium on Remote Sensing of Environment (pp. 931-941). ERIM. Ann Arbor, Michigan, USA.
- Leipnik, M. R. (1993). GIS and 3-D Modelling Fight Subsurface Contamination at Federal Site. GIS World, 6, 39-41.
- Levack, H. & Hinton, W. (1987). Sphagnum moss harvesting: South Westland. Letter to the Secretary for the environment, 29.6.87. Quoted in Ministry for the Environment (1987) "South Westland South of the Cook River Resource Management Study, Public Discussion Document, 6 November 1987. Ministry for the Environment. 88pp.
- Lewis, M. M. (1994). Species composition related to spectral classification in an Australian spinifex hummock grassland. International Journal of Remote Sensing, 15, 3223-3239.
- Lillesand, T. M., Hopkins, P. F., Buchheim, M. P., & Maclean, A. L. (1985). The Potential Impact of Thematic Mapper, SPOT and Microprocessor technology on Forest type mapping under Lake States conditions. In Pecora 10, (pp. 43-57). American Society for Photogrammetry and Remote Sensing.
- Lillesand, T.M. and Kiefer, R.W. (1987). Remote Sensing and Image Interpretation. John Wiley and Sons.
- Liu, Z. K., & Xiao, J. Y. (1991). Classification of remotely sensed image data using artificial neural networks. International Journal of Remote Sensing, 12, 2433-2438.
- Lo, C. P., & Shipman, R. L. (1990). A GIS Approach to Land-Use Change Dynamics Detection. Photogrammetric Engineering and Remote Sensing, 56, 1483-1491.
- Lodwick, W. A., Monson, W., & Svoboda, L. (1990). Attribute error and sensitivity analysis of map operations in geographical information systems. International Journal of Geographical Information Systems, 4, 413-428.
- Logan, B. J. (1993). Digital Orthophotography Bolsters GIS Base for Wetlands Project. GIS World, Special Issue June 1993, 58-61.
- Lopez, S., Gonzalez, F., Llop, R., & Cuevas, J. M. (1991). An evaluation of the utility of NOAA AVHRR images for monitoring forest fire risk in Spain. International Journal of Remote Sensing, 12, 1841-1851.
- Lowell, K. (1991). Utilizing discriminant function analysis with a geographical information system to model ecological succession spatially. International Journal of Geographic Information Systems, 5, 175-191.

- Lozano-Garcia, D. F., & Hoffer, R. M. (1993). Synergistic effects of combined Landsat TM and SIR-B data for forest resources assessment. International Journal of Remote Sensing, 14, 2677-2694.
- Lunetta, R. S., Congalton, R. G., Fenstermaker, L. K., Jensen, J. R., McGwire, K. C., & Tinney, L. R. (1991). Remote Sensing and Geographic Information System Data Integration: Error Sources and Research Issues. Photogrammetric Engineering and Remote Sensing, 57, 677-687.
- Lyon, J. G., & Greene, R. G. (1992). Use of Aerial Photographs to Measure the Historical Areal Extent of Lake Erie Coastal Wetlands. Photogrammetric Engineering and Remote Sensing, 58, 1355-1360.
- Lyon, J. G., Heinen, J. T., Mead, R. A., & Roller, N. E. G. (1987). Spatial data for modelling wildlife habitat. Journal of Surveying Engineering, 113, 88-100.
- Maffini, G. (1987). Raster vs Vector data encoding and handling: a commentary. Photogrammetric Engineering and Remote Sensing, 53, 1397-1398.
- Maguire, D. J. (1991). An overview and definition of GIS. In D. J. Maguire, M. F. Goodchild, & D. W. Rhind (Eds.), Geographic Information Systems (pp. 9-20). Longman Scientific and Technical.
- Maling, D. H. (1989). Measurement from Maps: Principles and Methods of Cartometry. Pergamon Press, Oxford, England.
- Malingreau, J. P., Stephens, G., & Fellows, L. (1985). Remote Sensing of forest fires: Kalimantan and North Borneo in 1982-1983. Ambio, 14, 314-321.
- Malingreau, J. P., & Tucker, C. J. (1988). Large scale deforestation in the South East Amazon Basin of Brazil. Ambio, 17, 49-55.
- Malingreau, J. P., Tucker, C. J., & Laporte, N. (1989). AVHRR for monitoring global tropical deforestation. International Journal of Remote Sensing, 8, 509-516.
- Marble, D. F., & Peuquet, D. J. (Ed.). (1983). Geographic Information Systems and Remote Sensing (2 ed.). American Society of Photogrammetry.
- Mark, A. F., & Smith, P. M. F. (1975). A lowland vegetation sequence in south Westland: Pakihi bog to mixed beech-podocarp forest. Part 1: the principle strata. Proceedings of the New Zealand Ecological Society, 22, 76-92.
- Martin, F. C. (1985). Using a geographical information system for forest land mapping and management. Photogrammetric Engineering and Remote Sensing, 51, 1753-1759.
- Masters, S. E., Holloway, J. T., & McKelvey, P. J. (1957). The National Forest Survey of New Zealand 1955. Volume 1: The Indigenous Forest Resources of New Zealand. New Zealand Government Printer, Wellington.
- Matson, M., & Holben, B. (1987). Satellite detection of tropical burning in Brazil. International Journal of Remote Sensing, 8, 509-516.
- McKelvey, P. J. (1984). Provisional classification of South Island virgin indigenous forests. New Zealand Journal of Forestry Science, 14, 151-178.

- McSweeney, G. D. (1982). Matai/totara flood plain forests in south Westland. New Zealand Journal of Ecology, 5, 121-128.
- Mechaffie, P. H., & Seargent, R. E. (1985). Detection and delineation of mine related subsidence in Western Kentucky Coalfields. In ACSM-ASPRS Fall Meeting, (pp. 538-554). Indianapolis, USA: American Society for Photogrammetry and Remote Sensing and American Congress on Surveying and Mapping.
- Mertz, T. (1993). GIS Targets Agricultural Nonpoint Pollution. GIS World, 6 (4), 41-46.
- Metcalf, L., & Godfrey, W. (1990). Lands disturbed by alluvial mining in Westland. In Issues in the restoration of disturbed land, (pp. 83-86). Massey University: Massey University Fertiliser and Lime Research Centre.
- Milne, A. K. (1988). Change Detection Analysis using Landsat imagery: a review of methodology. In 8th IGARSS Symposium, (pp. 541-544). Edinburgh, Scotland.
- Ministry for the Environment (1987) "South Westland South of the Cook River Resource Management Study, Public Discussion Document, 6 November 1987. Ministry for the Environment. 88pp.
- Montgomery, D. C., & Peck, E. A. (1982). Introduction to Linear Regression Analysis. John Wiley and Sons, New York.
- Morse, B. W. (1986). Forecasting Pest Hazard with a Geographic Information System. In Proceedings of the Geographic Information Systems Workshop, (pp. 255-161). April 1-4, 1986: American Society of Photogrammetry and Remote Sensing.
- Mroczynski, R. P., & Weismiller, R. A. (1982). Aerial Photography: A tool for strip mine reclamation. In C. J. Johannsen & J. L. Sanders (Eds.), Remote Sensing for Resource Management (pp. 331-337). Soil Conservation Society of America.
- Mukai, Y., Sugimura, T., Watanabe, H., & Wakamori, K. (1987). Extraction of areas infested by pine bark beetle using Landsat MSS data. Photogrammetric Engineering and Remote Sensing, 53, 77-81.
- Mukherjee, K. T., Bandyopadhyay, T. K., & Pande, S. K. (1991). Detection and delineation of depth of sub-surface coal mine fires based on an airborne multispectral scanner survey in a part of the Jharia coalfield, India. Photogrammetric Engineering and Remote Sensing, 57, 1203-1207.
- Natesan, U., & Subramanian, S. P. (1992). Study of the Ocean Parameters of Southern India from Space. In 6th Australasian Remote Sensing Conference, 1 (pp. 360-365). Wellington, New Zealand: Committee of the 6th Australasian Remote Sensing Conference.
- Nelson, R. (1983). Detecting forest canopy change due to insect activity using Landsat MSS. Photogrammetric Engineering and Remote Sensing, 49, 1303-1314.
- Nelson, R., & Holben, B. (1986). Identifying deforestation in Brazil using multi-resolution satellite data. International Journal of Remote Sensing, 7, 429-448.

- Nelson, R., & Horning, N. (1993). AVHRR-LAC estimates of forest area in Madagascar, 1990. International Journal of Remote Sensing, 14, 1463-1475.
- Nelson, R., Horning, N., & Stone, T. A. (1987). Determining the rate of forest conversion in Mato Grosso, Brazil using Landsat MSS and AVHRR data. International Journal of Remote Sensing, 8, 1767-1784.
- Nezry, E., Mougin, E., Lopes, A., Gastellu-Etchegorry, J. P., & Laumonier, Y. (1993). Tropical vegetation mapping with combined visible and SAR spaceborne data. International Journal of Remote Sensing, 14, 2165-2184.
- Nicol, E. R. (1993). Remote Sensing, Image Analysis and GIS in Natural and Historic Resource Management. In G. L. Benwell and N. C. Sutherland (Eds.), SIRC 93. University of Otago, 241-246.
- Norton, D. A. (1989). Floristics and structure of mire-forest ecotones, west coast South Island, New Zealand. Journal of the Royal Society of New Zealand, 19, 31-42.
- Norton, D. A., & Leathwick, J. R. (1990). The lowland vegetation pattern, south Westland, New Zealand. 1. Saltwater Ecological Area. New Zealand Journal of Botany, 28, 41-51.
- O'Donnell, C. F. J., & Dilks, P. J. (1986). Forest Birds in South Westland Status, Distribution and Habitat Use (Occasional Publication No. 10 No. New Zealand Wildlife Service.
- Openshaw, S. (1992). Learning to Live with Errors in Spatial Databases. In M. Goodchild & S. Gopal (Eds.), Accuracy of Spatial Databases (263-276). Taylor and Francis, London.
- Ormsby, J. P., & Lunetta, R. S. (1987). Whitetail Deer Food Availability Maps from Thematic Mapper Data. Photogrammetric Engineering and Remote Sensing, 53, 1081-1085.
- Oza, M. P., Srivastava, V. K., Pariswad, B. S., & Setty, K. R. V. (1989). Relationship between Landsat MSS data and forest type parameters. International Journal of Remote Sensing, 10, 1813-1819.
- Ozemoy, V. M., Smith, D. R., & Sicherman, A. (1981). Evaluating computerised geographic information systems using decision analysis. Interfaces, 11, 92-98.
- Paine, D.P. (1981) Aerial Photography and Image Interpretation for Resource Management. Wiley, New York.
- Pando, M., Lange, R.T., & Sparrow, A.D. (1992). Relations between reflectance in Landsat MSS wavebands and floristic composition of Australian chenopod rangelands. International Journal of Remote Sensing, 13, 1861-1867.
- Parent, P., & Church, R. (1987). Evolution of Geographic Information Systems as Decision Making Tools. In Second Annual International Conference, Exhibits and Workshops on Geographic Information Systems, ASPRS-ACSM.

- Park, A. B., Houghton, R. A., Kicks, G. M., & Peterson, C. J. (1983). Multitemporal change detection techniques for the identification and monitoring of forest disturbances. In 17th International Symposium on Remote Sensing of Environment, (pp. 77-97). Ann Arbor, Michigan, USA.
- Parker, H. D. (1988). The Unique Qualities of a GIS: A Commentary. Photogrammetric Engineering and Remote Sensing, 54, 1547-1549.
- Parks, N. F., Petersen, G. W., & Baumer, G. M. (1987). High Resolution Remote Sensing of Spatially and Spectrally Complex Coal Surface Mines of Central Pennsylvania: A Comparison between Simulated SPOT MSS and Landsat-5 Thematic Mapper. Photogrammetric Engineering and Remote Sensing, 53, 415-420.
- Pathan, S. K., Sastry, S. V. C., Dhinwa, P. S., Mukund R, Kajumdar, K. L., Kumar, D. S., Patkar, V. N., & Phatak, V. N. (1993). Urban growth trend analysis using GIS techniques - a case study of the Bombay metropolitan region. International Journal of Remote Sensing, 14, 3169-3179.
- Pavlidis, T. (1982). Algorithms for Graphics and Image Processing. Springer-Verlag, Berlin.
- Pech, R. P., Davis, A. W., Lamacraft, R. R., & Graetz, R. D. (1986). Calibration of LANDSAT data for sparsely vegetated semi-arid rangelands. International Journal of Remote Sensing, 7, 1729-1750.
- Pelletier, R. E. & Sader, S. A. (1985). The relationship between soils data and forest clearing and forest regrowth trends in Costa Rica. In Pecora 10, (pp. 276-285). August 20-22, Colorado State University, Colorado.
- Petrie, G. (1990). Digital Mapping Technology: Procedures and Applications. In T. J. M. Kennie & G. Petrie (Eds.), Engineering Survey Technology (pp. 329-389). Blakie, Glasgow and London.
- Peuquet, D. J. (1981 (a)). An examination of the techniques for reformatting digital cartographic data: Part 1 The raster to vector process. Cartographica, 18, 21-33.
- Peuquet, D. J. (1981 (b)). An examination of the techniques for reformatting digital cartographic data: Part 2: the vector to raster process. Cartographica, 18, 34-47.
- Peuquet, D. J. (1984). A Conceptual Framework and Comparison of Spatial Data Models. Cartographica, 21, 66-113.
- Phulpin, T., Jullien, J. P., & Lasselin, D. (1989). AVHRR data processing to study surface canopies in temperate regions. First results of HAPLEX-MOBILHY. International Journal of Remote Sensing, 10, 869-874.
- Pilon, P. G., Howarth, P. J., Bullock, R. A., & Adeniyi, P. O. (1988). An enhanced classification approach to change detection in semi-arid environments. Photogrammetric Engineering and Remote Sensing, 54, 1709-1716.
- Piwowar, J. M., & LeDrew, E. F. (1990). Integrating Spatial Data: A User's Perspective. Photogrammetric Engineering and Remote Sensing, 56, 1497-1502.

- Piwowar, J. M., LeDrew, E. F., & Dudycha, D. J. (1990). Integration of spatial data in vector and raster formats in a geographic information system environment. International Journal of Geographical Information Systems, 4, 429-444.
- Poole, A. L. (1937). A brief ecological survey of the Pukekura State Forest, south Westland. New Zealand Journal of Forestry, 4, 78-85.
- Poole, L., & Johns, J. (1992). Tomorrows Trees. The Caxton Press in association with Carter Holt Harvey.
- Pradham, K. P. (1990). Visual versus Digital Analysis of Landsat Data for Land-Use/Cover Mapping. Asian-Pacific Remote Sensing Journal, 3, 39-41.
- Preston, E. B. (1993). Remote Sensing, GIS Technologies Support Sea Ice Motion Monitoring. GIS World, 6 (1), 36-39.
- Preston, R. A. (1992). FERIS: An Integrated Remote Sensing and Environmental Modelling System for Assessment and Monitoring of Queensland's Forests. In 6th Australasian Remote Sensing Conference, 1 (pp. 263-270). Wellington, New Zealand: Committee of the 6th Australasian Remote Sensing Conference.
- Price, J. C. (1987). Calibration of Satellite Radiometers and the Comparison of Vegetation Indices. Remote Sensing of Environment, 21, 15-27.
- Price, J. E. (1986). Application of Geographic Information Systems for Assessment of Site Index and Forest Management Constraints. In Proceedings of the Geographic Information Systems Workshop, (pp. 263-292). April 1-4, 1986: American Society of Photogrammetry and Remote Sensing.
- Price, K.P., Pyke, D.A., & Mendes, L. (1992). Shrub dieback in a semiarid ecosystem: the integration of remote sensing and geographic information systems for detection of vegetation change. Photogrammetric Engineering and Remote Sensing, 58, 455-463.
- Quarmby, N. A., Townshend, J. R. G., Settle, J. J., White, K. H., Milnes, M., Hindle, T. L., & Silleos, N. (1992). Linear mixture modelling applied to AVHRR data for crop area estimation. International Journal of Remote Sensing, 13, 415-425.
- Ram, B. & Kolarkar, A. S. (1993). Remote sensing application in monitoring land-use changes in arid Rajasthan. International Journal of Remote Sensing, 14, 3191-3200.
- Reed, B. C. (1993). Using Remote Sensing and Geographic Information Systems for analysing landscape drought interaction. International Journal of Remote Sensing, 14, 3489-3503.
- Repic, R. L., Lee, J. K., & Mausel, P. W. (1991). An analysis of selected water parameters in surface coal mines using multispectral videography. Photogrammetric Engineering and Remote Sensing, 57, 1589-1596.
- Richards, J.A. (1986). Remote sensing digital image analysis. Springer-Verlag
- Richardson, A. J. (1982). Relating Landsat digital count values to ground reflectance in optically thin atmospheric conditions. Applied Optics, 21, 1457-1464.

- Richter, R. (1990). A fast atmospheric correction algorithm applied to Landsat TM images. International Journal of Remote Sensing, 11, 159-166.
- Rifai, H. S., Newell, C. J., & Bedient, P. R. (1993). GIS Enhances Water Quality Modelling. GIS World, 6(8), 52-53.
- Riggin, P. J., Brass, J. A., & Lockwood, R. N. (1993). Assessing Fire Emissions from Tropical Savanna and Forests of Central Brazil. Photogrammetric Engineering and Remote Sensing, 59, 1009-1015.
- Riordan, C. J. (1981). Change Detection for Resource Inventories using digital remote sensing data. In National Workshop on In-Place Resource Inventories: Principles and Practices, (pp. 278-283). University of Maine, Orono, Maine, USA.
- Ripple, W. J., Wang, S., Isaacson, D. L., & Paine, D. P. (1991). A preliminary comparison of Landsat Thematic Mapper and SPOT-1 HRV multispectral data for estimating coniferous forest volume. International Journal of Remote Sensing, 12, 1971-1977.
- Robinove, C. J. (1982). Computation of physical values from Landsat digital data. Photogrammetric Engineering and Remote Sensing, 48, 781-784.
- Rodbell, S. (1993). GPS/GIS Mapping Accurately Assesses Environmental Impact. GIS World, 6(12), 54-56.
- Rowland, E. B. (1986). Use of a GIS to Display Establishment and Spread of Gypsy Moth Infestations. In Proceedings of the Geographic Information Systems Workshop, (pp. 249-254). April 1-4, 1986: American Society of Photogrammetry and Remote Sensing.
- Rudorff, B. F. T., & Bastista, G. T. (1991). Wheat yield estimation at the farm level using Landsat TM and agrometeorological data. International Journal of Remote Sensing, 12, 2477-2484.
- Ryan, T. W., Sementilli, P. J., Yuen, P., & Hunt, B. R. (1991). Extraction of Shoreline Features by Neural Nets and Image Processing. Photogrammetric Engineering and Remote Sensing, 57, 947-955.
- Ryerson, R. A., Brown, R. J., Tambay, J. L., Murphy, L. A., & McLaughlin, B. (1981). A timely and accurate Potato estimate from Landsat: Results of a demonstration. In 15th International Symposium on Remote Sensing of Environment, (pp. 587-597). ERIM, Ann Arbor, Michigan, USA.
- Ryerson, R. A., Mosher, P., Wallen, V. R., & Stewart, N. E. (1979). Three tests of agricultural remote sensing for crop inventory in eastern Canada: Results, problems and prospects. Canadian Journal of Remote Sensing, 5, 53-66.
- Sader, S. A. (1987). Forest Biomass, Canopy Structure and Species Composition Relationships with Multipolarization L-Band Synthetic Aperture Radar Data. Photogrammetric Engineering and Remote Sensing, 53, 193-202.
- Schowengerdt, R. A. (1983). Techniques for Image Processing and Classification in Remote Sensing. Academic Press, New York, USA.

- Sellers, P. J. (1985). Canopy reflectance, photosynthesis and transpiration. International Journal of Remote Sensing, 6, 1335-1372.
- Senoo, T., Kobayashi, F., Tanaka, S., & Sugimura, T. (1990). Improvement of forest type classification by SPOT HRV with 20m mesh DTM. International Journal of Remote Sensing, 11, 1011-1022.
- Settle, J.J. & Drake, N.A. (1993). Linear mixing and the estimation of ground cover proportions. International Journal of Remote Sensing, 14, 1159-1177.
- Shelton, D. L., & Estes, J. E. (1981). Remote Sensing and Geographic Information Systems: An Unrealized Potential. Geo-Processing, 1, 395-420.
- Singh, A. (1987). Spectral separability of tropical forest cover classes. International Journal of Remote Sensing, 8, 971-979.
- Singh, A. (1989). Digital change detection techniques using remotely sensed data. International Journal of Remote Sensing, 6, 883-896.
- Singh, S. M. (1992). Fast atmospheric correction algorithm. International Journal of Remote Sensing, 13, 933-938.
- Six Dijkstra, H. G., Mead, D. J., & James, I. L. (1985). Stand structure in terrace rimu forests of south Westland and its implications for management. New Zealand Journal of Forestry Science, 15, 3-22.
- Skidmore, A. K., & Turner, B. J. (1988). Forest mapping accuracies are improved using a supervised non-parametric classifier. Photogrammetric Engineering and Remote Sensing, 54, 1415-1421.
- Skidmore, A. K. (1989). An Expert System classifies Eucalypt forest types using Thematic Mapper data and a Digital Terrain Model. Photogrammetric Engineering and Remote Sensing, 55, 1415-1421.
- Slater, P. H. (1980). Remote Sensing: Optics and Optical Systems. Addison-Wesley Publishing Company, Reading, Massachusetts.
- Smith, C., Pyden, N., & Cole, P. (1994). ERDAS Field Guide. ERDAS Inc, Georgia, USA.
- Smith, S. M., & Lee, W. G. (1984). Vegetation and soil development on a Holocene river terrace sequence, Arawata valley, south Westland, New Zealand. New Zealand Journal of Science, 27, 187-196.
- Smith, T. R., Menon, S., Starr, J. L., & Estes, J. E. (1987). Requirements and principles for the implementation and construction of large scale geographical information systems. International Journal of Geographical Information Systems, 1, 13-31.
- Soons, J. M. (1982). Westland: The West Coast of New Zealand. In J. M. Soons & M. J. Selby (Eds.), Landforms of New Zealand (pp. 300-313). Longman Paul Ltd.
- Sowden, J. R. (1986) Vegetation succession and soil development of a series of river terraces, south Westland. M.App.Sc., Lincoln College, University of Canterbury, Christchurch, New Zealand.

- Spanner, M. A., Pierce, L. L., Peterson, D. L., & Running, S. W. (1990). Remote sensing of temperate forest leaf area index: The influence of canopy closure, understorey vegetation and background reflectance. International Journal of Remote Sensing, 11, 95-111.
- Star, J., & Estes, J. (1990). Geographic Information Systems - An Introduction. Prentice Hall.
- Star, J. L., Estes, J. E., & Davis, F. (1991). Improved Integration of Remote Sensing and Geographic Information Systems: A Background to NCGIA Initiative 12/. Photogrammetric Engineering and Remote Sensing, 57, 643-645.
- Stenback, J. M., & Congalton, R. G. (1990). Using Thematic Mapper data to examine forest understorey. Photogrammetric Engineering and Remote Sensing, 56, 1285-1290.
- Stoms, D. M. (1992). Effects of Habitat Map Generalization in Biodiversity Assessment. Photogrammetric Engineering and Remote Sensing, 58, 1587-1591.
- Stoms, D. M., Davis, F. W., & Cogan, C. B. (1992). Sensitivity of Wildlife Habitat Models to Uncertainties in GIS data. Photogrammetric Engineering and Remote Sensing, 58, 843-850.
- Stow, D. A., Tinney, L. A., & Estes, J. A. (1980). Deriving land use/land cover change statistics from Landsat: a study of prime agricultural land. In 14th International Symposium on Remote Sensing of Environment, (pp. 1227-1237). Ann Arbor, Michigan, USA.
- Susilawati, S., & Weir, M. J. C. (1990). GIS Applications in forest land management in Indonesia. ITC Journal, 3, 236-244.
- Swain, P. H., & Davis, S. M. (1978). Remote Sensing: The Quantitative Approach. McGraw Hill Book Company, New York.
- SYSTAT (1992). SYSTAT for Windows: Statistics. Version 5. SYSTAT Inc, Evanston, IL. 750p
- Tanré, D., Deroo, C., Duhaut, P., Herman, M., Morcrette, J. J., Perbos, J., & Deschamps, P. Y. (1990). Description of a Computer Code to Simulate the Satellite Signal in the Solar Spectrum: The 5S code. International Journal of Remote Sensing, 11, 659-668.
- Thapa, K., & Bossler, J. (1992). Accuracy of Spatial Data used in Geographic Information Systems. Photogrammetric Engineering and Remote Sensing, 58, 835-841.
- Tom, C.H., & Miller, L. D. (1984). An automated land-use mapping comparison of the Bayesian maximum likelihood and linear discriminant analysis algorithms. Photogrammetric Engineering and Remote Sensing, 50, 193-207.
- Townshend, J. R. G. (1992). Land cover. International Journal of Remote Sensing, 13, 1319-1328.

- Townshend, J. R. G., Justice, C. O., & Kalb, V. (1987). Characterisation and classification of South American land cover types using satellite data. International Journal of Remote Sensing, 8, 1189-1207.
- Trotter, C. M., Stephens, P. R., Trustrum, N. A., Page, M. J., Carr, K. S., & DeRose, R. C. (1989). Application of remotely sensed and geographic information system data to quantitative assessment of landslide damage. In 1989 International Geoscience and Remote Sensing Symposium, (pp. 1990-1994). Vancouver, Canada.
- Trotter, C. M. (1991). Remotely-sensed data as an information source for geographical information systems in natural resource management: a review. International Journal of Geographical Information Systems, 5, 225-239.
- Trotter, C. M. (1994). The Vegetation Index and its application to measurement of possum browsing damage by remote sensing. In P. R. Stephens (Ed.), 4th National Remote Sensing and Geographic Information Systems Workshop, (pp. 47-54). Landcare Research NZ Ltd, Palmerston North, New Zealand.
- Tucker, C. J. (1978). A Comparison of satellite sensor bands for vegetation monitoring. Photogrammetric Engineering and Remote Sensing, 44, 1369-1380.
- Tucker, C. J., Holben, B. N., & Goff, T. E. (1984). Intensive forest clearing in Rodonia, Brazil, as detected by satellite remote sensing. Remote Sensing of Environment, 15, 255-261.
- Tuomisto, H., Linna, A., & Kalliola, R. (1994). Use of digitally processed satellite images in studies of tropical rainforest vegetation. International Journal of Remote Sensing, 15, 1595-1610.
- Turner, M. G., O'Neill, R. V., Gardner, R. H., & Milne, B. T. (1989). Effects of changing spatial scale on the analysis of landscape pattern. Landscape Ecology, 3, 153-162.
- van Beek, C. A. (1987). Letter to the Secretary for the Environment from Chairman of the West Coast Sphagnum Moss Industry Association. Quoted in Ministry for the Environment (1987) "South Westland South of the Cook River Resource Management Study, Public Discussion Document, 6 November 1987. Ministry for the Environment. 88pp.
- van der Knaap, W. G. M. (1992). The vector to raster conversion: (mis)use in geographical information systems. International Journal of Geographical Information Systems, 6, 159-170.
- van Diggelen, F. (1994). GPS for GIS - A comparative survey. GIS World, 7(10), 34-40.
- Venkatachalam, P., Murty, C., Chowdhury, S., & Sharma, I. N. (1991). Ground-Water Potential Zone Mapping Using a GIS Approach. Asian-Pacific Remote Sensing Journal, 4, 67-77.
- Veregin, H. (1992). Error Modelling in the map overlay function. In M. Goodchild & S. Gopal (Eds) Accuracy of Spatial Databases, (pp 3-18). Taylor & Francis.

- Vogelmann, J. E. (1988). Detection of forest change in the Green Mountains of Vermont using multispectral scanner data. International Journal of Remote Sensing, 9, 1187-1200.
- Vogelmann, J. E. (1990). Comparison between two vegetation indices for measuring different types of forest damage in the north-eastern United States. International Journal of Remote Sensing, 11, 2281-2297.
- Wallace, J. F., Campbell, N. A., Wheaton, G. A., & McFarlane, D. J. (1993). Spectral discrimination and mapping of waterlogged cereal crops in Western Australia. International Journal of Remote Sensing, 14, 2731-2743.
- Walsh, S. J., Vitek, J. D., & Gregory, M. S. (1982). Landsat digital analysis of forest clearcuts and reforestation. In C. J. Johannsen & J. L. Sanders (Eds.), Remote Sensing for Resource Management (pp. 159-171). Soil Conservation Society of America.
- Ward, L. I., & Weigle, B. (1993). To save a species: GIS for Manatee Research and Management. GIS World, 6(8), 34-37.
- Wardle, K., Foran, B., & Gibson, R. (1993). Developing Spatial Land Use Scenarios for the Dry Tussock Grasslands of New Zealand. In G. L. Benwell & N. C. Sutherland (Ed.), SIRC 93, University of Otago.
- Wardle, P. (1974). The kahikatea forest (*Dacrycarpus dacrydioides*) of South Westland. Proceedings of the New Zealand Ecological Society, 21, 62-71.
- Wardle, P. (1975). Vascular plants of Westland National Park (New Zealand) and neighbouring lowland and coastal areas. New Zealand Journal of Botany, 13, 497-545.
- Wardle, P. (1977). Plant communities of Westland National Park (New Zealand) and neighbouring lowland and coastal areas. New Zealand Journal of Botany, 15, 323-398.
- Wardle, P. (1978). Regeneration status of some New Zealand conifers with particular reference to *Libocedrus bidwillii* in Westland National Park. New Zealand Journal of Botany, 16, 471-477.
- Wardle, P. (1980). Primary succession in Westland national Park and its vicinity, New Zealand. New Zealand Journal of Botany, 18, 221-232.
- Welch, R., Remillard, M., & Alberts, J. (1992). Integration of GPS, Remote Sensing and GIS Techniques for Coastal Resource Management. Photogrammetric Engineering and Remote Sensing, 58, 1571-1578.
- Werle, D., Lee, Y. J., & Brown, R. J. (1986). The use of multispectral and radar remote sensing data for monitoring the forest clear cut and regeneration sites on Vancouver Island. In 10th Canadian Symposium on Remote Sensing, (pp. 319-329). Edmonton, Canada.
- White, B. (1992) New Zealand Official Yearbook. Department of Statistics. 707p.

- White, W. B. (1986). Modelling Forest Pest Impacts - Aided by a Geographic Information System in a Decision Support Framework. In Proceedings of the Geographic Information Systems Workshop, (pp. 238-248). April 1-4, 1986: American Society of Photogrammetry and Remote Sensing.
- Whitley, D. L., Wei-Ning, X., & Young, J. L. (1993). Use a GIS 'Melting Pot' to Assess Land Use Suitability. GIS World, 6(7), 48-51.
- Wier, C. W., Wobber, F. J., Orville, R. R., & Amato, R. V. (1973). Fracture mapping and strip mine inventory in the midwest by using ERTS-1 Imagery. Quoted in Rathore, C.S. and Wright, R. (1993) Monitoring environmental impacts of surface coal mining. International Journal of Remote Sensing, 14, 1021-1042.
- Williams, D. L., Irons, J. R., Markham, B. L., Nelson, R. F., Toll, D. L., Latty, R. S., & Stauffer, M. L. (1984). A statistical evaluation of the advantages of Landsat Thematic Mapper in comparison with Multi-spectral scanner data. I.E.E.E. Transactions on Geoscience and Remote Sensing, GE-22, 294-302.
- Williams, D. L., & Miller, L. D. (1979). Monitoring Forest Canopy Alteration around the World with Digital Analysis of Landsat Imagery. Quoted in Sader, S.A., Stone, T.A. and Joyce, A.T. (1990). Remote Sensing of Tropical Forests: An Overview of Research and Applications Using Non-Photographic Sensors. Photogrammetric Engineering and Remote Sensing, 56, 1343-1351.
- Williams, G. J. (1965). Economic Geology of New Zealand. In Eighth Commonwealth Mining and Metallurgical Congress, 4. Melbourne, Australia: Australian Institute of Mining and Metallurgy.
- Williams, V. L., Philipson, W. R., & Philpot, W. D. (1987). Identifying Vegetable Crops with Landsat Thematic Mapper Data. Photogrammetric Engineering and Remote Sensing, 53, 187-191.
- Williamson, H. D., & Eldridge, D. J. (1993). Pasture status in semi-arid grassland. International Journal of Remote Sensing, 14, 2535-2546.
- Wilson, J. D. (1993). GIS Supports Tax Reporting, Mine Management in Appalachian Coal Fields. GIS World, 6(3), 46-51.
- Wolf, P.F. (1974) Elements of Photogrammetry. McGraw Hill, New York.
- Wood, B. L., Beck, L. R., Washino, R. K., Palchick, S. M., & Sebesta, P. D. (1991). Spectral and spatial characteristics of rice field mosquito habitat. International Journal of Remote Sensing, 12, 621-626.
- Woodgate, P. W., & Ritman, K. T. (1992). Defining Old Growth Forests Using Remotely Sensed Imagery and GIS Techniques. In 6th Australasian Remote Sensing Conference, 1 (pp. 226-237). Wellington, New Zealand: Committee of the 6th Australasian Remote Sensing Conference.

- Woodwell, G. M., Houghton, T. A., Stone, T. A., Nelson, R. F., & Kovalick, W. (1987). Deforestation in the tropics: new measurements in the Amazon Basin using Landsat and NOAA AVHRR Imagery. Journal of Geophysical Research, 92, 2157-2163.
- Zhu, M. H., Yan, S. Y., Philipson, W. R., Yen, C. C., & Philpot, W. D. (1983). Analysis of Landsat for monitoring vegetables in New York mucklands. In 49th Annual Meeting of the American Society of Photogrammetry, (pp. 343-353). American Society of Photogrammetry, Falls Church, Virginia, USA.
- Zhu, Z., & Evans, D. L. (1992). Mapping Midsouth Forest Distributions: AVHRR satellite data and GIS help meet RPA mandate. Journal of Forestry, 90(12), 27-30.
- Zhu, Z., & Evans, D. L. (1994). US Forest Types and Predicted Percent Forest Cover from AVHRR Data. Photogrammetric Engineering and Remote Sensing, 60, 525-531.
- Zhuang, X., Engel, B. A., Baumgardner, M. F., & Swain, P. H. (1991). Improving classification of crop residues using digital land ownership data and Landsat TM imagery. Photogrammetric Engineering and Remote Sensing, 57, 1487-1492.

**APPENDIX 1: The rms error for the image-to-image registration in the  
Tuckers Flat alluvial gold mining study.**

The rms error between the 1943 and 1976 aerial photographs. The 1976 image was used as the base-image. The TIC-id column refers to Figure 5.8.

TIC id	1976 base-image tic coordinates		1943 image tic coordinates		Displacement between the images		Residuals <i>i.e.</i> (displacement) <sup>2</sup>	
	x	y	x	y	x	y	x	y
3	359.93	142.51	359.88	142.02	0.05	0.49	0.00	0.24
8	388.65	422.89	388.61	422.74	0.04	0.15	0.00	0.02
11	395.15	333.71	395.52	333.35	-0.37	0.36	0.14	0.13
13	450.79	135.65	450.33	136.12	0.46	-0.47	0.21	0.22
14	441.06	145.63	440.96	145.63	0.10	0.00	0.01	0.00
rms error x = 0.27 pixels, rms error y = 0.35 pixels Total rms error 0.44 pixels								

The rms error between the 1986 and 1976 aerial photographs. The 1976 image was used as the base-image. The TIC-id column refers to Figure 5.8.

TIC id	1976 base-image tic coordinates		1986 image tic coordinates		Displacement between the images		Residuals <i>i.e.</i> (displacement) <sup>2</sup>	
	x	y	x	y	x	y	x	y
1	242.63	272.98	242.41	273.06	0.22	-0.08	0.05	0.01
2	340.39	200.36	339.70	200.52	0.69	-0.16	0.47	0.02
3	359.93	142.51	360.04	142.82	-0.11	-0.31	0.01	0.10
5	312.80	334.48	312.54	334.44	0.26	0.04	0.07	0.00
9	242.79	359.21	242.64	359.35	0.15	-0.14	0.02	0.02
10	211.45	177.13	211.22	177.06	0.23	0.07	0.05	0.00
11	395.15	333.71	395.38	333.44	-0.23	0.27	0.05	0.07
12	392.65	314.12	392.38	314.14	0.27	-0.02	0.07	0.00
rms error x = 0.32 pixels, rms error y = 0.17 pixels Total rms error 0.36 pixels								

The rms error between the 1979 and 1976 aerial photographs. The 1976 image was used as the base-image. The TIC-id column refers to Figure 5.8.

TIC id	1976 base-image tic coordinates		1979 image tic coordinates		Displacement between the images		Residuals <i>i.e.</i> (displacement) <sup>2</sup>	
	x	y	x	y	x	y	x	y
2	340.39	200.36	339.66	200.30	0.73	0.06	0.54	0.00
3	359.93	142.51	359.60	142.53	0.33	-0.02	0.11	0.00
4	266.90	298.66	266.75	298.20	0.15	0.46	0.02	0.21
5	312.80	334.48	312.42	334.08	0.38	0.40	0.14	0.16
6	329.72	333.51	330.16	333.12	-0.44	0.39	0.20	0.15
9	242.23	359.21	242.23	359.16	0.56	0.05	0.32	0.00
11	395.15	333.71	395.03	333.40	0.12	0.31	0.02	0.10
12	392.65	314.12	391.98	314.24	0.67	-0.12	0.45	0.01
13	450.79	135.65	450.55	135.60	0.24	0.05	0.06	0.00
14	441.06	145.63	440.96	145.90	0.10	-0.27	0.01	0.07
rms error x = 0.43 pixels, rms error y = 0.27 pixels Total rms error 0.51 pixels								

The rms error between the 1988 and 1976 aerial photographs. The 1976 image was used as the base-image. The TIC-id column refers to Figure 5.8.

TIC id	1976 base-image tic coordinates		1988 image tic coordinates		Displacement between the images		Residuals <i>i.e.</i> (displacement) <sup>2</sup>	
	x	y	x	y	x	y	x	y
2	340.39	200.36	340.18	200.63	0.21	-0.27	0.04	0.08
3	359.93	142.51	359.65	142.65	0.28	-0.14	0.08	0.02
5	312.80	334.48	312.38	333.94	0.42	0.54	0.18	0.30
7	377.17	338.18	376.72	338.03	0.45	0.15	0.20	0.02
11	395.15	333.71	395.41	333.37	-0.26	0.33	0.07	0.11
12	392.65	314.12	392.55	313.65	0.10	0.47	0.01	0.22
14	441.06	145.63	440.98	145.72	0.08	-0.09	0.01	0.01
rms error x = 0.29 pixels, rms error y = 0.33 pixels Total rms error 0.44 pixels								